

**Montana Water Center
Annual Technical Report
FY 2008**

Introduction

The Montana University System Water Center is located at Montana State University in Bozeman, was established by the Water Resources Research Act of 1964. Each year, the Center's Director at Montana State University works with the Associate Directors from the University of Montana - Missoula and Montana Tech - Butte to coordinate statewide water research and information transfer activities. This is all in keeping with the Center's mission to investigate and resolve Montana's water problems by sponsoring research, fostering education of future water professionals and providing outreach to water professionals, water users and communities. To help guide its water research and information transfer programs, the Montana Water Center seeks advice from an advisory council to help set research priorities. During the 2007/2008 research year, the Montana Water Research Advisory Council members were:

Gretchen Rupp, Director and Steve Guettermann, Assistant Director for Outreach, Montana Water Center

Marvin Miller, Montana Bureau of Mines & Geology and MWC Associate Director

Don Potts, University of Montana and MWC Associate Director

Mark Aagenes, Montana Trout Unlimited, Conservation Director

Jeff Tiberi, Montana Association of Conservation Districts, Executive Director

J. P. Pomnichowski, Montana State Legislator

Daniel Sullivan, Montana Department of Agriculture, Technical Services Bureau Chief

Tyler Trevor, Montana University System, Associate Commissioner

Mike Volesky, Montana Governor's Office, Natural Resources Policy Advisor

Larry Dolan, Hydrologist - Montana Department of Natural Resources and Conservation

Hal Harper, Chief Policy Advisory - Governor's Office

John Kilpatrick, Director - Montana Water Science Center; U.S. Geological Survey

Glenn Phillips, Fisheries Division - Montana Fish, Wildlife & Parks

Richard Opper, Director - Montana Department of Environmental Quality

Research Program Introduction

Through its USGS funding, the Montana Water Center partially funded three new water research projects and continued funding for five other projects for faculty at three of Montana's state university campuses. The Montana Water Center requires that each faculty research project directly involve students in the field and/or with data analysis and presentations. This USGS funding also provided research fellowships to three students involved with water science and aquatic habitat research. Here is an introduction to their work, with the second year research projects listed first.

Dr. Chris Gammons of Montana Tech and his team, studied "Temporal and spatial changes in the concentration and isotopic composition of nitrate in the Upper Silver bow Creek drainage, Montana: Year 2." The project received \$6,800. Gammons' graduate student Beverly Plumb presented this work in her master's dissertation.

Dr. Joel Harper of the University of Montana received \$8,941 for his project titled "Historical and future streamflow related to small mountain glaciers in the Glacier Park Region, Montana." Considerable progress was made to use data garnered through field work and incorporate it into computer modeling.

Dr. Clayton Marlow and graduate student Richard Labbe, received \$2,000 for their work titled "Sediment and heavy metal source determination and reduction at a reclaimed abandoned mine site, Alta Mine, Jefferson County, Montana." Labbe presented the final results in his dissertation at Montana State University during the 2008 spring semester.

Dr. Lucy Marshall of Montana State University, received \$17,000 for her study of "Predictive modeling of snowmelt dynamics: thresholds and the hydrologic regime of the Tenderfoot Creek Experimental Forest, Montana." Work has focused on the development of conceptual snowmelt/hydrologic models.

Dr. Steve Parker, Montana Tech, received \$8,585 for his research project: "Carbon cycling and the temporal variability in the concentration and stable carbon isotope composition of dissolved inorganic and organic carbon in streams." This work has been key with getting a team of student field researchers involved in data collection and analysis of specific diel cycles.

Dr. Winsor Lowe of the University of Montana and his team was awarded \$6,930 for studying "The Importance of Ecologically Connected Streams to the Biological Diversity of Watersheds: a case study in the St. Regis River subbasin, Montana." This project promises to have impact in how the state will address its obligations under the national Clean Water Act.

Denine Schmitz of Montana State University's Department of Land Resources and Environmental Sciences received \$17,000 for research of "Modeling the Potential for Transport of Contaminated Sediment from a Mine-Impacted Wetland." Dr. Joel Cahoon assumed responsibility for the project when Schmitz and family assumed new job responsibilities out of state.

Dr. Andrew Wilcox in the Department of Geosciences at the University of Montana is capitalizing on the rare opportunity to study river channel changes following the removal of a 100 year old hydroelectric dam with his project "Evolution of channel morphology and aquatic habitat in the Middle Clark Fork River following removal of Milltown Dam." Wilcox was funded \$15,818.00.

Student Research Fellows The Water Center's Student Water Research Fellowship Program awarded research grants to three Montana University System graduate students. Each showed competence in studying a water resource problem that is impacting water quality or an aquatic species. They are:

Research Program Introduction

Matt Corsi, a Fish and Wildlife doctoral student at the University of Montana received \$3,000 for his study of "The Consequences of Introgressive Hybridization: Implications for Westslope Cutthroat Trout Conservation."

Sabrina Behnke of Montana State University's Center for Biofilm Engineering received \$1,000 for her drinking water quality work to determine how susceptible detached biofilm particles are to chlorine disinfection. Sabrina is continuing her work as a doctoral student.

Tyler Smith, a Master's student in MSU's Civil Engineering Department received \$1,000 for his work, "Predictive Modeling of Snowmelt and the Hydrologic Response: Tenderfoot Creek Experimental Forest, MT." An outcome of this project was the development of a piece of hydrologic modeling software called S.P.L.A.S.H. Tyler is also continuing his studies as a doctoral student.

Carbon cycling and the temporal variability in the concentration and stable carbon isotope composition of dissolved inorganic and organic carbon in streams

Basic Information

Title:	Carbon cycling and the temporal variability in the concentration and stable carbon isotope composition of dissolved inorganic and organic carbon in streams
Project Number:	2006MT89B
Start Date:	3/1/2006
End Date:	9/1/2009
Funding Source:	104B
Congressional District:	At large
Research Category:	Climate and Hydrologic Processes
Focus Category:	Geochemical Processes, Hydrogeochemistry, Water Quality
Descriptors:	
Principal Investigators:	Stephen Parker, Douglas Cameron

Publication

Temporal Variability in the Concentration and Stable Carbon Isotope Composition of Dissolved Inorganic and Organic Carbon in Two Montana, USA Rivers

Stephen R. Parker · Simon R. Poulson · M. Garrett Smith ·
Charmaine L. Weyer · Kenneth M. Bates

Received: 27 February 2009 / Accepted: 30 July 2009
© Springer Science+Business Media B.V. 2009

Abstract Here we report diel (24 h) and seasonal differences in the concentration and stable carbon isotope composition of dissolved inorganic (DIC) and organic carbon (DOC) in the Clark Fork (CFR) and Big Hole (BHR) Rivers of southwestern Montana, USA. In the CFR, DIC concentration decreased during the daytime and increased at night while DOC showed an inverse temporal relationship; increasing in the daytime most likely due to release of organic photosynthates and decreasing overnight due to heterotrophic consumption. The stable isotope composition of DIC ($\delta^{13}\text{C}$ -DIC) became enriched during the day and depleted over night and the $\delta^{13}\text{C}$ -DOC displayed the inverse temporal pattern. Additionally, the night time molar rate of decrease in the concentration of DOC was up to two orders of magnitude smaller than the rate of increase in the concentration of DIC indicating that oxidation of DOC was responsible for only a small part of the increase in inorganic carbon. In the BHR, in two successive years (late summer 2006 & 2007), the DIC displayed little diel concentration change, however, the $\delta^{13}\text{C}$ -DIC did show a more typical diel pattern characteristic of the influences of photosynthesis and respiration indicating that the isotopic composition of DIC can change while the concentration stays relatively constant. During 2006, a sharp night time increase in DOC was measured; opposite to the result observed in the CFR and may be related to the night time increase in flow and pH also observed in that year. This night time increase in DOC, flow, and pH was not observed 1 year later at approximately the same time of year. An in-stream mesocosm chamber used during 2006 showed that the night time increase in pH and DOC did not occur in water that was isolated from upstream or hyporheic contributions. This result suggests that a “pulse” of high DOC and pH water was advected to the sampling site in the BHR in 2006 and a model is proposed to explain this temporal pattern.

S. R. Parker (✉) · M. G. Smith · C. L. Weyer · K. M. Bates
Department of Chemistry and Geochemistry, Montana Tech of The University of Montana,
1300 W. Park St., Butte, MT 59701, USA
e-mail: sparker@mtech.edu

S. R. Poulson
Department of Geological Sciences and Engineering, University of Nevada-Reno, 1664 N. Virginia St.,
Reno, NV 89557-0138, USA

Keywords Dissolved organic carbon · Carbon isotopes · Dissolved inorganic carbon · Diel

1 Introduction

Investigations over the past 20 years have shown that diel (24 h) changes in the concentration of chemical species in flowing systems are reproducible processes that play an integral role in the health and water quality of river systems. Healthy rivers can exhibit large diel pH, dissolved O₂ (DO), and CO₂ cycles that are largely driven by aquatic plants and microbes which alternately consume or produce CO₂ depending on whether photosynthesis or respiration is the dominant process (Odum 1956; Pogue and Anderson 1994; Nagorski et al. 2003; Parker et al. 2005, 2007a). These short term variations are driven by the daily photoperiod, which influences: aquatic photoautotrophs; instream temperature cycles; changes in dissolved gas gradients between air and water; and affect either directly or indirectly concentration changes in metals and metalloids (e.g., Nimick et al. 2003, 2005; Jones et al. 2004; Gammons et al. 2005; Parker et al. 2007a, b and references therein). While researchers investigating the mechanisms influencing diel processes have provided great insight into the “driving forces” behind these daily changes, there is still much that is not well understood. By gaining deeper insight into the underlying mechanisms controlling diel concentration changes of important dissolved and particulate species we will be able to develop a better fundamental understanding of how streams function. This knowledge will help scientists, resource managers and others make better predictions on how streams will respond to shifting conditions caused by climate change, changing agricultural practices, restoration activities, nutrient fluxes and development.

Previous work has demonstrated that there is a significant and reproducible diel cycle in the stable isotope composition of dissolved inorganic carbon ($\delta^{13}\text{C}$ -DIC) in both the Clark Fork River (CFR) and Big Hole River (BHR) in Montana, USA as well as a substantial cycle in the ^{18}O composition of dissolved molecular oxygen ($\delta^{18}\text{O}$ -DO) in the BHR and other streams (Parker et al. 2005, 2007a, 2009). These daily changes in the isotope composition of the DIC and DO are caused by the combined effects of photosynthesis and respiration of aquatic plants and microbes as well as gas-exchange and groundwater influx. Additionally, $\delta^{13}\text{C}$ -DIC has been used as a tracer of the origins and sources of carbon in watersheds (e.g., Gaiero et al. 2005), but these data must be used carefully since substantial diel changes in $\delta^{13}\text{C}$ -DIC can occur (up to 4.5‰, Parker et al. 2009).

Dissolved organic carbon (DOC) represents a significant pool of reduced carbon in most aquatic ecosystems that is readily available to heterotrophic microorganisms as an energy source (McKnight et al. 1997; Volk et al. 1997). It has also been suggested that the DOC pool may be the largest source of carbon for microbial activity (Kaplan and Bott 1982; Hobbie 1992). Additionally, it has been shown that different size classes of DOC molecules exist and that the distribution can change over a diel period (Amon and Benner 1996; Zeigler and Fogel 2003). Depending on the size and composition of the DOC some classes of molecules may be more refractory than others and consequently consumed at different rates (Thurman 1985; Zeigler and Fogel 2003).

The types and concentration of the DOC can have a significant influence on the chemical composition of surface waters such as the bioavailability of metal ions and the absorption of

light in the visible and UV ranges (McKnight et al. 1997). Much of the literature examining DOC in rivers has concentrated on sources of organic carbon and its fate and transport to downstream areas (e.g., Thurman 1985; Olivie-Lanquet et al. 2001; Bianchi et al. 2004, 2007; Hood et al. 2005; Dalzell et al. 2007). Several researchers have shown that diel changes in DOC concentration occur in streams and can be attributed to daily changes in the level of productivity of algal communities (e.g., Manny and Wetzel 1973; Kaplan and Bott 1982; Harrison et al. 2005; Spencer et al. 2007). However, there is little literature that reports investigations of temporal changes in DOC and the ^{13}C -composition of DOC ($\delta^{13}\text{C}$ -DOC) simultaneously on a diel scale in surface waters (Zeigler and Fogel 2003). Since community respiration is using the DOC as a carbon source and other aquatic species are producing organic molecules as a consequence of their daily productivity, it is reasonable to expect changes in the isotopic composition of the DOC as it is influenced by the daily changes in the rates of metabolic activity (Barth and Veizer 1999; Zeigler and Fogel 2003; Zeigler and Brisco 2004).

DOC can include water soluble forms of amino acids, carbohydrates, organic acids, alcohols as well as fulvic and humic acids (Thurman 1985). Sources of DOC in streams can include decomposition of detrital organic matter, importation of organics from external (allochthonous) sources and in-stream production by aquatic plants and microbes (autochthonous). Microbes using DOC as a carbon source will produce CO_2 from respiration with a carbon isotope signature characteristic of the organic carbon substrate (Clark and Fritz 1997). In temperate regions, plant organic matter, that serves as the carbon source for microbial respiration has a $\delta^{13}\text{C}$ of -20 to -30% (Clark and Fritz 1997). In contrast, atmospheric CO_2 has $\delta^{13}\text{C}$ of -7 to -8.5% (NOAA 2008) and consequently DIC produced by gas exchange will be isotopically enriched compared to that produced by respiration.

A significant portion of DOC in natural waters falls in the category of natural organic matter (NOM), and most of the NOM fits into the operationally defined subcategories of fulvic acids (FA) and humic acids (HA; Thurman 1985; Macalady 1998). The fulvic and humic acids as well as other organic acids are well known for their ability to complex metal ions in solution (Saar and Weber 1982; Clapp et al. 1998). It is known that the fulvic and humic acids can contribute to daily variations in surface water iron concentrations by affecting Fe redox cycling through changes in the photoreactivity of Fe in the aqueous system (Voelker et al. 1997; Hrcir and McKnight 1998).

In this study, we investigated diel changes in the concentration of DOC and DIC in two different rivers systems (CFR and BHR). These rivers are geographically close but exhibited approximately inverse diel patterns in the concentration of DOC during the late summer of 2006. An in-stream mesocosm chamber was used in the BHR during 2006 to compare diel cycles and levels of DOC and DIC that were isolated from the flowing water column or hyporheic water exchanges. A follow-up study was conducted in the BHR 1 year later to assess the reproducibility of the diel DOC pattern observed the previous year. Additionally, in order to identify possible sources of DOC in the BHR a series of seeps (streamside springs) and shallow sediment water was sampled during the follow-up work in 2007. The rates of DOC consumption and DIC production in the CFR were compared in order to determine what portion of the inorganic carbon being produced resulted from the oxidation of DOC. The $\delta^{13}\text{C}$ -DOC was examined in the CFR as well as the $\delta^{13}\text{C}$ -DIC in the CFR and BHR. These isotope results are used here in conjunction with the seep and chamber data to investigate the relationship of the diel changes in DOC and DIC to the processes influencing these changes. Models are presented to help interpret the

diel behavior of DOC in the CFR and the differences in the diel behavior of DOC observed in the BHR between 2006 and 2007.

2 Field Sites

2.1 CFR Site

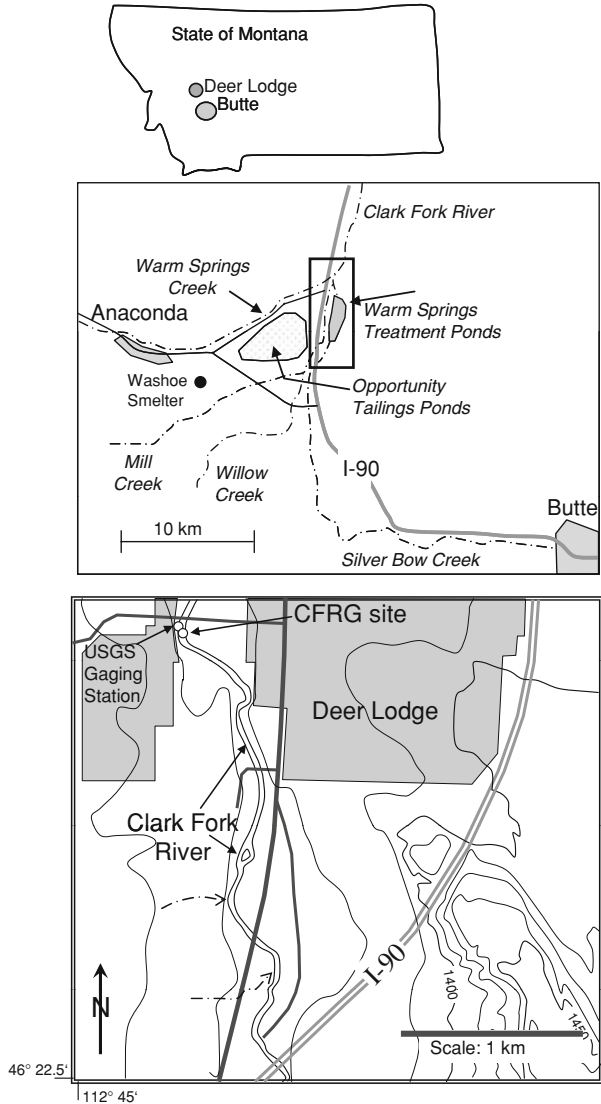
The field site on the Clark Fork River ($46^{\circ}23'51''\text{N}$; $112^{\circ}44'33''\text{W}$; sampling site CFRG) was within the city limits of Deer Lodge, MT and directly across from the USGS gaging station (Fig. 1, USGS Gage #12324200, 1,372 m elevation). Streamflow measurements were taken from the USGS gaging station which records every 15 min. The Clark Fork here is a second order stream with a discharge of roughly $0.6\text{--}60\text{ m}^3\text{ s}^{-1}$ depending on the time of year. The river in the study reach has moderate alkalinity ($\sim 3,200\text{--}3,700\text{ }\mu\text{eq l}^{-1}$; Parker et al. 2007a) and a pH range of about 8.0–9.0 during the summer months. Aquatic plants are dominated by *Cladophora* and diatom algae (Watson 1989). The mining and smelting centers of Butte and Anaconda are situated at the headwaters of the upper Clark Fork River along Silver Bow and Warm Springs Creeks, respectively (Fig. 1) such that the floodplain and streambed of the upper Clark Fork River contain highly elevated quantities of metals and metalloids (e.g., Fe, Cu, Zn, Pb, Cd, As) deposited as the result of mining, milling, and smelting activities (Moore and Luoma 1990). Currently, most of the heavy metal load in Silver Bow Creek is removed by a lime treatment facility at Warm Springs (Fig. 1). However, elevated concentrations of dissolved arsenic have been measured in the water exiting the treatment ponds ($>40\text{ }\mu\text{g L}^{-1}$) during summer base-flow periods (Duff 2001; Gammons et al. 2007). Diel changes in the concentration of metals and arsenic in the upper CFR have been previously characterized (Brick and Moore 1996; Parker et al. 2007a; Gammons et al. 2007).

2.2 BHR Site

The field site near the Mudd Creek Bridge on the Big Hole River ($45^{\circ}48'28''\text{N}$, $113^{\circ}18'51''\text{W}$; sampling site BHRG) was about 50 m upstream from the USGS gaging station (Fig. 2; USGS Gage #6024540, 1795 m). Annual flows range from 5 to $140\text{ m}^3\text{ s}^{-1}$ depending on time of year. Flow data for this site was obtained from the USGS gaging station which records discharge every 15 min. The BHR is a headwater tributary to the Missouri River and is a free-flowing river draining a sparsely-populated, high elevation basin ($\sim 1,900\text{ m}$ above sea level) of approximately $7,200\text{ km}^2$ in extent. This river is relatively pristine and there is little historical impact from mining or industrial sources. The principal activities in the basin are agriculture and recreation.

Previous work (Gammons et al. 2001; Ridenour 2002; Wenz 2003; Parker et al. 2005) has summarized the general geochemical characteristics of the Big Hole River. Overall, the Big Hole River at Mudd Creek Bridge can be classified as a Na–Ca–bicarbonate water, with alkaline pH and low to moderate alkalinity ($1,500\text{--}1,800\text{ }\mu\text{eq L}^{-1}$). The lower alkalinity of the BHR versus the CFR described above results in lower buffering capacity of the BHR stream water that often leads to larger ranges in and higher absolute values of pH during summer low flow periods.

Fig. 1 Location map of the upper Clark Fork River showing Butte, MT; Anaconda, MT; Warm Springs Ponds, Opportunity Ponds and the CFRG sampling site on the Clark Fork River near Deer Lodge, Montana, USA



3 Methods

3.1 Field Methods

3.1.1 Clark Fork River

Diel sample collection on the CFR began on 27 July 2006 at 11:15 and continued until 13:15 on 28th of July. All times are reported as local time (MDT, GMT−0600).

In situ temperature, pH, specific conductivity (SC), dissolved oxygen (DO) concentration and percent O₂ saturation were measured at each sampling time with a Hydrolab MS-5 datasonde (Luminescent DO probe) or an In Situ Troll 9000 (Clark DO probe) as

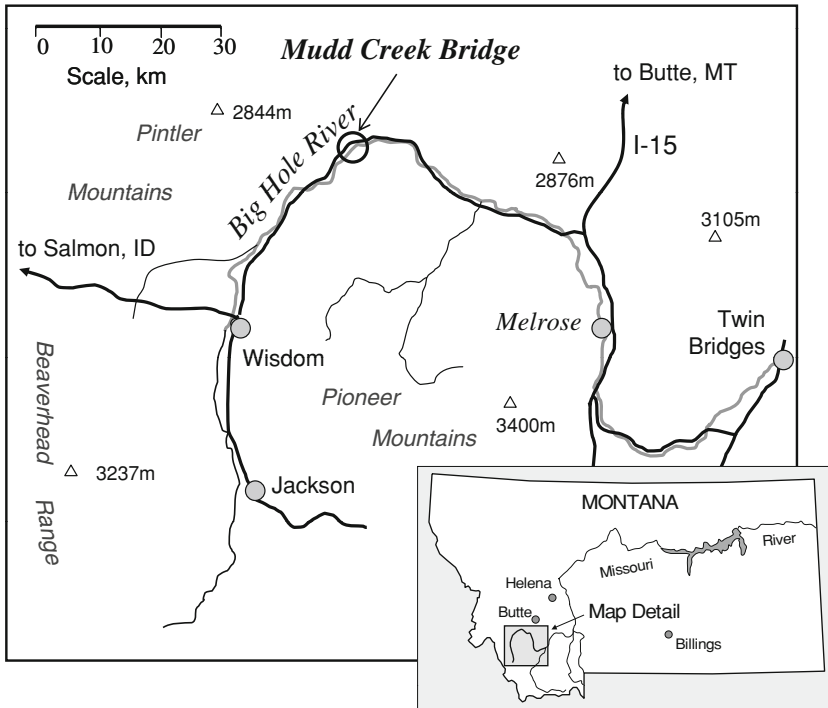


Fig. 2 Site map showing the Mudd Creek Bridge sampling area of the Big Hole River located in southwestern Montana, USA

well as a hand-held meter (WTW 340i). The instruments were calibrated according to the manufacturer's specifications.

Several samples were collected for laboratory analysis of DO using the Winkler method (Wetzel and Likens 1991). Unfiltered water was collected in 500 mL glass bottles with no head space and stored on ice until analysis in the laboratory within 48 h. The results of these analyses were compared to the DO measurements using hand and in situ instruments (shown in results).

Water was sampled from the main stem of the river in a well mixed, rapidly flowing reach approximately 0.5 m deep, 3 m from shore and at a depth approximately half way between surface and bottom. Filtration was done using a peristaltic pump and disposable 142 mm diameter 0.1 μm cellulose-ester filter membranes (for further details see Gammons et al. 2005). Samples (filtered) for DOC analysis were collected in 250 mL amber bottles that had been acid washed (5% HNO_3), triple rinsed with deionized water and oven dried (100°C). Filtered samples for ^{13}C -isotope analysis of dissolved inorganic carbon ($\delta^{13}\text{C}$ -DIC) were collected in 125 or 250 mL acid-washed, oven dried, glass bottles with no head-space and the DIC was precipitated in the laboratory as SrCO_3 after Usdowski et al. (1979).

A detector was used to measure photosynthetically active radiation (PAR) flux values (400–700 nm, $\mu\text{E m}^{-2} \text{s}^{-1}$) which were based on the manufacturer's calibration of the sensor. The PAR went to zero at 21:00 h in the evening and rose above zero at 06:30 in the morning. This *dark* period (zero PAR) is represented by the shaded region on all diel graphs.

All samples collected in the field were stored on ice, in sealed plastic bags and returned to the laboratory immediately following the field work.

3.1.2 Big Hole River

Two separate diel samplings occurred on the BHR approximately 1 year apart: 8 to 9 August 2006 and 31 July to 1 Aug 2007. Sampling was performed similar to that described in the previous section on the Clark Fork site. Alkalinity was measured in the field using a Hach titrator and standardized H_2SO_4 . Samples from seeps above the main sampling site were collected with a clean 60 mL syringe that was triple rinsed with sample water and then filtered using 0.2 μm PES syringe filters into glass bottles. Sediment pore water was collected at two locations near the sampling site with a 60 mL syringe that was inserted approximately 12 cm into the shallow sediments in the middle of the river. The syringe plunger was very slowly withdrawn to minimize water from being pulled around the barrel of the syringe from the above river; taking 2–3 min to fill the 60 mL volume. This water was filtered using 0.2 μm PES filters into glass bottles.

An isolation chamber was used during the 2006 sampling that was made from a 10 cm inside diameter clear acrylic plastic cylinder 22 cm long. One end was sealed and the other end was removable (both clear acrylic). Each end had a tubing connector fastened to a drilled and threaded hole in the center. Prior to the start of the diel sampling, the chamber was filled approximately half-full with cobbles ranging from 2 to 10 cm in diameter collected from the sampling site that were covered with attached periphyton and biofilms. The chamber lid was sealed with silicone vacuum grease and held in place with an elastic strap. Clear plastic tubing was used to connect the chamber to a peristaltic pump mounted on a tethered platform in the river, then to a low volume flow chamber on a datasonde and back to the chamber. The chamber and datasonde were placed on the river bottom at a depth of ~ 0.5 m. At the beginning of the sampling period, the chamber was flushed with river water, filled and purged to remove most of the trapped air. The chamber water was sampled every 2 h as described previously for DOC and DIC; then flushed and refilled with fresh river water. The datasonde connected to the chamber recorded pH, temperature, DO, and SC every 30 min throughout the diel period.

3.2 Analytical Methods

A pre-concentration step for samples for $\delta^{13}\text{C}$ -DOC analysis was performed by evaporating 250 mL of filtered river water to near-dryness at 50°C and resuspending in 4 mL of 1% H_3PO_4 .

The SrCO_3 precipitates (described above) for $\delta^{13}\text{C}$ -DIC and the DOC concentrates for $\delta^{13}\text{C}$ -DOC were analyzed using a Eurovector elemental analyzer interfaced to a Micromass Isoprime stable isotope ratio mass spectrometer after Harris et al. (1997) and Gandhi et al. (2004), respectively. Replicate analyses (three per sample set) indicated an average relative standard deviation (RSD) of 0.95‰ for $\delta^{13}\text{C}$ -DOC and 0.55‰ for $\delta^{13}\text{C}$ -DIC.

All analyses for total carbon (TC) and DOC were performed at Montana Tech using an Ionics (Model 1505) Total Carbon Analyzer (combustion method). All samples for TC analysis used filtered, unacidified water. Samples for DOC analysis used filtered water that was acidified to 1% (v/v) with concentrated H_3PO_4 and sparged for 5 min with N_2 . These samples were then sparged in the instrument for an additional 3 min with CO_2 -free air and analyzed. Standards were prepared from a stock solution of $1,000 \text{ mg l}^{-1}$ potassium hydrogen phthalate (KHP) prior to each analysis. All glassware used for carbon analyses

was acid-washed and oven dried prior to use (100°C). DIC was determined by subtracting DOC concentration from TC. Replicate analyses indicated an RSD of 5% for DOC and DIC.

3.3 Modeling

The partial pressure of dissolved (wet) CO₂ ($p\text{CO}_2$, μatm) was calculated for the CFR and BHR with the modeling program CO₂SYS (Lewis and Wallace 1998) using the temperature, pH and either the total alkalinity or DIC to determine the carbon speciation.

4 Results and Discussion

4.1 Clark Fork River

4.1.1 Field Results

Temperature, flow, pH, and specific conductivity from the diel sampling on the CFR in 2006 are shown in Fig. 3. A diel pH change of approximately 0.6 units (range 7.8–8.4) was observed which is attributed to daytime net consumption of CO₂ by aquatic photosynthesis and night time production of CO₂ by community respiration. The temperature reached a daytime maximum of 24.6°C and night time minimum of 16.5°C. A diel change in flow of approximately 13% was observed most likely due to evapo-transpiration in the streamside riparian zones (Bond et al. 2002). The dissolved oxygen reached a daytime high of 158% of saturation (385 $\mu\text{mol L}^{-1}$) and a night time low of 65% (164 $\mu\text{mol L}^{-1}$). DO concentrations ($n = 3$) determined by Winkler titration were in good agreement with instrument readings (Fig. 3c). The $p\text{CO}_2$ was above atmospheric partial pressure ($\sim 252 \mu\text{atm}$) during the whole diel period; decreasing during the day and increasing at night (Fig. 3c).

4.1.2 DOC and DIC

DOC showed a 1.8-fold diel change in concentration from a minimum of 124 to a maximum of 231 $\mu\text{mol C L}^{-1}$ (Fig. 4a). At the same time the average concentration of DIC was ~ 52 -times higher than that of the DOC. The DIC showed a ~ 5 -fold diel change in concentration from a minimum of 3.4 to a maximum of 17.0 mmol C L^{-1} (Fig. 4a). The diel change in DOC is most likely produced by release of soluble organic carbon compounds (i.e., amino acids, sugars, organic acids) by photosynthetic organisms during the daytime (Kaplan and Bott 1982; Vymazal 1994 and references therein) followed by consumption of those soluble organics by heterotrophic microbes during the night. The gradual increase in DOC after about 23:00 suggests a net accumulation due heterotrophic processing of larger insoluble organics from sediments or particulates (Zeigler and Fogel 2003). The DIC concentration decreased during the daytime due to removal of CO₂ by photosynthesis and increased at night due to community respiration.

The molar ratio of DIC/DOC reached a minimum of 16 at $\sim 17:00$ and a maximum of 104 at $\sim 06:00$ the following morning (Fig. 4b). This large increase in DIC relative to DOC at night suggests that oxidation of DOC contributed only a small part of the increase in DIC and that the majority of DIC was produced from other sources (e.g., aerobic or anaerobic respiration of microbes within the sediment bed; or groundwater influx). The

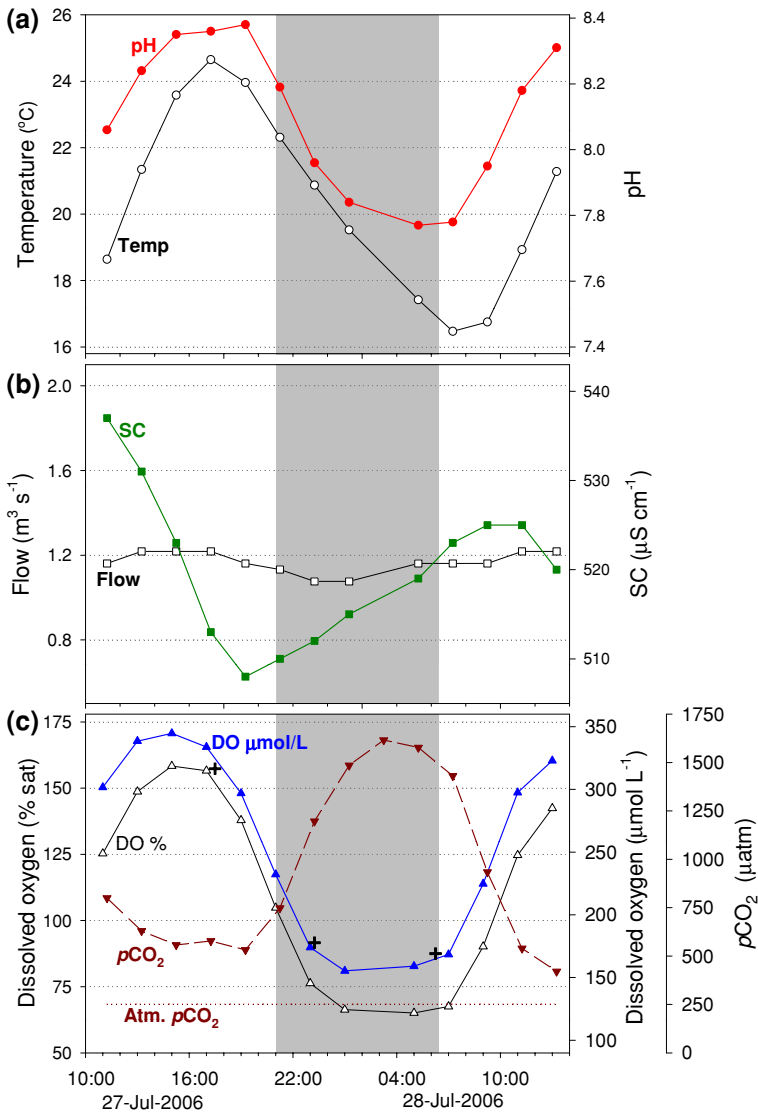


Fig. 3 Temperature and pH (a), specific conductivity (SC) and flow (b), dissolved oxygen (% saturation and $\mu mol L^{-1}$) and pCO_2 (c) at the Clark Fork River sampling site in Deer Lodge, MT. The cross marks (+) indicate Winkler DO measurements (see methods) performed to verify O_2 concentrations from instruments. Shaded bars in all diel graphs represent night time as determined by PAR signal of zero

rates of change in the concentration of DIC and DOC between sampling times can be compared to better understand how these two parameters were changing relative to each other (Fig. 4c). For example, at 19:15 the $\Delta DOC/\Delta t$ is about $-4.8 \mu mol C L^{-1} h^{-1}$ while the $\Delta DIC/\Delta t$ is approximately $1530 \mu mol C L^{-1} h^{-1}$; the concentration of DIC is increasing ~ 316 times faster than the concentration of DOC is decreasing. This also suggests that the majority of the increase seen in DIC was from sources other than the oxidation of the measured DOC.

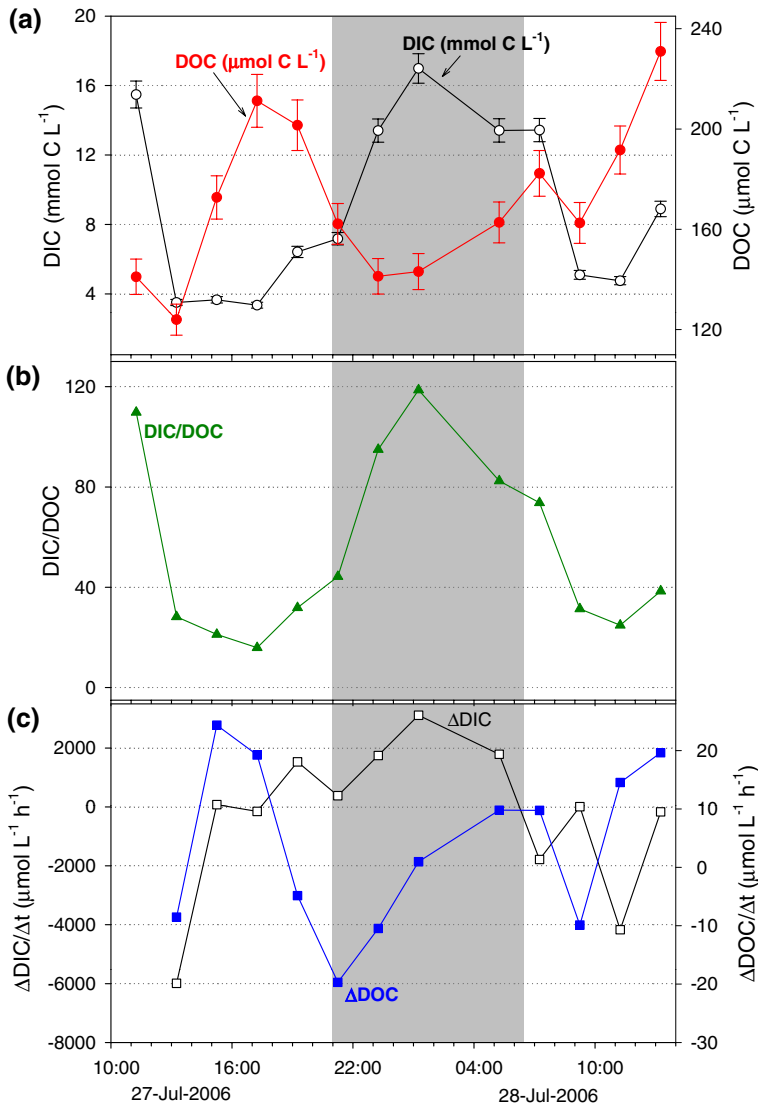


Fig. 4 DOC ($\mu\text{mol C L}^{-1}$) and DIC (mmol C L^{-1}) at CFRG during diel sampling in 2006 (a); molar ratio of DIC to DOC at CFRG (b) and the rate of change in DIC ($\text{mmol C L}^{-1} \text{h}^{-1}$) and DOC ($\mu\text{mol C L}^{-1} \text{h}^{-1}$) (c). Error bars represent 5% RSD based on replicate determinations

4.1.3 $\delta^{13}\text{C}$ -DOC and $\delta^{13}\text{C}$ -DIC

The isotopic composition of DOC ($\delta^{13}\text{C}$ -DOC) and DIC ($\delta^{13}\text{C}$ -DIC) also showed changes over the sampling period (Fig. 5). Diel changes in $\delta^{13}\text{C}$ -DIC have been observed previously in the CFR and BHR (Parker et al. 2005, 2007a). Photosynthesis removes CO_2 during the day with a reported isotopic depletion of about -29% (Falkowski and Raven 1997); such that the residual DIC becomes isotopically enriched. Gas-exchange with atmospheric

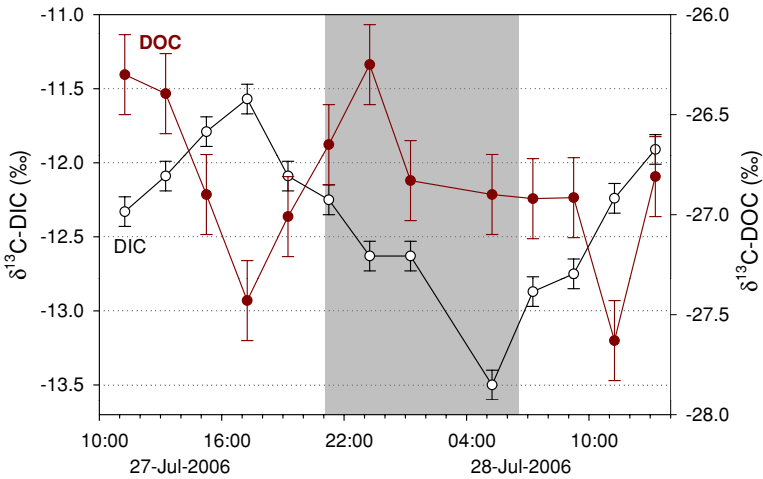


Fig. 5 $\delta^{13}\text{C-DOC}$ and $\delta^{13}\text{C-DIC}$ values measured during diel sampling in the CFR. Error bars represent a RSD of 0.95% for $\delta^{13}\text{C-DOC}$ and 0.55% for $\delta^{13}\text{C-DIC}$

CO_2 ($\delta^{13}\text{C} = -7$ to -8.5‰) will tend to elevate the $\delta^{13}\text{C-DIC}$ which had an average value over the diel period of -12.4‰ . However, as reported in Sect. 4.1.1 the $p\text{CO}_2$ was above atmospheric levels during the diel period such that the net flux of CO_2 would have been from the water to the atmosphere for the 24-h period. Diffusional fractionation associated with CO_2 outgassing should have caused the $\delta^{13}\text{C-DIC}$ to become isotopically heavier but the opposite was observed, with the $\delta^{13}\text{C-DIC}$ becoming increasingly depleted over night. This is consistent with community respiration being the dominant process which was influencing the $\delta^{13}\text{C-DIC}$.

The $\delta^{13}\text{C-DOC}$ showed the inverse isotopic diel trend to that of the DIC. The concentration of DOC increased during the day (Fig. 4a) due to soluble organics that were “leaking” from photosynthetic organisms and since photosynthesis discriminates against ^{13}C it follows that the DOC produced during this time will be isotopically depleted. Zeigler and Fogel (2003) suggested that the daytime decrease in $\delta^{13}\text{C-DOC}$ observed in a tidal wetland was due to the exudation of carbohydrates produced by phytoplankton and macrophytes. As photosynthesis decreased in the late afternoon ($\sim 17:00$), community respiration consumed this pool of soluble (isotopically light) organics, discriminating against the heavier isotope (kinetically) such that the remaining DOC pool becomes isotopically enriched (concentration decreasing, Fig. 4a). It is also possible that these “leaking”, isotopically light photosynthates such as carbohydrates are more readily bio-available and are used first for respiration (Zeigler and Fogel 2003). After $\sim 23:00$ the isotopic composition of the pool stabilizes at approximately -26.9‰ . The $\delta^{13}\text{C}$ of the local aquatic and streamside vegetation was not measured during this study, but temperate region C_3 plants should have an isotope composition in the range of -20 to -30‰ (Clark and Fritz 1997). Consequently, this $\delta^{13}\text{C-DOC}$ plateau from 01:00 to 09:00 may reflect the DOC being produced by microbial degradation of detritus with an isotope signature typical of temperate region vegetation. This is consistent with the increase in DOC concentration after 23:00 (discussed above) being due to heterotrophic degradation of organic detritus accumulated within the sediment bed.

During the night as community respiration consumes the isotopically light DOC and insoluble organic matter in the sediments, it produces light CO_2 which causes the $\delta^{13}\text{C}$ -DIC to continue dropping until photosynthesis reverses the trend starting about 06:30 (Parker et al. 2009).

4.2 Big Hole River

4.2.1 Field and Isolation Chamber Results

Diel samplings were conducted on the BHR in two successive years during late summer, low flow conditions (2006 and 2007) within 8 days of the same date each year (Fig. 6). The hydrographs for a 6–7-day period bracketing the sampling for the 2 years show that the average flow in 2007 was about 1.7-times higher than in 2006 during the sampling period and that different temporal flow patterns were present in the 2 years (Fig. 7). The flow during the diel sampling period in 2006 showed a ~ 2.7 -fold minimum to maximum increase and exhibited a sharp decrease during the late afternoon ($\sim 17:00$) followed by a gradual increase with a maximum at about 01:00–03:00 (Fig. 6b). The flow in 2007 showed a ~ 1.3 -fold minimum to maximum increase during the sampling period with a gradual decrease throughout the afternoon reaching a minimum about 21:00 through 02:00 followed by a gradual increase through the following morning (Fig. 6e). The 2007 pattern is more typical of one expected to be produced by evapo-transpiration from productive

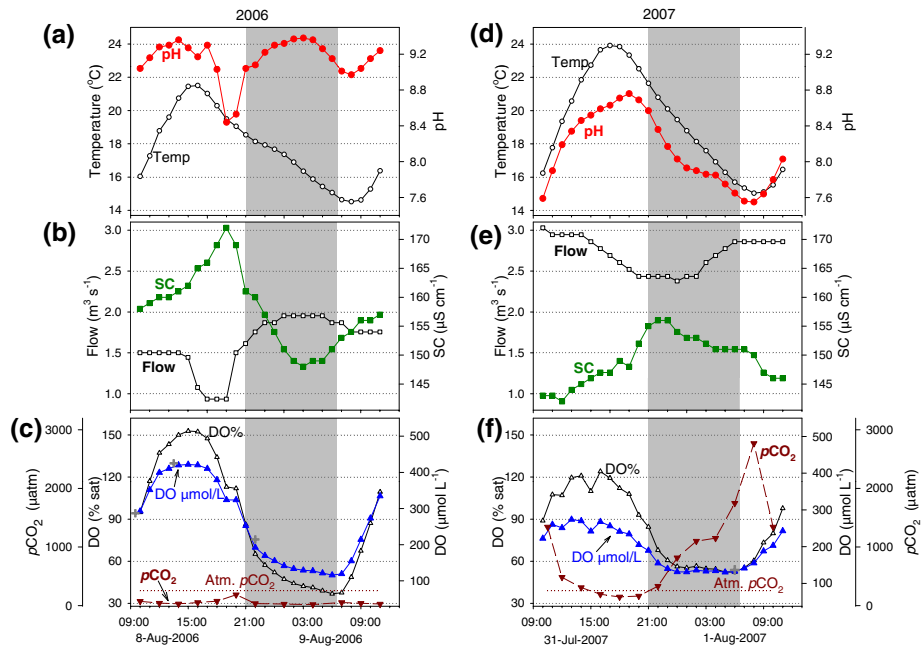


Fig. 6 Temperature and pH (a; 2006) and (d; 2007); flow and specific conductivity (SC) (b; 2006) and (e; 2007); and dissolved oxygen (% saturation and $\mu\text{mol L}^{-1}$) (c; 2006) and (f; 2007) for the BHR. The cross marks (+) indicate Winkler DO measurements (see methods) performed to verify O_2 concentrations from instruments

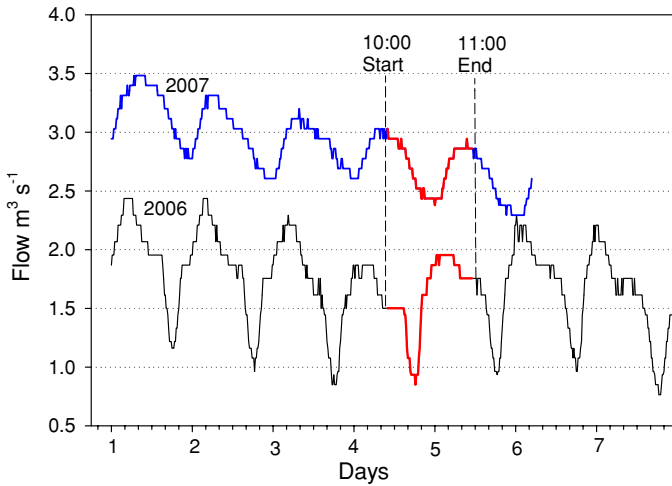


Fig. 7 Hydrographs (USGS gage data) for the BHR site for a 6–7 day period around the field work in 2006 and 2007. *Red lines* show the sampling period in both years and *dashed lines* show the approximate starting (10:00) and ending (11:00) times for sampling

upstream riparian zones (Bond et al. 2002) while the pattern observed in 2006 is not well understood (discussed below).

The pH variation observed in 2006 is very unusual with a sharp pH drop in late afternoon ($\sim 17:00$), at approximately the same time that the flow dropped (Fig. 6a). This was followed by a gradual increase in pH with a maximum at $\sim 03:00$; approximately the same time that the flow peaked in 2006. The late afternoon decrease in flow in 2006 described above was also accompanied by a sharp increase in specific conductivity (SC) at the same time ($\sim 18:00$, Fig. 6b). The SC dropped after this time with a minimum at $\sim 03:00$, the same time that the flow reached a maximum. The behavior of DO in 2006 was “normal” with the exception of a small shoulder at approximately 19:00 which corresponds to the sharp flow decrease in the late afternoon (Fig. 6c). In contrast to the CFR described above, the $p\text{CO}_2$ in the BHR in 2006 was below atmospheric levels ($\sim 252 \mu\text{atm}$) for the 24-h sampling period (Fig. 6c) which is due to the high pH (avg. 9.1) and high productivity as shown by the large diel change in O_2 concentration (37–152% sat.) during this base flow period. The late afternoon drop in pH described above ($\sim 17:00$) was mirrored by a small increase in $p\text{CO}_2$ followed by a night time decrease as the pH began to rise. This is an unusual $p\text{CO}_2$ pattern since it usually increases over night due to community respiration and decreasing pH, as observed in the CFR (Fig. 3c).

In 2007, the changes in flow, SC, and pH were more typical of “normal” stream behavior (Fig. 6d, e). The diel change in DO was not as large in 2007 as in 2006 and was possibly modulated by the larger flow (Fig. 6f). Maximum stream temperature was higher in 2007 than 2006 which also decreased O_2 solubility. The $p\text{CO}_2$ during 2007 was above atmospheric levels except for a brief period in the afternoon ($\sim 16:00$ – $20:00$) and showed a more “typical” pattern (Fig. 6f). The higher $p\text{CO}_2$ levels are in part due to the lower pH values in 2007 (avg. 8.1) versus 2006 (avg. 9.1).

An isolation chamber with stream water plus cobbles and attached periphyton was used during the 2006 sampling (Fig. 8a). This allowed a comparison of temperature, pH, and DO between the river and water in the chamber which was isolated from chemical species

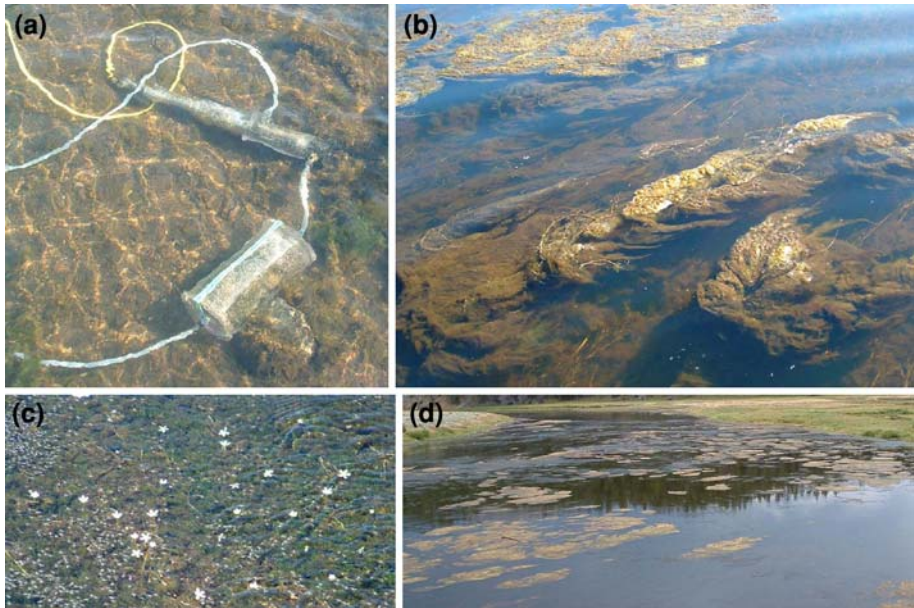


Fig. 8 Pictures of the isolation chamber (a), streaming algal mats (b), area of *Ranunculus aquatilis* (river buttercups, c) and river with algal mats near sampling area (d) in the BHR

transported to the sampling site from upstream or from hyporheic discharge (Fig. 9). Consequently, the observed changes in chemistry of the chamber water were dominated by interactions with the enclosed benthic materials. Temperature and DO both in the chamber and in the river were similar through the diel period although at night the DO in the chamber did reach a minimum of about $31 \mu\text{mol L}^{-1}$ versus $115 \mu\text{mol L}^{-1}$ in the river (Fig. 9a, c). This night time difference in DO was most likely due to the absence of gas exchange with the atmosphere in the chamber. The pH in the chamber did not show the same unusual pattern displayed in the river (Fig. 9b). Since the chamber was refilled with river water every 2 h, it does show evidence of a subdued version of the decrease in pH seen in the river at $\sim 19:00\text{--}20:00$. The pH in the water isolated in the chamber showed a 0.13 unit change in pH versus 0.86 units in the river in the time period from 17:00 to 19:00. Since the pH profile in the chamber was similar to the more typical pattern found in river systems (i.e., CFR Fig. 3a) and that it was refilled with river water every 2 h emphasizes the temporal period over which the pH modification can occur. The $p\text{CO}_2$ in the chamber (Fig. 9c), similar to pH, showed a more typical diel behavior and did not show the small increase around 19:00 as was seen in the river. The potential causes of these differences in the diel pH and $p\text{CO}_2$ patterns in 2006 between the river and the chamber will be discussed in the next section.

4.2.2 DOC and DIC

A 4.6-fold minimum to maximum diel change in DOC in the BHR was observed in 2006 while no regular diel change in DOC concentration was observed in 2007 (Fig. 10a, b). The night time peak in DOC concentration in 2006 occurred at $\sim 01:00$, which coincides

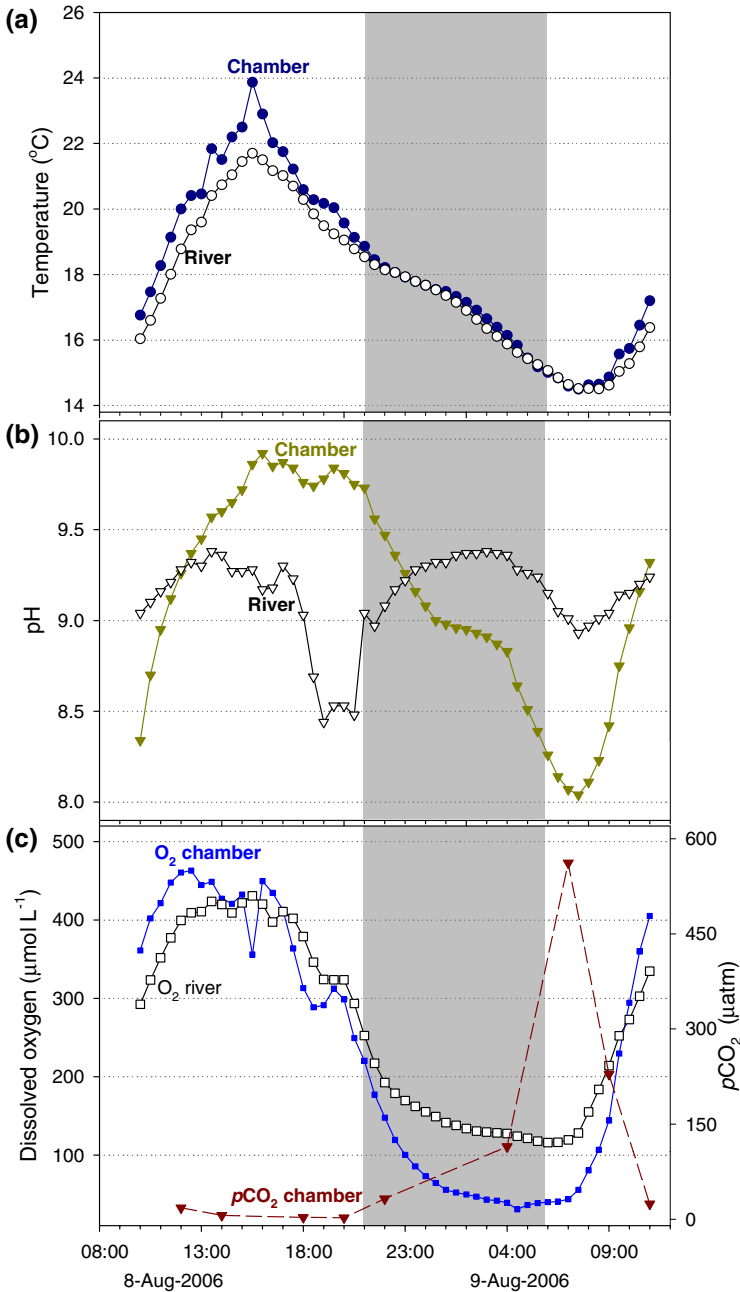


Fig. 9 Temperature (a), pH (b) and dissolved oxygen (% saturation and $\mu\text{mol L}^{-1}$) (c) for the isolation chamber and BHR during the 2006 sampling

approximately with the timing of the maximum values reached by both flow and pH (Fig. 6a, b). At the same time, the concentration of DIC both in 2006 and 2007 did not change significantly over the diel period. The load of DOC (concentration \times flow) in 2006

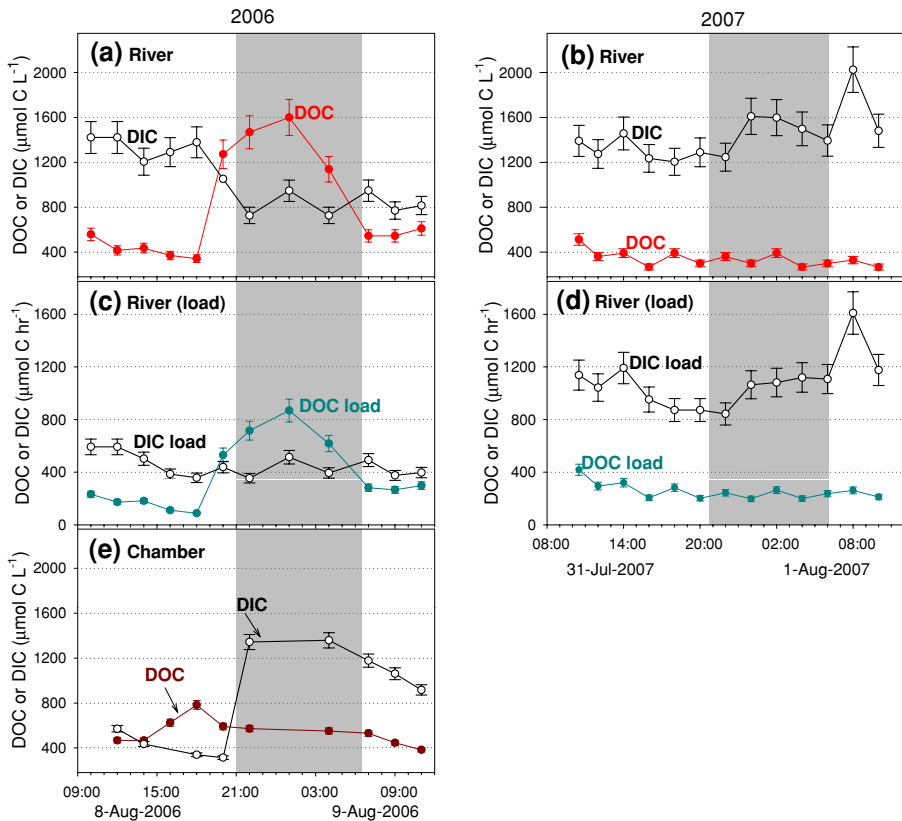


Fig. 10 Concentrations DIC and DOC in the BHR in 2006 (a) and 2007 (b); load of DOC and DIC in the BHR in 2006 (c) and 2007 (d); and DOC and DIC in the isolation chamber during 2006 (e). *Error bars* represent 5% RSD based on replicate determinations

shows the same night time increase with a maximum at $\sim 01:00$ when the flow peaked while there was no change in load of DOC over the diel period in 2007 (Fig. 10c, d). This indicates that the diel change in concentration in 2006 (Fig. 10a) was not an artifact of the change in flow (Fig. 6b) since the load of DOC increased simultaneously. Although the average load of DIC in 2007 was about 2.4 times higher than in 2006 there was no apparent regular diel pattern in either year (Fig. 10c, d).

One possible explanation for this significant late afternoon/night time increase in DOC in 2006 and not in 2007 may be linked to the unusual flow pattern observed in 2006. After the late afternoon decrease in flow in 2006 ($\sim 17:00$; Fig. 6b), the following increase may have included a groundwater influx from bank-storage and/or benthic sediments. This water may have carried additional concentrations of DOC from decaying organic matter producing the DOC increase observed in the river. In order to better address the DOC concentration and pH of bank storage/sediment pore waters during the 2007 sampling, water was collected from seeps (small springs) along the river bank as well as pore water withdrawn from the shallow stream bottom sediments. The seeps were on both sides of the river between 300 and 800 m upstream from the sampling site. The seeps all had higher

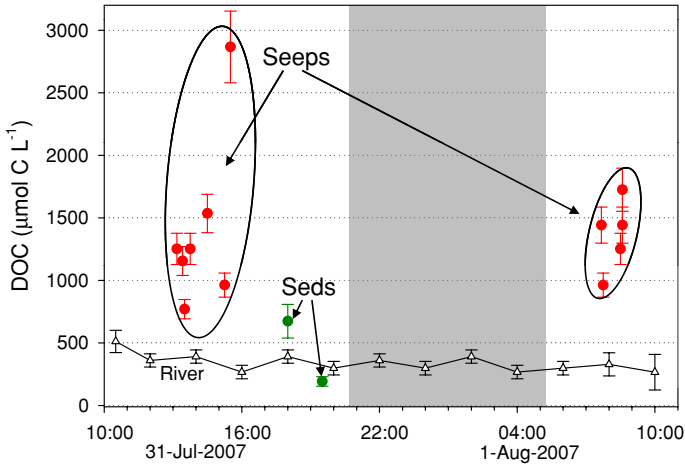


Fig. 11 Concentration of DOC ($\mu\text{mol C L}^{-1}$) in seeps (red), shallow sediments (green) and the BHR (open triangles) during the 2007 sampling site

DOC concentrations and lower pH values than the river water at the sampling site (Fig. 11; Table 1). The average DOC concentration of the seeps was $1,385 \mu\text{mol C L}^{-1}$ while the average DOC in the river over the diel period was $341 \mu\text{mol C L}^{-1}$. The DOC concentration of the shallow sediment water sampled was similar to that of the river (Fig. 11), which is characteristic of shallow, short range hyporheic flow paths (Poole et al. 2008). The average pH of the seep waters was 6.8 while the average pH of the river during the 2007 diel sampling was 8.1 (9.1 in 2006). This suggests that if the night time increase in DOC in 2006 was due to a significant influx of bank storage water, then the pH should have decreased simultaneously; not increased. This is not to suggest that streamside/groundwater contributions of DOC and other solutes did not occur but that those contributions were relatively constant while the large night time increase in DOC was produced by a separate process.

Another hypothesis that has been considered to explain the large diel changes in flow that have been observed periodically during late summer in the BHR has been the presence of large stretches of algae and macrophytes (*Ranunculus aquatilis* and other species) that float to the surface during the day while they are actively photosynthesizing, effectively forming an “in-stream” dam (see Fig. 8b–d). At night these photosynthetic organisms sink toward the bottom allowing the trapped water to flow down the river as a wave. This model is consistent with stream flow observations in this reach of the river during a similar flow regime in 2005 when the river stage (water level) increased and the flow decreased (C. Gammons personal communication). This might explain the decrease in flow in the late afternoon during 2006 followed by an increase in water at night from upstream as the in-stream damming action ceased. This pulse of water that was retarded by the plants and algae during the day may have been higher in pH due to photosynthetic removal of CO_2 and contain higher amounts of DOC due to leakage of organic photosynthates as discussed above in Sect. 4.1.2.

This model that conceptualizes a “wave” of water moving down the river can be further analyzed by looking at the SC of the water over the diel period. The average diel SC of the river was significantly lower in 2006 ($157 \mu\text{S cm}^{-1} \pm 6.7$; $n = 51$) than that of the seeps

Table 1 Concentrations of DOC from seeps and sediments from the Big Hole River sampled during 2007

Site	<i>T</i> (°C)	pH	SC	DO % sat	DO $\mu\text{mol/L}$	DOC $\mu\text{mol C/L}$	Location
Seep 1a	20.8	6.76	130	75.2	165	1,252	N 45°48.429'; W 113°19.147'
Seep 1b	NA	NA	NA	NA	NA	1,442	N 45°48.429'; W 113°19.147'
Seep 2a	25.2	6.88	129	105.2	206	1,155	N 45°48.433'; W 113°19.164'
Seep 2b	NA	NA	NA	NA	NA	963	N 45°48.433'; W 113°19.164'
Seep 3	19.5	6.23	157	52.0	117	770	N 45°48.433'; W 113°19.174'
Seep 4	23.0	7.12	157	135.5	288	1,252	N 45°48.436'; W 113°19.195'
Seep 5a	20.1	6.91	622	0.9	2.0	1,536	N 45°48.708'; W 113°19.564'
Seep 5b	11.7	7.05	608	43.9	119	1,252	N 45°48.708'; W 113°19.564'
Seep 6	23.4	6.91	167	104.7	214	964	N 45°48.439'; W 113°19.196'
Seep 7	15.6	6.23	124	123.4	278	2,867	N 45°48.439'; W 113°19.203'
Seep 8	11.4	6.83	582	25.0	68	1,442	N 45°48.712'; W 113° 19.579'
Seep 9	10.1	7.40	617	58.8	165	1,725	N 45°48.707'; W 113°19.567'
Sed 1	NA	NA	NA	NA	NA	674	N 45°48.450'; W 113°18.750'
Sed 2	NA	NA	NA	NA	NA	193	N 45°48.450'; W 113°18.750'

All seeps are between 300 and 800 m upstream from BHR sampling site

T temperature; pH in standard units; *SC* specific conductivity ($\mu\text{S/cm}$); *NA* not available

sampled in 2007 (avg. $329 \mu\text{S cm}^{-1}$; range: 124–622). Additionally, the effect of the higher *SC* of the seeps on the river *SC* was investigated with a synoptic survey through the sampling area in 2007. This survey showed consistently higher conductivity water near the stream banks (avg. $157 \pm 4.6 \mu\text{S cm}^{-1}$, $n = 8$) than in the middle of the channel (avg. $147 \pm 3.9 \mu\text{S cm}^{-1}$, $n = 49$) which shows that additions of water from streamside areas were entering the river. Assuming that the chemistry of the seep/groundwater was similar in the 2 years, the increase in *SC* of the river observed in 2006 (Fig. 6b) during the late afternoon when the flow decreased is consistent with a lower volume of river water (lower *SC*) relative to groundwater (higher *SC*). This was then followed by a decrease in *SC* as the flow increased in the first part of the night ($\sim 21:00$ – $01:00$; Fig. 6b) possibly related to an increase in the volume of river water being advected into the sampling area relative to the groundwater contributions.

In further support of this model, the *DOC* concentration and *pH* in the isolation chamber did not display the same night time increase observed in the river in 2006 (Fig. 10e). This difference in *DOC* and *pH* behavior between the chamber and the river is consistent with the model described above suggesting that a “slug” of water migrated downstream that was higher in *pH*; passing the BHR sampling site between 17:00 and 01:00. If the increase in *DOC* and *pH* was produced by aquatic vegetation in the direct area of the sampling site, it should have been observed at some level in the chamber as well as in the river. Additionally, the *DIC* concentration in the chamber showed a pattern that is more “typical” of productive systems with the *DIC* decreasing during the day, while photosynthesis is the dominant metabolic process, resulting in a net removal of CO_2 ; followed by increasing CO_2 at night as community respiration returns it to the water column (Fig. 10e). This was the same pattern observed for the *DIC* concentration in the CFR (Fig. 4a).

Another possible cause of the large and reproducible abnormal flow cycle observed in 2006 could have been a significant daily change in irrigation withdrawals upstream from

the sampling site. The hydrologist for the Montana Department of Natural Resources and Conservation indicated: (1) that there was no one irrigation structure that could remove that amount of water upstream from our site; (2) that the irrigators generally don't turn their ditches on and off, especially on a regular schedule; and (3) most irrigators were not withdrawing water at that time of year due to low flows (M. Roberts personal communication). Consequently it seems unlikely that there was any anthropogenic cause of the flow pattern observed in 2006.

These explanations for the abnormal flow, pH, and DOC behavior observed in 2006 are currently the focus of a continued investigation to better understand the hydrology and biogeochemistry of the upper Big Hole River.

4.2.3 Isotope Composition of DIC

The $\delta^{13}\text{C}$ -DIC was determined for both the 2006 and 2007 samplings in the BHR (Fig. 12). The pattern is typical of $\delta^{13}\text{C}$ -DIC reported previously (Parker et al. 2005, 2009) and similar to those observed in 2006 on the CFR (Fig. 5). There was no discernible diel pattern in DIC concentration in the BHR both during 2006 and 2007 and at the same time the minimum to maximum isotope composition change was ~ 3.3 and 2.7% in 2006 and 2007, respectively. Additionally, the $\delta^{13}\text{C}$ -DIC in 2006 did not show any influence of the aberrant pH and flow cycle (Fig. 8a, b) which appears to have been associated with the diel change in DOC (Fig. 9a). Diel changes in $\delta^{13}\text{C}$ -DIC are influenced by isotopically light CO_2 produced by community respiration, consumption of CO_2 by photosynthesis, gas exchange with the atmosphere, influx of groundwater and dissolution of carbonate minerals. Groundwater contributions of DIC do not appear to be significant in controlling the diel changes in $\delta^{13}\text{C}$ -DIC in 2006 and 2007 in the BHR at this site since these changes are not correlated with the flow cycles. The daytime increases in $\delta^{13}\text{C}$ -DIC have been attributed to kinetic fractionation associated with the consumption of CO_2 by photosynthesis. Since the average pH in 2006 was ~ 1 unit higher than in 2007 the $p\text{CO}_2$ was significantly lower in 2006 versus 2007 (Fig. 6e, f). In 2006 the $p\text{CO}_2$ was below atmospheric levels during the whole diel period while in 2007 the $p\text{CO}_2$ dipped below atmospheric levels during a brief period in the afternoon. During this afternoon period in 2007 when the $p\text{CO}_2$ was low, the net flux of CO_2 would have been from the atmosphere to the water which would have raised the $\delta^{13}\text{C}$ -DIC toward an equilibrium value of -1 to $+3\%$. However, the maximum afternoon $\delta^{13}\text{C}$ -DIC in 2006 and 2007 was -11.5% and -10.5% , respectively, indicating that a balance of metabolic processes was most significant in determining the isotopic composition of inorganic carbon. At night the $\delta^{13}\text{C}$ -DIC both in 2006 and in 2007 decreased during the period when respiration was the only metabolic process operating. In 2006 the $p\text{CO}_2$ remained below atmospheric levels during the whole diel period (Fig. 6c) while in 2007 $p\text{CO}_2$ increased well above atmospheric equilibrium over night (Fig. 6f). Gas exchange in 2006 at night should have resulted in a net influx of atmospheric CO_2 which should have caused an increase in $\delta^{13}\text{C}$ -DIC but since the $\delta^{13}\text{C}$ -DIC continued to decrease, community respiration producing light CO_2 must have been the most significant process affecting the isotope values. In 2007 the night time $p\text{CO}_2$ increased well above atmospheric levels which should have resulted in a net efflux of CO_2 from the water to the air. Diffusional fractionation associated with outgassing should have caused the $\delta^{13}\text{C}$ -DIC to increase but it continued to decrease overnight indicating again that community respiration was again the most significant process influencing the $\delta^{13}\text{C}$ -DIC in the absence of photosynthesis. This emphasizes the dynamic nature of the inorganic carbon pool. While the concentration is not changing in a regular manner, the isotopic

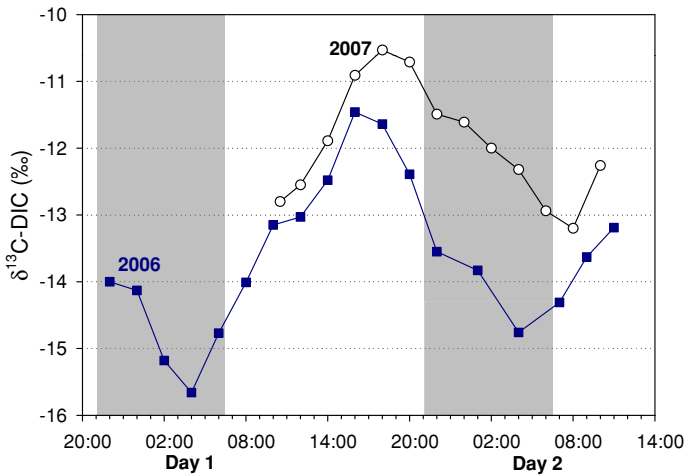


Fig. 12 $\delta^{13}\text{C-DIC}$ at the BHR site during the 2006 (blue squares) and 2007 (open circles) during diel samplings. Error bars represent 3% RSD based on duplicate determinations

composition of the pool was being modified by changing metabolic rates in this highly productive system and this was reflected by the diel pattern of $\delta^{13}\text{C-DIC}$.

5 Conclusions

Diel concentration cycles in DOC were observed in both the CFR and the BHR in 2006 but very different temporal patterns were observed in these two rivers. No change in DOC concentration was observed at the same location in the BHR approximately 1 year later (2007) suggesting that the presence of diel changes in DOC concentration are dependent on conditions that can change from year-to-year such as different flow regimes (Fig. 6b, e). The average flow in the BHR in 2007 was ~ 1.7 times higher than in 2006 and had a different temporal pattern suggesting that the presence of the observed diel changes in DOC may be linked to circumstances present during extreme low, base flow conditions. During these extreme low flow events the volume of water in the river is low in relation to the mass of attached periphyton which could amplify effects such as instream damming caused by aquatic plants and algae. These hydrologic and biogeochemical dynamics are not well understood and are the subjects of further study.

The DOC cycle in the BHR in 2006 reached a maximum concentration at $\sim 01:00$, which is approximately the time that the flow reached its maximum (Fig. 6b, 7). The pH during the 2006 sampling showed an unusual bi-phasic pattern with a maximum around 14:00 and then again at about 02:00. Between these two maximums there was a steep drop in pH with a minimum at $\sim 17:00$; coincident with the steep drop in flow. Normally pH will reach a minimum in the early morning ($\sim 07:00$ in 2007, Fig. 6d). This pH increase during the night could not have been caused *directly* by photosynthesis removing CO_2 from the water. However, since the flow increased at the same time this pattern is consistent with a mass of water moving into this reach that was chemically modified (higher pH, lower conductivity). Two hypotheses that have been suggested above to explain these data are: (1) increased flow from streamside regions and/or benthic sediments at night as evapo-transpiration decreased;

and (2) the possibility that algae and macrophytes in upstream reaches float up and partially dam the river during the day due to photosynthesis and then sink at night, releasing the water. The second hypothesis has been suggested to explain the large diel changes in flow previously observed in this middle reach of the BHR of up to $2.8 \text{ m}^3 \text{ s}^{-1}$ (100% minimum to maximum) in a period of as little as 2 h (USGS gage data, not shown). These large flow cycles observed in the past have had similar timing and trends to those of the 2006 flow reported in this study.

The first explanation is partially supported by preliminary results of samples collected from a number of seeps along the BHR above the sampling site in 2007. The water from these seeps had DOC concentrations ~ 4 -times higher on the average than the river (Fig. 11). At the same time water extracted from shallow benthic sediments had DOC concentrations similar to that of the river. The pH of the water from the seeps was in general lower than that of the river (avg., 6.8 vs. 8.1; Table 1). Consequently, this makes it seem unlikely that the increase in pH in conjunction with the increase in DOC observed in 2006 was due to a large influx of water from bank storage in streamside areas above the sampling site.

The latter explanation predicts a “slug” of water moving downstream that would be of higher pH due to photosynthetic removal of CO_2 during the day and have a higher concentration of DOC due to leakage of soluble organic photosynthates. It is interesting to note that the $\delta^{13}\text{C}$ -DIC during both 2006 and 2007 had the same pattern and in 2006 appeared to show no influence from the observed flow and pH increase during the night (Fig. 11). This suggests that the biologic processing of inorganic carbon is acting at a time scale resulting in a “normal” $\delta^{13}\text{C}$ -DIC pattern.

In the CFR, the DOC showed an inverse temporal pattern to that observed in the BHR in 2006. The DOC in the CFR reached a maximum concentration at $\sim 16:00$ which is consistent with “leakage” of photosynthates during this active photosynthetic period. The $\delta^{13}\text{C}$ -DOC became isotopically depleted during the afternoon most likely due to incorporation of “light” organics produced by photosynthesis and then became enriched during the night as microbial oxidation of DOC consumed lighter carbon containing compounds at a faster rate. It is also possible that the isotopically heavier DOC is in part a different class of compounds that was more recalcitrant and less readily oxidized than the isotopically lighter, recently synthesized compounds. Additionally, a comparison of the rates of change in the concentration of DOC and DIC indicates that the night time increase in DIC can not be solely attributed to microbial oxidation of DOC.

This study emphasizes the importance of the need for a better understanding of the dynamic nature of diel changes in the concentration of both dissolved inorganic and organic species in rivers. It also underscores the fact that different patterns of DOC concentration can occur seasonally in the same aquatic system. Additionally, it demonstrates a need to better quantify the types of organic compounds included in the DOC pool in relation to both the isotopic composition as well as how readily available these forms are for heterotrophic oxidation. These results also highlight the fact that significant short term temporal changes in DOC can occur and monitoring protocols for DOC need to take diel concentration changes into account. Also, predicting diel concentration patterns based on prior behavior may not always be reliable as shown by the BHR results for 2006 and 2007.

The night time pH maximum observed in the BHR during 2006 that coincided with the large concentration increase of DOC suggests that these two occurrences may have been caused by the same process which is also related to the simultaneous increase in flow. Unfortunately, these “anomalous” flow occurrences don’t happen every year as seen in 2007 but do need to be further investigated when they do happen. This may lead to

significant insight into the function and response of riverine systems to drought/low flow and changing land use conditions.

Acknowledgments We thank Heiko Langer, David Nimick and Blaine McClesky for their help with analytical work. Chris Gammons has been an invaluable resource of information on the CFR and BHR and provided productive critical insight for this work. This work was funded by the Montana Water Center through a grant from the USGS 104(b) Water Resources Research Program as well as the Montana Tech Undergraduate Research Program. S. Poulson was funded by NSF, EAR-0738912. This manuscript was greatly improved by the comments of two anonymous reviewers.

References

- Amon RMW, Benner R (1996) Bacterial utilization of different size classes of dissolved organic matter. *Limnol Oecoaogr* 41:41–51
- Barth JAC, Veizer J (1999) Carbon cycle in St. Lawrence aquatic ecosystems at Cornwall (Ontario), Canada: seasonal and spatial variations. *Chem Geol* 159:107–128
- Bianchi TS, Filley T, Dria K, Hatcher PG (2004) Temporal variability in sources of organic carbon in the lower Mississippi River. *Geochim Cosmochim Acta* 68:959–967
- Bianchi TS, Wysocki LA, Stewart M, Filley TR, McKee BA (2007) Temporal variability in terrestrial-derived sources of particulate organic carbon in the lower Mississippi River and its upper tributaries. *Geochim Cosmochim Acta* 71:4425–4437
- Bond BJ, Jones JA, Moore G, Phillips N, Post D, McDonnell JJ (2002) The zone of vegetation influence on baseflow revealed by diel patterns of streamflow and vegetation water use in a headwater basin. *Hydrol Process* 16:1671–1677
- Brick CM, Moore JN (1996) Diel variation of trace metals in the upper Clark Fork River, Montana. *Environ Sci Technol* 30:1953–1960
- Clapp CE, Hayes MHB, Senesi N, Griffith SM (eds) (1998) Humic substances and organic matter in soil and water environments: characterization, transformations, and interactions. International Humic Substances Society, Inc., St. Paul
- Clark ID, Fritz P (1997) Environmental isotopes in hydrogeology. Lewis Pub, New York
- Dalzell BJ, Filley TR, Harbor JM (2007) The role of hydrology in annual organic carbon loads and terrestrial organic matter export from a Midwestern agricultural watershed. *Geochim Cosmochim Acta* 71:1448–1462
- Duff BC (2001) Arsenic treatability study utilizing aeration and iron adsorption-coprecipitation at the Warm Springs Ponds. MS thesis, Montana Tech. Butte, MT USA
- Falkowski PG, Raven JA (1997) Aquatic photosynthesis. Blackwell Sciences, Malden
- Gaiero D, Probst JL, Depetris PJ, Gauthier-Lafaye F, Stille P (2005) $\delta^{13}\text{C}$ tracing of dissolved inorganic carbon sources in Patagonian rivers (Argentina). *Hydrol Process* 19(17):3321–3344
- Gammons CH, Ridenour R, Wenz A (2001) Diurnal and longitudinal variations in water quality along the Big Hole River and tributaries during the drought of August, 2000. Mont Bur Mines Geol 424:39 Open-File Report
- Gammons CH, Nimick DA, Parker SR, Cleasby TE, McClesky RB (2005) Diel behavior of iron and other heavy metals in a mountain stream with acidic to neutral pH: Fisher Creek, MT, USA. *Geochim Cosmochim Acta* 69:2505–2516
- Gammons CH, Grant TM, Nimick DA, Parker SR, DeGrandpre MD (2007) Diel changes in water chemistry in an arsenic-rich stream and treatment-pond system. *Sci Total Env* 384:433–451
- Gandhi H, Wiegner TN, Ostrom PH, Kaplan LA, Ostrom NE (2004) Isotopic (^{13}C) analysis of dissolved organic carbon in stream water using an elemental analyzer coupled to a stable isotope mass spectrometer. *Rapid Commun Mass Spectrom* 18:903–906
- Harris D, Porter LK, Paul EA (1997) Continuous flow isotope ratio mass spectrometry of carbon dioxide trapped as strontium carbonate. *Commun Soil Sci Plant Anal* 28:747–757
- Harrison JA, Matson PA, Fendorf SE (2005) Effects of a diel oxygen cycle on nitrogen transformations and greenhouse gas emissions in a eutrophied subtropical stream. *Aquat Sci* 67(3):308–315
- Hobbie JE (1992) Microbial control of dissolved organic carbon in lakes—research for the future. *Hydrobiologia* 229:169–180
- Hood E, Williams MW, McKnight DM (2005) Sources of dissolved organic matter (DOM) in a rocky mountain stream using chemical fractionation and stable isotopes. *Biogeochemistry* 74(2):231–255

- Hrncir DC, McKnight D (1998) Variation in photoreactivity of iron hydroxides taken from an Acidic Mountain Stream. *Environ Sci Technol* 32:2137–2141
- Jones CA, Nimick DA, McCleskey B (2004) Relative effect of temperature and pH on diel cycling of dissolved trace elements in Prickly Pear Creek, Montana. *Water Air Soil Pollut* 153:95–113
- Kaplan LA, Bott TL (1982) Diel fluctuations of DOC generated by algae in a piedmont stream. *Limnol Oceanogr* 27(6):1091–1100
- Lewis E, Wallace DWR (1998) Program developed for CO₂ system calculations. ORNL/CDIAC-105. Carbon Dioxide Information Analysis Center, Oak Ridge National Laboratory, U.S. Department of Energy, Oak Ridge, Tennessee; <http://cdiac.ornl.gov/oceans/co2rpr.html>
- Macalady DL (ed) (1998) Perspectives in environmental chemistry. Oxford University Press, New York
- Manny BA, Wetzel RG (1973) Diurnal changes in dissolved organic and inorganic carbon and nitrogen in a hardwater stream. *Freshw Biol* 3:31–43
- McKnight DM, Harnish R, Wershaw RL, Baron JS, Schiff S (1997) Chemical characteristics of particulate, colloidal and dissolved organic material in Loch Vale Watershed, Rocky Mountain National Park. *Biogeochemistry* 36:99–124
- Moore JN, Luoma SN (1990) Hazardous wastes from large-scale metal extraction. *Environ Sci Technol* 24:1279–1285
- Nagorski SA, Moore JN, McKinnon TE, Smith DB (2003) Scale-dependent temporal variations in stream water geochemistry. *Environ Sci Technol* 37:859–864
- Nimick DA, Gammons CH, Cleasby TE, Madison JP, Skaar D, Brick CM (2003) Diel cycles in dissolved metal concentrations in streams—occurrence and possible causes. *Water Resour Res* 39:1247. doi: [10.1029/WR001571](https://doi.org/10.1029/WR001571)
- Nimick DA, Cleasby TE, McCleskey RB (2005) Seasonality of diel cycles of dissolved trace metal concentrations in a Rocky Mountain Stream. *Env Geol* 47:603–614
- NOAA (2008) Climate monitoring and diagnostics laboratory, carbon cycle greenhouse gases 2008. <http://www.cmdl.noaa.gov/ccgg/iadv>
- Odum HT (1956) Primary production in flowing waters. *Limnol Oceanogr* 1:102–117
- Olivie-Lanquet G, Gruau G, Dia A, Riou C, Jaffrezic A, Henin O (2001) Release of trace elements in wetlands: role of seasonal variability. *Water Res* 35(4):943–952
- Parker SR, Poulson SR, Gammons CH, DeGrandpre MD (2005) Biogeochemical controls on diel cycling of stable isotopes of dissolved oxygen and dissolved inorganic carbon in the Big Hole River, Montana. *Environ Sci Technol* 39:7134–7140. doi: [10.1021/es0505595](https://doi.org/10.1021/es0505595)
- Parker SR, Gammons CH, Poulson SR, DeGrandpre MD (2007a) Diel changes in pH, dissolved oxygen, nutrients, trace elements, and the isotopic composition of dissolved inorganic carbon in the upper Clark Fork River, Montana, USA. *Appl Geochem* 22:1329–1343. doi: [10.1016/j.apgeochem.2007.02.007](https://doi.org/10.1016/j.apgeochem.2007.02.007)
- Parker SR, Gammons CH, Jones CA, Nimick DA (2007b) Role of hydrous iron oxide formation in attenuation and diel cycling of dissolved trace metals in a stream affected by acid rock drainage. *Water Air Soil Pollut* 181:247–2663. doi: [10.1007/s11270-006-9297-5](https://doi.org/10.1007/s11270-006-9297-5)
- Parker SR, Gammons CH, Poulson SR, Weyer CL, Smith MG, Babcock JN, Oba Y (2009) Diel behavior of stable isotopes (18-O & 13-C) of dissolved oxygen and dissolved inorganic carbon in Montana, USA rivers, and in a mesocosm experiment. *Chemical Geology*. doi: [10.1016/j.chemgeo.2009.06.016](https://doi.org/10.1016/j.chemgeo.2009.06.016)
- Parkhurst DL, Appelo CAJ (1999) User's guide to PHREEQC (Version 2)—a computer program for speciation, batch-reaction, one-dimensional transport, and inverse geochemical calculations: U.S. Geological Survey Water-Resources Investigations Report 99-4259: 310, http://wwwbr.cr.usgs.gov/projects/GWC_coupled/phreeqc/
- Pogue TR, Anderson CW (1994) Processes controlling dissolved oxygen and pH in the Upper Willamette River Basin. US Geol Surv. Water-Resources Investigations Report 95-4205
- Poole GC, O'Daniel SJ, Jones KL, Woessner WW, Bernhardt ES, Helton AM, Stanford JA, Boer BR, Beechie TJ (2008) Hydrological spiraling: the role of multiple interactive flow paths in stream ecosystems. *River Res Applic* 24(7):1018–1031. doi: [10.1002/rra.1099](https://doi.org/10.1002/rra.1099)
- Ridenour R (2002) A seasonal and spatial chemical study of the Big Hole River, Southwest Montana. M.S. Thesis, Montana Tech of The University of Montana, Butte, MT
- Saar RA, Weber JH (1982) Fulvic acid: modifier of metal-ion chemistry. *Environ Sci Technol* 16:510A–517A
- Spencer RGM, Pellerin BA, Bergamaschi BA, Downing BD, Kraus TEC, Smart DR, Dahlgren RA, Hernes PJ (2007) Diurnal variability in riverine dissolved organic matter composition determined by in situ optical measurements in the San Joaquin River (California, USA). *Hydrol Process* 21:3181–3189. doi: [10.1002/hyp.6887](https://doi.org/10.1002/hyp.6887)
- Thurman EM (1985) Organic geochemistry of natural waters. Kluwer Acad. Pub, Boston

- Usdowski E, Hoefs J, Menschel G (1979) Relationship between ^{13}C and ^{18}O fractionation and changes in major element composition in a recent calcite-depositing spring—a model of chemical variations with inorganic CaCO_3 precipitation. *Earth Planet Sci Lett* 42:267–276
- Voelker BM, Morel BM, Sulzberger B (1997) Iron redox cycling in surface waters: effects of humic substances and light. *Environ Sci Technol* 31:1004–1111
- Volk CJ, Volk CB, Kaplan LA (1997) Chemical composition of biodegradable dissolved organic matter in streamwater. *Limnol Oceanogr* 42(1):39–44
- Vymazal J (1994) Algae and element cycling in wetlands. Lewis Publishers, CRC Press, Inc., Boca Raton, p 222
- Watson V (1989) Maximum levels of attached algae in the Clark Fork River. *Proc Mont Acad Sci* 49:27–35
- Wenz AC (2003) Diurnal variations in the water quality of the Big Hole River. M.S. Thesis, Montana Tech of The University of Montana, Butte, MT
- Wetzel RG, Likens GE (1991) *Limnological analysis*, 2nd edn. Springer-Verlag, NY
- Zeigler SE, Brisco SL (2004) Relationships between the isotopic composition of dissolved organic carbon and its bioavailability in contrasting Ozark streams. *Hydrobiologia* 513:153–169
- Zeigler SE, Fogel ML (2003) Seasonal and diel relationships between the isotopic compositions of dissolved and particulate organic matter in freshwater ecosystems. *Biogeochemistry* 64:25–52

Temporal and spatial changes in the concentration and isotopic composition of nutrients in the upper Silver Bow Creek drainage, Montana: Year 2

Basic Information

Title:	Temporal and spatial changes in the concentration and isotopic composition of nutrients in the upper Silver Bow Creek drainage, Montana: Year 2
Project Number:	2007MT145B
Start Date:	3/1/2007
End Date:	12/31/2008
Funding Source:	104B
Congressional District:	at large
Research Category:	Water Quality
Focus Category:	Nitrate Contamination, Hydrogeochemistry, Surface Water
Descriptors:	
Principal Investigators:	Chris Gammons

Publication

1. Plumb, Beverly 2009 Geochemistry of Nutrients in Silver Bow Creek, Butte, Montana "MS Dissertation" Department of Geoscience, Montana Tech of the University of Montana, Butte, MT 85 pgs

Temporal and spatial changes in the concentration and isotopic composition
of nutrients in the upper Silver Bow Creek drainage, Montana: Year 2

Primary Investigator: Dr. Chris Gammons

Department of Geological Engineering

Montana Tech of the University of Montana

2009

Abstract

From the late 1800's to the 1970's, mine waste from mining activities in the Butte, Montana area was discharged into Silver Bow Creek. This created a toxic environment and destroyed most of the aquatic life in the stream. Beginning in 1999 and continuing to the present day, extensive reclamation activities along Silver Bow Creek and the historic mining district have improved environmental conditions in the Butte area, and metal concentrations in upper Silver Bow Creek now meet aquatic life standards. However, previous work has shown the existence of very high nutrient concentrations in Silver Bow Creek. Now that the metal toxicity has been eliminated, symptoms of severe eutrophication are evident, such as uncontrolled growth of aquatic plants and algae.

This research examined the geochemistry of nutrients (nitrate, nitrite, ammonia, phosphate) in upper Silver Bow Creek, with special attention to spatial and seasonal changes in nutrient concentrations and loads. Synoptic samples for nutrient analysis were collected at 10 to 15 monitoring locations every 4-6 weeks, beginning in May of 2006 and ending in August of 2007. Samples were collected on a regular basis at 4 sites on Blacktail Creek, at the mouth of Basin Creek, at 3 sites on upper Silver Bow Creek upstream of Rocker, and at the points-of-discharge from the Montana Pole, Lower Area One, and Butte Silver Bow wastewater treatment plant (WWTP) facilities. The results show that nutrient concentrations and loads in Silver Bow Creek as it leaves the Butte Summit Valley are very high, even when compared to national reference conditions for 'developed basins'. The largest nutrient source is the WWTP, which contributes over 80% of the total N load, mainly in the form of ammonia ($\text{NH}_4^+ + \text{NH}_3$). This ammonia is then gradually oxidized to nitrate, resulting in a substantial increase in the concentration and load of nitrate as Silver Bow Creek makes its way from Butte to Rocker. The oxidation process consumes dissolved oxygen (DO), and creates very low DO concentrations, in some cases to values less than 1 mg/L. Because the oxidation of ammonia to nitrate is faster in warm vs. cold water, the nighttime depletion of DO is most extreme during summer baseflow conditions. Diurnal changes in the rate of ammonia oxidation also result in 24-h changes in the concentrations of ammonia and nitrate in Silver Bow Creek.

Two sets of samples were also collected in this study for analysis of $\delta^{15}\text{N}$ -nitrate, $\delta^{18}\text{O}$ -nitrate and $\delta^{15}\text{N}$ -ammonia. The results show that both forms of N in Silver Bow Creek (ammonia, nitrate) are consistent with having been derived primarily from human and animal waste. There are few if any consistent differences between the isotopic compositions of the various point sources and non-point sources of N in the watershed. Attempts to use isotopes to fingerprint sources of nutrients are further complicated by the fact that in-stream fractionation of N-isotopes occurs during bacterial oxidation of ammonia to nitrate.

1.0 INTRODUCTION

1.1 Research Objectives

Starting in the late 1800's mine waste containing high metal concentrations from the mining, milling and smelting in and around Butte, MT was discharged into Silver Bow Creek. These high metal concentrations created a toxic environment in Silver Bow Creek and virtually annihilated aquatic life (Moore and Luoma, 1990). Beginning in 1999, a massive cleanup effort began to remove toxic tailings from the Silver Bow Creek floodplain, to reconstruct a new stream channel, and to reestablish floodplain and streamside vegetation. Restoration of the upper 10 km of Silver Bow Creek is now complete, and already there are signs that trout are returning to the stream (Frandsen, 2006; Forsell, 2006). However, whereas huge progress has been made to remove metals contamination from Silver Bow Creek, another serious issue has been neglected nutrient overload.

Although nutrients such as nitrate (NO_3^-) and phosphate (PO_4^{3-}) are essential for all forms of life, too many nutrients in a stream environment can have undesirable effects (e.g., Redfield, 1958; Mueller and Helsel, 1996). These include rapid growth of algae and weeds, increase in turbidity, blockage of sunlight, and large seasonal and diurnal (24-h) swings in pH and dissolved oxygen (DO) concentration. Collectively, these symptoms are often referred to as eutrophication. Nutrient levels in the Clark Fork River watershed are elevated, due to both point- and non-point source pollution (Samuels and Hallock, 1994; Watson and Gestring, 1996; Dodds et al., 1997; TSWQC, 2005, 2007). The former

include municipal sewage effluents, industrial discharges, and livestock feedlots. The latter include septic tanks, fertilizers, and domestic animal waste.

The main objective of this research was to collect samples of upper Silver Bow Creek and its main tributaries over a 16 month period to determine spatial and seasonal trends in nutrient concentrations and loads (load = concentration x stream discharge). The city of Butte is located at the headwaters of the Clark Fork watershed, and therefore any nutrients leaving the study area have an impact on downstream waters, including Silver Bow Creek and the upper Clark Fork River. Another objective was to collect preliminary information on the stable isotopic composition of nitrate and dissolved ammonium (NH_4^+) in Silver Bow Creek as well as the known point-sources of high N contamination. These data were then used to test if stable isotopes have potential to be used as tracers of the origins or chemical transformations of N throughout the upper Clark Fork watershed, as has been shown to be the case in previous studies elsewhere (e.g., Coplen, 1993; Wassenaar, 1995; Bohlke and Denver, 1996; Kendall, 1998; Kellman and Hillaire-Marcel, 2003; Deutsch et al., 2005).

1.2 Site Description

Silver Bow Creek begins at the confluence of Blacktail Creek and the Metro Strom Drain (MSD) in Butte, MT (Fig. 1). As of this writing, the population of Butte, MT is around 31,000. However, in the “heyday” of mining in the mid-1900s Butte is reported to have had a population of > 80,000 people. The average low temperature in

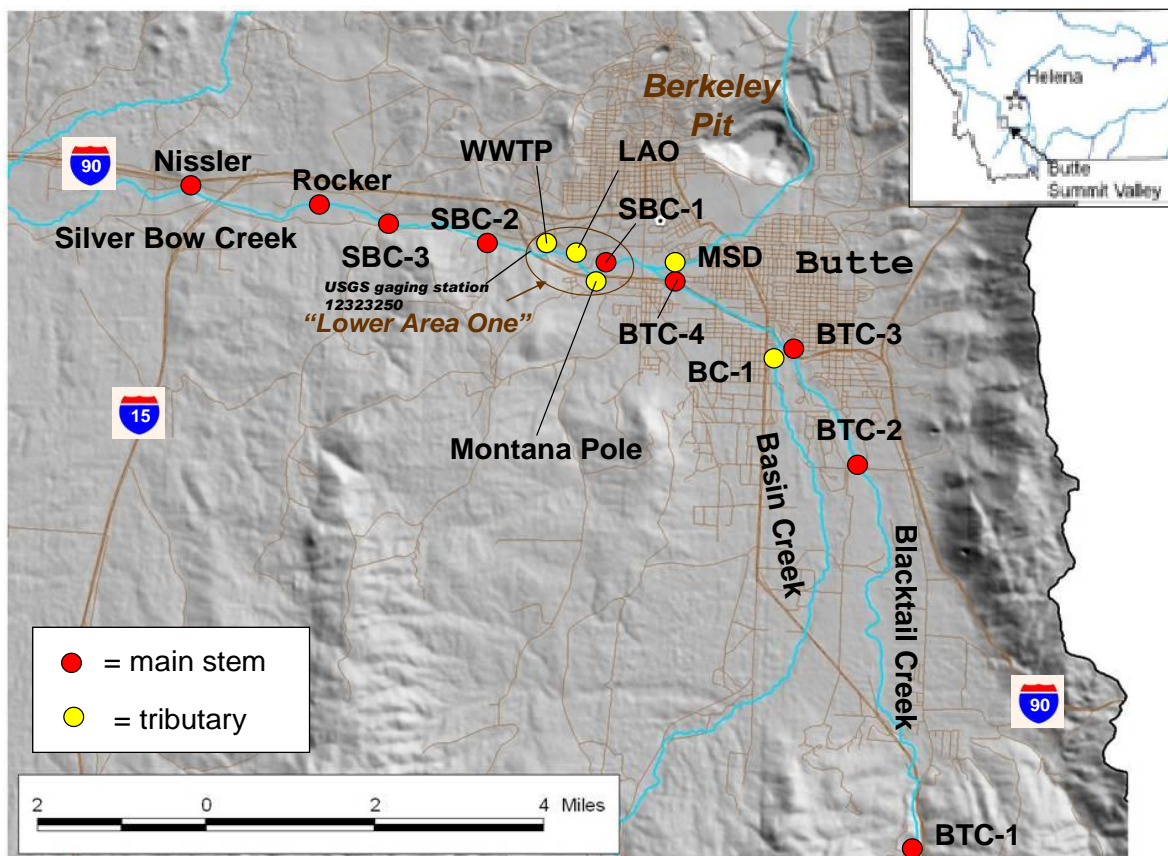


Figure 1. Map of the Butte Summit Valley showing sampling locations.

January is around -15°C and the average high in July is around 26.7°C . The large extremes in climate are explained by Butte's high elevation $\sim 5550\text{ ft}$ (1692 m), high latitude ($\sim 46^{\circ}\text{N}$), and high continentality, being located on the western crest of the Continental Divide separating the Columbia and Mississippi River drainages. The average annual precipitation is 12.8 inches (32.5 cm), although more rain and snow falls on the surrounding mountains, which attain elevations over 8000 ft (2438 m).

The Silver Bow Creek watershed upstream of USGS gaging station 12323250 covers an area of 268 km^2 . Most of the watershed is underlain by the Butte Quartz

Monzonite, a late Cretaceous granitic intrusion that also hosts the mineralization at Butte. Younger volcanic rocks (mainly rhyolite) of the Eocene Lowland Creek group also outcrop in the study area. Summit Valley extends to the south for ~ 10 km from the historic center of Butte, and contains alluvial gravel deposits derived from the surrounding granitic and volcanic highlands. The thickness of the alluvial aquifer is not known, but is believed to be > 100m in places (Botz, 1969). Homes near the southern end of the Summit Valley rely on wells completed in the alluvium or in fractured bedrock for their drinking water supply. Groundwater in the alluvium moves more or less in a direction parallel to the major streams, and discharges to Silver Bow Creek before exiting the valley at a bedrock shelf located near the point labeled “WWTP” in Figure 1.

1.3 Previous Work

There is a large amount of pre-existing information on nutrients in upper Silver Bow Creek, although some of the data are difficult to obtain. Sources of data include: 1) the Montana Bureau of Mines and Geology; 2) Butte Silver Bow; 3) BP-ARCO; and 4) the Montana Dept. of Environmental Quality.

The Montana Bureau of Mines and Geology (MBMG) have published a large amount of analytical data from locations throughout the State of Montana at their Ground Water Information Center website (GWIC, 2008). Although the majority of the samples analyzed in the Butte area are ground water, there are also quite a few analyses of surface waters, including upper Silver Bow Creek and Blacktail Creek. The MBMG laboratory routinely analyzes for nitrate (NO_3^-) and phosphate (PO_4^{3-}) by ion chromatography, but no data are available for ammonia ($\text{NH}_4^+ + \text{NH}_3$). Table 1 is a list of surface water

sampling sites for which historical chemical data are available in GWIC. Additional data exist on GWIC for sampling locations in the Lower Area One region that no longer exist, due to re-construction activities. As an example, Figure 2 shows GWIC data for Silver Bow Creek collected at USGS gaging station 12323250, which is located immediately downstream of the point of discharge for the Butte waste water treatment plant (WWTP). The data are inconsistent, both in terms of the concentrations measured and also with respect to the timing of when the samples were collected. Nonetheless, the results show many sampling dates with highly elevated nutrient concentrations (e.g., greater than 1 mg/L N or P), underscoring the nature of the nutrient problem in the watershed. Data collected by MBMG are fewer for most of the other Silver Bow Creek sampling stations listed in Table 1, and are not shown here.

Table 1. Surface water sampling station in GWIC database.

<i>GWIC ID#</i>	<i>Description</i>	<i>Site name, this research</i>
127593	Blacktail Creek at USGS gage 12323240	BTC-4
127536	Silver Bow Creek below Blacktail Creek	
217884	Silver Bow Creek above MT Pole, SW-06a	SBC-1
164317	Silver Bow Creek below MT Pole, SW-05	
161467	Montana Pole effluent	MT Pole
4851	BSB Sewage Treatment Plant effluent	WWTP
4930	Silver Bow Creek at USGS gage 12323250	
196457	Silver Bow Creek at SS-08, upstream of Rocker	SBC-3
217882	Silver Bow Creek at SS-14	
149881	Silver Bow Creek at Miles Crossing	

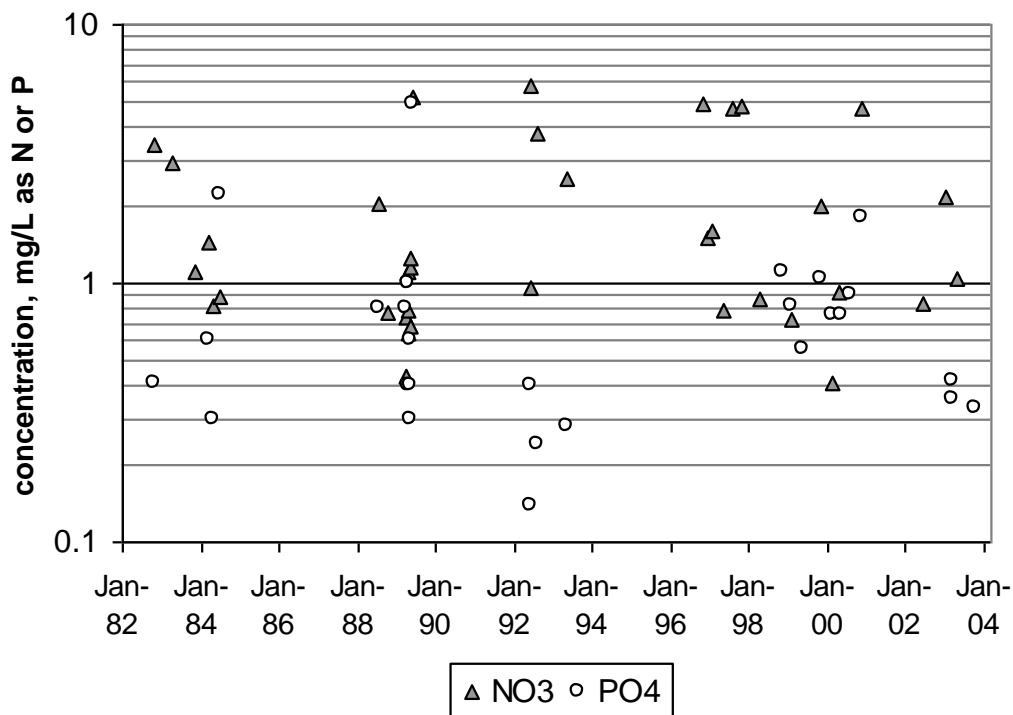


Figure 2. Concentrations of nitrate and phosphate in Silver Bow Creek at USGS gaging station 12323250 between 1982 and 2003. Data from GWIC (2008).

In 2004, the MBMG published a report (Carstarphen et al., 2004) that documented the occurrence of elevated nitrate levels in many shallow groundwater wells in the Butte Summit Valley. This report also included results from two synoptic sampling events along Blacktail Creek and upper Silver Bow Creek, down to the USGS gaging station 12323250. The study concluded that there were significant loadings of nitrate to Blacktail Creek as it makes its way through the Butte Summit Valley, and that the most likely cause of this nutrient contamination was groundwater influx. Carstarphen et al. (2004) also published some stable isotopic results for $\delta^{18}\text{O}$ and $\delta^{15}\text{N}$ of nitrate in Butte groundwater wells and concluded that the main source of nitrate was not synthetic fertilizer, but more likely human and/or animal waste. The more recent report of LaFave

(2008) expanded on the earlier work of Carstarphan et al. (2004), and drew similar conclusions.

During 2003-2004, a study was conducted on concentrations of nutrients in upper Silver Bow Creek by Water & Environmental Technologies, Inc. (WET, 2004). This one-year study gathered data from 8 locations in the watershed, including several stations sampled in the present research. The overall conclusions of the study were that upper Silver Bow Creek is severely impacted by high concentrations of nutrients, including nitrate, ammonia, and phosphate. Numerous point and non-point sources of nutrient contamination were inferred to be present, including the WWTP effluent and other discharging waters in the Lower Area One area, as well as suspected groundwater gains in the stream reach extending from Lower Area One downstream to Rocker. This study was one of the first investigations that documented high concentrations of ammonia in Silver Bow Creek.

Butte Silver Bow (BSB) monitors the effluent water chemistry from the WWTP on a monthly basis. Although this information is not freely available, data collected between 1996 and 2006 were kindly provided by BSB for this research, and are summarized in Figure 3. This graph shows a gradual increase in the concentrations of total N and total P in the WWTP effluent during the past 10 years. It also shows that very little of the nitrogen exiting the plant is present in oxidized form (e.g., as nitrite, NO_2^- , or nitrate, NO_3^-). The majority is ammonia ($\text{NH}_4^+ + \text{NH}_3$), with some additional N in dissolved organic form (data not shown). The scatter in the data underscores the high amount of short-term variability in the water quality discharged from the WWTP.

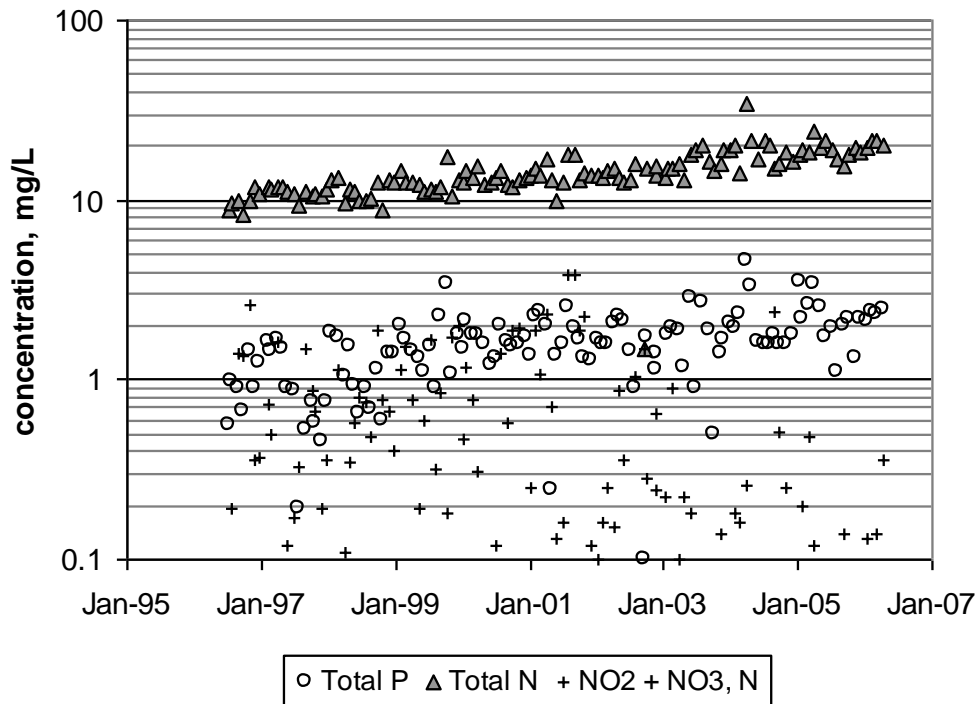


Figure 3. Concentrations of nutrients in the Butte WWTP effluent, 1995-2006.

BP-ARCO constantly monitors concentrations of metals and nutrients in Silver Bow Creek upstream of the Warm Spring Ponds Operable Unit (WSPOU). The WSPOU is a series of ponds and lagoons that treat Silver Bow Creek for heavy metals contamination. The WSPOU database (Pioneer Technical, 2005) is a good source of information on concentrations and loads of nutrients in lower Silver Bow Creek above the WSPOU. Data obtained during the period 1998-2005 are summarized in Figure 4. The data again show very high concentrations of nutrients (both N and P) in Silver Bow Creek, and also show clear seasonal trends. In most years, peak nutrient concentrations are seen during the fall and winter months, with lower concentrations during the spring and summer. Some of this variability is due to seasonal changes in streamflow, but other features in the data may reflect seasonal changes in temperature and/or biological

productivity of the stream. For example, it is interesting to note that the ammonia/(nitrate+nitrite) ratio of water entering the WSPOU is much higher in the winter than in the summer. This topic will be discussed in a later section of this research.

Finally, the Montana Dept. of Environmental Quality (MDEQ) has a large amount of monitoring data on the water quality of upper Silver Bow Creek available upon request, most of which is summarized in the form of annual reports (e.g., MDEQ, 2006).

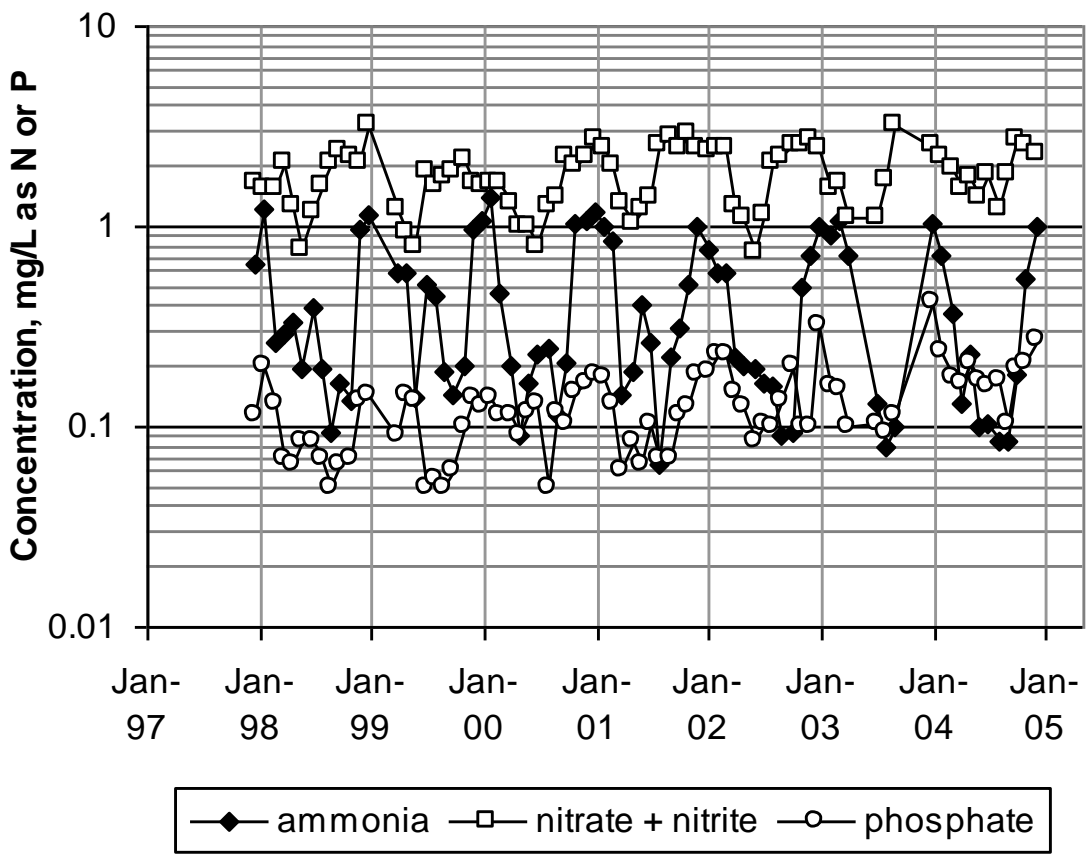


Figure 4. Nutrient concentrations in Silver Bow Creek above WSPOU, 1997-2005. Data from Pioneer Technical (2005).

3.0 METHODS

3.1 Field methods

3.1.1 Synoptic sampling

Twelve synoptic sampling events were conducted on Silver Bow Creek for this research and they occurred in May, June, October, November and December of 2006, and January, March, April, May, June, July, and August of 2007. Field measurements and water samples were taken at a number of sites along Silver Bow Creek and its major tributaries (Figure 1, Table 2

Table 2. Sample sites used in this study.

Site name	Location	km below BTC-1
BTC-1	Blacktail Creek at Thompson Park	0
BTC-2	Blacktail Creek at intersection with 4 Mile Road	8.0
BTC-3	Blacktail Creek at Father Sheehan Park	10.4
BC-1	Mouth of Basin Creek, near BTC-3	10.4
BTC-4	Blacktail Creek at Butte Visitors' Center, just upstream of USGS gage 12323240	13.5
MSD	Mouth of Butte Metro Storm Drain	13.7
SBC-1	Silver Bow Creek upstream of MT Pole	14.8
MT Pole	Point discharge from Montana Pole	14.8
LAO	Point discharge from Lower Area One	15.2
WWTP	Point discharge from Butte wastewater treatment plant	15.8
SBC-2	Silver Bow Creek at first frontage road bridge below I-90 overpass	16.9
SBC-3	Silver Bow Creek at second frontage road bridge, upstream of Rocker, MT	18.8
Nissler	Silver Bow Creek at old bridge near Nissler, just west of Interstate 15 overpass	22.5
Fairmont	Silver Bow Creek at bridge to Fairmont Hot Springs	39.8
Opportunity	Silver Bow Creek at bridge near USGS gage 12323600	45.9

The sites include four locations along Blacktail Creek (BTC), the mouth of Basin Creek (BC), the mouth of the Butte Metro Storm Drain (MSD), the effluent from the Montana Pole plant (MT Pole), the discharge from the Lower Area One treatment facility (LAO), the effluent from the Butte Wastewater Treatment Plant (WWTP), and several locations along Silver Bow Creek (SBC), stretching from Butte to Opportunity. Because the focus of this research was nutrient loading in the Butte Summit Valley, stations along Silver Bow Creek downstream of Rocker, MT were sampled infrequently.

Although many agencies collect water quality samples for Silver Bow Creek at USGS gaging station 12323250, the stream at this location is directly below the confluence of the WWTP effluent and upper Silver Bow Creek, and is poorly mixed. The zone of incomplete mixing extends for several hundred meters below the gaging station. For this reason, SBC-2 was used in this research to monitor nutrient loads in Silver Bow Creek at the point where it exits the Butte Summit Valley.

Figure 5 shows the hydrograph for Silver Bow Creek at USGS gaging station 12323250 during the 2-year study. Dates of sampling related to this research are shown by the green squares. It is worth noting that none of the sampling events in this study captured thunderstorms or major spring runoff events. This was intentional, as it was reasoned that downstream synoptic trends in nutrient concentrations and loads would be easier to see during steady, baseflow conditions. Measuring synoptic trends in nutrient concentrations and loads during storm events was not an original objective of the research, and would require more manpower and time.

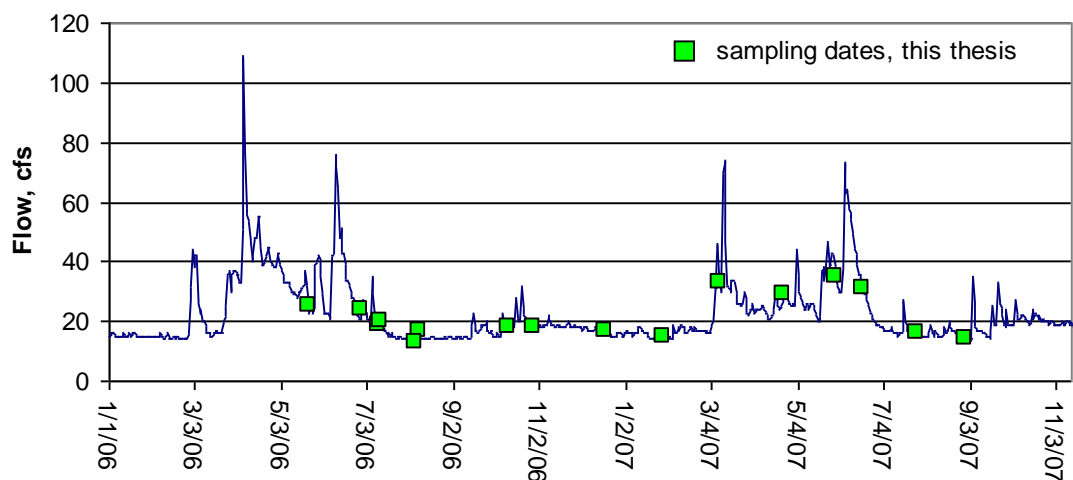


Figure 5. Hydrograph for Silver Bow Creek during the study period, showing dates of major sampling events in this research. Data were obtained from the USGS website for Station 12323250, Silver Bow Creek below Blacktail Creek.

At each site a width- and depth-integrated water sample was collected in a plastic 1-liter Nalgene bottle by holding the bottle at arms length upstream of the sampler and then progressing across the creek and up and down the water column. These samples were then filtered on site to 0.2 μm using a disposable PES syringe filter and transferred to high density polyethylene bottles for further sample analysis in the lab. These bottles were stored in a cooler on ice or in a refrigerator until analysis. A Hydrolab MS-5 datasonde was used to measure pH, dissolved oxygen (DO), water temperature, and specific conductivity (SC). The Hydrolab was calibrated in the laboratory to the manufacturer's instructions on the morning before sampling. Field parameters were recorded along with the date and time in a field book. Other field measurements, such as turbidity and alkalinity, were sometimes measured, following the methods outlined below.

Streamflow was measured directly at BTC-1, BTC-2, and BTC-3 using a Marsh-McBirney current meter, a measuring tape, and a top-setting wading rod. At least 10 velocity measurements were taken across each stream section at a depth of 4/10ths from the bottom of the streambed. Flows at MT Pole and WWTP were taken within 1 hour of a field visit from gages within the treatment plants at each site. Streamflows at BTC-4, SBC-2, and Opportunity were taken from USGS gaging stations 12323240, 12323250, and 12323600. Streamflows at Basin Creek and LAO were not measured directly, but instead were approximated using a specific conductivity (SC) mass balance, according to the following equation:

$$SC1*Q1 + SC2*Q2 = SC3*Q3$$

where Q1, Q2 and Q3 are the streamflows of the main stem upstream, the tributary stream, and the main stem downstream, respectively. By measuring the SC at each location, and by measuring either Q1 or Q3, it was then possible to estimate Q2, the flow of the tributary.

3.1.2 Diurnal sampling

On July 11-12, 2006, 10 samples were collected over a 24-h period at three locations to test for diurnal changes in nutrient concentration. The sites included the WWTP outfall, SBC-1B (Silver Bow Creek immediately upstream of the WWTP outfall), and SBC-3 (Silver Bow Creek upstream of Rocker). Samples were collected manually, filtered in the field, and analyzed for nutrient concentrations as described

above. Field measurements of water temperature (T), pH, SC, and DO were collected during each visit with hand-held meters.

The July diurnal investigation showed extremely low concentrations of dissolved oxygen at SBC-3 during the night. To further investigate this phenomenon, and to map out the extent of the night-time oxygen sag, a DO traverse of Silver Bow Creek was made in the pre-dawn hours of August 6, 2006. Two Montana Tech undergraduate students started sampling at 4:00 AM and quickly moved downstream from SBC-1B to Nissler, recording T-pH-SC-DO with the MS-5 datasonde. The last measurements were taken at 5:45 AM, just as the sky was starting to lighten. Also, 24-h profiles in T-pH-SC-DO were made using a Hydrolab Datasonde 3, a Hydrolab Minisonde 5, and an In-Situ Troll 9000 datasonde at 7 locations between August 14 and 17, 2006. All meters were calibrated on the morning of 8/14/06. The Datasonde 3 was put into the WWTP outfall, the Minisonde 5 was put into Silver Bow Creek at SBC-2, and the Troll was put into Silver Bow Creek immediately above the WWTP outfall (station SBC-1B). The next morning, the Datasonde 3 was moved to Silver Bow Creek at Rocker (behind the Town Pump station) and the Troll was moved to station SBC-3. Then, on the morning of August 16, all three units were moved to Silver Bow Creek at Nissler bridge, and side-by-side 24-h data sets were collected.

3.1.3 Collection of water samples for stable isotope analysis

Water samples for stable isotopic analysis of $\delta^{15}\text{N}$ -nitrate, $\delta^{18}\text{O}$ -nitrate and $\delta^{15}\text{N}$ -ammonia were collected on October 10, 2006, and June 26-28, 2007. At each site, 2 x 1

gallon HDPE containers were filled with filtered water, using a peristaltic pump and 142 mm diameter, 0.1 μm cellulose-ester filter membranes. The containers were first rinsed with 50 mL of filtered site water. One of the sample bottles was used for isotopic analysis of nitrate, while the other was used for ammonia. Duplicate filtered samples were collected in smaller plastic bottles for conventional nutrient analysis (see below), and field parameters were obtained using the MS-5 datasonde. Both bottles were filled to near volume and were frozen (the plastic bottles expanded upon freezing but did not break or leak). The bottles were shipped in a cooler to the stable isotope laboratory at the University of Waterloo, Ontario. Because of a lab error, no ammonia isotope results were obtained for the 2007 sampling.

3.2 Analytical Methods

3.2.1 Alkalinity

Alkalinity was measured by taking a raw, unfiltered sample and titrating it with a HACH digital titrator and 0.16 or 1.6 N sulfuric acid cartridges. A 100 mL volume of water was measured in a volumetric flask to obtain accurate volumes. Then the 100 mL sample was poured into an Erlenmeyer flask with a stirring rod. The Erlenmeyer flask was placed on a battery-operated stir plate. A bromcresol green-methyl red indicator packet was added to the flask and the stirrer was turned on to make sure adequate mixing took place. The solution started out blue-green in color (alkaline) and turned pinkish-red at the pH endpoint of 4.5. The alkalinity (units of $\text{mg/L CaCO}_3, \text{eq}$) was then measured directly from the readout on the titrator.

3.2.2 Turbidity

Turbidity measurements were taken in the field with a HACH 2100P portable turbidimeter. The 1-L composite sample bottle was used, and was shaken to re-suspend any solids before loading the cuvette for the instrument. Two measurements were taken on each sample and the average of the measurements was used. The turbidimeter was periodically calibrated with standards ranging between 0 and 100 NTU (Nephelometric Turbidity Units).

3.2.3 Ammonia

Filtered and refrigerated samples were analyzed for total dissolved ammonia ($\text{NH}_4^+ + \text{NH}_3$) within 12-h of collection using a HACH portable spectrophotometer. The Nessler Method (HACH method 8038) was used, which is accurate for a range of 0.02 to 2.50 mg/L NH_3 as N. The Nessler Method uses the Nessler Reagent, which is a solution of potassium tetraiodomercurate(II) in potassium hydroxide. The Nessler Reagent reacts with ammonia and gives a yellow color. Waste from this procedure contains mercury and was therefore treated as hazardous waste. The colorimeter was zeroed with a solution of deionized (DI) water to which the HACH reagents were added. Calibration was checked during each analytical session by running at least one standard solution containing 0.1 to 1.0 mg/L NH_3 as N. Some of the samples collected in this study had NH_3 concentrations above the linear range of the colorimeter, and therefore were diluted prior to analysis.

3.2.4 Nitrite

Filtered and refrigerated samples were analyzed for dissolved nitrite (NO_2^-) within 12-h of collection using a HACH portable spectrophotometer. The Diazotization Method (HACH Method 8507) was followed, which uses sulfanilic acid and chromotropic acid to react with nitrite to produce a pink color. Method 8507 is good for a range of 0.002 to 0.300 mg/L NO_2^- as N. For samples with high nitrite concentrations, an independent measure of NO_2^- was obtained by ion chromatography (IC) (see below). In most cases, the agreement between the colorimetric and IC results for nitrite was excellent (see Appendix 3), despite the fact that the sample holding times for IC analysis were often > 1 week. Because of its lower detection limits, all results reported in this research were obtained by colorimetry unless specified otherwise.

3.2.5 Phosphate

Filtered and refrigerated samples were analyzed for soluble reactive phosphate (PO_4^{3-}) within 12-h of collection using a HACH portable spectrophotometer. The PhosVer 3 method (HACH Method 8048) was used, in which molybdate is added to the sample water after pH adjustment, and then ascorbic acid reduces this complex and gives the solution a blue color. This method is accurate for concentrations of phosphate in the range of 0.01 to 1.6 mg/L PO_4^{3-} as P. The instrument was calibrated during each session using freshly prepared PO_4^{3-} standards. For samples with high phosphate concentrations, an independent measure of PO_4^{3-} was obtained by ion chromatography (IC) (see below).

In most cases, the agreement between the colorimetric and IC results for phosphate was good (see Appendix 3). Because of its lower detection limits, all results reported in this research were obtained by colorimetry unless specified otherwise.

3.2.6 Nitrate

Early in this project concentrations of dissolved nitrate were determined by colorimetry, following the Cd-reduction method (HACH Method 8171). However, laboratory analysis of split samples by IC showed that the colorimetric method was inaccurate, and therefore was discontinued after June, 2006. After this time, all nitrate analyses were performed by IC (see below).

3.2.7 Anions/Ion Chromatography

Beginning in July of 2006, all samples collected in this study were analyzed for a suite of anions by ion chromatography (IC) at the Murdock Environmental Laboratory, Missoula, MT. Filtered samples for IC analysis were collected in 60 cc HDPE bottles and stored on ice or in the refrigerator prior to shipment to the Murdock lab. Samples shipped to Missoula were transported in a small cooler with ice packs, and the samples were analyzed within 2 weeks of collection. No preservative was added to the bottles. The Murdock lab followed standard EPA procedures, and provided quantification of dissolved nitrate, nitrite, phosphate, chloride, sulfate, and fluoride. As pointed out above, most of the data reported in this research for nitrite and phosphate were obtained colorimetrically. Nonetheless, the IC results provided a convenient check on the

colorimetry results. At least one field duplicate sample was taken during each sampling event, and submitted to the laboratory.

3.2.8 Metals/ICP-AES

One set of synoptic samples collected in March, 2007 was submitted to the Murdock lab for analysis of major and trace metals by inductively-coupled plasma atomic emission spectroscopy (ICP-AES). Samples were filtered to 0.2 μm and collected in 60 mL HDPE bottles to which 0.6 mL of concentrated Trace Metal grade HNO_3 was added. ICP-AES analysis followed the “USN” EPA method, which employs ultra-sonic nebulization.

4.0 RESULTS

4.1 Synoptic Sampling

All field and laboratory data collected in this research during synoptic sampling of upper Silver Bow Creek and tributaries are given in Table A1 of the Appendix. Laboratory results for ICP-AES analyses performed on synoptic samples collected in January 2007 are given in Table A2 of the Appendix. Results for synoptic trends in concentrations and loads of nitrate, ammonia and phosphate are shown in the following series of graphs (Figures 6-16). The data are briefly summarized here for each nutrient.

4.1.1 Ammonia

Ammonia concentrations and loads were typically low before the addition of the WWTP at km 15.8. An exception was March 2007, when significant concentrations of ammonia were detected in lower Blacktail Creek. The source of this ammonia loading could have been melting of valley snow and washing of animal waste stored over the winter period into the streams. However, on all sampling dates, by far the biggest increase in ammonia load occurred from the WWTP. The WWTP effluent averaged about 12 mg/L ammonia as N during the study period, which is consistent with historical data supplied by BSB (Fig. 3). Since the flow of the WWTP discharge is a significant fraction of the total flow in Silver Bow Creek, this resulted in a very sharp increase in ammonia concentrations and loads in the main stream. On several sampling dates, concentrations of total dissolved ammonia ($\text{NH}_4^+ + \text{NH}_3$) at SBC-2 exceeded EPA regulatory standards for aquatic life, which are dependent on both pH and temperature (EPA, 1999). Below SBC-2, the ammonia concentrations in Silver Bow Creek steadily decrease with further distance downstream, as ammonia is oxidized to nitrite and nitrate. During the cold winter months ammonia concentrations stayed elevated all the way to the Warm Springs treatment ponds, a trend that is also seen in the historical data from the WSPOU (Fig. 4). As discussed below, this is probably mostly due to the slower rates of ammonia oxidation in cold vs. warm water.

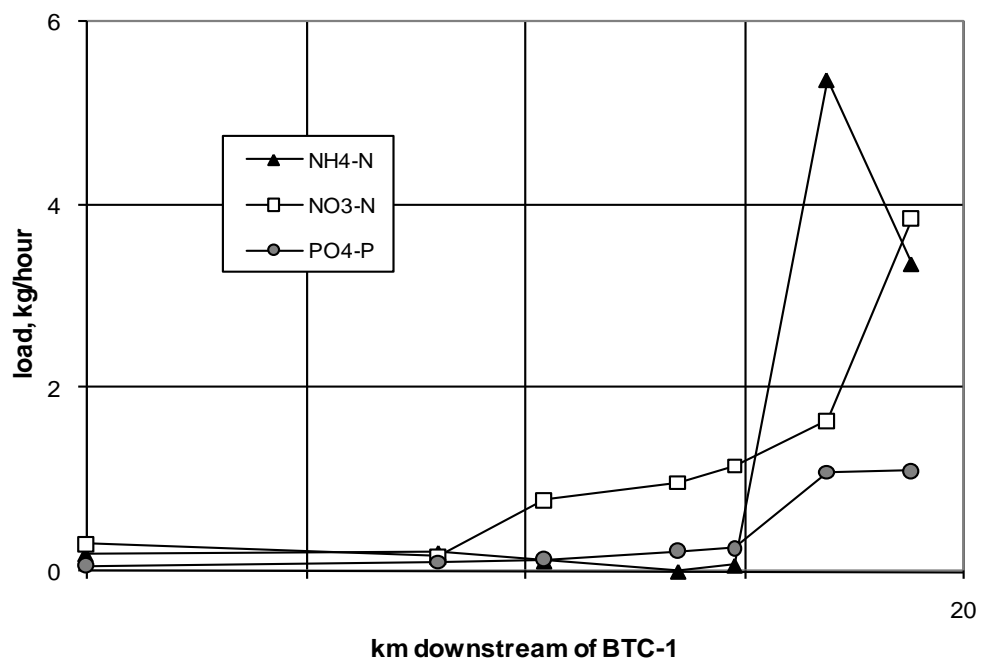
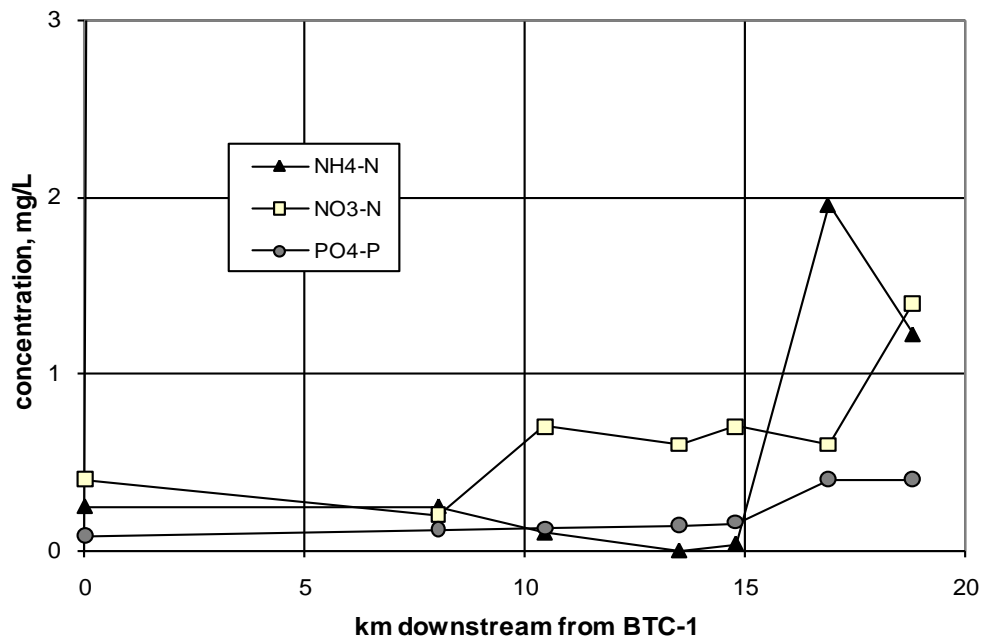


Figure 6. Synoptic samples of May 22, 2006

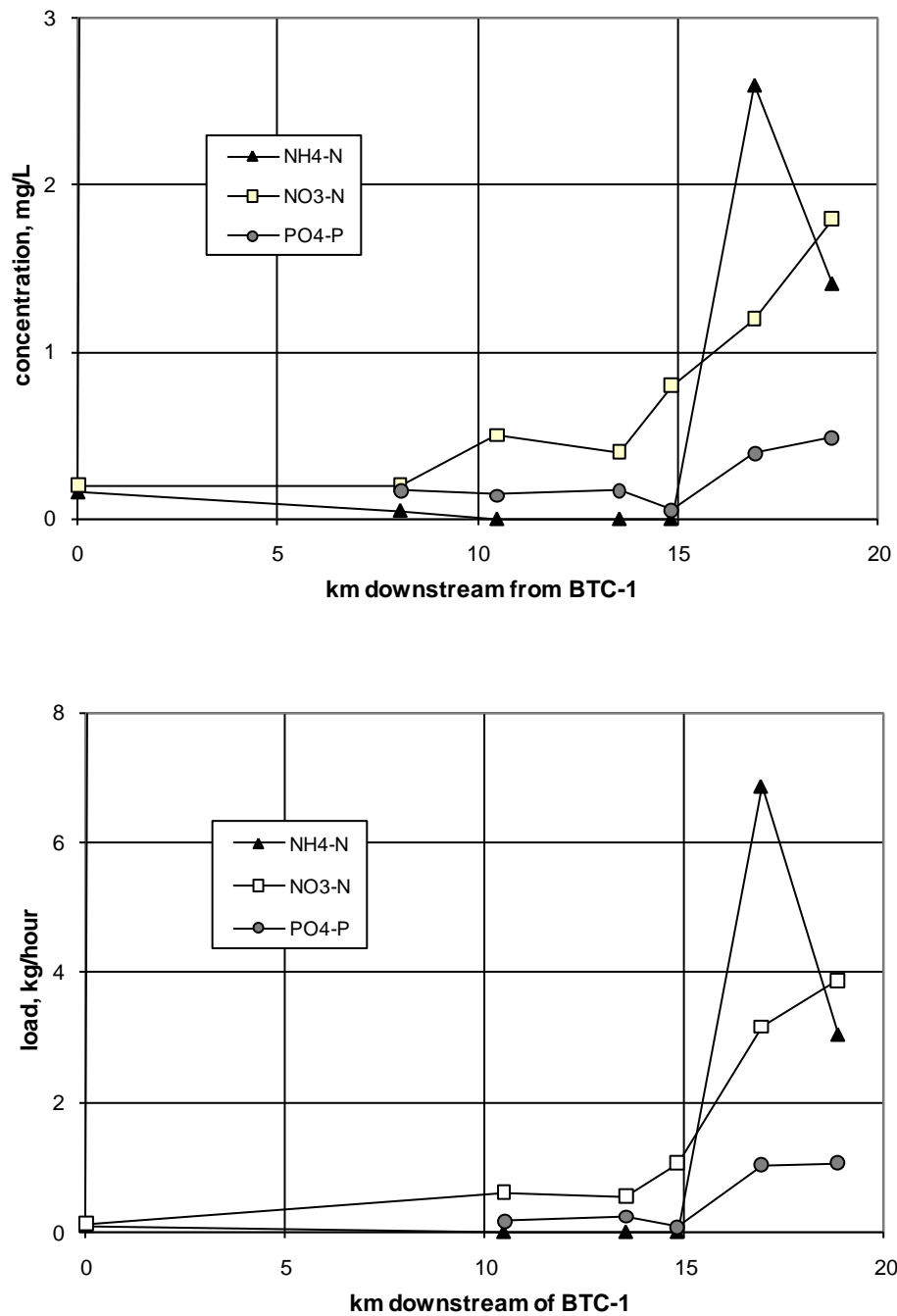


Figure 7. Synoptic samples of June 29, 2006

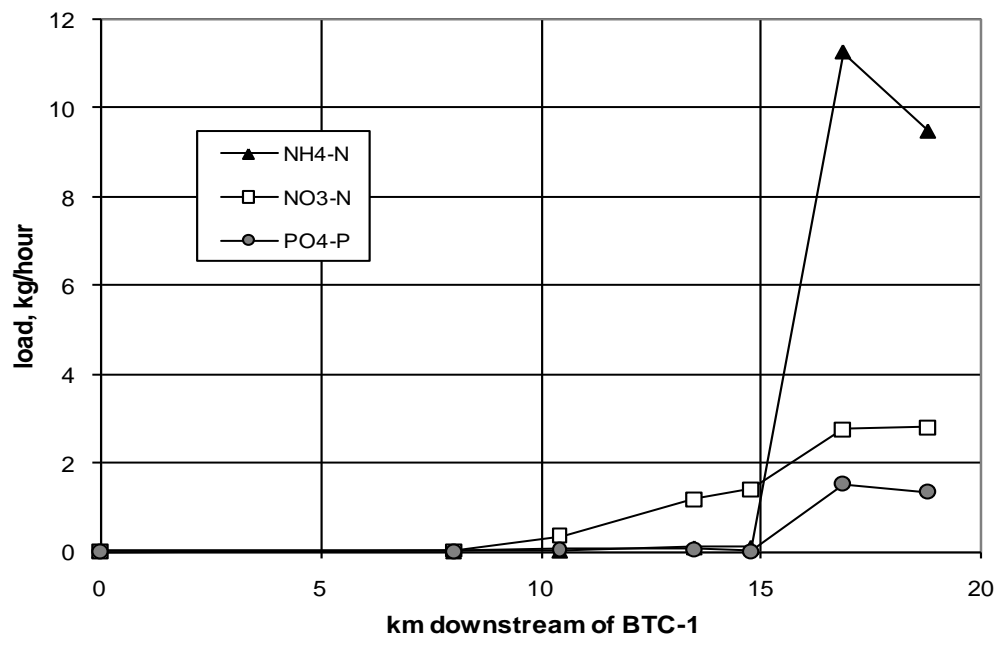
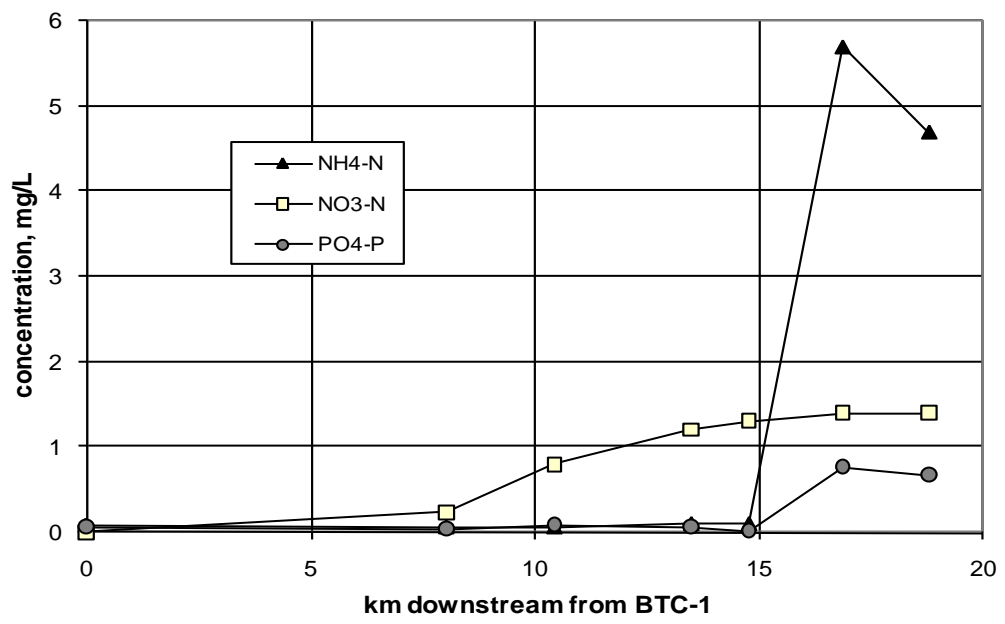


Figure 8. Synoptic samples of October 10, 2006

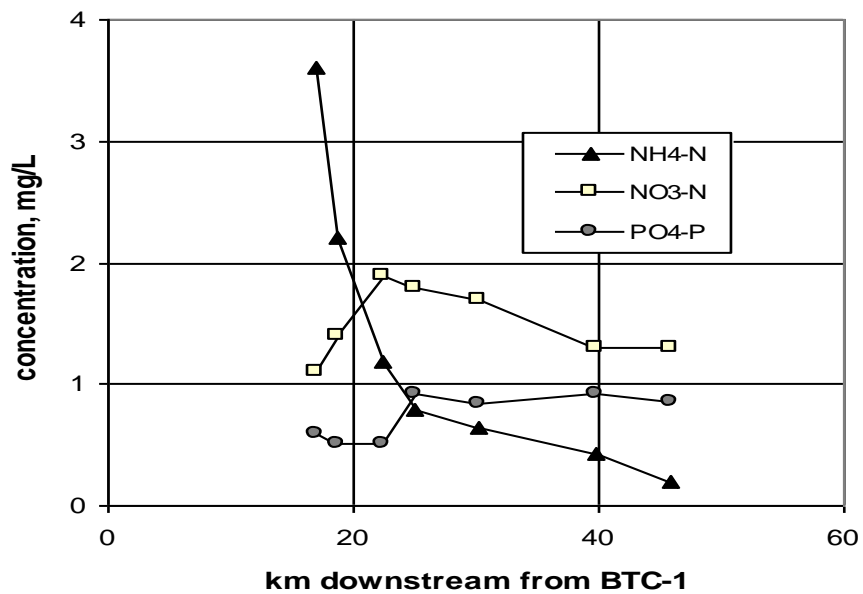


Figure 9. Detailed synoptic samples of Silver Bow Creek below the WWTP outfall, October 28, 2006

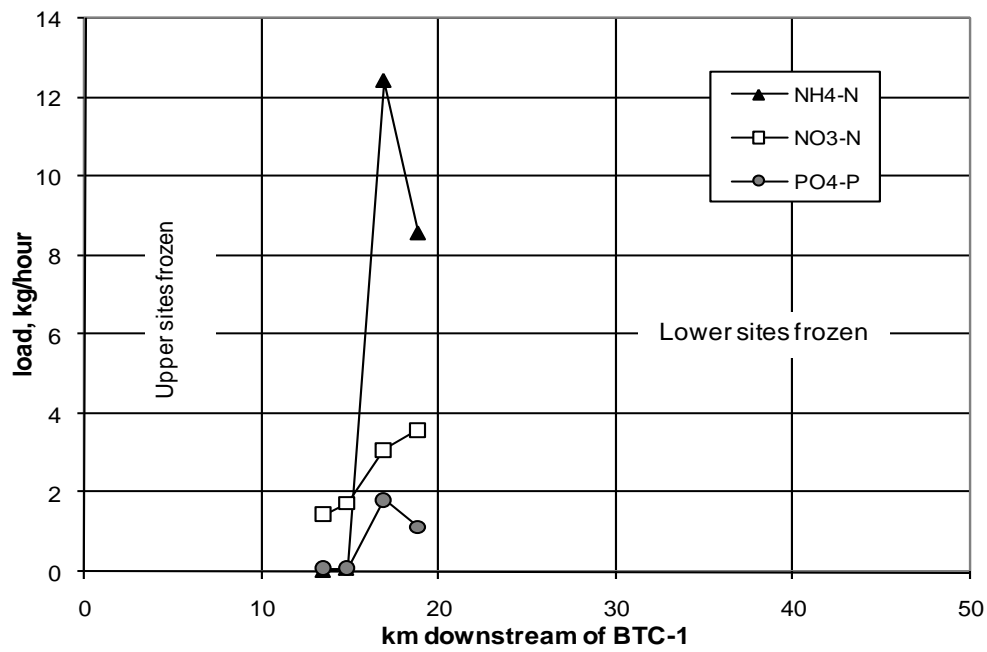
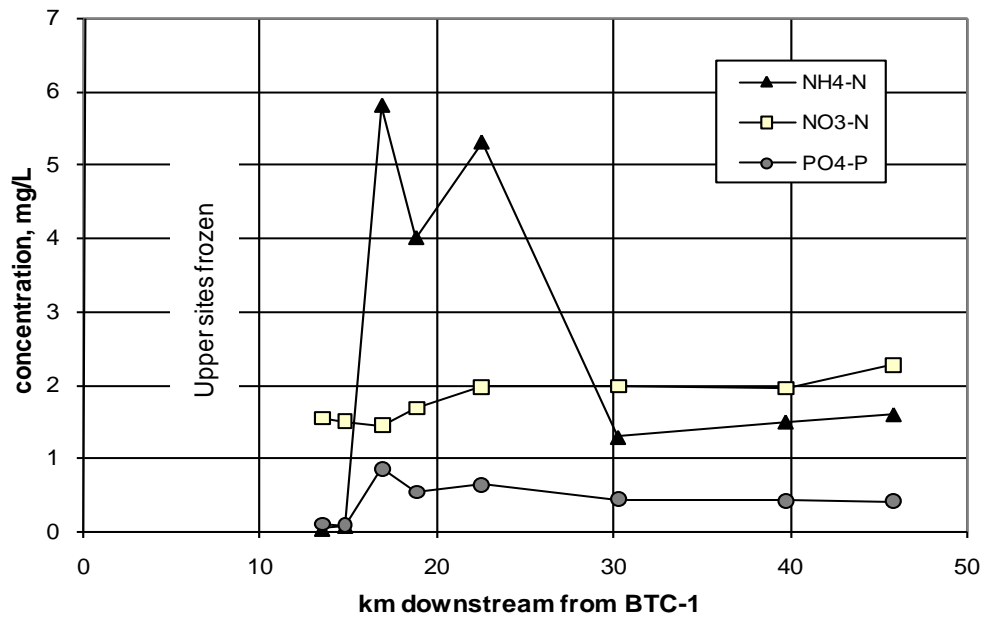


Figure 10. Synoptic samples December 18, 2006

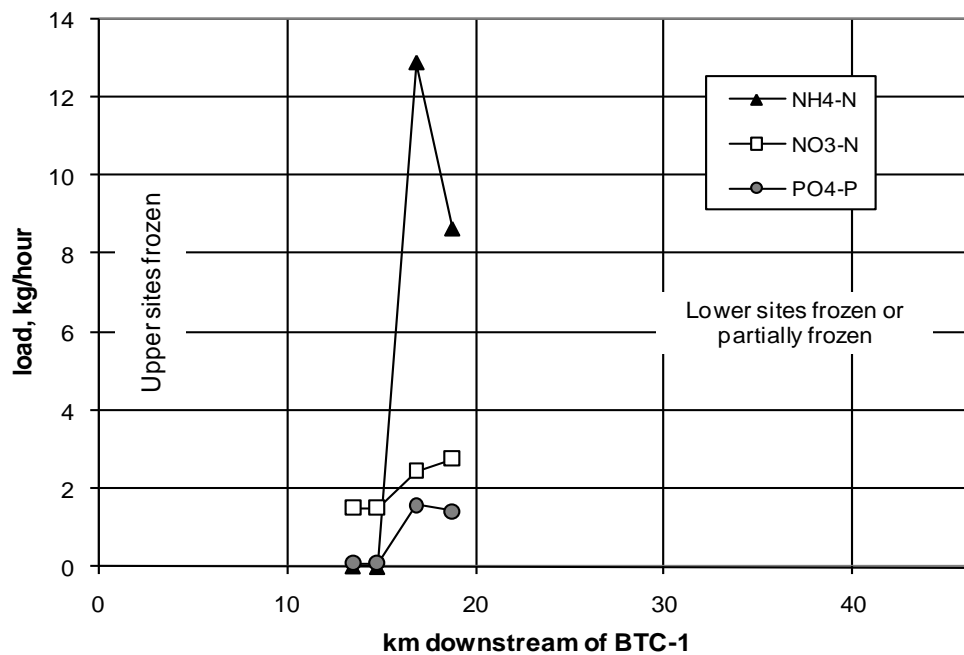
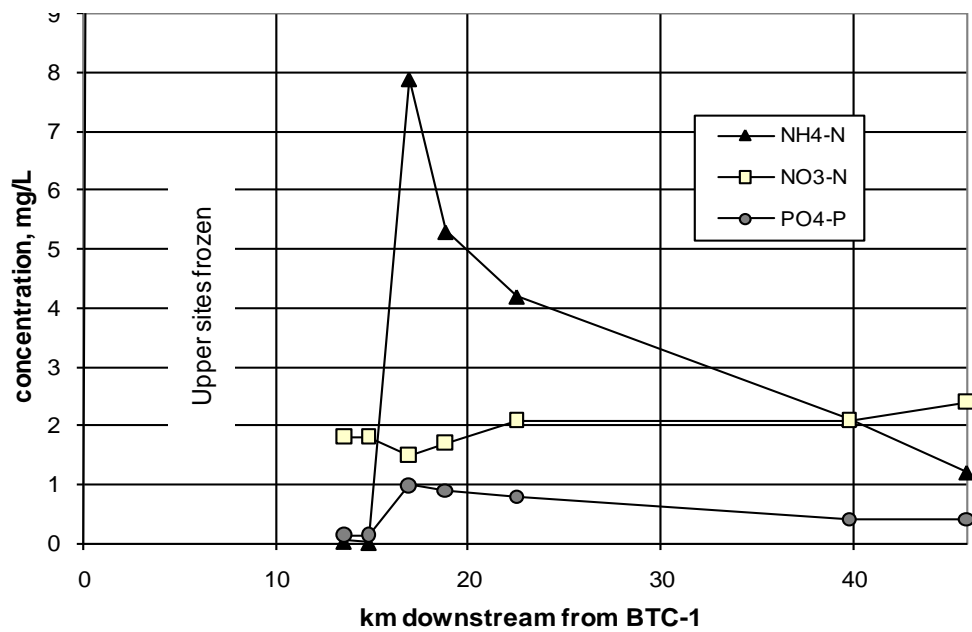


Figure 11. Synoptic samples of January 29, 2007

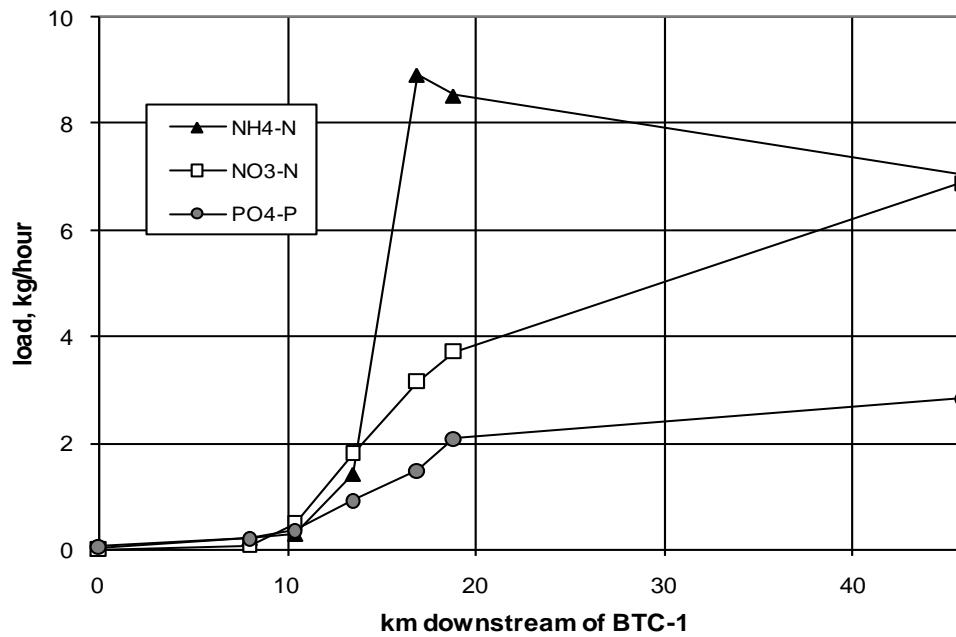
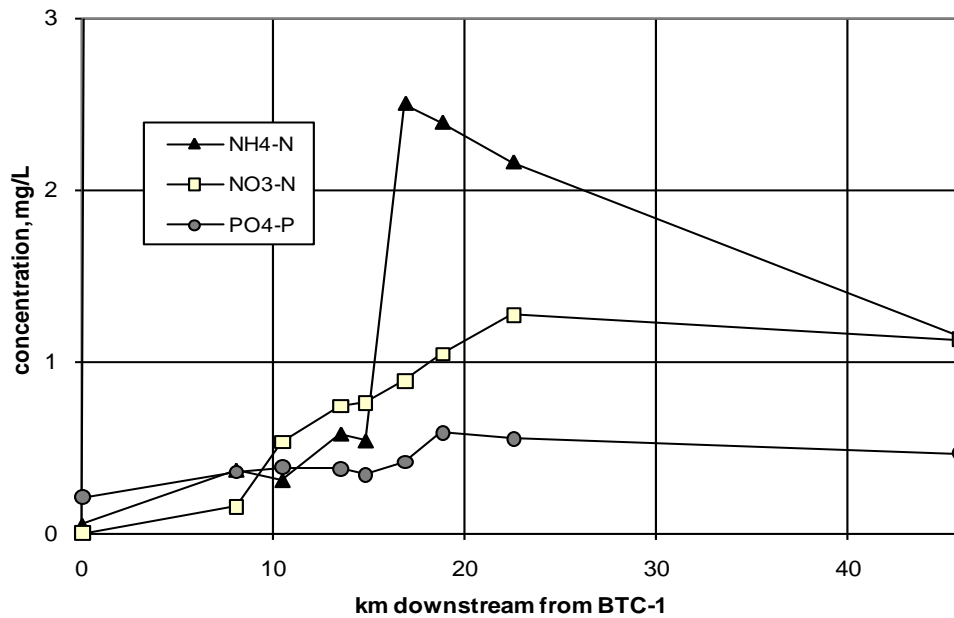


Figure 12. Synoptic samples of March 9, 2007

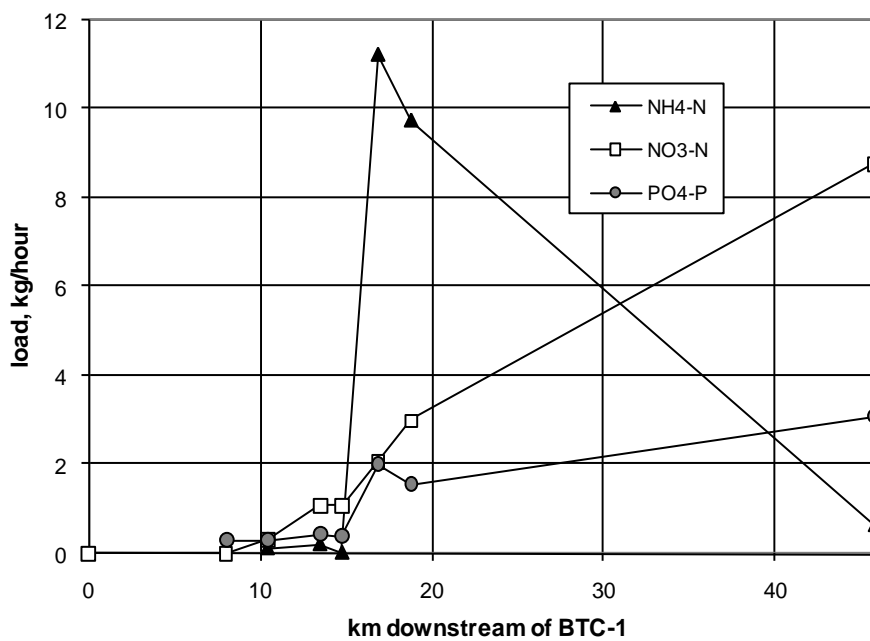
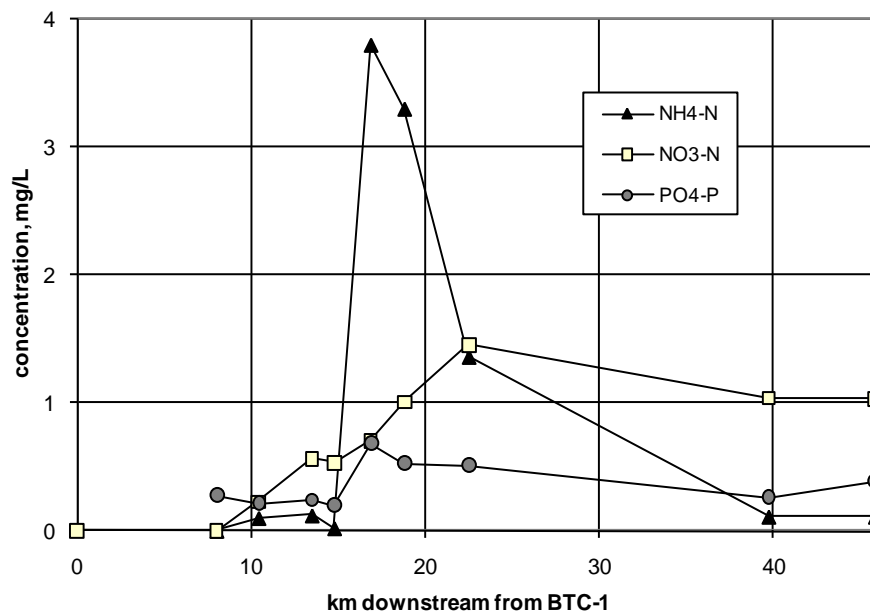


Figure 13. Synoptic samples of April 24, 2007

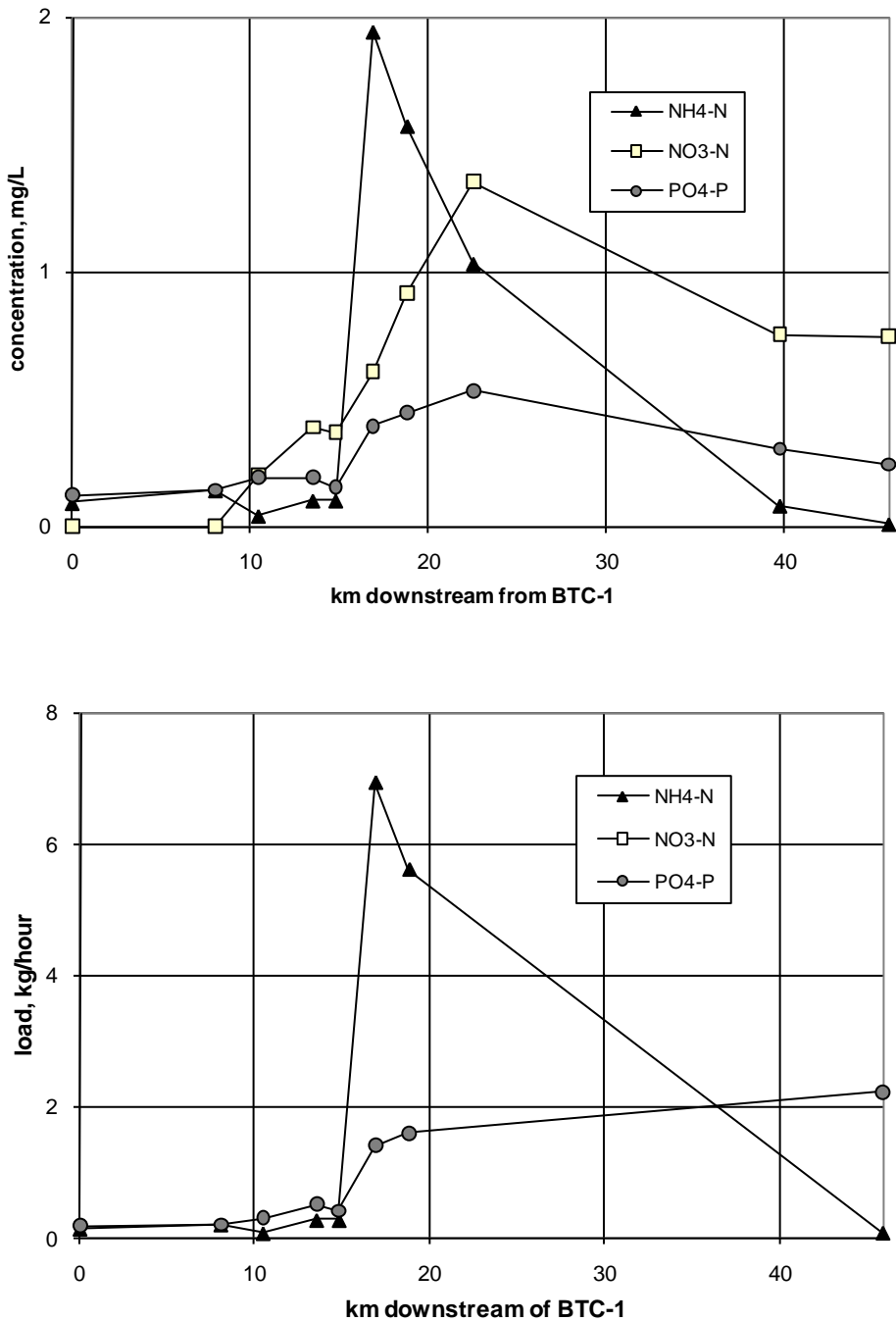


Figure 14. Synoptic samples of May 31, 2007

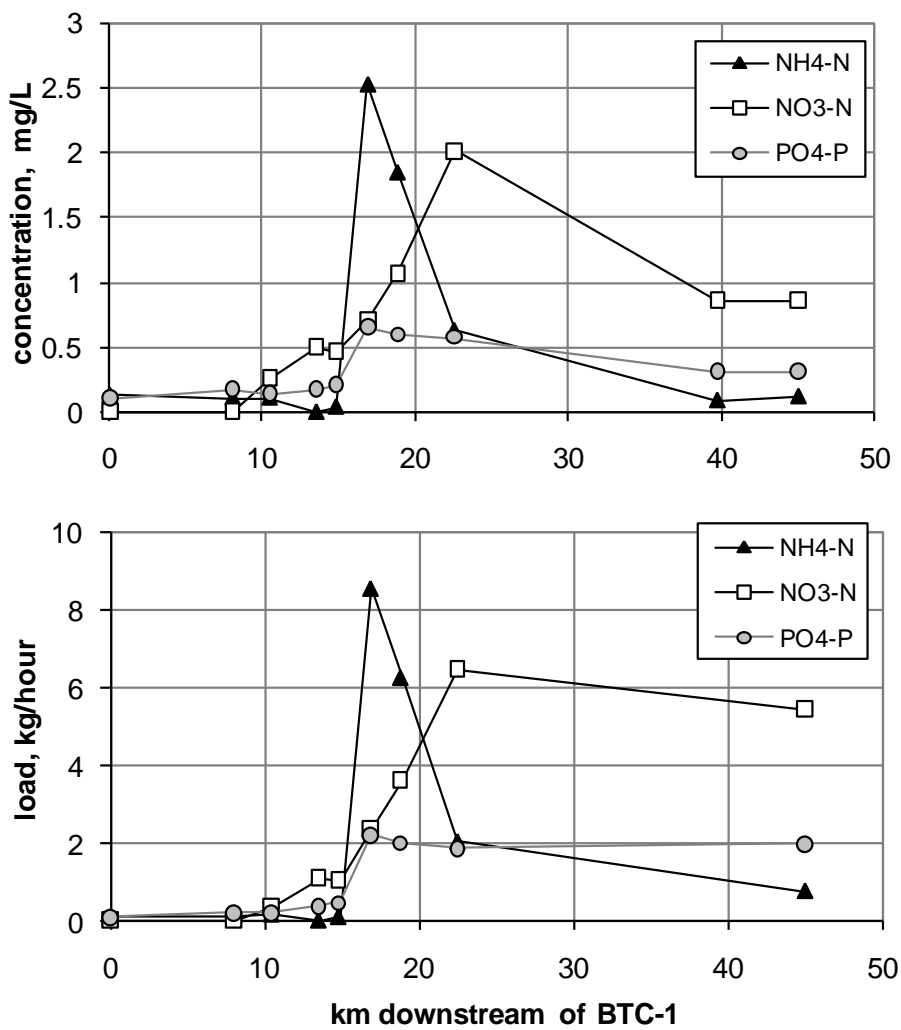


Figure 15. Synoptic samples of June 19, 2007

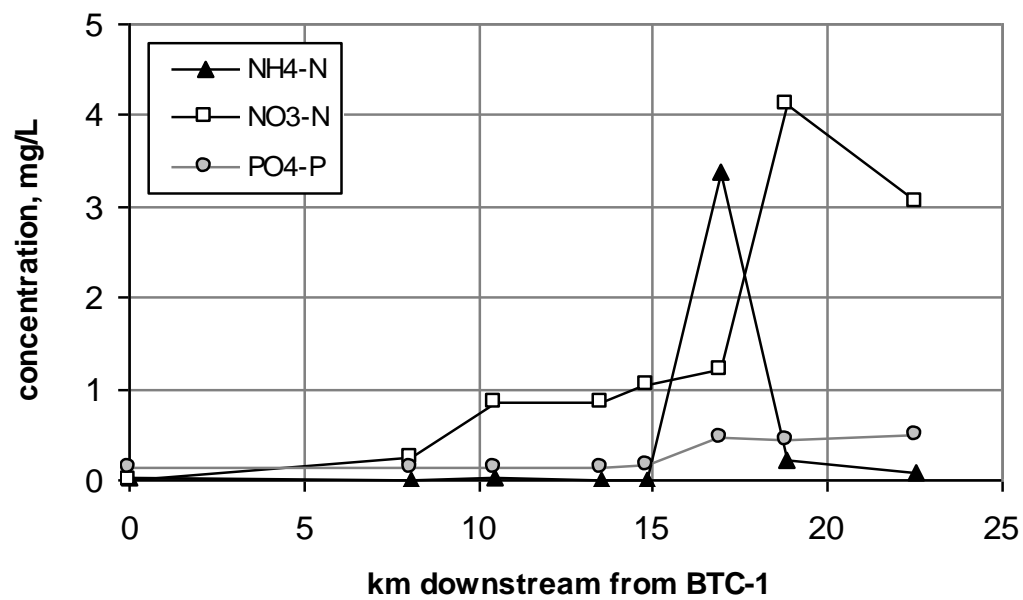


Figure 16. Synoptic samples of July 27, 2007

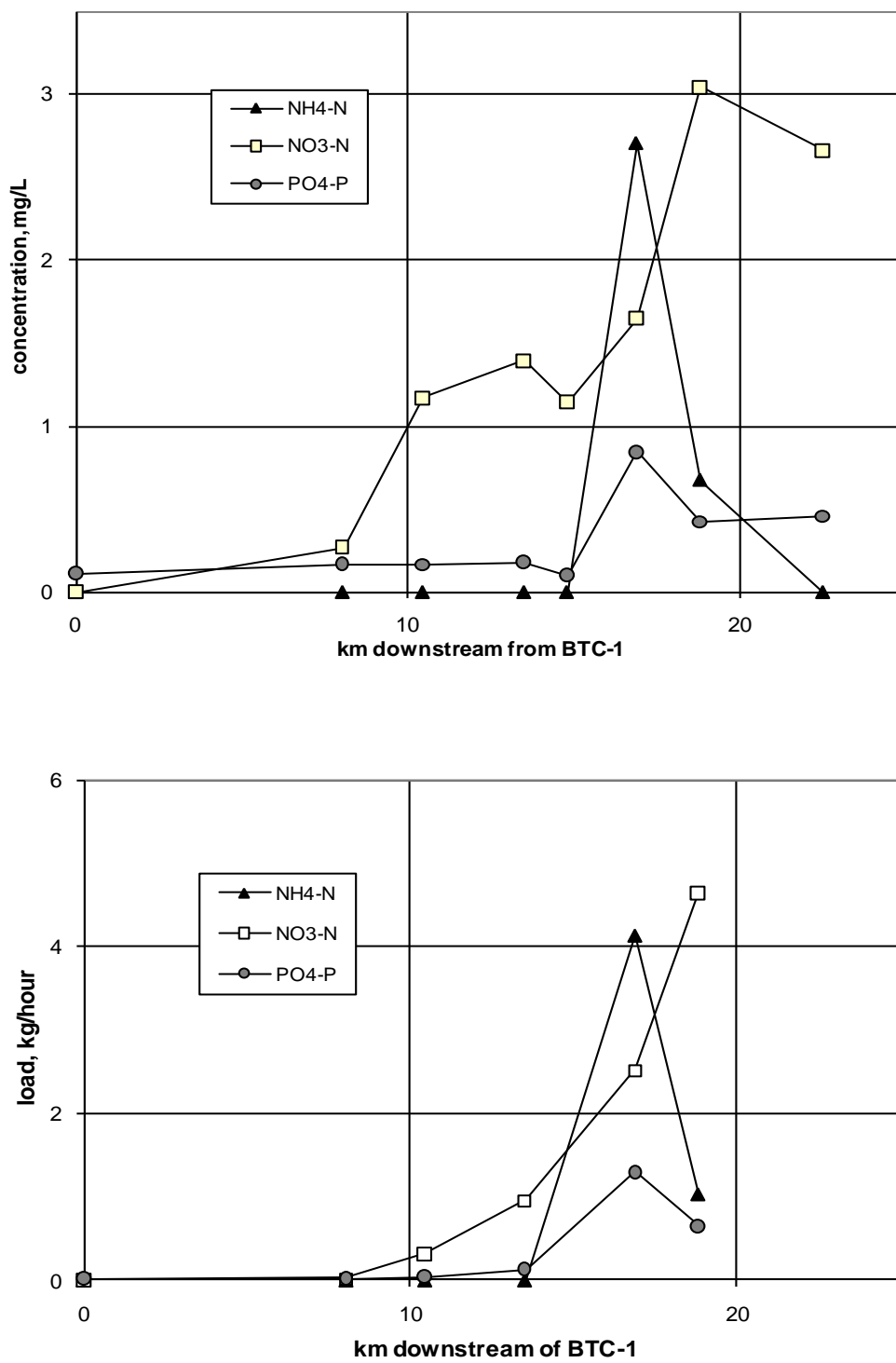


Figure 17. Synoptic samples of August 31, 2007

4.1.2 Nitrate

Nitrate concentrations and loads showed a significant increase between sites BTC-1 and BTC-4. Concentrations of dissolved nitrate exceeded 1 mg/L as N on most sampling dates at BTC-4 and SBC-1. This has been shown in other studies (WET, 2004; Carstarphen et al., 2004; Lafave, 2008) and been attributed to the effects of non-point sources of nutrients as Blacktail Creek makes its way through the Butte Summit Valley. Below station SBC-1, further additions of nitrate come from the Montana Pole and Lower Area One (LAO) treatment facilities. The WWTP discharge adds relatively little nitrate directly to Silver Bow Creek, since most of the nitrogen leaving the WWTP is in reduced form as ammonium ion. However, oxidation of ammonium to nitrate is probably the main reason for the observed increases in nitrate concentrations and loads on most dates in Silver Bow Creek between Lower Area One and SBC-3. Because the rate of this oxidation is slower in the cooler months, nitrate values increase more gradually downstream of SBC-2 in winter as opposed to summer.

The above findings cast doubt on the conclusion of WET (2004) that increases in nitrate concentration below Lower Area One are due to discharging groundwater and/or seepage of nutrients from a nearby meat packing operation. Based on specific conductance transects (C. Gammons, pers. commun.), it is considered unlikely that much groundwater enters Silver Bow Creek below the Interstate 90 bridge at Lower Area One during normal baseflow conditions.

4.1.3 Phosphate

Concentrations and loads of phosphate were typically low in Blacktail Creek and upper Silver Bow Creek (at SBC-1). The confluence of the WWTP effluent caused an abrupt increase in phosphate concentrations and loads. Below the WWTP, concentrations of phosphate-P in Silver Bow Creek were highly elevated on all sampling dates, falling in the range 0.3 to 1.0 mg/L as P.

4.1.4 Oxidation of ammonia to nitrate

Figure 18 shows detailed changes in the speciation of dissolved nitrogen below the WWTP outfall, measured on samples collected August 9, 2006. The WWTP typically discharges 3 to 10 cfs of water containing dissolved ammonium concentrations above 10 mg/L as N. This ammonium is then oxidized by microbes to nitrite, as shown by the following equation:



Microbes that oxidize ammonia to nitrite include species of the genera *Nitrosomonas*, and *Nitrosospira* (Kowalchuk 2001). The nitrite is then further oxidized to nitrate, as shown by the following equation:



Bacteria that oxidize nitrite to nitrate include *Nitrobacter*, and *Nitrospira* (Kowalchuk 2001). The combination of reactions (1) and (2) result in the observed synoptic profiles in nitrate, nitrite, and ammonia concentrations shown in Figure 18. In general, nitrite

concentrations are elevated until all of the ammonia is oxidized, at which point nitrite drops to undetectable levels.

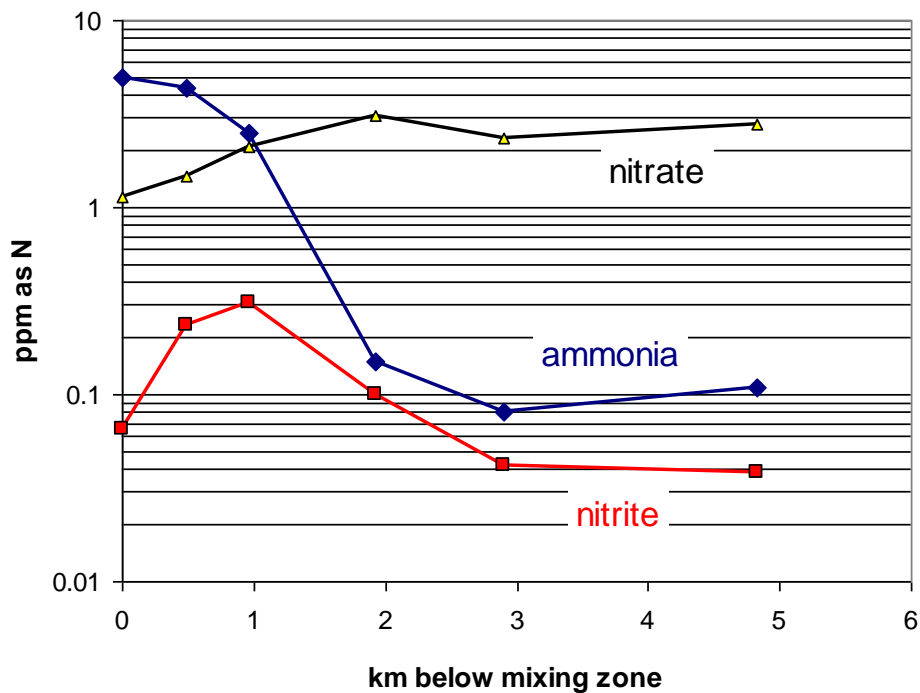


Figure 18. Detailed changes in speciation of nitrogen below the WWTP outfall on August 9, 2006.

4.1.5 Comparison of nutrient loads in Lower Area One

Tables 3 to 6 give a more detailed summary of the percentage contribution of the total load of each nutrient as Silver Bow Creek passes through Lower Area One. Station SBC-1 is located immediately upstream of the MT Pole discharge, and therefore the load at this point is the sum of all non-point sources of nutrients upstream in the watershed. As shown in Table 3, non-point sources account for a little more than half of the total nitrate load exiting the Butte Summit Valley. The Montana Pole discharge is the next largest source at roughly 1/3 of the total nitrate load, whereas the LAO and WWTP contribute smaller percentages. The WWTP is overwhelmingly the dominant source of

Table 3. Comparison of nitrate loads in Lower Area One

Date	Total load kg/hour	% contribution to the total load			
		SBC-1	MT Pole	LAO	WWTP
10/10/06	2.42	59	32	5	4
12/18/06	2.85	61	25	8	7
1/29/07	2.61	57	30	5	8
4/24/07	2.06	53	37	0	10
5/31/07	1.91	51	38	0	11
6/19/07	1.97	52	35	0	13

Table 4. Comparison of ammonia loads in Lower Area One

Date	Total load kg/hour	% contribution to the total load			
		SBC-1	MT Pole	LAO	WWTP
5/22/06	8.15	1	0	0	99
6/29/06	11.2	0	0	0	100
10/10/06	8.86	1	0	0	99
12/18/06	12.8	1	0	0	99
1/29/07	9.79	0	0	0	100
4/24/07	10.2	0	0	0	100
5/31/07	8.04	3	0	0	97
6/19/07	11.2	1	0	0	99

Table 5. Comparison of total N loads (ammonia + nitrate loads)

Date	Total load kg/hour	% contribution to the total load			
		SBC-1	MT Pole	LAO	WWTP
5/22/06	10.7	11	2	3	84
6/29/06	14.1	8	4	2	87
10/10/06	11.3	14	7	1	78
12/18/06	15.6	12	5	1	82
1/29/07	12.4	12	6	1	81
4/24/07	12.2	9	6	0	84
5/31/07	10.0	12	7	0	80
6/19/07	13.1	9	5	0	86

Table 6. Comparison of phosphate loads in Lower Area One

Date	Total load kg/hour	% contribution to the total load			
		SBC-1	MT Pole	LAO	WWTP
5/22/06	1.31	19	1	1	79
6/29/06	1.40	5	1	1	93
10/10/06	1.55	1	1	0	97
12/18/06	1.82	4	1	0	95
1/29/07	1.81	6	1	0	93
4/24/07	3.23	13	1	1	85
5/31/07	1.19	34	2	1	63
6/19/07	3.58	13	1	8	79

ammonia and phosphate loading (Tables 4, 6). When nitrate and ammonia are combined (total dissolved N), the WWTP contributed > 78% of the total N load on all sampling dates (Table 5). As mentioned above, most of the ammonia that is released by the WWTP eventually oxidizes to nitrate. Thus, the total N load is a more useful metric than nitrate alone to evaluate the impacts of the WWTP on nutrients in Silver Bow Creek.

4.1.6 Comparison of Nutrient Loads in Silver Bow Creek to Reference Conditions

To better compare the nutrient loads in Silver Bow Creek to other watersheds nationwide, the average annual load exiting the Butte Summit Valley was divided by the drainage area of the basin (103 sq. miles) and then converted to metric units to calculate the “nutrient yield” ($\text{kg}/\text{km}^2/\text{year}$). This was compared to the average runoff (cm/year), which was taken as the average discharge at USGS gaging station 12323250 over the entire 2006 and 2007 calendar years divided by the area of the watershed. Figure 19 shows how Silver Bow Creek compares with reference conditions established for U.S. rivers in “developed” and “undeveloped” basins (Smith et al. 2003). The results show that the N and P yields for Silver Bow Creek plot well above the national trends for “developed” basins. However, if the effects of the WWTP were removed Butte Summit Valley would have nutrient loads below the national average yields of other developed basins. This is an important result, and underscores the need to improve nutrient removal in the Butte Silver Bow wastewater treatment plant to restore Silver Bow Creek to a more natural condition. Of course, any new upgrades to the treatment plant are unlikely to remove 100% of the nutrient load. However, even if nutrient removal were 80-90%, this would go a long ways to improving the eutrophication problem in Silver Bow Creek

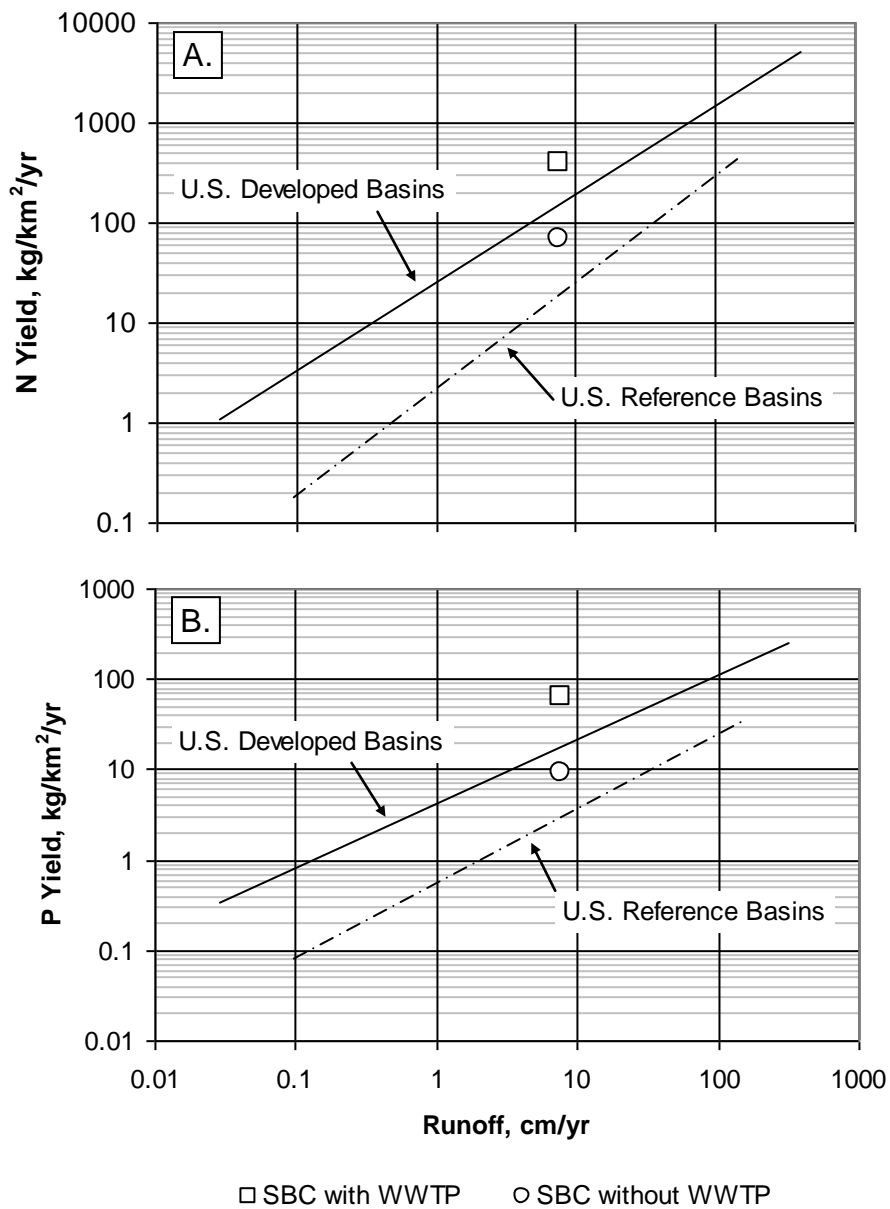


Figure 19. Comparison of estimated annual N and P yield from Silver Bow Creek with national average for developed and reference basins (from Smith et al., 2003)

4.2 Diurnal sampling

4.2.1 Diurnal nutrient sampling of July, 2006

On July 11-12, 2006, a set of diurnal samples was taken at three locations (SBC-1B, WWTP, and SBC-3) to see how the nutrient levels changed throughout the day.

Although the data are scattered, there appears to have been an increase in nitrate concentrations during the night at SBC-1B, which is above the WWTP outfall. Previous studies have shown that dissolved nitrate concentrations have a tendency to increase at night in streams in the upper Clark Fork River basin (Brick and Moore, 1996; Gammons et al., 2007; Parker et al., 2007), and elsewhere (Scholefield et al., 2005) although the reasons why are not known with confidence. Neither ammonia nor nitrite followed a clear diurnal pattern at SBC-1B, although there is a possible trend to higher concentrations during the day (Figure 20). The single very high nitrite value at 13:00 may have been an error.

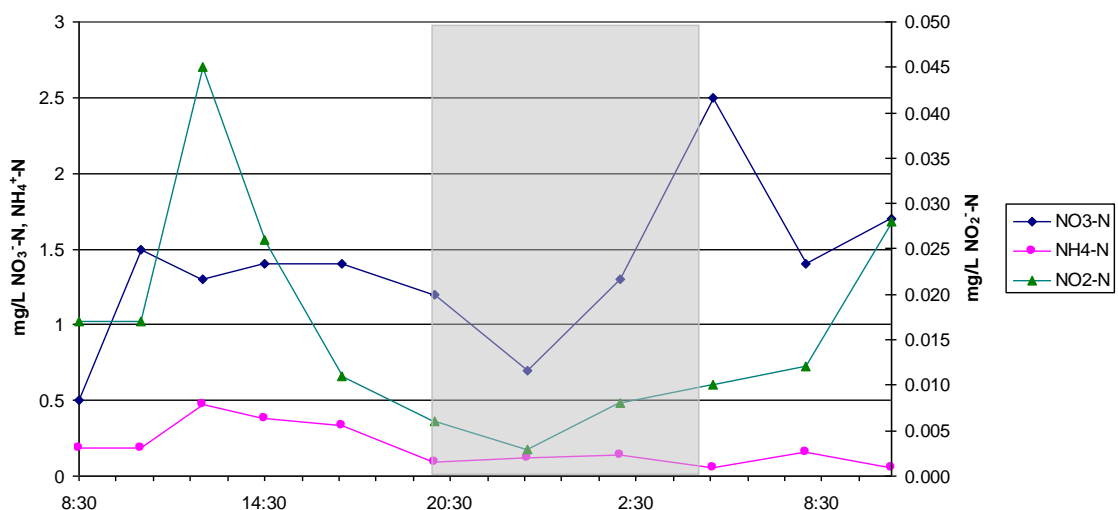


Figure 20. Diurnal changes in nutrients at SBC-1B

The concentrations of nutrients in the WWTP outfall showed quite a bit of variation over the 24-h period (Fig. 21), but the changes didn't follow a clear diurnal pattern. Concentrations of ammonia-N were much higher than nitrate-N at all times of the day, although there is a possible trend of higher ammonia/nitrate ratios at night and lower ratios during the day. This could reflect a more rapid rate of oxidation of ammonia to nitrate during the warm daylight hours. Concentrations of nitrite also increased at night, relative to daytime.

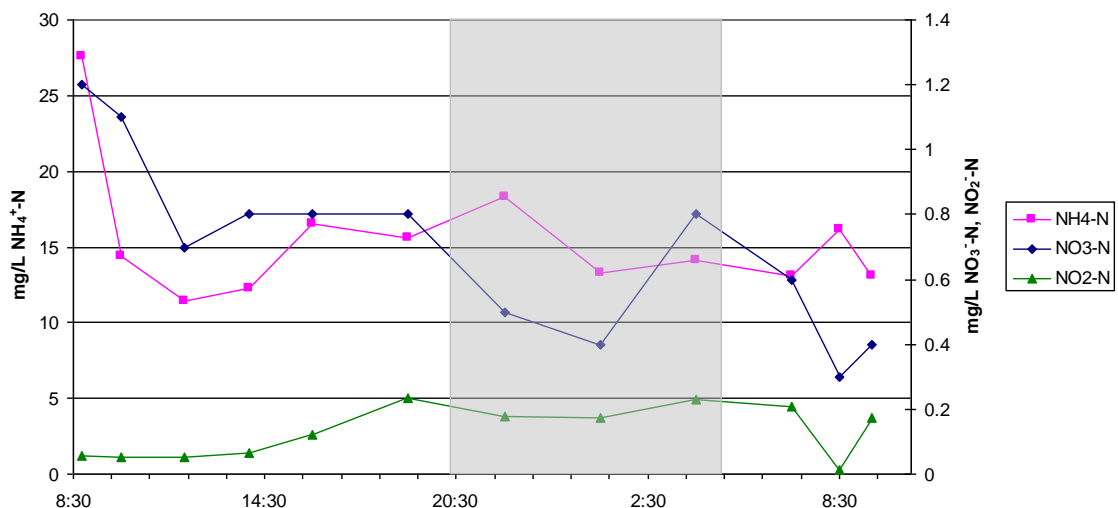


Figure 21. Diurnal changes in nutrients at the WWTP outfall.

More systematic diurnal changes in nutrient concentration were noted at SBC-3 compared to the other stations (Fig. 22). Concentrations of ammonia and nitrite increased at night, and decreased during the day, whereas nitrate followed the reverse pattern. These diel patterns are due to the biological activity in the water, which is dependent on both sunlight and temperature. During the day when the water temperatures are higher and dissolved oxygen is being produced by photosynthesis, the ammonia oxidizes faster. This causes the ammonia concentrations to be lower during the day and higher at night. Since ammonia oxidizes to nitrate, the concentrations of nitrate vary in an inverse fashion to those of ammonia. Overall the diurnal trends in nitrite appear to follow ammonia closer than nitrate, although the correlation isn't perfect.

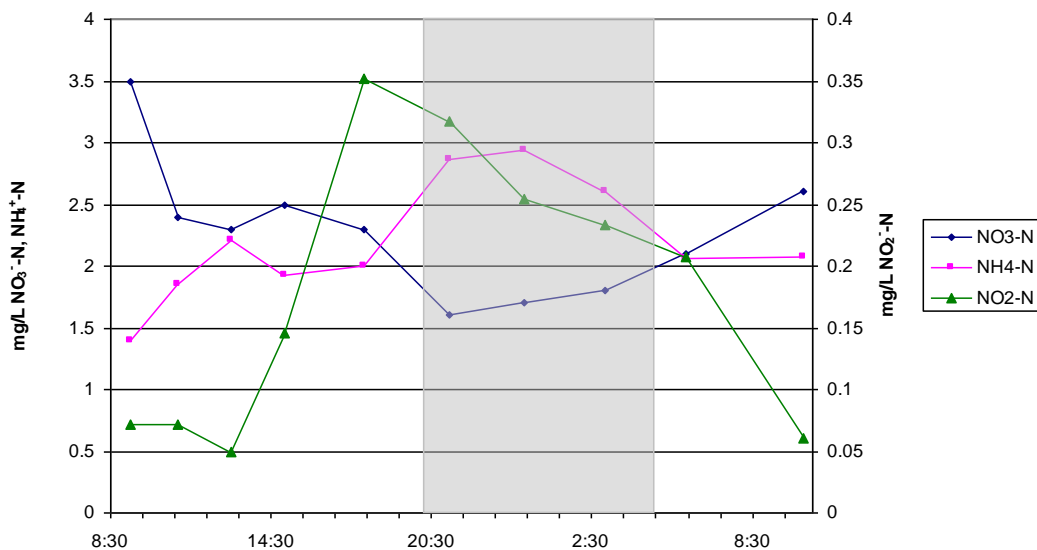


Figure 22. Diurnal changes in nutrients at SBC-3.

Based on the preliminary data collected in this research, it is clear that concentrations of ammonia and nitrate in Silver Bow Creek change depending on the time of day. These changes are more noticeable below the WWTP outfall as compared to above the outfall. More detailed investigations of diurnal nutrient cycling in Silver Bow Creek are in progress (Babcock and Gammons, 2008; Babcock, in preparation).

4.2.2 Dissolved Oxygen Concentrations and the Silver Bow Creek “Dead Zone”

On August 6, 2006, starting at 4:00 a.m. and ending around 6:00 a.m., DO concentrations were taken at 8 locations along Silver Bow Creek in the pre-dawn hours. The results (Fig. 23) show that DO values above the WWTP were near 8 mg/L in the pre-dawn hours. However, the DO concentrations for all stations below the WWTP fell below 5 mg/L, with the most severe DO depletions (< 2 mg/L) at the SBC-3 and “Town Pump” monitoring sites. These unusually low DO concentrations are believed to be caused by the oxidation of ammonia from the WWTP in the absence of photosynthesis (e.g., see Dunnette and Avedovech, 1983). The reach of critically low DO concentrations is denoted the “Dead Zone” in Figure 23. This term is often used to describe hyper-eutrophic waters, including ocean waters such as the northern Gulf of Mexico (Malakoff, 1998; Dodds, 2006), that show extreme hypoxia during certain times of the year. In the middle part of the Silver Bow Creek Dead Zone, concentrations of DO clearly dropped to levels that would be lethal to trout on the morning of August 6, 2006.

To further investigate the extent of the Silver Bow Creek Dead Zone, 24-h changes in dissolved oxygen concentration were measured at 6 locations above and below the WWTP outfall on August 14-17, 2006 (Figure 24). The DO profile above the WWTP showed higher DO concentrations during the daytime and lower concentrations at night, as expected, although the levels stayed above the aquatic life standard of 5 mg/L over the entire 24 hour period. The WWTP outlet had a fairly steady DO concentration around 4 mg/L, indicating O₂ consumption. This value was also close to the DO levels measured at the WWTP outfall during each monthly visit (see data in Appendix A1).

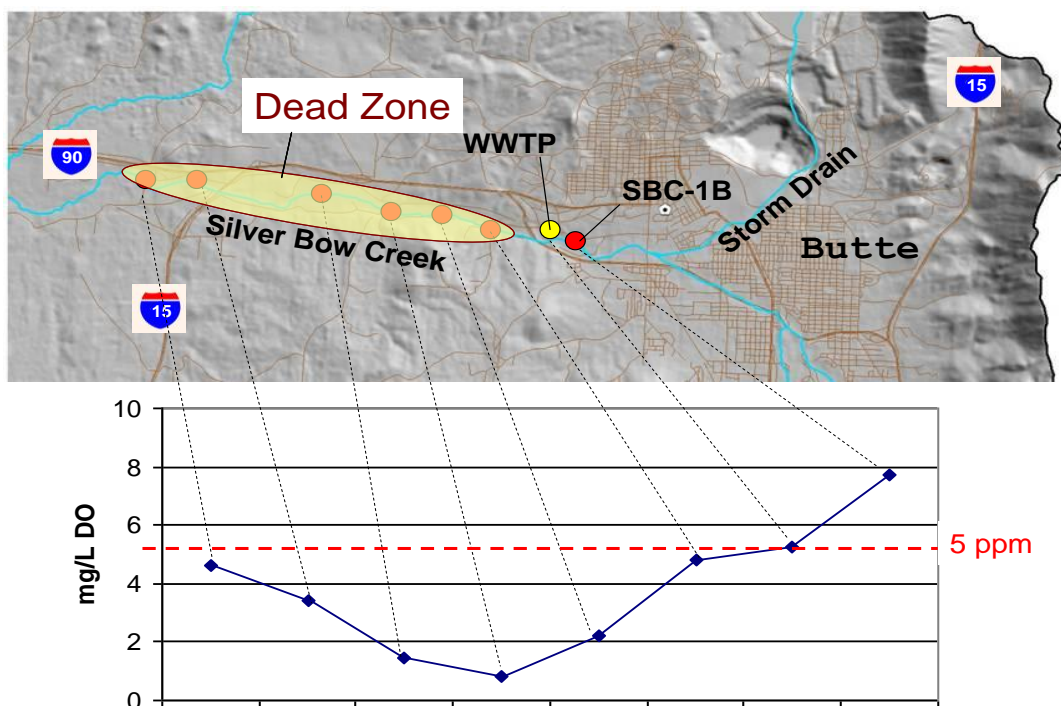


Figure 23. Dissolved oxygen concentrations in Silver Bow Creek in the pre-dawn hours of August 6, 2006

Monitoring stations in Silver Bow Creek below the WWTP clearly showed the serious impacts of the sewage treatment outfall. At SBC-2, DO concentrations dropped below 4 mg/L during both nights (Fig. 24). At SBC-3, DO concentrations dropped below 1 mg/L for roughly 10 hours during the late afternoon and nighttime period. At the Town Pump site, nighttime O_2 concentrations dropped below 2 mg/L. By the time the stream got to the Nissler site, most of the ammonia was probably already oxidized, and therefore the nighttime depletion in O_2 was less extreme. Nonetheless, Figure 24 shows that O_2 levels dropped below 4 mg/L at Nissler for over 6 hours. At Nissler, all three datasondes were placed in the water side-by-side over the 24 hour sampling period. Figure 24 shows how well their DO profiles matched.

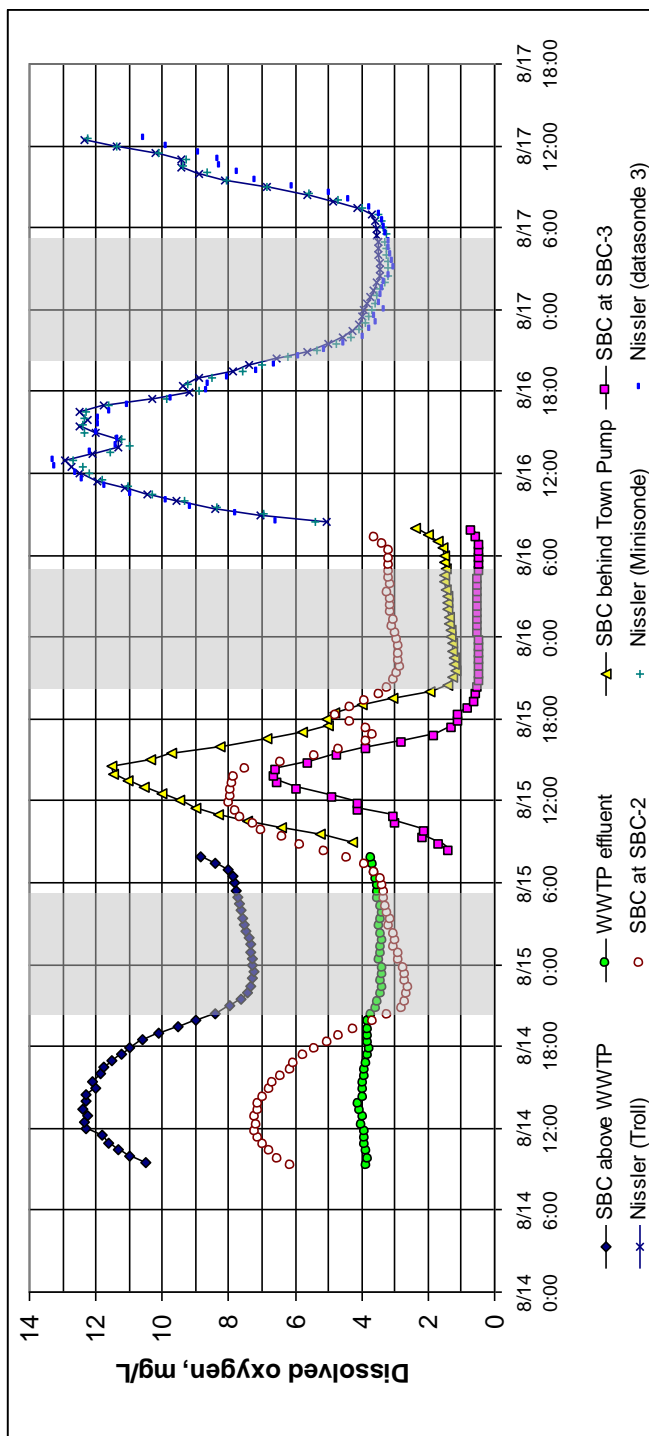


Figure 24. Diurnal changes in dissolved oxygen measured at 6 locations above and below the WWTP outfall during August 14-17, 2006.

4.2 Stable isotopes

The results of stable isotope analysis of samples collected in this research during October 2006 and June 2007 are summarized in Table 7 and Figure 25. The 2006 samples were collected at the same time as the synoptic nutrient sampling of 10/10/06.

Table 7. Stable isotope results

<i>Location</i>	<i>Sample Date</i>	$\delta^{15}\text{N-NO}_3$	$\delta^{18}\text{O-NO}_3$	$\delta^{15}\text{N-NH}_4$
Samples from October, 2006				
MT Pole	10/10/06	12.1	0.7	n.a.
LAO	10/10/06	9.9	10.0	n.a.
WWTP	10/10/06	n.a.	n.a.	10.1 (7.6)
SBC-1	10/10/06	10.5	-1.2	n.a.
SBC-3	10/10/06	5.0 (5.3) ¹	-2.4 (-1.9) ¹	16.5 (14.9) ¹
Samples from June, 2007				
MT Pole	6/26/07	12.7 (12.3) ¹	2.0	n.a.
SBC-1	6/26/07	11.2	3.2	n.a.
SBC-2	6/28/07	8.6	5.4	n.a.
SBC-2B ²	6/28/07	7.9	1.7	n.a.
SBC-3	6/28/07	7.8	-3.0	n.a.
Town Pump	6/28/07	8.3	-5.0	n.a.
Nissler	6/28/07	11.4	-5.4	n.a.

¹ Values in parentheses are laboratory duplicates. ² SBC-2B is located mid-way between SBC-2 and SBC-3. n.a. = not analyzed.

Supporting field and nutrient concentration data for the 2007 isotope samples are given in Table A1 of the Appendix.

As shown in Figure 25, the stable isotopic compositions of nitrate from the various waters sampled in this study are similar to those collected by previous workers for shallow alluvial groundwater wells in the Butte Summit Valley. As discussed by LaFave (2008), the range in isotopic composition for nitrate in Summit Valley groundwater is most consistent with derivation of N from human or animal waste, although lesser contributions from other sources (such as chemical fertilizer, munitions, or acid rain) cannot be discounted. Ammonium from the WWTP shows an N-isotope

composition within the ranges of $\delta^{15}\text{N-NO}_3$ from the groundwater wells and Silver Bow Creek samples and therefore cannot be used to differentiate the WWTP from other nitrogen sources.

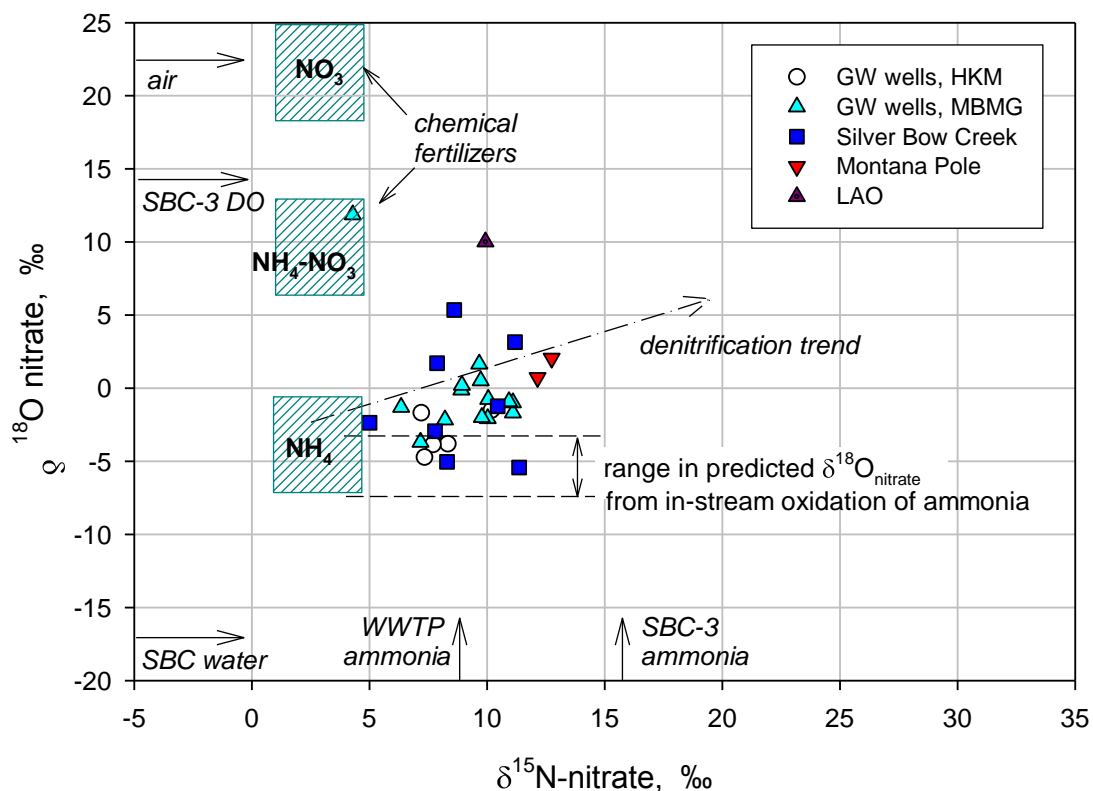


Figure 24. Stable isotope composition of nitrate from Silver Bow Creek compared to other results. The green-hatched boxes show the isotopic composition of nitrate that would be obtained after leaching and oxidation of synthetic NO_3 , synthetic NH_4 , or a 1:1 mixt

Nitrate from the MT Pole effluent is isotopically enriched in $\delta^{15}\text{N}$ relative to the rest of the samples, and this may reflect denitrification of nitrate in the anaerobic plume at Montana Pole. The line labeled “denitrification trend” in Figure 25 shows the predicted pathway that residual nitrate would take during microbial denitrification (reduction of NO_3^- to N_2). This is a slope of 1:2 on the graph (Böttcher et al., 1990).

Overall, isotopic evidence for denitrification is weak for the groundwater and surface waters sampled in this study, even for Montana Pole.

None of the samples, with one possible exception, plot in the boxes for synthetic (chemical) fertilizer. The exception is a Montana Pole groundwater monitoring well collected by MBMG. The reason that there are 3 boxes for chemical fertilizer is that the source of the fertilizer could be nitrate, ammonium-nitrate, or ammonium. Synthetic *nitrate* always has $\delta^{18}\text{O}$ -nitrate close to $\delta^{18}\text{O}$ -air, which is near +23 ‰ (Kroopnik and Craig, 1972). If synthetic *ammonium* was the fertilizer source used, then oxidation of this ammonium after application would result in nitrate that has 1/3 of its O from air, and 2/3 from water. This is because, in the microbial oxidation of ammonium to nitrate, two O atoms come from water and one from air (Wassenaar, 1995; Clark and Fritz, 1997; Kendall and Aravena, 2000). Stream water in Butte is isotopically light, and has an average $\delta^{18}\text{O}$ value near -17 ‰ (Gammons et al., 2006). The central position of the box labeled “NH₄” was thus calculated by mass balance: $2/3 * -17\text{‰} + 1/3 * 23\text{‰}$ (air) = -3.7 ‰. For a *mixed ammonium-nitrate* fertilizer, 2/3rds of the O atoms in the final nitrate would be inherited from air, and 1/3 from local water, resulting in a predicted $\delta^{18}\text{O}$ -nitrate value of +9.7 ‰.

SBC-3 ammonia is highly enriched in ¹⁵N compared to ammonia coming from the WWTP outfall: the $\delta^{15}\text{N}$ -NH₄ values are +16‰ and +8‰, respectively (Table 7). The enrichment in ¹⁵N with distance downstream may be due to preferential oxidation of isotopically-light ammonium by microbes such as *Nitrosomonas* sp., leaving isotopically

heavy ammonia behind in the water column. Preferential oxidation of isotopically light NH_4^+ to NO_3^- could also explain the drop in $\delta^{15}\text{N}\text{-NO}_3$ between the SBC-1 and SBC-3 sites (Fig. 26). There is also an interesting trend of decreasing $\delta^{18}\text{O}\text{-nitrate}$ with distance below the WWTP (Fig. 26), which is also most likely due to the in-stream addition of nitrate formed by oxidation of ammonia. Overall, the fact that the N and O isotopic

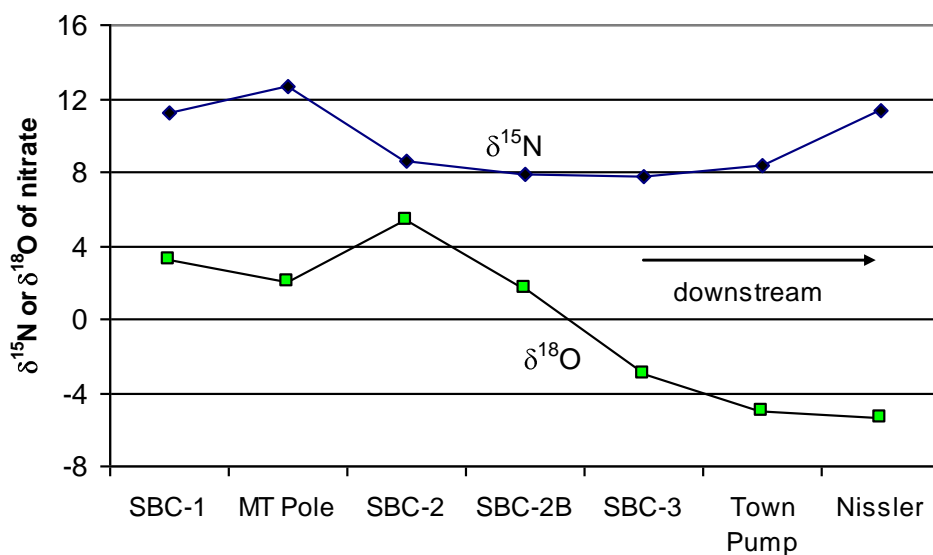


Figure 25. Changes in the isotopic composition of nitrate with distance downstream on 6/26/07.

composition of nitrate changes over a short, 5 km stream reach is interesting, but makes it even less likely that stable isotopes could be useful to pin-point sources of nitrate in Silver Bow Creek or the upper Clark Fork River.

5. Conclusions and Recommendations

5.1 Conclusions

This study has shown that Silver Bow Creek has very high nutrient concentrations and loads as it leaves the Butte Summit Valley. In terms of nutrient yield ($\text{kg}/\text{km}^2/\text{year}$),

the amount of N and P leaving the watershed is far in excess of average national trends for “developed basins” (Smith et al., 2003). The largest source of nutrient contamination is the Butte wastewater treatment plant (WWTP), which contributes over 80% and 60% of the total N and total P loads, respectively, during normal baseflow conditions. When the contribution from the WWTP is removed, Silver Bow Creek has a nutrient yield more consistent with national averages for developed basins. Besides the WWTP, significant loads of nitrate and phosphate in upper Silver Bow Creek come from non-point sources in the Butte Summit Valley, as well as discharges of groundwater from the Montana Pole and Lower Area One treatment plants.

Most of the N exiting the WWTP is in the form of ammonium (NH_4^+). The ammonium is then oxidized to nitrate by bacteria as the water moves downstream, and this oxidation reaction occurs faster when the temperature is warmer. Since the rate of oxidation is temperature dependent, both seasonal and diurnal fluctuations occur in ammonia and nitrate concentrations in Silver Bow Creek. Oxidation of ammonia to nitrate also results in downstream increases in nitrate concentrations and loads. These should not be misinterpreted as being due to the influx of nitrate-rich groundwater.

During mid-summer, low-flow conditions, dissolved oxygen concentrations in Silver Bow Creek below the WWTP drop below 2 mg/L during the night, creating a “dead zone” where aquatic life is severely impaired. Oxidation of ammonium is believed to be the main source of this extreme depletion in dissolved oxygen. Besides playing a dominant role in consumption of dissolved oxygen, concentrations of ammonium in

Silver Bow Creek below WWTP are sometimes high enough to be toxic to aquatic life based on current EPA standards.

The stable isotopic composition of nitrate and ammonium in Silver Bow Creek is most consistent with derivation from human and animal waste. With the possible exception of the discharge pipe from the Montana Pole plant, none of the waters sampled show clear isotopic evidence for denitrification. Below the WWTP outfall, oxidation of ammonium to nitrate results in significant changes in the O and N isotopic composition of nitrate, making it difficult if not impossible to use stable isotopes to discriminate between multiple sources of N contamination to the watershed.

5.2. Recommendations

Based on this study, it is clear that improvements should be made to the Butte-Silver Bow wastewater treatment plant to remove N and P prior to discharge to Silver Bow Creek. The “dead zone” between Butte and Rocker will most likely return each summer so long as current conditions prevail. As well, nutrient loads from the WWTP create a large crop of biomass (aquatic plants and algae) in the stream that is further evidence of hyper-eutrophic conditions. If improvements are made to the WWTP, nutrient loads in SBC would be much closer to nation-wide reference conditions for developed watersheds.

Future nutrient monitoring efforts in upper Silver Bow Creek should include both ammonia-N and nitrate-N. Apparent increases in nitrate concentration and load in Silver Bow Creek between the WWTP outfall and the town of Rocker are likely due to

oxidation of ammonia, not to the input of nitrate from groundwater or additional off-stream sources. Future nutrient monitoring should also take diurnal cycling into account, especially below the WWTP outfall. Concentrations measured depends on the time of day. This is especially true for dissolved oxygen and the nitrogen compounds (nitrate and ammonium).

The USGS monitoring station below the WWTP is not a good place to collect water quality samples because Silver Bow Creek is poorly mixed at this location. Samplers need to take care to collect width- and depth-integrated samples to obtain a representative bulk sample. Better yet, it is recommended to move the water quality collection point to the first frontage road bridge, roughly 0.6 km downstream (SBC-2 of this study).

All of the data in this research were collected during baseflow-to-moderately high flow conditions. Additional studies should be undertaken to look at loads and concentrations of nutrients exiting Butte during Spring runoff and storm events. For example, it is possible that there is a flush of nutrients off Butte Hill during storms, some of which is incompletely processed through the WWTP, and some of which enters directly into the streams.

Based on the results of this research, it seems unlikely that stable isotopes of N can be used to pinpoint sources of N-contamination in the upper Silver Bow Creek basin. However, this study did show interesting changes in $\delta^{18}\text{N}$ and $\delta^{18}\text{O}$ of nitrate as it passes downstream from Butte to Rocker and beyond. Further work is recommended to investigate the causes of these isotopic trends..

6.0 References

- Babcock J. (in preparation) Diurnal cycling of metals and nutrients in Silver Bow Creek, Montana. M.S. Research, Montana Tech of The University of Montana.
- Babcock J. and Gammons C.H. (2008) Diurnal cycling of nutrients in a hyper-eutrophic stream: Silver Bow Creek, Montana. Proc. 2008 Montana Water Center Conference, http://www.awra.org/state/montana/pdfs/2008_proceedings_screen.pdf
- Bohlke J.K. and Denver J.M. (1996) Combined use of groundwater dating, chemical, and isotopic analysis to resolve the history and fate of nitrate contamination in two agricultural watersheds, Atlantic Coastal Plain, Maryland: *Water Resources Research* 31, 2319-2339.
- Böttcher J., Strebel O., Voerkelius S. and Schmidt H. L. (1990) Using isotope fractionation of nitrate-nitrogen and nitrate-oxygen for evaluation of microbial denitrification in a sandy aquifer. *Journal of Hydrology* 114, 413-424.
- Botz M. K. (1969) Hydrogeology of the upper Silver Bow Creek drainage area, Montana. Montana Bureau of Mines and Geology, Bulletin 75, 32 pp.
- Brick C. M. and Moore J. N. (1996) Diel variation of trace metals in the upper Clark Fork River, Montana. *Envir. Sci. Technol.* 30, 1953-1960.
- Carstarphen C.A., LaFave, J.I., and Patton, T.W. (2004) Water levels and nitrate in Warne Heights, upper Summit Valley, Silver Bow County, Montana, *Mont. Bur. Mines Geol. Ground-water Open-File Report* 18, 52 pp.

- Clark I. and Fritz P., 1997. *Environmental Isotopes in Hydrogeology*. Lewis Pub., New York.
- Coplen T. B. (1993) Use of environmental isotopes, in Alley, W.A., ed, *Regional Ground-Water Quality*: New York, Van Nostrand Reinhold, Chap. 10, p. 227-254.
- Deutsch B., Liskow I., Kahle P. and Voss M. (2005) Variations in the $\delta^{15}\text{N}$ and $\delta^{18}\text{O}$ values of nitrate in drainage water of two fertilized fields in Mecklenburg-Vorpommern (Germany). *Aquatic Sciences* 67, 156-165.
- Dodds W.K. (2006) Nutrients and the “dead zone”: the link between nutrient ratios and dissolved oxygen in the northern Gulf of Mexico. *Frontiers in Ecology and the Environment* 4(4), 211-217.
- Dodds W.K., Smith V.H., and Zander B. (1997) Developing nutrient targets to control benthic chlorophyll levels in streams: A case study of the Clark Fork River. *Water Research* 31, 1738-1750.
- Dunnette D.A. and Avedovech R.M. (1983) Effect of an industrial ammonia discharge on the dissolved oxygen regime of the Willamette River, Oregon. *Water Research* 17, 997-1007.
- EPA (1999) 1999 Update of ambient water quality criteria for ammonia. U.S. Environmental Protection Agency, Document EPA-822-R-99-014, 153 pp.
- Forsell, R. (2006) “Fish in Silver Bow Creek”. *Montana Standard*. October 14, 2006.
- Frandsen A. (2006) Mining megasite cleanup. *The Water Report*, Envirotech Publ, Eugene OR, v. 26, 10-25.

- Gammons C. H., Poulson S. R., Pellicori D. A., Roesler A., Reed P. J., Petrescu E. M. (2006) The hydrogen and oxygen isotopic composition of precipitation, evaporated mine water, and river water in Montana, USA. *Journal of Hydrology* 328, 319-330.
- Gammons C.H., Grant T.M., Nimick D.A., Parker S.R., and DeGrandpre M.D. (2007) Diel changes in water chemistry in an arsenic-rich stream and treatment-pond system. *Science of the Total Environment* 384, 433-451.
- GWIC (2008) Ground Water Information Center. Montana Bureau of Mines and Geology, <http://mbmgwic.mtech.edu/>
- Kellman, L.M. and Hillaire-Marcel, C. (2003) Evaluation of nitrogen isotopes as indicators of nitrate contamination sources in an agricultural watershed. *Agriculture, Ecosystems and the Environment* 95, p. 87-102.
- Kendall C. (1998) Tracing nitrogen sources and cycles in catchments. In: C. Kendall and J. J. McDonnell (eds.), *Isotope Tracers in Catchment Hydrology*. Elsevier, Amsterdam, pp. 519–576.
- Kendall, C.A. and Aravena, R. (2000) Nitrate isotopes in groundwater systems, in Cook, P.G. and Herczeg, A.L eds, *Environmental Tracers in Subsurface Hydrology*: Boston, Kluwer Academic Publishers, Chap. P, p. 261 – 298.
- Kowalchuk, G.A. and Stephen, J. (2001) Ammonia-Oxidizing Bacteria: A Model for Molecular Microbial Ecology. *Annu. Rev. Microbiol* 55: 485-529.
- Kroopnik P.M. and Craig H. C. (1972) Atmospheric oxygen: Isotopic composition and solubility fractionation. *Science* 175, 54-55.

- LaFave J. (2008) Nitrate in the ground water and surface water of the Summit Valley near Butte, Montana. Montana Bureau of Mines and Geology, Ground-Water Open File Report 22, 26pp.
- Malakoff D. (1998) Death by suffocation in the Gulf of Mexico. *Science* 281, 190-192.
- MDEQ (2006) Monitoring report for 2005: Streamside Tailings Operable Unit, Silver Bow Creek/Butte Area NPL Site. Montana Department of Environmental Quality, Helena, MT, 139 pp.
- Moore J.N. and Luoma S.N. (1990) Hazardous wastes from large-scale metal extraction. *Environmental Science and Technology* 24, 1279-1285.
- Mueller D. K. and Helsel D. R. (1996) Nutrients in the nation's waters too much of a good thing? U.S. Geological Survey, Circular 1136, 24 p.
- Parker S. R., Gammons C. H., Poulson S. R., and DeGrandpre M. D. (2007) Diel changes in pH, dissolved oxygen, nutrients, trace elements, and the isotopic composition of dissolved inorganic carbon in the upper Clark Fork River, Montana, USA. *Applied Geochemistry* 22, 1329-1343.
- Pioneer Technical (2005) Warm Springs Ponds five-year review report. Pioneer Technical Services, Inc., Butte, Montana, 40 pp. plus figures.
- Redfield A.C. (1958) The biologic control of chemical factors in the environment. *American Scientist* 64, 205-221.
- Scholefield D., Le Goff, T., Braven J., Ebdon L., Long T., and Butler M. (2005) Concerted diurnal patterns in riverine nutrient concentrations and physical conditions. *Science of the Total Environment* 344, 201-210.

- Smith R.A., Alexander R.B., and Schwarz G.E. (2003) Natural background concentrations of nutrients in streams and rivers of the conterminous United States. *Environmental Science and Technology* 37, 3039-3047.
- TSWQC (2005) Status Report: The Clark Fork River Voluntary Nutrient Reduction Program, 2002-2005. Document available online at the following Tri-State Water Quality Council website: http://www.tristatecouncil.org/documents/05vnrp_eval.pdf.
- TSWQC (2007) Clark Fork-Pend Oreille Watershed Management Plan: Management Strategies for the Next Decade: 2007-2017. Document available online at the following Tri-State Water Quality Council website: http://www.tristatecouncil.org/documents/07cfpo_wmplan_000.pdf
- Wassenaar L.I. (1995) Evaluation of the origin and fate of nitrate in the Abbotsford Aquifer using the isotopes of ^{15}N and ^{18}O in NO_3^- . *Applied Geochemistry* 10, 391-405.
- Watson, V. and Gestring, B. (1996) Monitoring algae levels in the Clark Fork River. *Intermountain Journal of Sciences*. 2:2, 17-26.
- WET (2004) Nutrient source assessment, Upper Silver Bow Creek watershed. Water & Environmental Technologies (WET). Available online at: http://www.tristatecouncil.org/documents/04ucf_goal1.pdf.

Appendix A1: Field Parameters for Samples Collected

Samples of 5/22/06

Date/time	Site	Temp °C	SC µS/cm	pH s.u.	alkalinity mg/L CaCO ₃	DO % sat	DO mg/L	Turbidity NTU	Flow cfs
5/22/06 9:45	BTC-1	8.5	140	7.56	41	91	8.5	3.33	7.5
5/22/06 10:45	BTC-2	11.7	184	7.47	54	98	8.6	4.25	8.1
5/22/06 12:20	BTC-3	13.3	211	7.45	69	104	8.7	2.94	11.0
5/22/06 12:30	BC-1	15.3	280	7.95	99	109	8.8	1.96	1.5
5/22/06 14:00	BTC-4	14.7	269	7.75	84	108	8.8	3.28	15.9
5/22/06 14:20	MSD	14.0	188	7.54	60	99	8.3	2.56	0.3
5/22/06 15:30	SBC-1	15.7	282	7.87	85	100	8.0	4.41	16.2
5/22/06 15:20	MT Pole	8.7	1012	7.03	187	85	8.1	0.85	0.7
5/22/06 16:40	LAO	17.9	1149	8.78	45	120	9.4	na	2.4
5/22/06 17:00	WWTP	13.2	504	6.98	120	58	4.8	3.49	7.7
5/22/06 17:45	SBC-2	15.8	419	7.53	94	110	8.6	4.65	27.0
5/22/06 18:00	SBC-3	16.7	421	7.45	110	96	7.6	4.16	27

Location	mg/L, colorimetry			
	NO ₂ -N	NO ₃ -N	NH ₄ -N	PO ₄ -P
BTC-1	na	0.4	0.25	0.08
BTC-2	na	0.2	0.25	0.11
BTC-3	na	0.7	0.10	0.12
Basin	na	0.4	<0.02	0.12
BTC-4	na	0.6	<0.02	0.14
MSD	na	0.2	<0.02	0.06
SBC-1	na	0.7	0.04	0.15
MT Pole	na	3.4	<0.02	0.11
LAO	na	1.1	<0.02	0.03
WWTP	na	1.1	10.3	1.32
SBC-2	na	0.6	1.95	0.40
SBC-3	na	1.4	1.22	0.40

Samples of 6/29/2006

Date/time	Site	Temp °C	SC µS/cm	pH s.u.	alkalinity mg/L CaCO ₃	DO % sat	DO mg/L	Turbidity NTU	Flow cfs
6/29/06 16:10	BTC-1	13.8	163	7.87	56	98	8.1	4.08	5.8
6/29/06 16:50	BTC-2	na	193	7.59	na	89	7.0	7.72	na
5/22/06 15:00	BTC-3	17.9	216	7.77	74	113	8.7	5.14	11.8
5/22/06 15:20	BC-1	20.0	248	8.46	na	109	8.1	na	3.3
5/22/06 14:00	BTC-4	18.6	279	8.17	93	141	11.0	3.08	13.5
5/22/06 13:30	SBC-1	18.3	298	8.70	94	159	12.4	3.15	13.0
5/22/06 13:00	MT Pole	8.6	1035	7.20	184	98	9.5	1.15	1.1
5/22/06 10:20	LAO	20.8	1111	8.86	88	102	7.5	1.10	1.7
5/22/06 11:00	WWTP	15.6	530	7.10	145	43	3.5	3.22	11.2
5/22/06 9:20	SBC-2	16.1	475	7.61	104	105	8.6	3.68	25.9
5/22/06 8:30	SBC-3	15.2	469	7.48	98	110	9.1	2.06	21.2

Location	mg/L colorimetry			
	NO ₂ -N	NO ₃ -N	NH ₄ -N	PO ₄ -P
BTC-1	na	0.2	0.16	na
BTC-2	na	0.2	0.05	0.17
BTC-3	na	0.5	<0.02	0.14
Basin	na	0.3	0.21	0.15
BTC-4	0.009	0.4	<0.02	0.17
SBC-1	0.046	0.8	<0.02	0.05
MT Pole	na	4.6	<0.02	0.18
LAO	0.009	1.6	<0.02	0.05
WWTP	0.028	0.9	9.8	1.14
SBC-2	0.054	1.2	2.60	0.39
SBC-3	0.091	1.8	1.41	0.49

Samples of 10/10/06

Date/time	Site	Temp °C	SC µS/cm	pH s.u.	alkalinity mg/L CaCO ₃	DO % sat	Turbidity NTU	Flow cfs
10/10/06 17:00	BTC-1	3.8	197	7.57	61	99	1.60	3.1
10/10/06 16:50	BTC-2	6.5	238	7.53	64	112	2.00	1.6 ^a
10/10/06 15:50	BTC-3	8.6	275	7.89	105	108	1.70	4.4
10/10/06 16:30	BC-1	7.8	335	7.77	112	111	0.96	0.7
10/10/06 15:30	BTC-4	9.0	349	7.41	109	113	3.30	9.8
10/10/06 15:30	MSD	7.9	465	6.85	99	108	2.15	0.5
10/10/06 14:40	SBC-1	8.2	363	7.48	110	110	6.60	10.7
10/10/06 14:20	MT Pole	9.4	1076	6.90	202	109	0.27	0.9
10/10/06 13:40	LAO	8.8	1134	8.67	35	100	0.40	1.4
10/10/06 13:16	WWTP	15.5	548	6.79	146	57	4.10	6.4
10/10/06 12:15	SBC-2	9.7	512	7.26	116	99	12.60	19.4
10/10/06 11:15	SBC-3	9.1	516	7.25	116	111	9.40	19.8

^avalue in question due to very low stream velocities

Location	mg/L, colorimetry			IC-Murdock					
	NO ₂ -N	NH ₄ -N	PO ₄ -P	NO ₂ -N	NO ₃ -N	PO ₄ -P	F	Cl	SO ₄
BTC-1	0.012	0.08	0.07	<0.2	<0.13	<0.25	0.27	5.0	25.5
BTC-2	0.008	0.06	0.04	<0.2	0.24	<0.25	0.25	8.4	33.8
BTC-3	0.017	0.06	0.09	<0.2	0.80	<0.25	0.21	9.0	32.4
Basin	0.005	<0.02	0.19	<0.2	0.65	<0.25	0.24	5.7	48.0
BTC-4	0.017	0.10	0.07	<0.2	1.20	<0.25	0.30	13.8	40.1
MSD	0.016	0.12	0.05	<0.2	0.29	<0.25	0.58	11.3	110
SBC-1	0.050	0.10	0.02	<0.2	1.30	<0.25	0.36	15.3	48.7
MT Pole	0.028	0.12	0.14	<0.2	8.30	<0.25	0.48	52.2	267
LAO	0.023	<0.02	0.03	<0.2	0.89	<0.25	0.74	51.0	488
WWTP	0.044	13.4	2.31	0.24	0.16	2.10	0.23	42.5	44.5
SBC-2	0.034	5.7	0.77	<0.2	1.40	0.46	0.28	28.5	86.4
SBC-3	0.035	4.7	0.67	<0.2	1.40	0.44	0.34	28.6	86.5

Samples 10/28/06

Date/time	Site	Temp °C	SC μS/cm	pH s.u.	DO % sat
10/28/06 10:50	WWTP	13.8	538	6.70	48
10/28/06 11:15	SBC-2	7.0	521	6.88	88
10/28/06 11:25	SBC-3	6.1	524	6.95	98
10/28/06 12:05	Nissler	5.7	525	7.19	110
10/28/06 12:50	MT Livestock	6.0	519	7.23	113
10/28/06 13:00	Miles Xing	5.7	553	7.13	99
10/28/06 13:45	Fairmont	5.6	491	7.55	114
10/28/06 14:00	Opportunity	6.9	484	7.55	116

Location	mg/L, colorimetry			
	NO ₂ -N	NO ₃ -N	NH ₄ -N	PO ₄ -P
WWTP	0.177	0.8	12.8	1.80
SBC-2	0.073	1.1	3.60	0.59
SBC-3	0.076	1.4	2.20	0.51
Nissler	0.055	1.9	1.18	0.51
MT livestock	0.045	1.8	0.79	0.92
Miles Xing	0.035	1.7	0.65	0.84
Fairmont	0.026	1.3	0.42	0.92
Opportunity	0.024	1.3	0.20	0.85

Samples of 12/18/06

Date/time	Site	Temp °C	SC μS/cm	pH s.u.	DO % sat	flow cfs
12/18/06 12:55	BTC-4 ^a	1.5	340	6.63	93	9.2
12/18/06 13:35	SBC-1	-0.1	363	7.17	96	11.4
12/18/06 13:25	MT Pole	9.2	1061	6.83	109	0.9
12/18/06 14:25	LAO	1.6	1264	8.74	101	1.6
12/18/06 14:10	WWTP	9.8	554	6.96	50	7.3
12/18/06 14:45	SBC-2	2.7	520	7.10	87	21.0
12/18/06 15:00	SBC-3	1.9	500	7.23	95	21
12/18/06 15:20	Nissler	-0.1	534	7.41	93	frozen
12/18/06 15:40	Miles Xing	-0.2	587	7.16	88	frozen
12/19/06 12:30	Fairmont	0.0	541	7.22	108	frozen
12/19/06 12:55	Opportunity	-0.1	596	7.33	111	frozen

^aSites upstream of BTC-4 were frozen.

Location	mg/L, colorimetry			IC-Murdock					
	NO ₂ -N	NH ₄ -N	PO ₄ -P	NO ₂ -N	NO ₃ -N	PO ₄ -P	F	Cl	SO ₄
BTC-4	0.035	0.03	0.09	<0.06	1.5	<0.25	0.24	13.2	41.5
SBC-1	0.012	0.07	0.07	<0.06	1.5	<0.25	0.27	15.1	44.6
MT Pole	0.019	0.01	0.14	<0.3	7.6	<1.25	0.43	51.7	257
LAO	0.009	0.04	0.03	<0.6	1.4	<2.5	0.79	61.4	508
WWTP	0.164	17.1	2.32	0.22	0.25	1.9	0.22	42.6	40.3
SBC-2	0.080	5.80	0.85	<0.12	1.4	0.84	0.29	28.3	80.3
SBC-3	0.071	4.00	0.53	<0.06	1.7	0.47	0.31	26.2	81.8
Nissler	0.065	5.30	0.63	<0.12	2.0	0.56	0.31	30.2	90.3
Miles Xing	0.019	1.28	0.43	<0.06	2.0	0.34	0.49	44.8	119
Fairmont	0.015	1.49	0.41	<0.06	2.0	0.28	0.36	33.4	97.2
Opportunity	0.014	1.59	0.40	<0.06	2.3	0.27	0.43	35.1	114

Samples of 1/29/07

Date/time	Site	Temp °C	SC µS/cm	pH s.u.	alkalinity mg/L CaCO ₃	DO % sat	flow cfs
1/29/07 13:30	BTC-4	2.4	349	6.88	na	93	8.1
1/29/07 13:00	SBC-1	1.5	371	7.12	77	101	8.1
1/29/07 12:45	MT Pole	8.8	1055	6.40	153	95	1.0
1/29/07 13:50	LAO	0.9	1326	9.17	52	na	1.0
1/29/07 13:30	WWTP	8.6	558	6.76	150	44	6.1
1/29/07 14:25	SBC-2	4.3	583	7.30	114	na	16.0
1/29/07 14:45	SBC-3	3.7	578	7.43	78	na	16
1/29/07 16:35	Nissler	2.8	568	7.63	86	na	na
1/29/07 16:00	Fairmont	-0.2	569	7.50	80	na	frozen
1/29/07 15:30	Opportunity	-0.1	569	7.61	na	na	frozen

Location	mg/L, colorimetry			mg/L, IC-Murdock					
	NO ₂ -N	NH ₄ -N	PO ₄ -P	NO ₂ -N	NO ₃ -N	PO ₄ -P	F	Cl	SO ₄
BTC-4	0.004	0.03	0.13	<0.06	1.8	<0.25	0.24	11.9	39.6
SBC-1	0.008	0.01	0.12	<0.06	1.8	<0.25	0.27	14.0	45.0
MT Pole	0.007	<0.02	0.17	<0.06	7.8	<0.25	0.46	46.6	262
LAO	0.003	0.01	0.08	<0.06	1.3	<0.25	0.85	64.3	504
WWTP	0.183	15.7	2.71	0.230	0.32	2.30	0.30	39.9	38.7
SBC-2	0.097	7.90	0.98	0.150	1.5	0.86	0.34	31.3	99.8
SBC-3	0.113	5.30	0.88	0.160	1.7	0.77	0.37	31.1	99.5
Nissler	0.081	4.20	0.79	0.120	2.1	0.65	0.39	30.5	99.1
Fairmont	0.015	2.12	0.39	<0.06	2.1	0.29	0.42	30.4	107
Opportunity	0.011	1.21	0.39	<0.06	2.4	0.25	0.44	30.4	109

Samples of 3/9/07

Date/time	Site	Temp °C	SC µS/cm	pH s.u.	DO % sat	DO mg/L	Turbidity NTU	flow cfs
3/9/07 10:45	BTC-1	0.6	202	7.09	101	11.9	3.50	2.1
3/9/07 11:30	BTC-2	1.1	165	6.44	91	10.4	4.72	5.6
3/9/07 12:30	BTC-3	3.4	204	6.55	98	10.6	5.20	9.2
3/9/07 12:30	Basin	0.6	158	6.61	92	10.8	53.0	7.6
3/9/07 13:30	BTC-4	3.9	241	6.77	93	10.0	16.3	24.0
3/9/07 14:00	MT Pole	8.7	1056	6.78	120	11.0	0.75	1.0
3/9/07 14:30	SBC-1	4.2	252	6.80	96	10.2	15.5	25
3/9/07 15:10	LAO	2.5	1101	8.67	87	9.6	0.55	2.1
3/9/07 15:00	WWTP	9.1	511	6.50	55	5.1	3.70	6.5
3/9/07 15:40	SBC-2	5.6	376	7.01	92	9.4	11.5	35.0
3/9/07 15:50	SBC-3	6.2	397	6.94	98	9.8	10.0	35
3/9/07 16:20	Nissler	6.6	413	7.10	106	10.6	9.00	na
3/9/07 16:50	Opportunity	na	na	na	na	na	na	60.0

Location	mg/L, colorimetry			mg/L, IC-Murdock					
	NO ₂ -N	NH ₄ -N	PO ₄ -P	NO ₂ -N	NO ₃ -N	PO ₄ -P	F	Cl	SO ₄
BTC-1	0.004	0.05	0.21	<0.06	<0.13	<0.25	0.23	9.1	17.7
BTC-2	0.009	0.37	0.36	<0.06	0.16	<0.25	0.12	8.3	15.9
BTC-3	0.009	0.31	0.38	<0.06	0.53	<0.25	0.13	9.0	21.7
Basin	0.013	0.82	0.49	<0.06	<0.13	0.35	0.12	5.3	12.3
BTC-4	0.010	0.58	0.38	<0.06	0.74	<0.25	0.14	9.8	25.1
SBC-1	0.014	0.54	0.34	<0.06	0.76	<0.25	0.14	10.8	27.0
MT Pole	0.006	<0.02	0.25	<0.3	7.4	<1.25	0.46	49.0	254.9
LAO	0.010	0.04	0.16	<0.6	<1.3	<2.5	0.85	74.0	410.0
WWTP	0.173	12.1	1.99	0.25	0.63	1.20	0.44	38.8	41.6
SBC-2	0.043	2.50	0.41	0.073	0.89	0.35	0.27	21.1	53.4
SBC-3	0.056	2.39	0.58	0.076	1.0	0.36	0.31	22.5	60.3
Nissler	0.047	2.16	0.55	0.073	1.3	0.36	0.35	24.0	66.1
Opportunity	0.014	1.15	0.46	<0.06	1.1	0.28	0.34	21.0	59.3

Samples of 4/24/07

Date/time	Site	Temp °C	SC µS/cm	pH s.u.	DO % sat	DO mg/L	Turbidity NTU	flow cfs
4/24/2007 10:10	BTC-1	2.6	133	6.15	102	11.4	8.70	10.3
4/24/2007 11:00	BTC-2	7.4	175	6.61	106	11.1	4.30	11.3
4/24/2007 11:35	BTC-3	7.1	203	6.74	109	10.7	3.30	13.8
4/24/2007 12:00	BC-1	8.9	319	7.40	120	11.3	7.40	1.0
4/24/2007 12:40	BTC-4	9.5	261	7.32	129	12.1	2.40	19.0
4/24/2007 13:15	SBC-1	10.6	276	7.48	128	11.6	2.80	20.0
4/24/2007 13:10	MT Pole	8.8	1027	6.85	116	10.7	0.40	1.0
4/24/2007 14:00	LAO	10.3	1101	8.58	103	9.3	0.55	1.9
4/24/2007 13:55	WWTP	11.7	514	6.65	49	4.3	12.7	6.7
4/24/2007 14:30	SBC-2	12.5	407	7.09	107	9.3	3.70	29.0
4/24/2007 14:45	SBC-3	13.5	414	7.29	112	9.5	6.70	29
4/24/2007 15:30	Nissler	15.0	423	7.64	127	10.5	4.00	na
4/24/2007 16:00	Fairmont	12.1	400	8.24	123	11.1	na	na
4/24/2007 15:20	Opportunity	11.6	399	8.65	133	12.3	na	59.0

Location	mg/L, colorimetry			mg/L, IC-Murdock					
	NO ₂ -N	NH ₄ -N	PO ₄ -P	NO ₂ -N	NO ₃ -N	PO ₄ -P	F	Cl	SO ₄
BTC-1	na	na	na	<0.06	<0.13	<0.25	0.14	6.2	15.1
BTC -2	0.004	1.78 ^a	0.29	<0.06	<0.13	<0.25	0.21	8.3	21.0
BTC-3	0.002	0.1	0.22	<0.06	0.2	<0.25	0.21	9.2	24.6
BC-1	na	na	na	<0.06	0.5	<0.25	0.23	6.4	44.6
BTC-4	<.002	0.1	0.24	<0.06	0.6	<0.25	0.25	11.9	32.2
SBC-1	0.008	0.0	0.20	<0.06	0.5	<0.25	0.27	12.8	34.9
MT Pole	0.003	0.5	0.27	<0.3	7.5	<1.25	0.43	49.3	265
LAO	0.002	0.01	0.20	<0.6	<1.3	<2.5	0.88	50.4	459
WWTP	0.181	14.9	4.04	0.3	0.3	2.24	0.23	43.4	41.2
SBC-2	0.062	3.8	0.68	0.1	0.7	0.48	0.31	23.5	68.3
SBC-3	0.100	3.3	0.53	0.2	1.0	0.43	0.32	23.6	71.4
Nissler	0.098	1.36	0.52	0.2	1.5	0.37	0.35	24.5	75.2
Fairmont	0.028	0.11	0.27	<0.06	1.0	<0.25	0.31	19.2	74.3
Opportunity	0.020	0.11	0.38	<0.06	1.0	<0.25	0.33	19.3	75.5

^aValue seems too high.

Samples of 5/31/07

Date/time	Site	Temp °C	SC µS/cm	pH s.u.	Alkalinity mg/L CaCO ₃	DO % sat	DO mg/L	Turbidity NTU	flow cfs
5/31/2007 11:45	BTC-1	8.6	137	7.15	36	na	na	5.0	14.5
5/31/2007 12:15	BTC-2	11.0	181	7.09	65	107	9.6	5.9	13.8
5/31/2007 12:45	BTC-3	12.6	202	7.20	67	105	9.1	3.0	15.9
5/31/2007 13:15	BC-1	15.1	202	7.53	63	113	9.2	2.1	6.4
5/31/2007 13:45	BTC-4	15.2	236	7.52	75	117	9.5	3.6	26
5/31/2007 14:45	SBC-1	15.9	260	7.71	76	118	9.5	3.2	25.9
5/31/2007 14:29	MT Pole	8.4	1099	6.50	186	96	9.1	0.4	1.0
5/31/2007 15:30	LAO	16.0	1145	8.70	37	110	8.8	0.8	1.7
5/31/2007 15:10	WWTP	14.0	531	6.84	123	52	4.3	3.5	6.4
5/31/2007 16:00	SBC-2	17.0	376	7.28	88	94	7.4	2.3	35
5/31/2007 16:45	SBC-3	18.0	384	7.26	79	90	6.9	2.8	35
5/31/2007 17:15	Nissler	19.1	399	7.28	83	91	6.8	3.9	na
5/31/2007 17:45	Fairmont	9.6	330	7.57	88	103	9.6	6.8	na
5/31/2007 18:15	Opportunity	11.0	335	7.81	85	110	9.8	9.1	90.0

Location	mg/L, colorimetry			mg/L, IC-Murdock					
	NO ₂ -N	NH ₄ -N	PO ₄ -P	NO ₂ -N	NO ₃ -N	PO ₄ -P	F	Cl	SO ₄
BTC-1	0.002	0.09	0.12	<0.06	<0.13	<0.25	0.14	4.2	12.6
BTC-2	0.004	0.14	0.14	<0.06	<0.13	<0.25	0.23	5.9	15.4
BTC-3	0.001	0.04	0.19	<0.06	0.20	<0.25	0.22	6.6	18.2
BC-1	<.002	0.09	0.15	<0.06	<0.13	<0.25	0.14	2.2	26.7
BTC-4	0.003	0.10	0.19	<0.06	0.39	<0.25	0.23	8.0	25.3
SBC-1	0.004	0.10	0.15	<0.06	0.37	<0.25	0.26	9.0	27.9
MT Pole	<.002	<0.02	0.21	<0.3	7.1	<1.25	0.44	49.8	267
LAO	0.004	<0.02	0.10	<0.6	<1.3	<2.5	0.91	46.2	445
WWTP	0.290	12.0	1.16	0.39	0.33	1.6	0.28	38.4	42.5
SBC-2	0.075	1.94	0.39	0.11	0.61	0.27	0.30	17.1	55.1
SBC-3	0.106	1.57	0.44	0.14	0.91	0.29	0.31	17.7	57.5
Nissler	0.124	1.03	0.53	0.16	1.4	0.34	0.32	18.9	60.7
Fairmont	0.020	0.08	0.30	<0.06	0.75	<0.25	0.23	10.5	50.9
Opportunity	0.014	0.01	0.24	<0.06	0.75	<0.25	0.26	10.7	53.1

Samples of 6/19/07

Date/time	Site	Temp °C	SC μS/cm	pH s.u.	DO % sat	DO mg/L	Turbidity NTU	Flow cfs
6/19/07 9:30	BTC-1	9.4	148	7.36	99	9.2	4.4	6.8
6/19/07 10:10	BTC-2	12.2	182	6.98	95	8.3	3.4	10.8
6/19/07 8:36	BTC-3	12.7	208	6.94	88	7.6	2.7	13.7
6/19/07 8:55	Basin Creek	13.1	216	7.17	91	7.6	2.5	4.3
6/19/07 10:30	BTC-4	14.5	262	7.37	109	9.0	2.7	21.5
6/19/07 0:00	MT Pole	8.8	1097	7.02	84	7.9	0.4	0.90
6/19/07 12:05	SBC-1	16.1	277	7.58	120	9.6	2.8	22
6/19/07 12:40	LAO	18.9	1214	8.71	110	8.2	0.8	2.0
6/19/07 12:30	WWTP	15.1	555	6.72	51	4.1	2.3	8.1
6/19/07 13:00	SBC-2	17.9	422	7.25	100	7.6	2.2	33.0
6/19/07 13:30	SBC-3	18.7	410	7.34	102	7.7	1.7	33
6/19/07 14:02	Nissler	19.0	428	7.00	111	8.3	1.6	31.5
6/19/07 15:00	Fairmont	19.3	389	8.17	118	8.8	4.3	na
6/19/07 14:44	Opportunity	19.5	386	8.31	120	8.9	3.4	62.0

Location	mg/L, colorimetry			mg/L, IC-Murdock					
	NO ₂ -N	NH ₄ -N	PO ₄ -P	NO ₂ -N	NO ₃ -N	PO ₄ -P	F	Cl	SO ₄
BTC-1	<.002	0.13	0.10	<0.06	<0.13	<0.2	0.15	3.4	11.2
BTC-2	<.002	0.11	0.17	<0.06	<0.13	<0.2	0.22	5.0	12.9
BTC-3	<.002	0.11	0.14	<0.06	0.26	<0.2	0.22	5.6	16.5
Basin	<.002	0.02	0.14	<0.06	<0.13	<0.2	0.15	2.4	19.5
BTC-4	<.002	<0.02	0.17	<0.06	0.50	<0.2	0.24	7.8	24.0
SBC-1	<.002	0.04	0.20	<0.06	0.46	<0.2	0.26	9.2	27.2
MT Pole	<.002	0.01	0.29	<0.3	7.47	<1	0.46	51.3	262.9
LAO	<.002	0.01	1.37	<0.6	<1.3	<2	0.90	48	455.1
LAO-D	<.002	0.03	1.48	na	na	na	na	na	na
WWTP	0.308	13.4	3.42	0.41	0.31	3.3	0.28	40.5	47
SBC-2	0.098	2.53	0.65	0.16	0.70	0.4	0.31	20.2	59.6
SBC-3	0.173	1.85	0.59	0.23	1.07	0.4	0.31	19.5	57.0
Nissler	0.189	0.63	0.57	0.28	2.01	0.3	0.34	20.9	64.5
Fairmont	0.002	0.09	0.31	<0.06	0.86	<0.2	0.31	14.7	57.3
Opportunity	0.004	0.12	0.31	<0.06	0.86	<0.2	0.33	14.4	57.9

Samples of 7/27/07

Date/time	Site	Temp °C	SC μS/cm	pH s.u.	DO % sat	DO mg/L	Turbidity NTU	Flow cfs
7/27/07 8:30	BTC-1	12.0	212	7.16	96	8.4	2.5	2.3
7/27/07 9:00	BTC-2	14.5	244	6.83	82	6.8	6.1	1.7
7/27/07 10:00	BTC-3	13.8	289	7.30	104	8.8	3.3	4.0
7/27/07 10:30	BC	13.7	352	7.77	104	8.8	4.0	0.44
7/27/07 12:00	BTC-4	17.5	354	7.72	134	10.5	1.8	9.2
7/27/07 12:20	SBC-1	18.0	394	8.16	151	11.6	2.2	9.2
7/27/07 12:18	MT Pole	9.75	1079	6.99	75	7.0	1.8	na
7/27/07 12:20	WWTP	18.4	518	6.92	56	4.3	na	7.4
7/27/07 14:00	SBC-2	20.9	559	7.77	118	8.6	na	na
7/27/07 14:20	SBC-3	22.0	548	7.77	108	7.7	na	na
7/27/07 15:00	Nissler	21.3	543	8.49	161	11.7	na	na

Location	mg/L, colorimetry			mg/L, IC-Murdock					
	NO ₂ -N	NH ₄ -N	PO ₄ -P	NO ₂ -N	NO ₃ -N	PO ₄ -P	F	Cl	SO ₄
BTC-1	na	0.02	0.14	<0.06	<0.13	<0.2	0.29	4.1	9.6
BTC-2	na	<0.02	0.13	<0.06	0.24	<0.2	0.24	6.3	18.5
BTC-3	na	0.04	0.13	<0.06	0.85	<0.2	<0.05	8.4	26.8
Basin	na	<0.02	0.09	<0.06	0.42	<0.2	0.21	5.7	41.0
BTC-4	na	<0.02	0.12	<0.06	0.86	<0.2	<0.05	8.4	26.8
MT Pole	na	<0.02	0.18	<0.6	7.6	<2	<0.5	51.3	261
SBC-1	0.007	<0.02	0.16	<0.06	1.0	<0.2	0.31	15.9	41.5
WWTP	0.168	7.05	1.30	<0.06	0.15	0.68	0.28	38.2	40.8
SBC-2	0.157	3.38	0.47	<0.06	1.2	0.24	0.36	30.5	90.4
SBC-3	0.123	0.23	0.43	<0.06	4.1	0.25	0.40	30.4	94.8
Nissler	0.220	0.09	0.49	<0.06	3.1	0.27	0.45	29.3	103

Samples of 8/31/07

Date/time	Site	SC μS/cm	pH s.u.	DO % sat	DO mg/L	flow cfs
8/30/07 13:30	BTC-1	213	8.28	82	7.1	1.3
8/30/07 14:00	BTC-2	253	8.76	62	5.2	0.61
8/30/07 15:00	BTC-3	296	8.12	90	7.6	2.6
8/30/07 14:45	BC-1	327	8.56	89	7.7	0.39
8/31/07 11:55	BTC-4	369	7.66	55	5.0	6.7
8/31/07 11:40	SBC-1	401	8.18	103	9.1	na
8/31/07 11:30	MT Pole	1033	6.90	80	7.6	na
8/31/07 12:30	WWTP	479	6.96	91	6.8	na
8/31/07 12:50	SBC-2	650	7.61	54	4.4	15
8/31/07 13:10	SBC-3	579	7.68	80	6.5	15
8/31/07 13:25	Nissler	590	8.37	64	5.3	na

Location	HACH colorimetry			IC-Murdock					
	NO ₂ -N	NH ₄ -N	PO ₄ -P	NO ₂ -N	NO ₃ -N	PO ₄ -P	F	Cl	SO ₄
BTC-1	0.003	<0.02	0.11	<0.1	<0.13	<0.1	0.35	4.3	11.8
BTC-2	0.007	<0.02	0.17	<0.1	0.27	<0.1	0.22	7.9	31.5
BTC-3	0.008	<0.02	0.16	<0.1	1.2	<0.1	0.17	9.5	33.4
Basin	0.006	<0.02	0.06	<0.1	0.30	<0.1	0.19	5.6	44.6
BTC-4	0.018	<0.02	0.18	<0.1	1.4	<0.1	0.29	15.3	37.5
SBC-1	0.0017	<0.02	0.09	<0.1	1.1	<0.1	0.37	17.6	51.1
MT Pole	0.003	<0.02	0.29	<0.5	7.7	<0.5	0.41	50.8	263.2
WWTP	0.451	7.6	1.00	0.59	1.0	0.55	0.29	38.2	40.6
SBC-2	0.261	2.7	0.85	0.32	1.6	0.23	0.43	33.9	132.3
SBC-3	0.208	0.68	0.42	0.27	3.0	0.32	0.44	33.5	131.7
Nissler Bridge	0.007	<0.02	0.45	<0.1	2.7	0.33	0.47	32.1	147.5

Diel Samples of WWTP July 11-12, 2006

Date/time	pH	Temp °C	SC μS/cm	alkalinity CaCO ₃
7/11/2006 8:45	7.21	13.6	532	140
7/11/2006 9:45	7.16	15.8	538	135
7/11/2006 10:00	7.16	15.9	538	136
7/11/2006 12:00	7.15	16.4	536	135
7/11/2006 14:00	7.08	16.5	550	134
7/11/2006 16:00	7.09	17.4	560	136
7/11/2006 19:00	7.03	17.0	563	141
7/11/2006 22:00	7.03	16.6	557	149
7/12/2006 1:00	7.00	16.0	550	143
7/12/2006 4:00	7.03	15.9	545	140
7/12/2006 7:00	7.05	15.8	537	146

Date/time	mg/L, colorimetry				
	NO ₃ -N	NH ₄ -N	NO ₂ -N	Cl	PO ₄ -P
7/11/2006 8:45	1.2	27.6	0.057	0.05	3.86
7/11/2006 10:00	1.1	14.4	0.053	0.1	3.65
7/11/2006 12:00	0.7	11.4	0.054	0.46	3.52
7/11/2006 14:00	0.8	12.3	0.063	1.07	3.65
7/11/2006 16:00	0.8	16.5	0.122	0.19	3.93
7/11/2006 19:00	0.8	15.6	0.232	0.16	4.04
7/11/2006 22:00	0.5	18.3	0.179	0.08	3.65
7/12/2006 1:00	0.4	13.3	0.174	0.04	3.7
7/12/2006 4:00	0.8	14.1	0.231	0.07	1.11
7/12/2006 7:00	0.6	13.1	0.208	0.01	3.33

Diel Samples of SBC-1B July 11-12, 2006

Date/time	pH	temp °C	SC µS/cm	alkalinity CaCO ₃	staff gage	flow
7/11/2006 8:30	7.9	13.6	532	95	0.69	19.1
7/11/2006 10:30	8.4	15.2	517	95	0.67	17.7
7/11/2006 12:30	8.6	17.7	508	93	0.68	18.4
7/11/2006 14:30	8.7	19.4	502	95	0.67	17.7
7/11/2006 17:00	8.7	20.8	501	91	0.67	17.7
7/11/2006 20:00	8.4	19.1	479	96	0.67	17.7
7/11/2006 23:00	7.8	17.4	514	93	0.67	17.7
7/12/2006 2:00	7.7	16.0	519	101	0.66	17.1
7/12/2006 5:00	7.7	15.0	542	97	0.62	14.4

Date/time	mg/L, colorimetry				
	NO ₃ -N	NH ₄ -N	NO ₂ -N	Cl ₂	PO ₄ -P
7/11/2006 8:30	0.5	0.19	0.017	0.02	0.33
7/11/2006 10:30	1.5	0.19	0.017	0.50	0.32
7/11/2006 12:30	1.3	0.47	0.045	0.22	0.37
7/11/2006 14:30	1.4	0.38	0.026	0.03	0.24
7/11/2006 17:00	1.4	0.33	0.011	0.08	0.35
7/11/2006 20:00	1.2	0.09	0.006	0.02	0.31
7/11/2006 23:00	0.7	0.12	0.003	0.01	0.68
7/12/2006 2:00	1.3	0.14	0.008	0.02	0.27
7/12/2006 5:00	2.5	0.06	0.010	0.02	0.2
7/12/2006 8:00	1.4	0.16	0.012	0.01	0.33

Diel Samples of SBC-3 July 11-12, 2006

Date/time	pH	temp °C	SC µS/cm	DO	DO	alkalinity CaCO ₃	staff gage	flow
7/11/2006 9:15	7.75	14.7	522	8.6	103	94	0.46	18.2
7/11/2006 11:00	7.93	17.4	527	10.1	129	103.5	0.52	21.6
7/11/2006 13:00	7.73	19.7	517	8.8	117	NA	0.525	21.9
7/11/2006 15:00	8.11		511	10.5	144	98	0.52	21.6
7/11/2006 18:00	7.46	21.2	515	5.9	81	88	0.5	20.5
7/11/2006 21:10	7.2	18.4	523	2.53	33	95	0.51	21.0
7/11/2006 23:59	7.21	17	525	2.6	33	104	0.5	20.5
7/12/2006 3:00	7.2	15.8	526	2.4	30	106	0.49	19.9
7/12/2006 6:00	7.23	14.8	534	2.6	32	106.9	0.42	16.0

Date/time	mg/L, colorimetry				
	NO ₃ -N	NH ₄ -N	NO ₂ -N	Cl	PO ₄ -P
7/11/2006 9:15	3.5	1.40	0.072	0.13	1
7/11/2006 11:00	2.4	1.85	0.071	0.14	1.25
7/11/2006 13:00	2.3	2.21	0.05	0.2	1.08
7/11/2006 15:00	2.5	1.92	0.146	0.07	1.15
7/11/2006 18:00	2.3	2.00	0.352	0.04	1.37
7/11/2006 21:10	1.6	2.86	0.32	0.02	1.27
7/11/2006 23:59	1.7	2.94	0.25	0.02	1.31
7/12/2006 3:00	1.8	2.61	0.23	0.00	1.06
7/12/2006 6:00	2.1	2.06	0.21	0.01	1.02

time	km below mixing zone	pH	SC	Temp	NH ₄ ⁺ as N	NO ₂ ⁻ as N	NO ₃ ⁻ as N
13:30	0.0	7.15	566	17.7	5.00	0.065	1.1
14:15	0.5	7.24	558	17.7	4.38	0.235	1.5
14:30	1.0	7.19	552	18.5	2.52	0.310	2.1
14:40	1.9	7.30	545	17.2	0.15	0.099	3.1
14:50	2.9	7.75	557	16.2	0.08	0.042	2.4
15:10	4.8	8.75	559	17.5	0.11	0.038	2.8

Appendix A2: ICP-AES analyses of synoptic samples (filtered to 0.2 µm) collected in January 2007. All data in mg/L. PQL = practical quantification limit.

	PQL	B	Ba	Ca	Cu	K	Li	Mg
WWTP		0.17	0.021	27.9	0.02	11.5	0.013	7.9
FAIRMONT		0.06	0.031	57.4	0.03	9.3	0.024	12.4
FAIRMONT-B		0.06	0.031	57.7	0.03	8.9	0.023	12.4
LAO		0.21	0.011	155.7	b.d.	12.1	0.121	40.6
MT. POLE		0.07	0.040	129.8	b.d.	9.4	0.050	29.6
NISSLER		0.10	0.034	51.2	b.d.	9.8	0.024	12.3
SBC-1		0.02	0.051	39.5	b.d.	7.5	0.012	9.7
Opportunity		0.07	0.030	58.1	0.03	8.6	0.026	12.6
SBC-3		0.10	0.034	50.6	b.d.	10.2	0.024	12.2
BTC-4		0.02	0.053	38.6	b.d.	6.7	0.008	9.5
SBC-2		0.10	0.035	50.9	b.d.	9.3	0.024	12.4
	PQL	Mn	Na	P	S	Si	Sr	Zn
WWTP		0.08	38.9	2.43	13.5	9.23	0.15	0.061
FAIRMONT		0.32	29.1	0.34	32.2	12.46	0.32	0.289
FAIRMONT-B		0.32	29.0	0.33	32.5	12.47	0.32	0.288
LAO		0.72	60.7	b.d.	178.0	8.41	1.04	0.033
MT. POLE		b.d.	41.5	0.10	83.5	14.81	0.70	0.004
NISSLER		0.24	31.6	0.75	30.3	10.90	0.32	0.085
SBC-1		0.16	15.9	b.d.	14.6	12.04	0.24	0.044
Opportunity		0.29	29.3	0.32	33.2	12.44	0.32	0.287
SBC-3		0.24	31.3	0.90	30.4	10.52	0.30	0.083
BTC-4		0.05	14.6	b.d.	13.1	12.10	0.22	0.013
SBC-2		0.20	30.4	0.97	30.7	10.60	0.29	0.066

NOTE: The following elements were analyzed but were below detection (PQL shown in parentheses): As (0.028), Cd (0.004), Fe (0.1), Mo (0.01), Ni (0.01), Pb (0.09).

Appendix A3: QA/QC

Table A3-1 contains values of standards measured with the HACH spectrophotometer. The ammonia and phosphate values all agreed within 0.2 mg/L or less. The nitrate values were at times greater than 1.0 mg/L off. Independent checks of samples by HACH and ion chromatography (IC) showed that the HACH method was unreliable. Therefore nitrate values starting in August were taken from the IC rather than the HACH. Table A3-2 shows laboratory duplicates measured with the HACH spectrophotometer. Again, these results show poor reproducibility for the HACH nitrate method, and therefore the IC was used for nitrate analysis beginning in August 2006.

Table A3-1. Measurement of standards (all units in mg/L as N or as P)

Nutrient	Date	Conc. Standard	Conc. Measured	difference
Ammonia	5/18/2006	1.2	1.1	0.1
Ammonia	6/30/2006	1.0	1.0	0.0
Ammonia	6/30/2006	2.0	2.1	0.1
Ammonia	5/31/2007	1.0	0.80	0.2
Nitrate	9/25/2006	0.50	0.70	0.2
Nitrate	9/25/2006	0.05	0.10	0.0
Nitrate	9/25/2006	0.11	0.20	0.1
Nitrate	9/25/2006	0.16	0.30	0.1
Nitrate	12/18/2006	0.27	0.30	0.0
Nitrate	5/18/2006	3.0	3.1	0.0
Nitrate	6/30/2006	10.0	7.3	2.7
Nitrate	6/30/2006	1.0	1.1	0.1
Nitrate	7/11/2006	2.0	1.0	1.0
Nitrate	7/11/2006	3.0	1.7	1.3
Phosphate	12/18/2006	1.0	1.1	0.1
Phosphate	5/31/2007	1.0	1.2	0.2

Table A3-2. Laboratory duplicates. All data in mg/L as N or P.

Nutrient	Date	Site	Measurement	Duplicate	Difference
Ammonia	7/11/2006	SBC-3	1.9	1.9	0.1
Ammonia	10/10/2006	WWTP	19.0	15.3	3.7
Ammonia	12/18/2006	MT Pole	0.00	0.00	0.00
Ammonia	12/18/2006	SBC-2	7.4	6.7	0.7
Nitrate	7/11/2006	WWTP	0.70	1.10	0.40
Nitrate	8/8/2006	MT Pole	5.0	4.5	0.5
Nitrate	10/10/2006	WWTP	0.70	0.90	0.20
Nitrite	7/11/2006	SBC-3	0.15	0.14	0.01
Nitrite	7/11/2006	SBC-3	0.35	0.35	0.00
Nitrite	7/11/2006	SBC-3	0.25	0.25	0.01
Nitrite	8/8/2006	BTC-4	0.03	0.02	0.01
Nitrite	10/10/2006	SBC-2	0.04	0.03	0.00
Nitrite	12/18/2006	Nissler	0.07	0.07	0.00
Nitrite	8/29/2007	SBC-3	0.20	0.22	0.02
Phosphate	5/22/2006	LAO	0.09	0.09	0.00
Phosphate	1/29/2007	SBC-2	3.0	2.9	0.1

Table A3-3 shows field duplicates that were taken and analyzed as separate samples with the HACH spectrophotometer. All duplicate samples gave values for all nutrients within 0.04 mg/L.

Table A3-3. Field duplicates

Nutrient	Date	Site	Measurement	Duplicate	Difference
Ammonia	5/31/0007	Basin Creek	0.11	0.08	0.03
Nitrite	5/31/0007	Basin Creek	0.00	0.00	0.00
Phosphate	5/31/0007	Basin Creek	0.45	0.49	0.04
Ammonia	8/29/2007	Nissler	-0.02	-0.05	0.03
Nitrite	8/29/2007	Nissler	0.02	0.02	0.00
Phosphate	8/29/2007	Nissler	1.4	1.4	0.0

For samples with high PO₄ concentration it was possible to get independent analyses of PO₄ from the HACH spectrophotometer as well as by IC. Figure A3-1 shows a generally good agreement between the two methods, although the HACH values overall were slightly higher than those from the IC. From personal communication with the Murdock laboratory manager (Heiko Langner) it was found that the IC-PO₄ numbers have a large associated uncertainty due to overlaps on the IC column with more abundant solutes. Therefore, the HACH results were used in this study. It was also possible to get independent checks on nitrite by HACH and IC (Fig. A3-2). In general the results were well-correlated, but the HACH numbers were consistently lower than the IC values. The most likely reason for the discrepancy is the longer holding times for the IC compared to the HACH analyses. Ammonia is unstable in the presence of oxygen, and therefore it is almost certain that some oxidation of ammonia to nitrite occurred during storage and prior to IC analysis.

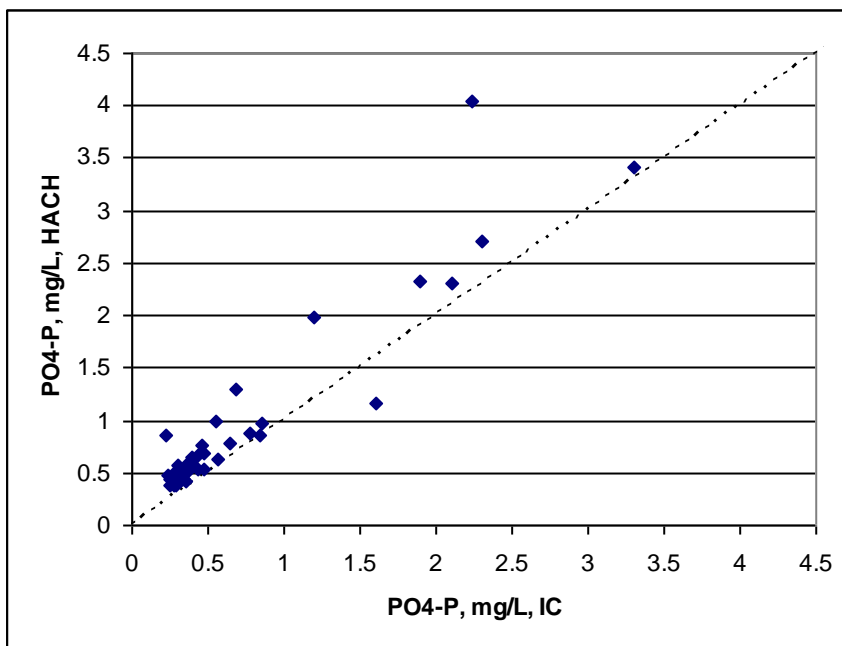


Figure A3-1: Phosphate comparison IC and HACH

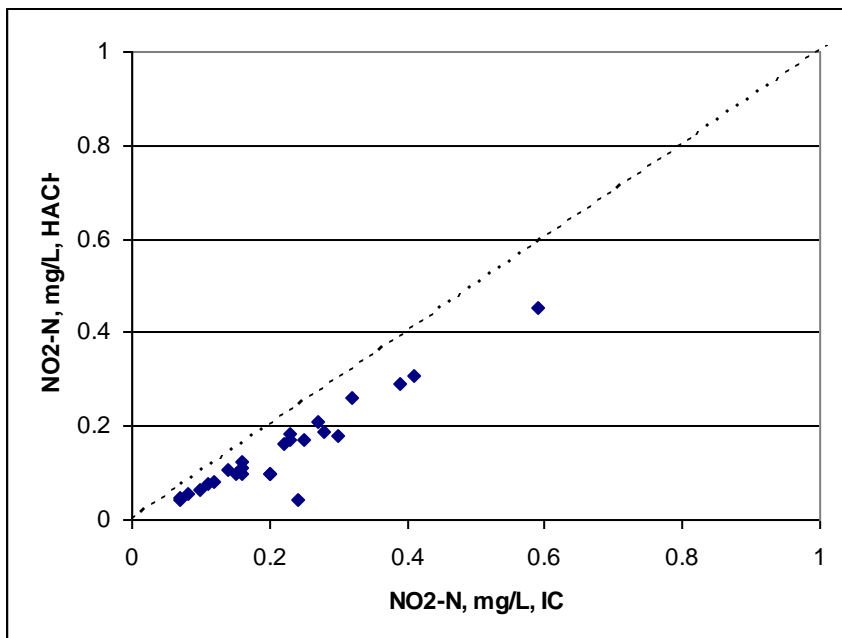


Figure A3-2. Nitrite comparison IC and HACH

Historical and Future Streamflow Related to Small Mountain Glaciers in the Glacier Park Region, Montana

Basic Information

Title:	Historical and Future Streamflow Related to Small Mountain Glaciers in the Glacier Park Region, Montana
Project Number:	2007MT148B
Start Date:	3/1/2007
End Date:	2/28/2009
Funding Source:	104B
Congressional District:	At large
Research Category:	Climate and Hydrologic Processes
Focus Category:	Climatological Processes, Water Supply, Models
Descriptors:	
Principal Investigators:	Joel Harper

Publication

1. Meierbachtol, T W, J.T. Harper, J.N. Moore, 2007, Modeling Spring Snowmelt Dynamics in a Northern Rockies Basin using a Modified Temperature-Index Model, Eos Trans. AGU, 88(52), Fall Meet. Suppl., Abstract C21B-0475.
2. Bleha, J. A. and J.T. Harper, 2007, Snowmelt Water Generation in a Large Mountain Basin of Northwest Montana from a MODIS Driven Model, in M. Gribb, editor, Proceedings of Symposium on Environmental Sensing, Oct. 25-26, 2007, Boise Id, Inland Northwest Research Alliance Inc., p. 83-86.
3. Reardon, B.A., J.T. Harper, and D.B. Fagre, 2008, Mass balance of a cirque glacier in the U.S. Rocky Mountains, Proceedings of The Mass Balance Measurement and Modeling Workshop, 26-28 March 2008, Skeikampen, Norway, International Glaciological Society, p. 1-5.
4. Reardon, B.A., J.T. Harper, and D.B. Fagre, 2008, Volume and Surface Mass Balance Changes of Sperry Glacier, Glacier National Park, Montana, Abstracts Mountain Climate Research Conference, Silverton, Colorado, Consortium for Integrated Climate Research in Western Mountains.
5. Kramer, M., and J. T. Harper (2007), Historical Changes in Streamflow Related to Small Mountain Glaciers in the Glacier Park Region, Montana, U.S.A., paper presented at Workshop on Glaciers in Watershed and Global Hydrology, International Commission for Snow and Ice Hydrology, IAHS, Obergurgl, Austria.
6. Nathan Taylor, UM Geosciences. Ice Volume Changes in Sperry Glacier, Glacier National Park, From 1950-2007 Completed: 5/2008

Historical and Future Streamflow Related to Small Mountain Glaciers in the Glacier Park Region, Montana

Funded by U.S.G.S 104b program, Montana Water Center

Joel Harper
Department of Geosciences
University of Montana

Final Report - April 25, 2009

ABSTRACT

This research focused on long term change in water runoff from Sperry Glacier, Glacier National Park, Montana. Research activities followed three main avenues of investigation. 1) Field measurement of present day surface mass balance. Measurements were made over water years 2005-2008. These data are used to understand factors driving mass balance and how these factors vary across the glacier. Further, these data are used to constrain modeling of historical and future change on the glacier. 2) Modeling of historical mass balance and water runoff of the glacier. 3) Future scenarios of Sperry Glacier's mass balance based on downscaled ocean-atmosphere global circulation model output. In two of the three water years (2005 and 2006) Sperry Glacier had a negative mass balance, while in 2008 the glacier experienced a strongly positive mass balance. The glacier's positive mass balance in 2008 was not associated with 'extreme' cold or wet conditions at high elevations. It was unexpected that conditions resulting in a positive mass balance are not extreme outliers. The timing of the onset of summer melt conditions (i.e., a cold/wet or warm/dry Spring) appear to be important to dictating the summer balance. Modeling shows that substantial change in summer water discharge from Sperry Glacier has occurred since the start of the 20th century. The glacier is likely to persist in some form throughout the 21st century unless the most extreme warming scenarios are realized.

1. Mass Balance for Water Years 2005-2008

1.1 Overview

The annual balance is an estimate of the total change in mass at the glacier surface over a year. For Sperry Glacier, the year is defined as the water year, which runs from October 1 to September 30. The sum of accumulated and ablated mass at a given point on the glacier surface is the point net balance b_n . The mean b_n for all points on the glacier is the annual net balance B_n . It can also be understood as the change in mass at the glacier surface divided by the glacier area.

The point net balance b_n can be calculated for any point for which both b_w and b_s are known by summing the two values. A positive sum represents a net gain in mass at the point, while a negative sum represents a net loss in mass. For Sperry Glacier, a direct calculation of b_n is possible for the ablation stake points each year. The interpolated b_w and b_s values also allow b_n to be estimated for each 10 m cell by summing the two grids. The mean value for the cells approximates the annual net balance B_n . This method for determining B_n can be used for 2005 and 2006 because there were sufficient snow depth measurements to interpolate b_w across the glacier. For 2007 and 2008, B_n is estimated by adding the scaled B_w and the B_s determined through interpolation.

1.2 Methodology

We used two methods for calculating B_n . For 2005 and 2006, grids of interpolated b_w and b_s were both available, allowing calculations of b_n for each of the 10 m cells by summing the two grids. The mean b_n value is equivalent to the B_n for the glacier as a whole. For 2007 and 2008, only one of the two grids was available, the grid of interpolated b_s values. We calculated B_n by summing the B_w value for each year derived via scaling and the B_s value for each year taken from the interpolated grid of b_s values.

1.3 Results for 2005 and 2006 water years

Maps of interpolated b_n for 2005 and 2006 show similar spatial patterns. In both years, the area with the most negative b_n values was near the west margin of the glacier, in the area of crevasses and shallow snow. The areas with the highest values were below the headwall and the cirque walls, while the headwall itself showed both positive and negative mass balances. In both years, most of the lower part of the glacier had b_n values between -1.00 to -2.00 m w.e. However, while the line where accumulation and ablation are equal – the zero contour – was at different elevations in the two years. In the basin below the headwall, the line was between 2500 and 2550 m elevation both years but in 2006 the line was lower and extended northeast under the cirque wall whereas in 2005 there were only a few patches of positive mass balance under the cirque wall.

The maps also showed that the two years had very different accumulation- area ratio (AAR). This measure is the ratio of the area in which the b_n is positive to the area of the entire glacier surface. For the glacier area in the denominator of this ratio we used the total area of the interpolated cells – 0.828 km² - which is slightly smaller than the actual area of the glacier - 0.841 km². The AAR for 2005 was 0.08, only 1/3 the of 2006 value of 0.24. Both values are well below the ratio of 0.6-0.7 considered typical of a glacier with a positive mass balance.

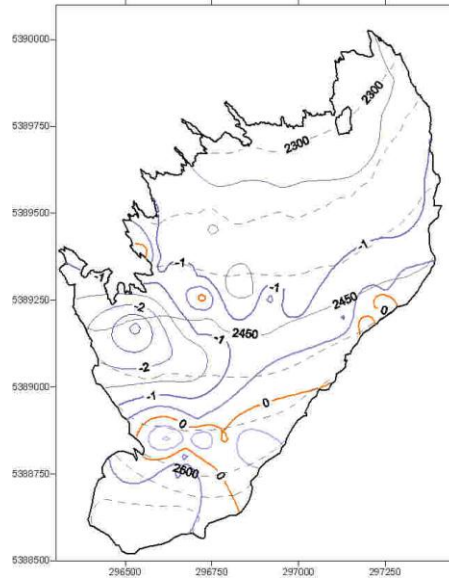


Figure 1. Contour map of 2005 calculated b_n values and surface elevations. Blue contours depict b_n in 0.5 m w.e. contour intervals, with orange line marking line of zero balance. Grey lines depict surface elevation in 50 m intervals, with solid dark line marking approximate mean elevation of glacier.

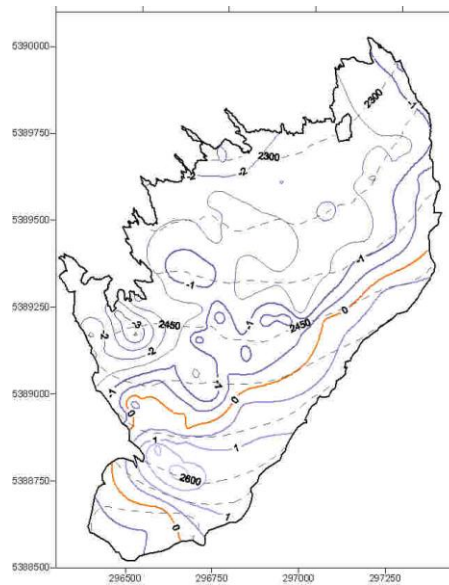


Figure 2. Contour map of 2006 calculated b_n values and surface elevations. Blue contours depict b_n in 0.5 m w.e. contour intervals, with orange line marking line of zero balance. Grey lines depict surface elevation in 50 m intervals, with solid dark line marking approximate mean elevation of glacier.

The differences between the 2005 and 2006 interpolated b_n values were greatest at the extremes. The median values for the two years were nearly identical, as were the 75th-percentile values, with the 25th percentile values similar. Thus the middle 50% of the values were both similar and similarly distributed. For the other two quartiles, particularly the uppermost quartile, the two year's values were more different. In 2005, the mean and median values were with 0.05 m w.e.; in 2006, the mean was considerably further from the median and closer to the 75th percentile.

In 2005, the glacier lost $8.88 \times 10^5 \text{ m}^3$ water while gaining just $2.3 \times 10^4 \text{ m}^3$, for a net volume change of $-8.65 \times 10^5 \text{ m}^3$ of water. Dividing that net change by the gridded area results in an annual net balance B_n for the year of -1.04 m w.e. That figure is slightly lower than the mean interpolated b_n due to the equation used to determine volume on the grid; the latter is likely a slightly better estimate of b_n because the math is simpler.

The volume of water lost at the glacier surface in 2006 was $8.53 \times 10^5 \text{ m}^3$, only slightly lower than in 2005. The volume gained, however, was $1.54 \times 10^5 \text{ m}^3$, 6.5 times greater than in the prior year. The resulting net change for the year was $-6.99 \times 10^5 \text{ m}^3$ of water, for an annual net balance of -0.84 m w.e. The mean b_n of -0.81 was slightly more positive and is again a slightly better estimate of B_n .

1.4 Results 2007 and 2008 water years

For these two years, computing the B_n required subtracting the interpolated B_s from the B_w value derived by scaling. However, the ablation stake data provided measured b_w values that could be included in the scaling, so the B_w estimate was revised (Table 1). The revised B_w values were each 0.04 m w.e. greater than the previous versions, but the increases seem reasonable. The 2005 value is still within 3% of the interpolated value, and the mean measured b_w for 2007 and 2008 are almost certainly underestimate the actual values.

Table 1	2007	2008
Scaled B_w	2.35	3.08
Interpolated B_s	-3.97	-2.36
$B_w - B_s$	-1.62	0.72
Mean stake b_w	2.44	3.18
Mean stake b_s	-3.97	-2.4
Mean stake b_n	-1.53	0.78
Total Grid Area (m^2)	808900	808900
Net delta	-	
Volume (m^3)	1309090	584952

Without interpolating values we cannot compare spatial patterns with previous years, but other comparisons are possible. Multiplying the total grid area for the B_s

computations – slightly smaller than the grid used for the previous two years – by the B_n provides an estimate of net volume change for the glacier in each of the two years. In 2007, the glacier lost a net volume of $1.31 \times 10^6 \text{ m}^3$ of water – 86% more than the previous year. In contrast, the glacier gained $5.85 \times 10^5 \text{ m}^3$ of water.

1.5 Cumulative Balance:

Over the four years of study, an average of 10.4 m w.e. accumulated at any given point on the glacier surface, but 13.11 m w.e. was ablated over the same period (Table 2). The cumulative mass balance for the four years was -2.77 m w.e., with a mean annual balance of -0.69 m w.e. The average volume change each year was $-5.72 \times 10^5 \text{ m}^3$ of water, for a net volume change over the period was $-2.29 \times 10^6 \text{ m}^3$.

Table 2.

	2005	2006	2007	2008	Cumulativ e Sum	Annual Mean	Range
B_w (m w.e.)	2.18	2.79	2.35	3.08	10.4	2.60	0.9
B_s (m w.e.)	-3.18	-3.60	-3.97	-2.36	-13.11	-3.28	1.61
B_n (m w.e.)	-1.06	-0.81	-1.62	0.72	-2.77	-0.69	2.34
Net D	-	-	-	58495	-	-	189404
Volume (m ³)	864819	698469	1309090	2	-2287426	571857	2

2. Historical Change in Sperry Glacier

2.1. Change in Runoff over the 20th Century

Direct measurements of runoff from Sperry Glacier (or any other GNP glacier) are not available. We employ two methods to compute present day summer ablation from the glacier and make the assumption that all ablation results in runoff. First, we employed a distributed energy balance model, adjusted from Brock and Arnold (2000), using data from an on-site meteorological station. This modeling supports the notion that little ablation results from sublimation or evaporation and that shortwave energy is the dominant source for melting the ice. Second, we made direct measurement of surface melt using an ablation stake network and continuous measurements of melt at a single point with a sonic ranger. Ablation measurements showed daily melt rates averaged 56 to 59 mm w.e. during summer and revealed little to no elevation gradient along the glacier. The distributed energy balance model slightly underestimated the daily melt, and had a

tendency to produce a stronger elevation gradient in the melt rate than indicated by direct observations.

We examined scenarios for runoff from Sperry Glacier in 1850 by employing a numerical reconstruction of the glacier (Figure 2). We used a cellular automata technique which includes rules for surface accumulation and ablation, including snow accumulation from avalanching off the cirque walls, and down-valley mass transfer by glacier motion (Harper and Humphrey, 2003). Here we focus on one end-member scenario that considers no change in the glacier's accumulation gradient (only increased ablation due to warming) between 1850 and present. This assumption along with the modeled annual mass balance gradient yields a solution for the 1850 summer ablation along the glacier.

Total melt runoff from Sperry Glacier in 1850 is estimated to be $17 \times 10^6 \text{ m}^3$. Our methods and assumptions suggest summer runoff from Sperry Glacier has decreased on the order of 75%, from approximately $17 \times 10^6 \text{ m}^3$ in 1850 to approximately $4.3 \times 10^6 \text{ m}^3$ in 2005. Such a reduction has likely had a significant impact on basin ecological systems and represents an important water resource to local downstream users in this dry summer climate regime.

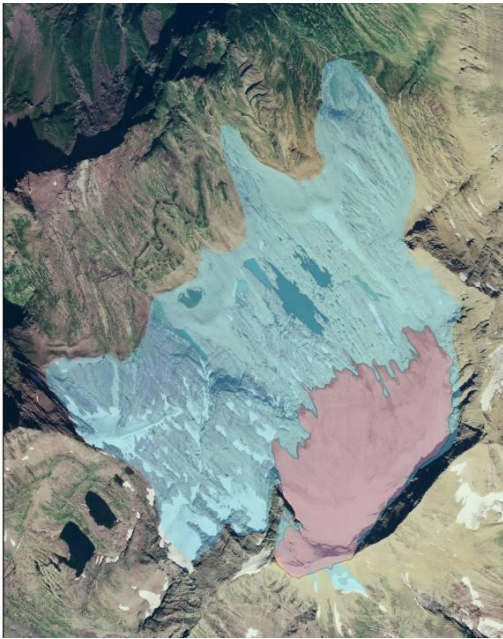


Figure 3. Satellite image of Sperry Glacier showing extent of the glacier in 1850 (blue) and 2007 (red).

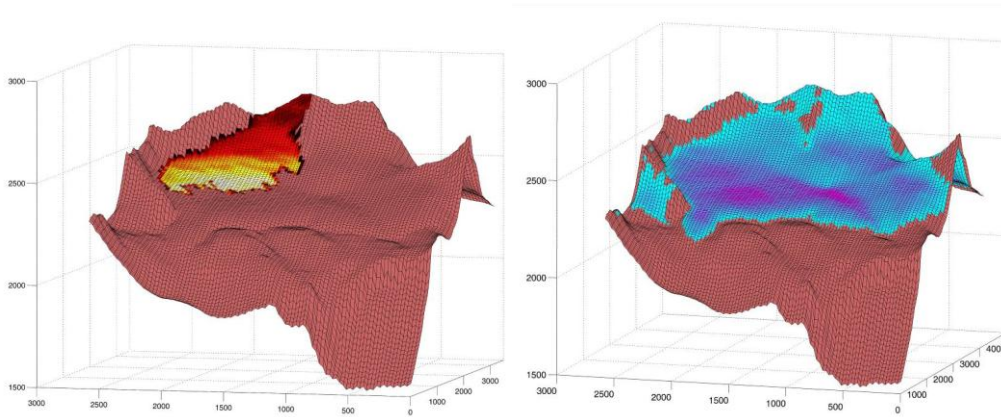


Figure 4. Modeled geometry and mass balance of Sperry Glacier. Left panel shows 2007 extent of the glacier. Colors indicate surface mass balance from a spatially distributed energy balance model. Hotter colors indicate more negative mass balance. Right panel shows 1850 geometry of the glacier from a cellular automata model and a spatially prescribed net mass balance.

2.2. Ice Volume Changes 1950-2007

Digital elevation models of Sperry Glacier were constructed from two USGS topographic maps based on surveys of the glacier conducted in 1950 and 1960. A third digital elevation model was produced from data collected during a 2007 survey of the glacier’s surface and surrounding rock margin. This latter survey was done with a kinematic GPS survey system utilizing an established local base station and a rover outfitted with Trimble R7 receivers. Post processing of these data allowed for cm-scale vertical and horizontal accuracy. Digital elevation models were gridded into 10m² cells via a standard Kriging algorithm. The grids were differenced in order to calculate volume changes between the survey years.

These results provide insight into the rate of ice volume loss of glaciers in Glacier National Park, and constitute figures from which mass balance values could be derived and then compared to current on-going field measurements. The implications of this research are highly relevant at both local and global scales. Locally, up to 75% of water resources in the Rocky Mountain West come from mountain snow, with glaciers filling an important niche as storage reservoirs that provide water during the late summer drought typical for the region. Global scale implications include insight into the fate of runoff from small mountain glaciers. These glaciers are the dominant contributor to current worldwide sea level rise, though the functions by which this is occurring are not yet fully understood.

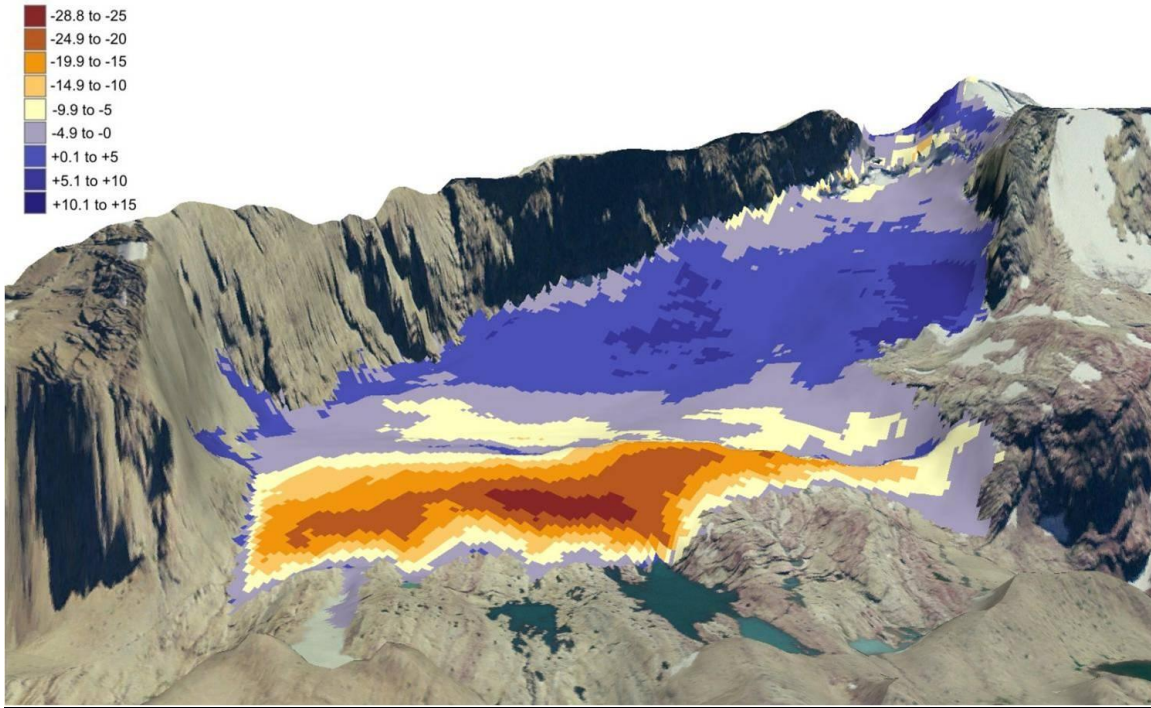


Figure 5. Ice volume change of Sperry Glacier, 1950-1960. Hot colors show areas of glacier thinning ($-5.4 \times 10^6 \text{ m}^3$); cold colors show areas of glacier thickening ($+1.4 \times 10^6 \text{ m}^3$).

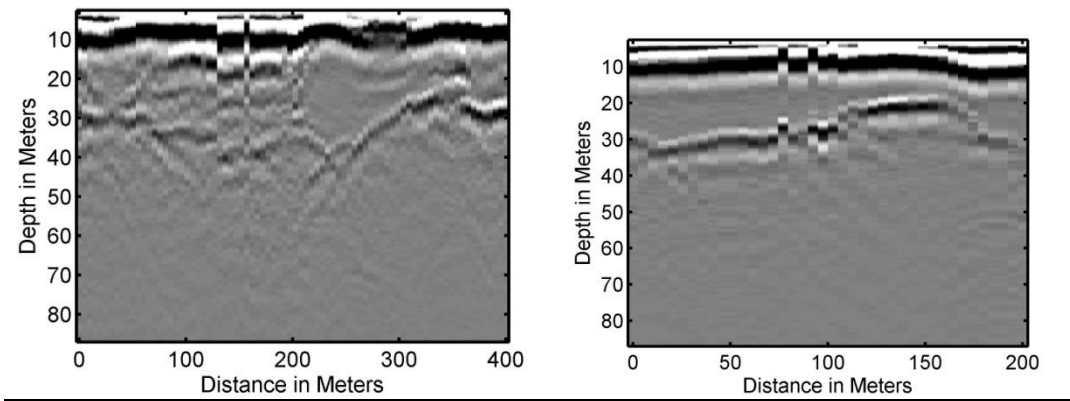


Figure 6. Example ice penetrating radar transects of Sperry Glacier collected in 2008. Radar data were used to map the glacier bed and compute the present day ice volume.

3. 21st Century Change

We use a simplified glaciological model to determine the minimum regional change in climate that would be needed to completely melt Sperry Glacier. Although any single mountain glacier has no measurable influence globally, Sperry Glacier is important because it is used as a Benchmark for climate change in the mountainous areas of the northern Rocky Mountains. This modeling is not intended to be a predictive model for the future of Sperry Glacier, but rather is an investigation of the range of conditions under which Sperry Glacier may undergo significant change or perhaps disappear. We used a cellular automata approach to model coupled ice flow and surface mass balance conditions. Mass balance is modeled as a change from current measured conditions (see above) using downscaled global circulation model output for the 21st century. We determine that it is likely that Sperry Glacier will persist through the year 2100 if regional temperature changes do not increase more than 1^o C, however, if temperature increases 4 or more degrees C by 2100 our model indicates total ablation of Sperry is likely by 2100.

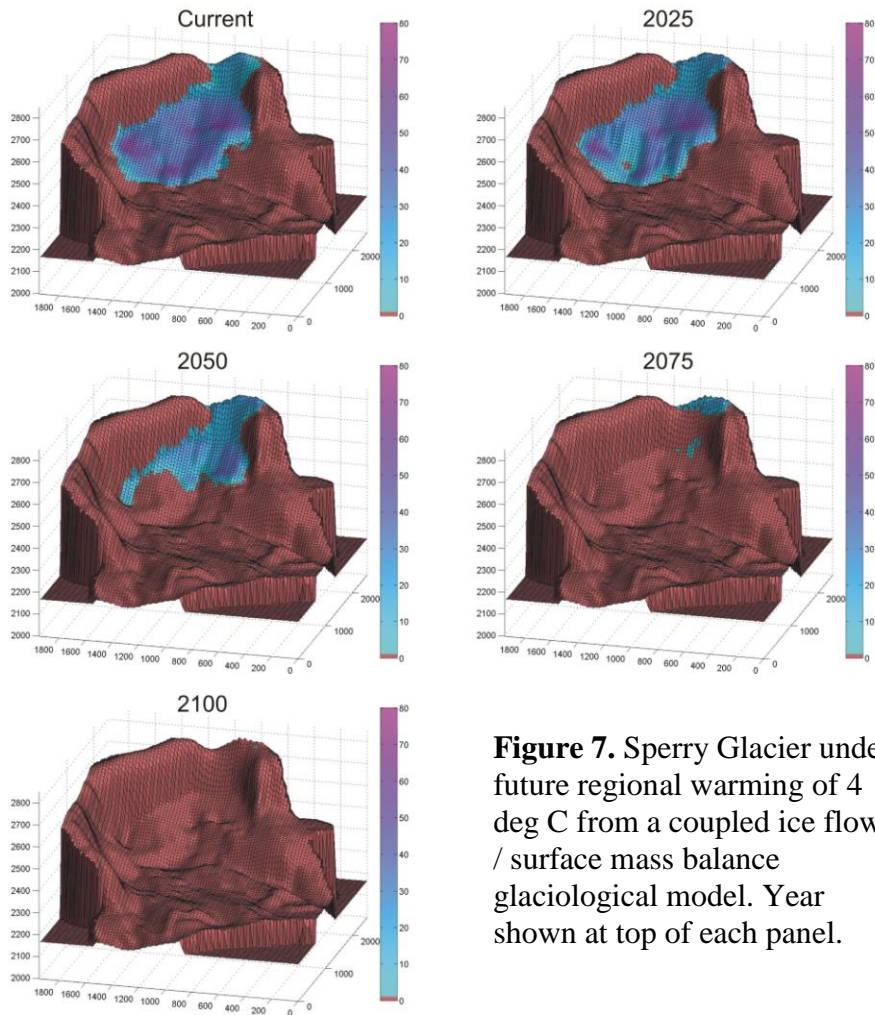


Figure 7. Sperry Glacier under future regional warming of 4 deg C from a coupled ice flow / surface mass balance glaciological model. Year shown at top of each panel.

Students Involved In (And Supported By) This Research

Joel Brown, Ph.D. candidate, Geophysics

Michiel Kramer, Ph.D. candidate, Geosciences

Blase Reardon, M.S. candidate, Geosciences

Nathan Taylor, undergraduate senior, Geosciences

James St. Clair, undergraduate senior, Geosciences and Physics

Public Outreach Involving This research

- Presentation. “Role of Ice Movement in the Response of Glacier Park Glaciers to Climate Change” Waterton-Glacier Parks Science and History Day, July 27, 2006.
- Invited guest speaker, Big Sky Science Partnership Summer Institute, June 19, 2008
- Presented an afternoon session on Climate Change and Climate Science Research to ~45 middle school teachers.
- Keynote Address (1 hr banquet address) “Glacier Melt and Sea Level Rise: Myths, Realities and Wildcards”, NOAA Great Divide Weather Workshop, Great Falls, MT. October 4, 2007.
- Invited Presentation, Glacier-Waterton Peace Park Science Symposium “From Glacier Park to Greenland: Why Small Glaciers Matter to Sea Level Rise”. July 22, 2008.

Undergraduate Senior Thesis

Nathan Taylor, UM Geosciences. “Ice Volume Changes in Sperry Glacier, Glacier National Park, From 1950-2007” Completed: 5/2008

Conference Presentations and Publications

Kramer, M., and J. T. Harper (2007), Historical Changes in Streamflow Related to Small Mountain Glaciers in the Glacier Park Region, Montana, U.S.A., paper presented at Workshop on Glaciers in Watershed and Global Hydrology, International Commission for Snow and Ice Hydrology, IAHS, Obergurgl, Austria.

Reardon, B. A., J. T. Harper, and D. B. Fagre (2008), Mass Balance Sensitivity Of Cirque Glaciers In The Northern U.S. Rocky Mountains, Montana, U.S.A, in Workshop on mass balance measurements and modeling, edited by J. O. Hagen, et al., pp. 1-5, International Glaciological Society, Skeikampen, Norway.

Reardon, B.A., J.T. Harper, and D.B. Fagre, 2008, Climatic And Topographic Influences On The Mass Balance Of A Receding Cirque Glacier, Glacier National Park, Montana, Mountain Climate Research Conference, Silverton Colorado, Consortium for Integrated Climate Research in Western Mountains.

Moore, J. N., J. T. Harper, W. W. Woessner, and S. Running (2007), Headwaters of the Missouri and Columbia Rivers WATERS Test Bed site: Linking Time and Space of Snow Melt Runoff in the Crown of the Continent, Eos Trans. AGU, 88(52), Fall Meet. Suppl., Abstract H13A-0964.

Predictive Modeling of Snowmelt Dynamics: Thresholds and the Hydrologic Regime of the Tenderfoot Creek Experimental Forest, Montana

Basic Information

Title:	Predictive Modeling of Snowmelt Dynamics: Thresholds and the Hydrologic Regime of the Tenderfoot Creek Experimental Forest, Montana
Project Number:	2007MT150B
Start Date:	3/1/2007
End Date:	2/28/2009
Funding Source:	104B
Congressional District:	At Large
Research Category:	Climate and Hydrologic Processes
Focus Category:	Hydrology, Climatological Processes, Models
Descriptors:	
Principal Investigators:	Lucy Marshall, Brian Leonard McGlynn, Tyler Smith

Publication

- Jencso, K. J., B. L. McGlynn, M. N. Gooseff, S. M. Wondzell, and K. E. Bencala. 2009. Hydrologic Connectivity Between Landscapes and Streams: Transferring Reach and Plot Scale Understanding to the Catchment Scale, *Water Resources Research*. doi:10.1029/2008WR007225.
- Smith, T. J., and L. A. Marshall (2008), Bayesian methods in hydrologic modeling: A study of recent advancements in Markov chain Monte Carlo techniques, *Water Resources Research*, 44, W00B05, doi:10.1029/2007WR006705.
- Smith, T. J., and L. A. Marshall (2009), Exploring uncertainty and model predictive performance concepts via a modular snowmelt-runoff modeling framework, *Environmental Modelling & Software*, Under Review
- Smith, T. J. 2008. A Conceptual Precipitation-Runoff Modeling Suite: Model Selection, Calibration and Predictive Uncertainty Assessment. M.S. thesis, Montana State Univ., Bozeman, MT.
- Smith, T. J., and L. A. Marshall. 2008. Development and Application of a Parsimonious Snow-Hydrologic Modeling Suite: Investigating the Link Between Model Complexity and Predictive Uncertainty. *Eos Trans. AGU*, 89(53), Fall Meet. Suppl. AGU Fall Meeting 2008. December 15-19. San Francisco, California.
- Jencso, K. J., B. L. McGlynn, M. N. Gooseff, S. M. Wondzell, and K. E. Bencala. 2009. Hydrologic Connectivity Between Landscapes and Streams: Transferring Reach and Plot Scale Understanding to the Catchment Scale, *Water Resources Research*. doi:10.1029/2008WR007225.

Final Report for USGS 104b Grant: Predictive Modeling of Snowmelt Dynamics: Thresholds and the Hydrologic Regime of the Tenderfoot Creek Experimental Forest, Montana

Principal Investigators:

Lucy Marshall, Assistant Professor of Watershed Analysis, Department of Land Resources and Environmental Sciences, Montana State University.

Brian McGlynn, Associate Professor of Watershed Hydrology, Department of Land Resources and Environmental Sciences, Montana State University.

Abstract

This project was aimed at advancing understanding of the first-order controls on snowmelt runoff processes for improved forecasting and water resource management. The need for this improved insight is particularly relevant given our reliance in the inland northwest region on mountain water resources, and our relatively poor understanding of thresholds and controls on runoff generation in mountain environments. We addressed these themes via a synthesis of field observations, data analyses and conceptual model development. We undertook our activities at a regional test watershed, the Tenderfoot Creek Experimental forest, located in the Little Belt Mountains in central Montana.

Our field observations and modeling approaches provided insight to the variables controlling runoff source areas and the utility of different data for quantifying these. Our analyses indicated topographic controls on runoff and the variability of this through time. We implemented a modular suite of 30 model structures to assess the relative importance of different elements of watershed runoff. Our results emphasize the importance of characterizing the spatial distribution of snowmelt (strongly correlated to aspect and elevation), and its temporal variability according to climatic indicators such as temperature and radiation. These results are transferable to other catchments and will help guide future conceptual models of watershed behavior in mountainous regions.

A self-contained graphical user interface was developed to integrate the modeling framework and associated analyses into a freely available modeling software package. The Simulation and Prediction Lab for Analysis of Snowmelt Hydrology (SPLASH) has been successfully programmed to perform model selection, parameter calibration, uncertainty analysis, and model evaluation.

This project provided training for two graduate students in field hydrology methods and modeling. These students were highly productive and successful over the duration of the project. Additionally, three journal manuscripts and numerous presentations disseminated the main scientific findings of this project to the greater scientific community.

Introduction and Overview

In mountainous areas across the western United States including Montana, winter snowpack controls regional water resources, supplying water to downstream, lower elevation valleys partially because of

reduced evaporation, greater water deposition, and storage until spring snowmelt. To date, little research has been conducted in the Montana region on the linkages between snow accumulation, melt timing, topographic structure, runoff source areas, and streamflow residence time. Although there is a strong desire to more efficiently predict and model snowmelt driven streamflow yield and timing, the primary controls on watershed runoff and flow dynamics are poorly understood.

Forecasting watershed response to incident and accumulated precipitation is more easily achieved via the use of simulation modeling. Such hydrological models play an important role in testing our understanding of the watershed response to precipitation, whether it is to elucidate more information on the unobservable processes occurring or to simulate past or future scenarios for better water resource management. In recent years, hydrologic modelers have increasingly recognized the importance of incorporating uncertainty in the modeling process. Modeling by its nature is only an approximation of the processes occurring and significant uncertainties arise in mathematically expressing complex non-linear watershed dynamics.

This project aimed to improve understanding and quantitative modeling of snow accumulation and melt, watershed streamflow generation, and the effect of watershed topographic structure on watershed processes. We focused our efforts on continued data collection, isotopic analyses of streamflow residence times, and conceptual model comparisons.

Research was conducted at Tenderfoot Creek Experimental Forest (TCEF). The TCEF was established in 1961, and consists of seven gauged watersheds (Figure 1). The forest is representative of the vast expanses of lodgepole pine found east of the continental divide and is the only USDA experimental forest formally dedicated to research on subalpine forests on the east slope of the northern Rocky Mountains.

Objectives

1. To synthesize extensive existing field observations at the Tenderfoot Creek Experimental Forest into a conceptual predictive modeling framework evaluating the first order controls on spatio-temporal runoff dynamics, new snowmelt/old groundwater runoff partitioning and the impact of terrain and forest practices.

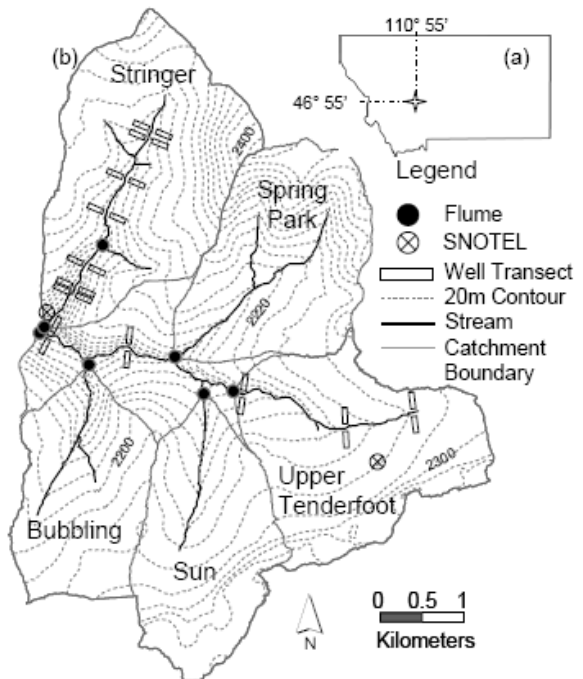


Figure 1. Site location and instrumentation of the TCEF catchment. (a) Catchment location in the Rocky Mountains, MT. (b) Catchment flumes, well transects, and SNOTEL instrumentation locations. Transect extents are not drawn to scale.

2. To initiate watershed tracer experiments quantifying new snowmelt runoff direct contributions to streamflow and resident (old) groundwater contributions to spring runoff across sub-watersheds to explicate the residence time of new water within in each of 7 watersheds and better inform conceptual model underpinnings.

Methodology

This project focused on three main activities: hydrometric and isotopic data collection, analysis of detailed field measurements to inform conceptual modeling, and implementation of a modular predictive modeling framework.

Hydrologic Data Collection

This project helped support existing infrastructure and allowed for new data collection at the project test watershed. Under this project, continuing data collection included:

Stream flow

- Monitored discharge at the outlets of 7 nested watersheds

- Monitored real time specific conductance and temperature at 8 locations

Wells and piezometers

- Installed (many existing) and monitored (real-time water level data collection)

 - 100 wells

 - 20 piezometers

Lysimeters

- Installed recording snowmelt lysimeters

Rainfall

- Built and installed an incremental rainfall sampler

- Monitored 5 existing recording rain gauges

We additionally collected water samples for isotopic, dissolved organic carbon (DOC), and major ion analysis from stream flumes, groundwater wells, piezometers, snow and soil lysimeters, and rainfall sampler.

Data Analyses

Since the project inception (and following reviewer comments), the project evolved to consider topographic and water table data (additional to isotopic analyses) to help inform conceptual model underpinnings and to address major project objectives. In steep headwater catchments with shallow soils, topographic convergence and divergence is a hypothesized first-order control on the distribution of soil water and groundwater. Additionally, hillslope-riparian water table connectivity represents the linkage between the dominant catchment landscape elements (hillslopes and riparian zones) and the channel network. To explore these concepts, we combined digital elevation model (DEM) based terrain analyses with high frequency water table measurements. Using these, we tested the relationship between watershed topography and hillslope-riparian- stream shallow groundwater connectivity.

We quantified water table connectivity (Figure 2) based on 146 recording wells and piezometers distributed across transects within Tenderfoot Creek.

Correlations were observed between the longevity of water table connectivity and the size of each transect's upslope accumulated area (Jencso et al., 2009). We

applied this relationship to the entire stream network to quantify landscape scale connectivity through time and determine its relationship to catchment scale runoff dynamics. We found that the shape of the estimated annual landscape connectivity duration curve was highly related to the catchment flow duration curve (Figure 2). This research suggests internal catchment landscape structure (topography and topology) as a 1st order control on runoff source area and whole catchment response characteristics.

We made additional analyses of isotopic data to discretize new (snowmelt runoff) and old (groundwater) contributions to streamflow. The model we implemented computes transfer functions for event water and pre-event water calculated from a time-variable event water fraction (Weiler et al., 2003). This undertaking helped to identify several obstacles in using traditional residence time analyses for a watershed system such as TCEF. The biggest stumbling block to these analyses is adequately characterizing the

snowmelt contribution to runoff, due to the strong spatial variability of snow melt patterns across the watershed. Figure 3 illustrates the inability of classical transfer function models to capture patterns of

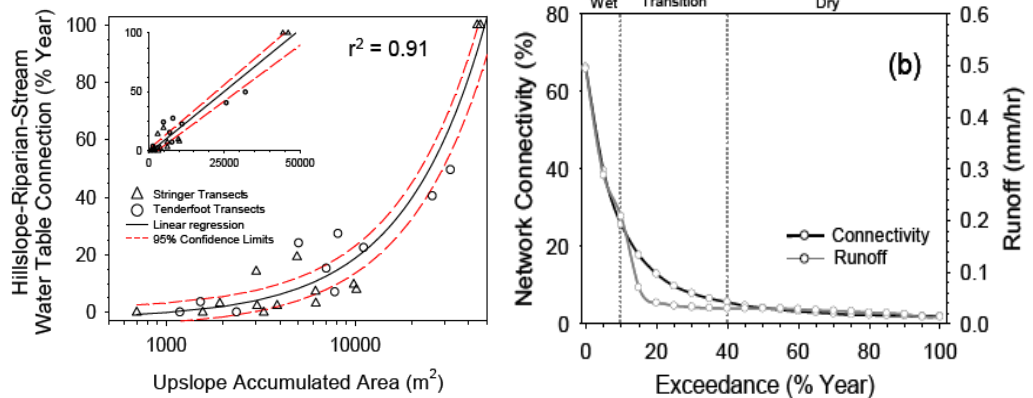


Figure 2. A) Upland-stream water table connectivity as a function of upslope accumulated area. This relationship defines the fraction of the stream network hydrologically connected to uplands and can be used either as a spatially explicit variable or as a space-time distribution. B) Flow duration curve and fractional upland stream connectivity curves for one TCEF subwatershed. Note relationship between connectivity and discharge.

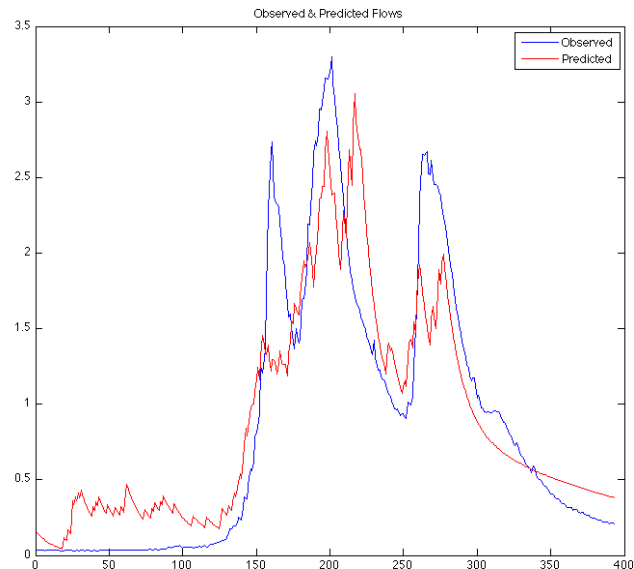


Figure 3. Observed and predicted streamflow from runoff component of residence time model

runoff. These findings helped support conceptual model methodologies (detailed following). Our project evolved to focus on characterizing the variability in snow melt rates due to elevation and aspect across the watershed.

Modeling

We developed and implemented a modular modeling framework that applies model parameter estimation and uncertainty analysis quantification for a range of hydrologic models. We applied the modeling framework using existing observations from the Stringer Creek watershed, located within TCEF. Thirty unique modular structures, ranging in complexity from very simple to moderately complex, were developed and included in the modeling suite. The suite of models was constructed in a modular, component-wise fashion to allow for different conceptualizations of soil moisture accounting, runoff routing, and snowmelt accounting. We used findings from our data analyses to help guide conceptual modeling development, focusing on characterizing spatial variability in snowmelt rates, and spatial variability in runoff source areas.

In implementing the modeling approach we compared three recently developed Markov chain Monte Carlo algorithms necessary to for model calibration (parameter estimation) and uncertainty analysis under a Bayesian inferential approach (Smith and Marshall, 2008). The predictive modeling framework was used to assess the effect of model structural complexity on model predictive performance (Figure 4). We assessed each of the models based on their predictive performance, the uncertainty associated with the model simulations and parameters, and their ability to predict snow water equivalents (Smith and Marshall, 2009).

A self-contained graphical user interface was developed to integrate the modeling framework and associated analyses into a freely available modeling software package. The Simulation and Prediction Lab for Analysis of Snowmelt Hydrology (SPLASH) has been successfully programmed to perform model selection, parameter calibration, uncertainty analysis, and model evaluation. This software package simplifies the complexities required to implement a predictive modeling study and shifts the focus toward the modeling problem itself through the application of forward-looking methods in computational hydrology.

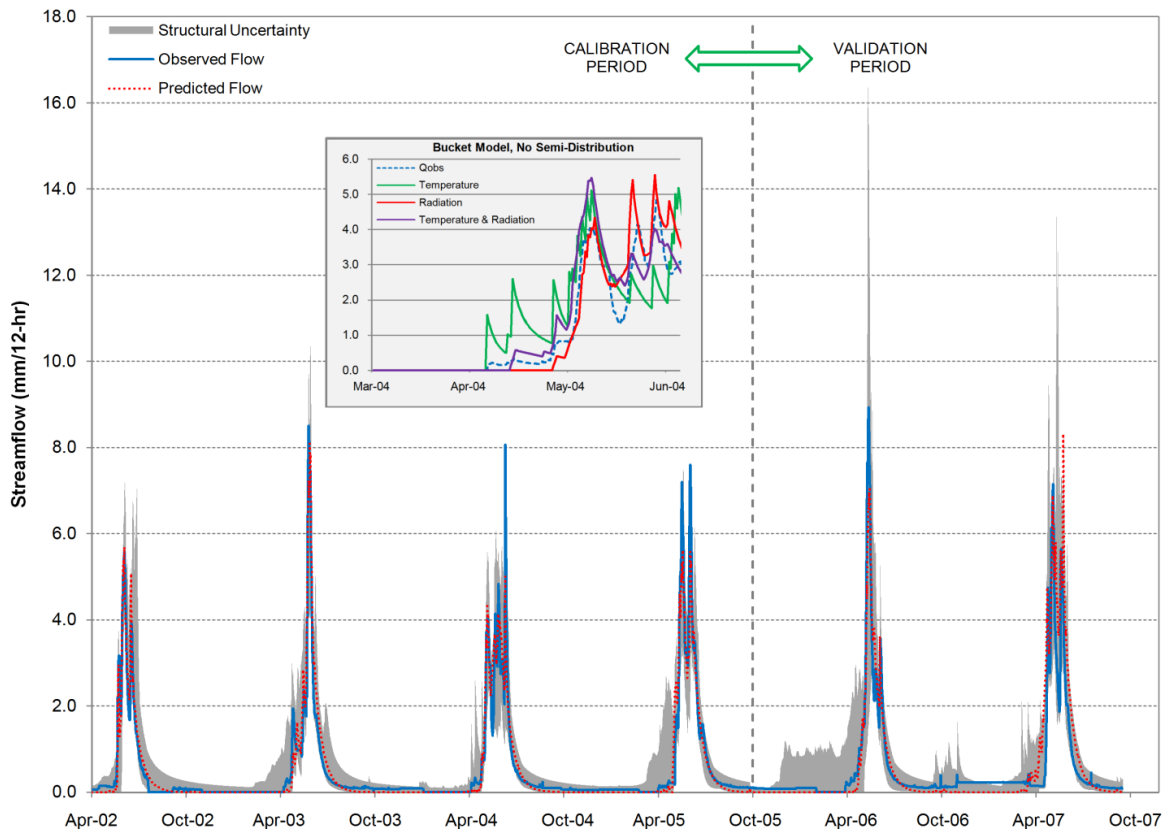


Figure 4. Modeling framework structural uncertainty and streamflow simulation for 'optimal' modular structure. **Inset** shows three model simulations corresponding to different conceptualizations of snowmelt.

Results and Conclusions

Overall, the project was successful and productive from three main viewpoints: scientific merit and furthering scientific understanding, graduate student training, and disseminating results via publications and presentations. These areas are detailed following.

Scientific Merit

Our analyses of water table connectivity strongly indicates topography (as represented by upslope accumulated area) controls upland-stream connectivity and that this drives runoff generation through time. The transformative nature of this research is strongly evident. How hillslope inputs along stream networks are linked to catchment-scale response has traditionally been poorly understood, with research efforts focused on a specific plot/stream reach. This project provides implications for watershed drivers that may be transferable to other catchments and allows development of general principles that can guide future conceptualizations of watershed models.

In undertaking conceptual model development at our test site, we focused on model selection, calibration, uncertainty analysis, and overall assessment. The results of this case study suggest that a modular framework is useful in identifying the interactions between and among different process representations and their resultant predictions of stream discharge. Such an approach can strengthen model building and address an oft ignored aspect of predictive uncertainty; namely, model structural

uncertainty. Our modeling approach offers insight into the interplay among the modular components and predictive performance for TCEF. The overriding conclusions are (1) precipitation semi-distribution methods did little more than provide another degree of freedom to the model structures; (2) net radiation is an important component in conceptualization of snowmelt accounting methods; and (3) a model based on topographic similarity may inhibit the overall calibration performance due to the model's rigidity in structure.

While the research undertaken in this project has been focused at a local test-site, the methods and models developed are broad reaching and could be applied to other watersheds. This research should have significant impact for better understanding of the link between model reliability and predictive uncertainty in streamflow forecasting for mountainous snow driven watersheds, and for conceptualizing watershed response based on topographic structure.

Student Training

Two high achieving graduate students were trained under this project. Kelsey Jencso is pursuing a PhD degree in the department of Land Resources and Environmental Sciences under the tutelage of Dr Brian McGlynn. Kelsey's work focused on hydrologic data collection and data analyses related to hydrologic connectivity. Kelsey has been very successful while working on this project, and was twice awarded the American Geophysical Meeting Outstanding Student Paper award. He recently published a high quality manuscript describing his work under this project and is continuing work focused at TCEF. Tyler Smith recently completed a Master's degree and was advised by Dr Lucy Marshall. Tyler's work focused on model development, model uncertainty assessment, and construction of the modular modeling software suite. Tyler published one paper describing the uncertainty methods used in this project, and has an additional manuscript under review describing the modeling framework. Tyler was additionally awarded an American Geophysical Meeting Outstanding Student Paper award. This is a highly competitive award, and it speaks highly of the quality of students supported under this project that both students received the award. Tyler is continuing his research efforts, and has recently commenced a PhD degree at Montana State University.

Publications

Several journal papers and numerous presentations resulted out of this project.

Journal Manuscripts

Jencso, K. J., B. L. McGlynn, M. N. Gooseff, S. M. Wondzell, and K. E. Bencala. 2009. Hydrologic Connectivity Between Landscapes and Streams: Transferring Reach and Plot Scale Understanding to the Catchment Scale, *Water Resources Research*. doi:10.1029/2008WR007225.

Smith, T. J., and L. A. Marshall (2008), Bayesian methods in hydrologic modeling: A study of recent advancements in Markov chain Monte Carlo techniques, *Water Resources Research*, 44, W00B05, doi:10.1029/2007WR006705.

Smith, T. J., and L. A. Marshall (2009), Exploring uncertainty and model predictive performance concepts via a modular snowmelt-runoff modeling framework, *Environmental Modelling & Software*, Under Review

Smith, T. J. 2008. A Conceptual Precipitation-Runoff Modeling Suite: Model Selection, Calibration and Predictive Uncertainty Assessment. M.S. thesis, Montana State Univ., Bozeman, MT.

Presentations

Jencso, K, B L McGlynn, M N Gooseff, R Payn, S Wondzell. 2008. Landscape Structure as a 1st Order Control on Whole Catchment Hydrologic and Solute Response Characteristics Across Contrasting Climate Conditions. Fall AGU.

Jencso, K, B.L. McGlynn, M.N. Gooseff, S.M. Wondzell, K.E. Bencala, and R.A. Payn. 2008. Topographic controls on hillslope–riparian water table continuity in a set of nested catchments, Northern Rocky Mountains, Montana. CUAHSI (Consortium of Universities for the Advancement of Hydrologic Sciences) Biennial Colloquium on Hydrologic Science and Engineering

Jencso, K, B.L. McGlynn, M.N. Gooseff, S.M. Wondzell, K.E. Bencala, and R.A. Payn. 2007. Topographic controls on hillslope–riparian water table continuity in a set of nested catchments, Northern Rocky Mountains, Montana. American Geophysical Union Fall Meeting. Fall, 2007.

Marshall, L. A.. 2008. Modeling the Catchment Via Mixtures: an Uncertainty Framework for Dynamic Hydrologic Systems. Uncertainty Quantification Workshop. April 25-26, 2008. University of Arizona, Tucson, Arizona.

Marshall, L. A. and T. J. Smith. 2008. A Study of Recently Developed MCMC Techniques for Efficiently Characterizing the Uncertainty of Hydrologic Models. Eos Trans. AGU, 89(53), Fall Meet. Suppl. AGU Fall Meeting 2008. December 15-19. San Francisco, California.

Marshall, L. A. 2007. University of New South Wales, Sydney, Australia (Invited Seminar). Water resources research in Montana. [INVITED]

McGlynn, B.L., K. Jencso, K. Gardner, M. Gooseff, and R. Payn. 2008. Climate variability effects on landscape hydrologic connectivity, riparian buffering potential, and solute fluxes. American Geophysical Union Fall Meeting. Fall, 2008. [INVITED]

McGlynn, B.L. 2008. Hydrologic connectivity from hillslope to landscape scales: Implications for runoff generation and water quality. NSF EPSCoR Water Dynamics Workshop, Burlington, VT, Nov 9-11, 2008. [INVITED]

McGlynn, B.L., K. Jencso, R. Payn, M. Gooseff, T. Covino, and J. Seibert. 2007. Conceptualizing, testing, and transferring watershed characteristic-runoff generation relationships. Fall AGU [INVITED]

Smith, T. J., and L. A. Marshall. 2008. A Flexible Modeling Framework For Rainfall And Snowmelt. Montana Section of the American Water Resources Association 25th Annual Meeting. October 2-3, 2008. Big Sky, Montana

Smith, T. J., and L. A. Marshall. 2008. Development and Application of a Parsimonious Snow-Hydrologic Modeling Suite: Investigating the Link Between Model Complexity and Predictive Uncertainty. Eos Trans. AGU, 89(53), Fall Meet. Suppl. AGU Fall Meeting 2008. December 15-19. San Francisco, California.

Smith, T, L. Marshall. Predictive modeling of snowmelt and the hydrologic response: Tenderfoot Creek Experimental Forest, MT. American Water Resources Association Montana Section 24th Annual Meeting. October 11-12, 2007. Lewistown, Montana.

Smith, T, L. Marshall. A Bayesian uncertainty framework for conceptual snowmelt and hydrologic models applied to the Tenderfoot Creek Experimental Forest. Eos Trans. AGU, 88(52), Fall Meeting Supplement. American Geophysical Union Fall Meeting. 10-14 December 2007. San Francisco, CA.

References Cited

Jencso, K. J., B. L. McGlynn, M. N. Gooseff, S. M. Wondzell, and K. E. Bencala. 2009. Hydrologic Connectivity Between Landscapes and Streams: Transferring Reach and Plot Scale Understanding to the Catchment Scale, Water Resources Research. doi:10.1029/2008WR007225.

Smith, T. J., and L. A. Marshall (2008), Bayesian methods in hydrologic modeling: A study of recent advancements in Markov chain Monte Carlo techniques, Water Resources Research, 44, W00B05, doi:10.1029/2007WR006705.

Smith, T. J., and L. A. Marshall (2009), Exploring uncertainty and model predictive performance concepts via a modular snowmelt-runoff modeling framework, Environmental Modelling & Software, Under Review

Weiler, M., B. McGlynn, K. McGuire, and J. McDonnell 2003. How does rainfall become runoff? A combined tracer and hydrologic transfer function approach, Water Resources Research, 39, 1315-1327.

Sediment and Heavy Metals Source Determination and Reduction at a Reclaimed Abandoned Mine Site, Alta Mine, Jefferson County, MT

Basic Information

Title:	Sediment and Heavy Metals Source Determination and Reduction at a Reclaimed Abandoned Mine Site, Alta Mine, Jefferson County, MT
Project Number:	2007MT152B
Start Date:	3/1/2007
End Date:	2/28/2009
Funding Source:	104B
Congressional District:	At large
Research Category:	Water Quality
Focus Category:	Water Quality, Hydrogeochemistry, Sediments
Descriptors:	
Principal Investigators:	Clayton B. Marlow

Publication

1. Labbe, Richard 2008 "Sediment and Heavy Metals Source Determination and Reduction at a Reclaimed Abandoned Mine Site, Alta Mine, Jefferson County, MT" M.S. Dissertation; Department of Land Resources and Environmental Sciences; Montana State University, Bozeman, MT (73 pgs)

SEDIMENT AND HEAVY METALS SOURCE DETERMINATION AND
REDUCTION AT A RECLAIMED ABANDONED MINE SITE
ALTA MINE, JEFFERSON COUNTY, MT

by

Richard James Labbe

Advising Faculty Professor

Dr. Clayton Marlow

ABSTRACT

Abandoned hardrock metal mines can have an antagonistic effect on soil productivity, vegetation, and water quality. Specifically, abandoned mines that actively generate acidity in soil are phytotoxic due to low pH and increased bioavailability of heavy metals. Arsenic concentrations in mine soils are often elevated, but may not be as mobile as heavy metals at low pH. Acid mine drainage migration from abandoned mines is problematic because it leads to water quality impairments that limit water use for certain activities (i.e. stock watering and irrigation). In this work, a previously reclaimed abandoned lead and silver mine (Alta Mine Jefferson County, MT) was characterized for its persistent impacts on soil, vegetation, and water quality. A progressive monitoring effort linked offsite water quality impacts to deep underground mine workings, shallow ground water, and metalliferous soils found at the Alta mine. Water quality impacts were of importance because they significantly hindered the attainment of Total Maximum Daily Load (TMDL) allocations that were established shortly before this study. Vegetative cover on the previously reclaimed portion of the mine was measured in 16 transects in conjunction with 30 soil pits excavated on the reclaimed site. By regression and analysis of variance, sparse vegetative cover was significantly ($p < 0.1$) linked to pH and acid generation potential. To overcome acidic soil conditions, lime and compost amendments were tested on site. The amendments significantly ($p < 0.1$) neutralized soil acidity; however, a corresponding increase in vegetative cover was not observed. Erosion of the bare unstable slopes caused greater than anticipated seed bank loss that precluded vegetation establishment. It is anticipated that successful establishment of a dense vegetative cover on the abandoned mine could prevent erosion and water quality impacts due to sedimentation. Vegetation may also have minor impacts on landscape sources of arsenic and heavy metals that were identified in the study; but the most significant source of water quality impairment, deep underground mine workings, will persist at the Alta mine under any land treatment.

INTRODUCTION

The science of land rehabilitation integrates principles of soil physiochemistry, plant physiology, and water interactions. Rehabilitation implies the return to a previous condition; thus, scientists must examine soil characteristics, plant growth requirements, and the hydrologic regime of disturbed lands if they are to return them to their original state. In application, land rehabilitation is the practice of attenuating earth disturbances and revegetating them by ameliorative, adaptive, or agricultural treatment (Ye et al. 2000, Tordoff et al. 2000). Mining, timber harvest, agriculture, road building, and other construction activities commonly result in land disturbances that require rehabilitation. Watershed processes are explicitly linked to land use; thus, the same suite of disturbances that often require land rehabilitation may also lead to impairments in bodies of water. Poor agricultural practices, such as over-fertilization or cattle feeding operations, may lead to excess nutrient loads in streams; also, mine waste may be an important non-point source of stream impairment by heavy metals. Nearly all anthropogenic land uses, including those previously named, are potential sources of excess sediment. The interconnectedness between land disturbance and watershed impairment is important for scientists, land managers, and regulatory agencies to understand if they are to implement effective land rehabilitation and watershed restoration strategies.

Problem Statement

The specific problems addressed in this research are the factors that limit the rehabilitation of lands disturbed by historic, acid-producing, hard rock metal mines and the persistent impact that these mines have on water quality on the watershed scale. Sulfide mineral oxidation resulting in low pH and increased heavy metal toxicity reduces soil productivity and plant vigor; however, it is not the only process that limits the successful rehabilitation of mined lands. Soil texture, drought, erosion, lack of organic matter (OM), low nutrients, and steep slopes exemplify the universe of limitations on effective mine rehabilitation. In addition, site specific limitations may occur due to abandoned mine features (i.e. adits, shafts, dumps), site accessibility, and budget constraints. When chemical, physical, logistical, and fiscal limitations are not overcome, land rehabilitation is not effective; thus, the potential exists for water quality impairments downstream. Impairments such as sediment, heavy metals, arsenic, sulfates, and pH may limit water use for drinking, swimming, irrigation, fish and other organisms.

Water Quality in Mined Watersheds

Acid Mine Drainage Impairments

Acid drainage is a term assigned to solutions produced from sulfide mineral weathering that are characterized by low pH and often contain high levels of potentially toxic trace elements (e.g. Cd, Zn, Pb, Cu, As). Mining disturbances are a common source of exposed sulfide minerals; so acid drainage is frequently referred to as acid mine drainage (AMD). A copious amount of work has been published regarding the formation of AMD. Comprehensive manuscripts (OSU 1971, Evangelou 1995) discuss the production chemistry, kinetics, role of microorganisms, and control of AMD. Pyrite (FeS_2) is the most common acid-producing Fe-sulfide mineral and is found in many geological environments (OSU 1971). The oxidation of pyrite by O_2 and subsequent acid production is the summation of 3 intermediate reactions: 1) dissolution of FeS_2 ; 2) oxidation of Fe^{2+} to Fe^{3+} ; and 3) hydrolysis of Fe^{3+} . Reactions 1 and 3 produce a total of 5 moles of H^+ ; while 1 mole of H^+ is consumed in reaction 2, resulting in 4 moles of acidity produced for every mole of FeS_2 reacted. Also, at low pH (below 3.5) ferric iron (Fe^{3+}) oxidation of pyrite can accelerate acid production to a rate of 16 moles of acid per 1 mole of pyrite reacted (Jennings and Dollhopf, 1995). Reactions assigned to AMD production, though they are charge and mass balanced, have no molecular, mechanistic, or rate reaction meaning because pyrite oxidation involves many other metastable species (Evangelou 1995).

The products of AMD have a significant impact on water quality that is not limited to the spatial confines of mine disturbances. Rather, historic metal mine disturbances produce water quality impairments that persist throughout entire watersheds (Sullivan et al. 2000, Caruso 2003, Herr et al. 2003, U.S. EPA 2006). Sediment, metal hydroxides, and toxic trace elements (e.g. As, Cd, Cu, Pb, and Zn) from abandoned mine sources have been shown to cause impairments in fluvial ecosystems (Henry et al. 1999, Soucek et al. 2000a, Soucek et al. 2000b, Niyogi et al. 2001, Niyogi et al. 2002).

AMD Characterization

Products of AMD and evidence of their negative ecological impact may extend to all reaches within a watershed; however, several factors make it difficult to characterize and/or model AMD systems. Heavy metal and As transformations and pH shifts can occur rapidly in AMD systems at the confluence of waters not impacted by AMD or by rapid dilution during snowmelt or rainfall events (Brooks et al. 2001, Sullivan et al. 2001, MacDonald et al. 2007). Mixing with alkaline or neutral streams causes distinct changes in the chemical signature of AMD (Broshears 1996). Metal hydroxide precipitation in mixing zones is important in determining downstream aqueous chemical composition.

Heavy metal concentrations decrease in mixing zones due to coprecipitation with metal hydroxides (Runkel and Kimball 2002, Butler II 2006).

In addition to chemical changes brought on by hydrologic influences, the character of AMD impacted streams is dependent on biological and physical factors. Reduced stream flows due to evapotranspiration by riparian vegetation can amplify heavy metal concentrations, as photoreduction and microbial reduction of Fe(III) to Fe(II) is increased during periods of low flow (Sullivan and Drever 2001, Butler II 2006). Concentrations of heavy metals in the water column increase when Fe is reduced, either microbially or by photoreduction, because of decreased adsorption on Fe-hydroxides (Sullivan and Drever, 2001).

Abandoned metal mines that produce AMD have the potential to discharge As and heavy metals from a variety of sources. Heavy metals and As may be transported in leachate from tailings, waste rock, and contaminated soils or may be discharged from mine workings such as portals, shafts, and adits. For this reason, site specific factors are possibly the most important in determining how products of AMD are transported in streams. Kimball et al. (2002) identified numerous inflows springs, bogs, diffuse sources, seeps, and adits along a 12 km reach of Cement Creek, Colorado. Depending on the nature of each source, inflows either attenuated or contributed to the transport of heavy metals and other products of AMD. Recent monitoring and modeling efforts concluded that abandoned mine features (point sources) were likely the most significant sources of AMD products (Runkel and Kimball 2002, Kimball et al. 2002, Caruso 2003, and Herr et al. 2003).

Sediment from Abandoned Mines

As early as the beginning of the 20th century, impacts of excess sediment from mining sources were assessed (Gilbert 1917). Hydraulic gold mining led to the production of nearly 8 billion m³ of mining debris in the Yuba, Bear, and American river watersheds, some of which negatively impacted the San Pablo, San Francisco, and Suisun Bays. The spatial extent of sediment delivery from abandoned hard rock mines is not as vast as that from large hydraulic mine sources but resulting overbank deposits and silted stream channels are the same. Soda Butte Creek drains the historic New World gold mining district near Yellowstone National Park. A tailings impoundment failure in 1950 resulted in exposed over-bank tailings deposits as far as 25 km downstream (Marcus et al. 2001). The source of the sediment was unmistakably linked to the tailings impoundment failure by sand-sized pyrite grains, strong oxidation, and sparse vegetative cover. The tailings also filled abandoned channels as deep as 0.7 m.

Bonta (2000) monitored 3 Ohio watersheds for suspended sediment in their natural condition, during active mining and reclamation, and after final reclamation. Maximum suspended sediment concentrations were the highest in each watershed during mining and reclamation activities; while, minimum concentrations were always in the undisturbed condition. In one watershed, average post reclamation suspended sediment loads were decreased by 75% of the load in the undisturbed condition. The decrease was

attributed to increased vegetative cover and not lack of stream power because average stream flows had actually increased following reclamation.

Limits on Soil Productivity and Vegetation Establishment

Establishing a vegetative cover on land disturbed by historic hard rock mining is an effective way to reduce erosion, limit heavy metal and As leachate, and improve water quality within a watershed (Brown 2005); however, there are many chemical and physical limitations to vegetation establishment on these sites.

Mine Waste

Tailings deposits and waste rock dumps are common remnants of abandoned mine disturbances that produce AMD. Tailings are the by-product of the ore milling and concentrating process; as such, they are generally made of fine-grained material (Tordoff 2000). Residual sulfide ore minerals and metals content is high in historic mine tailings because of inefficiencies in past separation processes (Alloway 1995). Poor vegetation establishment on fluviially deposited tailings on the banks of the upper Clark Fork River and on the historic Keating gold and copper mine tailings in Montana are just 2 of the countless examples of the phytotoxicity of tailings (RRU-BRI 2004, Neuman et al. 2005). Further, pyrite oxidation occurring as deep as 1 m within mine tailings heaps may lead to a decline in vegetative cover where increased sulfur oxidizing bacteria are present and neutralization potential is depleted (Schippers et al. 2000).

In contrast to tailings deposits, waste rock piles are typically composed of larger rock fragments that have been removed from their native location but have not been milled or processed. Waste rock piles also have the potential to produce AMD by sulfide mineral oxidation (Lefebvre et al. 2001, Sracek et al. 2004). It cannot be assumed that tailings or waste rock pile removal will result in successful remediation of AMD. As a result of AMD solution leaching from waste rock, native soils beneath waste rock piles may be enriched with metals in soluble secondary minerals (Zhixum 1997). Low pH in mine waste substrates and soils in contact with mine waste is a crucial limiting factor to vegetation establishment.

Revegetation and Rehabilitation

Rehabilitation is successful when acid-metalliferous substrates (i.e. impacted soils, tailings, waste rock) cease to inhibit plant growth and are no longer mobile in the environment. In situ amendment of substrate that reduces toxic trace element bioavailability and raises soil pH has emerged as a commonly practiced treatment in abandoned acid-metal mine rehabilitation

Amendments are chosen for the ameliorative effects that they will have on soil and substrate character. Organic amendments such as biosolids, peat, and compost are added to substrate to increase water and nutrient holding capacity, provide a source of nutrients, increase cation exchange capacity, and form organic complexes with potentially toxic trace elements (Tordoff 2000). Calcium carbonate (agricultural lime), steel sludge, furnace slag, zeolites, and red mud by-product from alumina production are among the host of inorganic materials available for acid-metalliferous substrate amendment (Chen 2000, Friesl et al. 2003). The principle of inorganic amendment addition is to reduce heavy metal availability by raising soil pH and binding or precipitating heavy metals. Recent work has confirmed the effectiveness of both organic and inorganic amendments at increasing productivity of abandoned acid metal mine substrates (Friesl et al. 2003, Walker et al. 2004, Brown et al. 2005, Neuman et al. 2005, O'Dell 2007).

Purpose of Work

The purpose of this work was to characterize a previously reclaimed abandoned Pb and Ag mine for site specific limitations on vegetative succession and sources of impairment on water quality. A vast area of sparse vegetation on the reclaimed site was studied for its soil chemical and physical composition and other environmental factors that have often been attributed to poor vegetative cover in the current land rehabilitation literature. The extent of heavy metal and As discharge from soil, shallow groundwater, and deep underground mine workings were examined through an extensive water quality monitoring effort. The water quality monitoring plan was designed such that the temporally variable contribution of contaminants from the mine could be compared to Montana's aquatic life standards (MT DEQ 2006) and recently established federally mandated maximum contaminant load allocations.

Two (2) hypotheses were tested by our site characterization:

1. Waters that drain the site are the significant source of impairment to downstream water quality in terms of total maximum As, Cd, Cu, Pb, Zn, and sediment load;
2. A chemical or physical variable or combination of physical and chemical variables consistent with acid mine disturbed lands control vegetative cover on site, despite previous reclamation attempts.

The first hypothesis was tested by direct comparison of monitored site discharge to measured background loads of As and heavy metals in receiving waters. Hypothesis 2 was tested by statistical significance (linear regression and ANOVA) of pH, soil heavy metal and As concentrations, OM, nutrients, EC, acid-base potential, and slope aspect control on vegetative cover.

Beyond site characterization, a third hypothesis tested the effectiveness of lime and compost amendments at increasing soil productivity and vegetative cover in a field experiment. A healthy vegetative cover would not only indicate effective mine

rehabilitation but could potentially reduce sediment, heavy metal, and As loads from soils and shallow groundwater. The third hypothesis was:

3. Lime and compost amendments will increase soil productivity and vegetative cover on experimental treatment plots on the disturbed site.

This hypothesis was tested by the statistical significance of end of growing season soil and vegetative cover characteristics compared to end of growing season controls.

The results of this work are important to private, state, and federal stakeholders who may be responsible for the rehabilitation of similar mines in roughly the same geographic region. This work also exemplifies the complex link between water quality impairments and acid mine land disturbances. Watershed planners and conservation districts may consider the results of this work when assessing the impact of abandoned mines in watersheds of comparable size and character.

Study Site

Location

The study site, located approximately 30 km south of Helena, MT, consists of the abandoned Alta Mine complex, a small stream referred to as the Alta tributary, and Corbin Creek immediately above and below its confluence with the Alta tributary (Figure 2). The abandoned Alta mine complex is included in the Colorado Mining District of Jefferson County, MT (Pioneer 1994). As an abandoned mine, the Alta is not unique. In fact, it is one of an estimated 6,000 inactive mining and milling sites across Montana (Pioneer 1994).

The Alta mine complex is divided into an upper mine site and a lower mine site. The lower site is located in Section 10, T7N, R4W; and the upper site is distributed between Sections 9 and 10, T7N, R4W. The Alta tributary drains the Alta mine diagonally from SW to NE across Section 10, T7N, R4W, until it reaches a confluence with Corbin Creek in the SW1/4 of SW1/4 Section 2, T7N, R4W. The Alta tributary and Corbin Creek are found at the southern edge of the Lake Helena Watershed in the Upper Missouri River Drainage Basin. Corbin Creek drains an estimated 442 ha above its confluence with the Alta tributary. The Alta tributary subwatershed accounts for approximately 19% (82 ha) of the drainage area. The streams drain to Prickly Pear Creek, which is the largest stream in the Lake Helena Watershed.

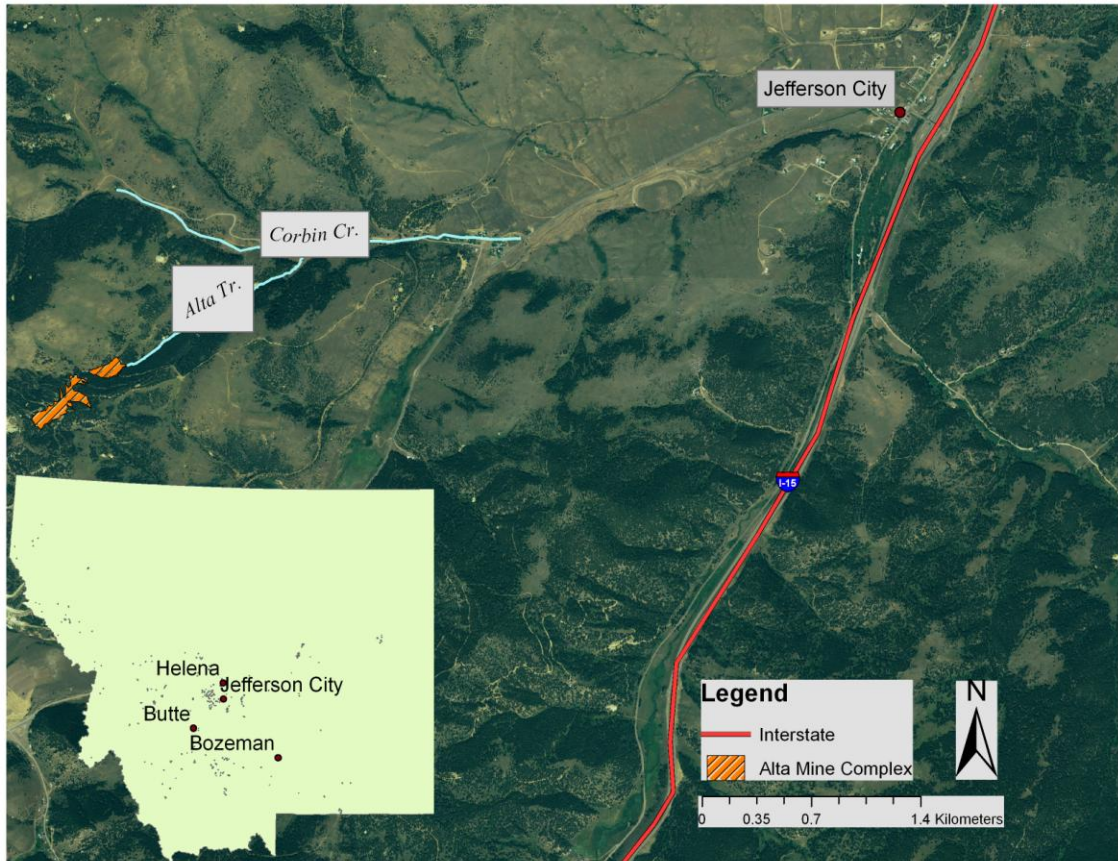


Figure 1. Alta Mine Site Location. Points on Montana inlay represent abandoned mines.

Geology and Climate

The elevation of the study site ranges from approximately 1,500 m above mean sea level (amsl) at the confluence of the Alta tributary and Corbin Creek to 1,905 m-amsl at the summit of Alta Mountain. Snow in the winter, rain in the spring, and intermittent thundershowers throughout summer and fall account for precipitation at the site. Snow in the Alta drainage accumulates primarily on the slopes with northern aspect; while, snow on the south facing slope tends to melt or sublimate rapidly. The 30-year average cumulative annual precipitation at the nearest weather station in Boulder, MT is 28.7 cm. Cumulative precipitation for the latest complete year of record (2006) was 29.3 cm. Both Deckler (1982) and Tetra Tech (1997) suggested increased precipitation at the Alta Mine due to orographic effects; and observations made in the summer of 2007 seem to corroborate this assumption. Cumulative precipitation at the Alta Mine—approximately 190 m above the Boulder weather station—was nearly 6% greater than that observed in Boulder. Site temperature varies from extreme cold in winter to extreme heat in summer. Average Monthly temperatures (from Boulder weather station) range from -12 °C to 0 °C in January and from 7 °C to 26 °C in July (Tetra Tech 1997).

The study site is at the north end of the Boulder Batholith and Elkhorn Mountain volcanics formations. Both formations are igneous and Cretaceous in age; however, the Batholith is intrusive, while the Elkhorn Mountain volcanics are remnant of lava flows and volcanic ejecta (Veseth and Montagne 1980). Rocks present on site are representative of both formations. Quartz monzonite is the primary batholithic rock; while, rhyolite and dacite tuffs and lava flows account for much of the volcanics (Veseth and Montagne 1980, Tetra Tech 1997).

Mining History

The Alta mine was the most productive underground lead and silver mine in the area, owing to an extensive ore body of galena (presumably argentiferous galena), pyrite, tetrahedrite, and sphalerite (Becraft et al. 1963). Ore was discovered there in 1869; and the mine operated at its greatest capacity from 1883 to 1896. Minimal amounts of silver and lead ore were produced after 1896; however, low grade ore, used as silica flux in the East Helena smelter, was mined in the 1950s. When mining ceased, the site was abandoned as a pile of waste rock, 13 levels of underground mine workings, and a series of shafts and adits that opened to the surface on the east side of Alta Mountain. Most notably, the #8 shaft was a continuous source of metals laden AMD that discharged from beneath the lower waste rock pile. The waste rock piles consisted of ore minerals sparsely and heterogeneously distributed within volcanic and batholithic rock materials. In addition to sulfide minerals from within the Alta ore body, limonite, chalcopyrite, and quartz were deposited on the lower Alta waste rock dump after exploration in a separate vein immediately to the southwest. Ore samples from this vein contained 11 % copper. Samples of crude ore from the Alta ore body were shown to contain 18 – 35 % lead; and concentrated samples had 12 % zinc.

Reclamation History

Of the estimated 6,000 abandoned mines in Montana, a list of 270 priority abandoned mine sites was compiled (Pioneer 1994). In 1993, nearly all of the 270 mines were characterized for their risk to human health and the environment by chemical degradation and hazardous abandoned structures. Upon characterization, sites were compared and ranked according to severity of risk. Alta was ranked 17th amongst the most threatening mine sites due to metals laden AMD that exceeded nearly all of Montana's numeric water quality standards and for its abundance of actively eroding waste rock dumps with elevated levels of Pb and As (Pioneer 1994).

Reclamation of priority abandoned mine sites is funded largely by the Surface Mining Control and Reclamation Act (SMCRA) of 1977 and is administered by the Montana Department of Environmental Quality (MT DEQ 2005). MT DEQ reclaimed the Alta mine in the summer of 1999. Work done during the reclamation effort included: removing 117, 741 m³ of waste rock; transporting waste rock to a 2.3 ha repository;

reconstructing 274 m of stream channel; re-contouring the 40% slopes with terraces; and fertilizing, seeding, and mulching the re-contoured area (Tetra Tech 2002). Risk-based As, Pb, and Mn concentrations were used to determine which portions of the waste rock to remove. All of the waste rock removal and subsequent reclamation activities were done exclusively on the lower Alta mine site; while, waste rock piles at the upper mine and in the Alta tributary below the reclaimed area were left in place. The reclamation effort did not include surface water or groundwater treatment; however, a failed attempt to seal the #8 shaft was made in order to eliminate surface discharge (Tetra Tech 2002).

Watershed Restoration

The Clean Water Act (CWA), as amended in 1977, includes programs that aim to limit the discharge of pollution from industrial point sources, regulate effluent from waste water treatment plants, and reduce nonpoint source pollution impacts (Gallagher and Friedman 2001). Section 303(d) of the CWA maintains that each state must assemble a list of waters that are impaired and the contaminants that impair them. Each state must assess contaminant sources (point and nonpoint) for a given body of water and determine the reduction in contaminants needed to support beneficial water uses. The reduced load is known as a Total Maximum Daily Load (TMDL).

Corbin Creek, the receiving waters of the Alta tributary, has been found to be impaired by As, Cd, Cu, Pb, Zn, and sediment from its headwaters to its mouth (U.S. EPA 2006). TMDLs have been established for each of these constituents, along with the current estimated daily load and the percent reduction required for TMDL attainment (Table 2). Abandoned mines are estimated to account for 59%, 99%, 96%, 86%, 98%, and 5% of the As, Cd, Cu, Pb, Zn, and sediment loads in Corbin Creek, respectively. The remainder of the current load is attributed to dirt roads, timber harvest, natural sources, and stream bank erosion. Extensive mining and reclamation activities have taken place in the Corbin Creek watershed above the Alta tributary but not below. Of the many abandoned metal mines with a potential impact on Corbin Creek, the Alta mine complex is mentioned by name in the Framework Water Quality Restoration Plan for the Lake Helena Watershed Planning Area (US EPA 2006); however, the mine's contribution of sediment and heavy metals is not directly estimated. Moreover, the document suggests that the #8 shaft had been sealed during reclamation. While the document recognizes that limited revegetation of the Alta mine may be a source of sediment and toxic trace elements, it accounts for less than 0.5 ha of bare ground.

Table 1. Corbin Creek TMDL Attainment Goals and Estimated Current Maximum Loads (US EPA 2006).

Constituent	Estimated Current Load (kg day ⁻¹)	% Reduction Required	TMDL (kg day ⁻¹)
Arsenic	0.06	25%	0.045
Cadmium	0.11	97%	0.003
Copper	1.32	89%	0.141
Lead	0.12	66%	0.041
Zinc	72.72	97%	2.045
Siltation	0.59	23%	0.455

Precedent Research

More than a decade before the massive abandoned mine characterization effort launched by the state of Montana, Deckler (1982) characterized soils and substrates at the Alta mine. Consistent with the efforts of the state, he found the site to include 2 large waste piles that were uninhabited by vegetation. The upper Alta waste rock pile was less acidic (pH from 5.5 to 6.2), coarse textured (and homogenous), and contained lower concentrations of potentially toxic trace elements than the lower pile. Erosion, nutrient availability, and overly drained soils were suspected to limit vegetation on the upper pile. The lower pile was finer textured and more acidic (pH=3.0). Extractable metal levels were high on the lower waste rock pile but soluble metal levels were low. There was evidence that metals had leached from upper portions of the waste profile; thus, it is possible that they reached native soils below. Deckler made several suppositions about the future reclamation of the site. He concluded that: sufficient cover soil depth must be maintained on lower slopes to sustain vegetation; upper waste rock material may be used as a barrier between lower waste rock and cover soil; and mulches would provide nutrients and decrease incident solar radiation from the bare waste rock piles. Finally, Deckler (1982) noted that tailings from the nearby Bertha mine were located directly in the Corbin Creek channel above the Alta tributary at the time of his study. These tailings were removed in 2002 in a reclamation project separate from the Alta reclamation effort (MT DEQ 2008).

Schroth (2001) and Schroth and Parnell (2005) provide a thorough account of geochemical transformations within the Alta waste rock pile prior to its removal and in the Alta channel following relocation of the pile. They found that schwertmannite precipitation was an important metal sink within the waste rock pile. It was further discovered that metal hydroxide precipitation increased upon pile removal; however, trace element concentrations did not actively decrease by coprecipitation with schwertmannite. Pre and post waste rock removal concentrations of selected trace elements in the Alta tributary immediately above Corbin Creek remained relatively constant (Figure 3).

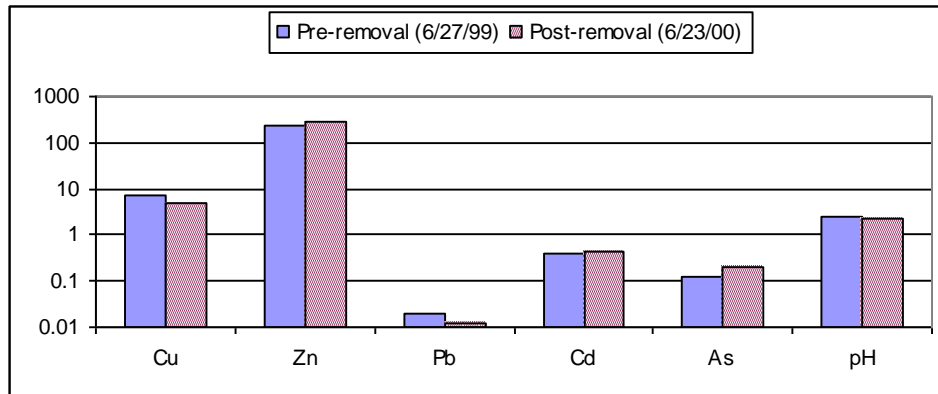


Figure 2. Heavy Metal and As Concentrations (mg kg^{-1}) in Alta Tributary Before and After Waste Rock Removal. Data are from Schroth (2001).

In effect, Schroth and Parnell (2005) concluded that trace element attenuation by the waste rock pile was equal to that of attenuation by coprecipitation with Fe-hydroxides in the channel. All trace elements except for Cu were found to decrease in the direction of flow in the Alta tributary both before and in the summer after pile removal (Figure 4).

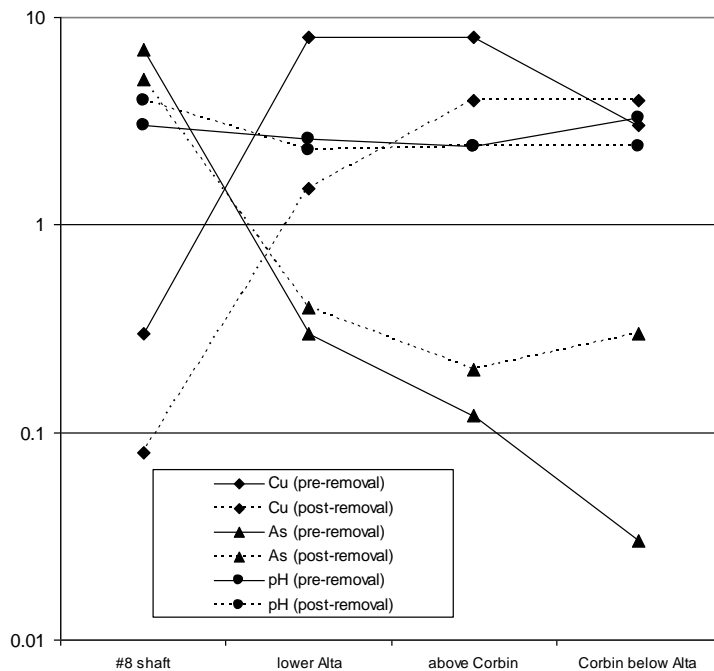


Figure 3. Cu, As, (mg L^{-1}) and pH (standard) Along Longitudinal Profile of Alta Tributary Before and After Waste Rock Removal. Data are from Schroth (2001).

The longitudinal profiles substantiate the idea that pile removal did little to influence downstream concentrations of heavy metals and arsenic in the first year after reclamation. Hydrologic regime appears to play an important role in determining concentrations in Corbin Creek. No surface flow was observed in the creek above the Alta tributary in 2000. As a result, pH below the Alta tributary was 1 unit less than in

1999. Concentrations of Cu and As decreased after mixing with Corbin Creek surface flows in 1999 but increased or remained constant in 2000—when no flow was observed in the creek above the confluence with the Alta tributary.

The findings of previous researchers are a time-specific representation of conditions, processes, and events at the Alta mine. The relevance of each work was dictated by prevailing site conditions at the time of study. As a means to assess reclamation alternatives, Deckler (1982) examined the characteristics of two waste rock piles that had been abandoned for nearly 30 years. Schroth (2001) provided a narrative of geochemical processes that occurred as a result of transient conditions during the reclamation effort in the summer of 1999. The current study expands the temporal coverage of our knowledge about the abandoned Alta mine to include a characterization of post reclamation site conditions and water quality impacts. The study is relevant because of an apparent vegetation failure on reclaimed slopes and because of recently established TMDLs in Corbin Creek.

METHODS AND MATERIALS

Soil Survey

Soil Pit Excavation

Post-reclamation soils were surveyed on the Lower Alta reclaimed site in the summer of 2006. Sharpshooter shovels were used to dig 30 soil pits to completed depths between 0.6 m and 0.75 m. In most cases, pits were started by scraping surface-exposed material from the edge of a terrace (Sobek et al. 1978); then, pits were completed by excavating through topsoil of the adjacent lower terrace to the desired depth. Soil profiles were described in field notes according to soil color, mottling, moisture, root zone, and apparent texture. The pits were located on an approximate 25 m grid of the reclaimed area (Figure 5).

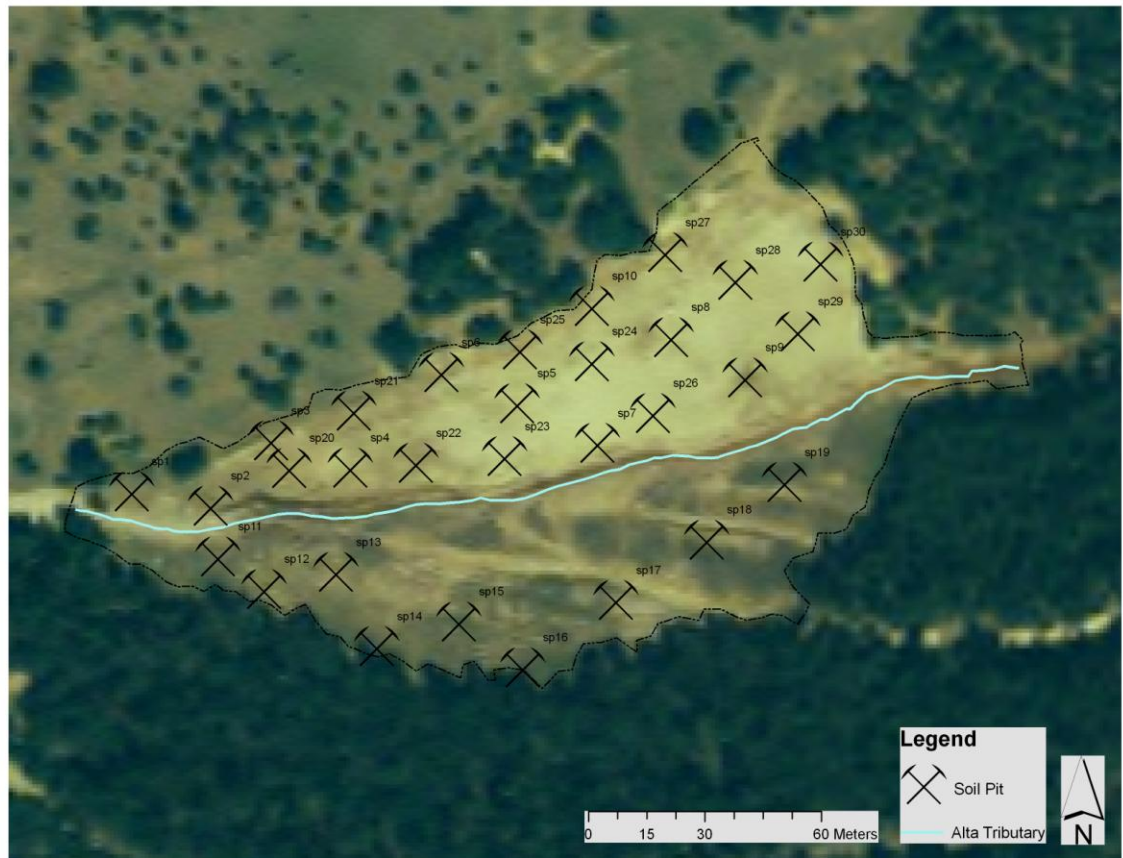


Figure 4. Soil Pit Locations on the Lower Alta Mine Site.

To prevent cross contamination between soil pits, they were dug with 2 alternating shovels. Upon completion of a pit, the first shovel was washed and allowed to air dry while another soil pit was completed with the second shovel. Shovels were decontaminated with Alconox® detergent dissolved in ambient temperature de-ionized water at 10 g/L. Decontamination included scrubbing with a wire brush; scrubbing with a synthetic-bristled brush; and rinsing with de-ionized water for 10 seconds. The decontamination station was located on the tailgate of our field vehicle. It consisted of a 19 L tub of detergent solution and 15 L of de-ionized rinse water. Shovels were decontaminated at the end of each sampling day to prevent uncontrolled offsite transfer of impacted soils.

Soil Sample Collection

Each of the pits was sampled at two intervals: 0 - 15 cm; and 60 - 75 cm. Sampling at these intervals was completed to remain consistent with the EEECA sampling protocol (PRC EMI 1997). Between 1 and 1.5 kg of soil was collected from each interval with multiple scoops of a Corona CT3020 polished aluminum trowel. Soils were stored and transported in sealed plastic bags, each labeled with soil pit name, date, and depth interval. As was done with the sharpshooter shovels, trowels were washed between samples. Four trowels were used for soil sample collection such that two trowels were in use while the other two were washed. Trowels were carried from the decontamination station in a separate, clean, dry plastic bag. In addition to soils, controlled 1.2 mm silica sand was collected with trowels that had been decontaminated at the time of sampling. The sand, which was transported to the site in a sealed, clean, dry, plastic bag, underwent all further sample preparation and analysis steps as a blind control. Like soil samples, it was sampled in 1 to 1.5 kg increments. Trowels were decontaminated at the end of the day to prevent uncontrolled offsite transfer of impacted soils.

Soil Sample Preparation

Soil samples were first homogenized by mixing within the sealed plastic bags in which they were originally collected and transferred; then, they were removed from their bags and spread onto sheets of brown kraft paper (Sobek et al. 1978) to air dry for at least 24 hours. Each sample was placed on a separate piece of paper and labeled with its soil pit name, date, and depth interval. While on the kraft paper, each soil sample was mixed with its own clean spatula in order to accelerate drying and to further homogenize the samples.

Once samples were dry, they were transferred to clean aluminum pans and weighed on 10-kg capacity scale. The total weight of each sample was recorded before it was sieved through a USA Standard No. 10 sieve with 2 mm openings. Each sample was shaken by hand for approximately 1 minute or until the sample was sufficiently separated. The samples, less the fraction with particle diameter greater than 2 mm, were

returned to their aluminum pans, weighed, and recorded. Only the fraction of each sample with particle diameter less than 2 mm was retained for soil chemical and textural analyses. Retained samples were returned to clean, dry, plastic bags and labeled by soil pit name, depth interval, and date collected. All samples underwent this process as a minimum of preparation. Additional preparation and methods of specific soil analyses are outlined below.

Soil Sample Analyses

A multitude of soil physical and chemical properties, known to affect vegetative succession, were considered in the characterization of the Lower Alta reclaimed site. The list includes Acid Base Accounting (ABA), heavy metals and arsenic, pH, EC, texture, rock content, nutrients, and organic matter. Some of the analyses were performed on the campus of Montana State University; while, others were completed by an independent laboratory—namely Energy Laboratories Inc. of Billings, MT (Energy Labs).

Rock Content. Rock content of Alta soils was determined as the amount of material that did not pass through a USA Standard No. 10 (2 mm) sieve (USDA, NRCS 2007). Specifically, rock content of each sample was expressed as a percent of the total sample by mass.

Soil Texture. Soil texture and class were determined by the hydrometer method described in Tan (2005) and the USDA Soil Texture Triangle. A mechanical blender was used to blend 100 g of soil, distilled water (to within 10 cm of the top of a stainless steel blender cup), and 10 ml of 0.25 M (NaPO₃)Na₂O (sodium metaphosphate) solution for 15 minutes. The mixture was transferred to a glass ASTM soil testing cylinder; and distilled water was added until the suspension reached the 1205 ml level. A stirrer was used to thoroughly mix the suspension; then, a hydrometer was placed in the cylinder. Hydrometer readings were taken twice at 40 s and again after 2 hrs. The averaged 40 s readings were taken to be the silt and clay fraction of the soil matrix; and the 2 hr reading was clay alone. The temperature of the suspension was recorded and used to correct hydrometer readings to the calibration temperature of 68 °F (20°C).

Paste pH and EC. Saturated pastes (2:1, soil:water) were prepared with soils from each of the 30 soil pits and sampled depth intervals. The pastes were prepared in 200 ml paper cups according to Sobek (1978), except that less than 10 mesh soils were used instead of less than 60 mesh soils. The soils were allowed to wet by capillary action before being stirred to a thin paste with a spatula. The spatula was rinsed with a jet of de-ionized water before stirring each sample.

EC was measured with a YSI 3100 Benchtop Conductivity Meter. Before making EC measurements, the cell constant of the instrument was set at 1.00/cm and it was calibrated with 8,974 µS and 2,764 µS standard solutions. Additional calibrations were performed after every 10 soil samples. The YSI 3100 was set to automatically adjust EC readings with changes in temperature. Measurements were recorded when the digital EC

reading was stable. Between measurements, the probe and cell were rinsed with a jet of and stored in a beaker of de-ionized water.

Paste pH was measured with a Fisher Scientific Accumet 15 pH Meter on the same set of saturated pastes used for EC measurement. Measurements were recorded when the digital pH reading was stable. The probe and electrode were rinsed with de-ionized water between samples. The pH meter was calibrated prior to use and after every 10 measurements with pH 4.0 and pH 7.0 standard buffer solutions.

Heavy Metals and Arsenic. Both total and soluble heavy metal and arsenic concentrations were determined for Alta mine soils. Energy Labs performed the analysis with Inductively Coupled Plasma Mass Spectroscopy (ICPMS). Total As, Pb, and Zn were determined for each of the 30 soil pits at both the 0 – 15 cm interval and the 60 – 75 cm interval. Sub-samples of approximately 150 g of less than 10 mesh air-dried soils were sent to the lab, where they were digested according to SW-846 EPA Method 3050 (US EPA 1995) before ICPMS analysis.

Soluble metals in the 0 – 15 cm interval were determined for 18 of the 30 soil pits. The analysis was limited to soils from the 0 – 15 cm depth because this was the observed rooting depth of vegetation on site. Also, only 18 samples had a sufficient amount of soil remaining—for additional preparation—once the soils had been sub-sampled for prior analyses. Additional sample preparation for soluble metals and arsenic included: making 2:1 saturated soil pastes; obtaining soil water extracts (SWE) by centrifugation; filtering the SWE; and acidifying the filtrate. The 2:1 saturated soil pastes were made in the same manner as those used in pH and EC determination, except these were made directly in clean 250 ml centrifuge tubes. First, approximately 200 g of soil were weighed in the tubes; then, approximately 100 g of water was added. The soils were allowed to wet by capillary action before being stirred to a thin paste with a spatula. The spatula was rinsed with a jet of de-ionized water before stirring each sample. SWE was obtained by centrifuging saturated pastes at 9,000 rpm for 10 minutes in a refrigerated centrifuge. The separated SWE was then evacuated from the centrifuge tubes with 60 ml BD syringes. From the syringes, the SWE was filtered through 0.2 µm membranes into 15 ml Falcon tubes. Each 0.2 µm membrane was used only once and discarded; however, the 50 ml BC syringes were used for multiple samples. Before reuse, each syringe was flushed 3 times with de-ionized water. Finally, filtrate was acidified with HNO₃ to pH < 2 and stored at < 4 °C until samples were shipped to Energy Labs for ICPMS analysis.

Acid Base Potential. Acid base potential (ABP) was completed by Energy Labs with the Modified Sobek Method (Sobek et al. 1978). The method considers both the neutralization potential (amount of neutralizing bases in a sample) and the maximum acid generating potential by total sulfur determination. Total ABP was calculated as the difference between neutralization potential and acid generating potential in T-CaCO₃/1kT-soil.

Nutrients and Organic Matter. Soils sent to Energy Labs were analyzed for N, P, K, and OM. Nitrate, as N, analysis was done with Method 38-8.1 (ASA, SSSA 1982). P

was extracted by Method 24-5.4 (ASA, SSSA 1982) and analyzed with Method E365.1 (EPA, NERL 1993). K was extracted with ammonium acetate according to Method 13-3.5 (ASA, SSSA 1982) and analyzed with ICPMS. Finally, OM was extracted with the Walkley-Black Procedure, Method 29-3.5.2 (ASA, SSSA 1982), and analyzed by spectrophotometry.

Vegetation Survey

Concurrent with soil pit excavation, a pair of 50 m transects were centered, perpendicular to each other, at each of the first 16 soil pits. Vegetation transects were only established at just over half of the soil pits; yet, they provided adequate coverage of the Lower Alta reclaimed area without overlapping each other. Canopy cover (Daubenmire 1959) was estimated in eight 20 cm x 50 cm (0.1 m²) frames per pair of transects. Average vegetative cover of the eight frames was calculated for each pair of transects. The average was considered representative of the vegetative cover for the soil pit at which transects were centered.

Soil Amendments and Revegetation

Materials Handling and Plot Construction

The efficacy of lime and compost amendments at increasing vegetative cover was tested on 16 - 54 m² plots on the lower Alta mine site. Restricted access, remoteness of the site, and rough steep terrain limited the type of materials and number of agronomic practices available. Rather than having lime and compost delivered to the site in bulk, the amendments were purchased in smaller more manageable units. Some materials, 64 bags of lime (23 kg each) and 6 rolls of silt fence (30 m each), were stockpiled at the lower Alta site prior to construction. Compost, 20 super sacks (272 kg each), was transported to the lower Alta mine site on a ¾-ton flatbed truck. In order to ensure safe passage of the transport vehicle, the access road was improved with a Link-Belt 2700 excavator and a John Deere skid steer. Improvements included smoothing, widening, and removing rocks in the road that would cause undue stress on the transport truck. Upon completion of road work, compost was transported from an offsite staging and loading area established near the confluence of the Alta tributary and Corbin Creek. The skid steer was used to load super sacks at the staging area and the excavator was used to unload them at the lower Alta site.

Steep rough terrain made it impossible to prepare treatment plots with conventional agricultural equipment; instead, an excavator was used. A 1 m x 1 m trench was dug approximately 30 m upslope and parallel to the area chosen for plot construction in order to protect treatments from excessive erosion. Also, silt fences were installed below treated plots to prevent soil loss from reaching the Alta tributary. Terraces on the area to be treated were returned to the approximate original contour of the hillside. As

terraces were excavated, all substrate that had the appearance of topsoil (i.e. more apparent organic matter, finer texture) was stored upslope from the plots. The apparent topsoil was the last substrate returned to each plot to be used as the seed bed. For treatments that required amendments, the teeth on the bucket of the excavator were used to incorporate lime and/or compost into the top 15 – 20 cm of soil. All work performed on the excavator was done by Arrowhead Reclamation, a private contractor. Plot construction was completed on April 30, 2007.

Compost

Compost made from sawdust, agricultural wastes, and dairy, steer, and horse manure was purchased from Earth Systems Compost. The compost, which was analyzed by an independent laboratory, was found to contain 32.9% OM, 0.793% N, 0.393% P, and 2.16% K. Plots amended with compost received approximately 2 m³ each, which corresponded to an addition of roughly 2.25% OM in the top 15 cm of the soil profile. Accounting for background OM concentrations, a target of 2-6% OM was set in the 0 -15 cm interval on plots that received compost.

Lime

Lime product used on treatment plots was 97.5% pure agricultural lime (CaCO₃). Nominal grain sizes listed by the manufacturer were between 0.297 and 0.8 mm. An actual fineness factor (FF) of 61% was determined by the method of Whitney and Lamond (1993). By this method, grains < 0.25 mm are 100% reactive, grains between 0.25 - 2.4 mm are 50% reactive, and grains > 2.4 mm are not considered. Lime product was applied at a rate of 1.45% (14.5 T-lime 1kT-soil⁻¹). The purity (CaCO₃ equivalence) and FF reduced the effective rate of calcium carbonate addition to 8.6 T-CaCO₃ 1kT-soil⁻¹. A target pH of 6.5 was the goal of lime amendment.

Seeded Species

Plots were seeded on May 4, 2007 with a bulk seed mix that contained equal portions of 5 native grass species and 1 forb species (Table 3). Each species was included in the seed mix for a specific adaptation to the Alta mine site or to AMD site conditions in general.

Spring wheat was also seeded in each of the 16 plots as a cover crop. All plots received 34 kg-pls ha⁻¹ of bulk seed mix and 42 kg-pls ha⁻¹ spring wheat. Alfalfa seed (5.5 kg-pls ha⁻¹) was applied to half of the plots as an additional cover crop. Seed was broadcasted onto the soil surface with 9-kg capacity Solo® model 421S portable seed spreaders and then lightly raked into the soil by hand.

Table 2. Seeded Species of Grasses, Gorbbs, and Trees.

Common Name	Scientific Name	Variety	Reason
<i>Grasses</i>			
Bluebunch wheatgrass	<i>Pseudoroegneria spicatum</i>	Goldar	drought tolerant, bunchgrass
Idaho Fescue	<i>Festuca idahoensis</i>	Joseph	found on site,

Big bluegrass	<i>Poa ampla</i>	Sherman	bunchgrass acid tolerant
Canada wildrye	<i>Elymus canadensis</i>	Mandan	drought and acid tolerant
Slender wheatgrass	<i>Agropyron trachycaulum</i>	Copperhead	acid tolerant
<i>Forbs</i>			
Lewis flax	<i>Linaria lewisii</i>	Appar	found on site
<i>Cover Crops</i>			
Alfalfa	<i>Medicago sativa</i>	falcata	N-fixing cover crop
spring wheat	<i>Triticum spp.</i>		cover crop
<i>Trees</i>			
Douglas-fir	<i>Pseudotsuga menziesii</i>	harvested near site	
Limber Pine	<i>Pinus flexilis</i>	harvested near site	
Aspen	<i>Populus tremuloides</i>	harvested near site	

The possibility of successfully establishing deciduous and coniferous trees on the lower Alta mine site was also examined. Roots of aspen trees from 2 separate aspen stands within 100 m of the lower Alta site were collected in early June 2006. Seventy (70) root cuttings were harvested and cultivated in a greenhouse according to MacDonald (1986). Saplings were removed from the greenhouse in the fall and exposed to winter conditions in a standard horticultural lath house; thereby, trees entered a dormant state and acquired winter hardiness. Freshly fallen Limber pine and Douglas fir cones were collected on August 21, 2006 from tree stands adjacent to and at the same elevation as the Alta mine. Seeds were plucked from the cones with tweezers, planted in individual growth containers, and vernalized according to MacDonald (1986). Following the 6 week vernalization, conifer seeds were planted in 2.5 x 15 cm containers filled with standard greenhouse potting soil. Containerization was completed in December 2006. Emerging seedlings were watered weekly and held at 25°C until they were planted on site. At the time they were transplanted, seedlings were approximately 2.5 – 6 cm tall. Aspen saplings and Douglas fir and Limber pine seedlings were transplanted to the lower Alta reclaimed area on May 4, 2007. Saplings and seedlings were planted into unamended soils above and below treatment plots.

Experimental Design

The 16 plots consisted of 4 treatments, each replicated 4 times. Treatments included: compost alone, lime alone, lime and compost, and seeded controls. Replicates were equally divided and randomly applied to either of 2 blocks: trees; or alfalfa. Plots in

the alfalfa block were seeded with bulk seed mix and an additional 5.5 kg pls ha⁻¹ alfalfa. The trees block received only the bulk seed mix; but the conifer seedlings and deciduous saplings were planted in unamended soils around its perimeter (Figure 6).

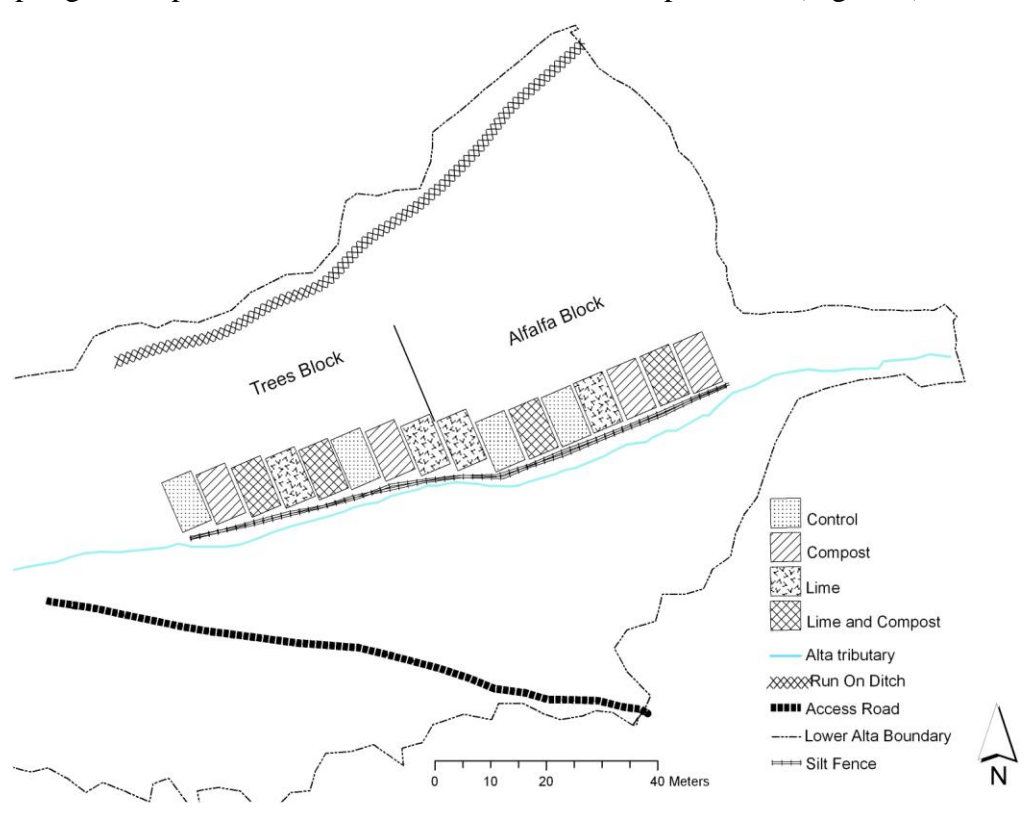


Figure 5. Treatment Plot Layout for Experimental Revegetation Trials.

Quantification of Vegetative Cover

As was done in the baseline vegetation survey, canopy cover at the end of the 140-day growing season was measured with the Daubenmire method (1959). A single diagonal transect from the southeast corner to the northwest corner of each treatment plot was established. Cover was determined by species in 6 – 0.1 m² frames spaced approximately 1.8 m apart on each transect. Tree mortality was determined by counting the number of living and dead trees at the end of the growing season.

Quantification of Soil Productivity

A composite soil sample from the amended soil depth was collected for each plot from 4 locations, spaced approximately 2.7 m apart, on the diagonal transect. Samples were collected in 1 L disposable cups and transferred to plastic bags. Samples were homogenized by a thorough mixing within the plastic bags and during the drying process of Sobek et al. (1978).

Soil samples derived from the treated plots were analyzed for OM, pH, EC, and water extractable Cd, Cu, Pb, Zn, and As. Methods of analysis were consistent with those previously described except for OM and water extractable heavy metals and As. OM was determined by the loss on ignition method (Nelson and Sommers 1996) because it could be done cheaply in-house. Soils subject to loss on ignition (LOI) were ground first, for 2 minutes in a SPEX Certiprep 8000D ball mill, with 1.27 cm diameter ceramic balls. Water extractable heavy metals and As were determined from a 1:10 soil solution because subsamples that remained after LOI were too small to yield a viable extract from a 2:1 saturated paste; however, ICPMS was still used to determine heavy metal and As concentrations.

Water Quality Monitoring

Surface Water Monitoring Locations

Paired stream flow measurements and sediment, As, and heavy metals samples were collected at 6 surface water monitoring locations in both the Corbin Creek watershed and Alta subwatershed throughout the summer of 2007 (Figure 7).

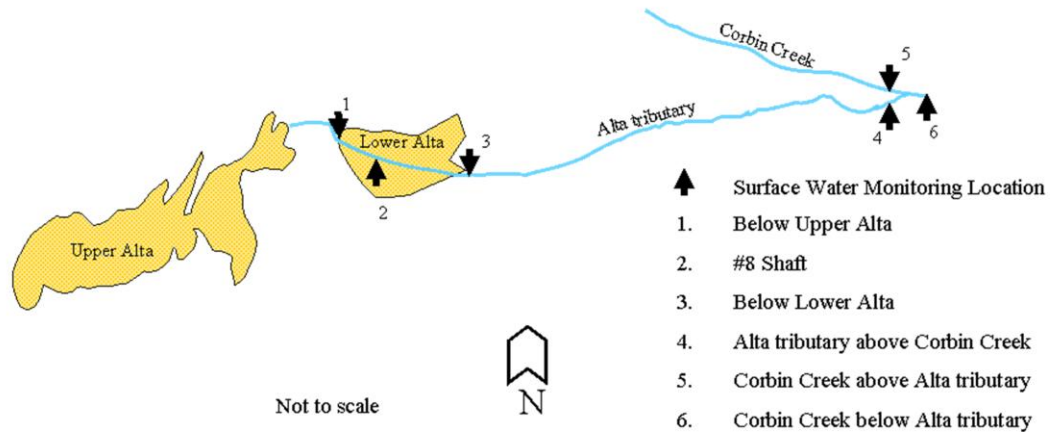


Figure 6. Summer 2007 Alta Sub-Watershed Surface Water Monitoring Locations.

The 6 sampling locations were: below the Upper Alta waste rock pile; at the #8 shaft; below the Lower Alta reclaimed area; above the confluence of the Alta tributary and Corbin Creek (in the tributary); above the confluence of the Alta tributary and Corbin Creek (in the creek); and below the confluence of the 2 streams. Monitoring locations in the Alta tributary were situated in the approximate location described by Scroth (2001). While the exact geographic location of 1999 and 2000 sample points was not known, the locations proposed above are likely a close fit. The monitoring location in Corbin Creek below the Alta tributary was situated well below the mixing zone (Thomann and Mueller 1987) determined by maximum stream velocity, depth, and width. Monitoring locations allowed for comparison of 2007 As and heavy metal concentrations to heavy metal and As concentrations present during reclamation (1999) and 1 year removed (2000). In

addition, paired solute concentrations and discharge measurements taken over the course of summer 2007 at the monitoring locations above and below the confluence with the Alta tributary in Corbin Creek were used to determine the Alta tributary's contribution to Corbin Creek water quality impairments by As and heavy metals. Metal loads were compared to TMDL goals and previously estimated maximum loads for Corbin Creek (US EPA 2006). No direct measures of water quality impacts on aquatic life were monitored; however, in stream concentrations of As and heavy metals were compared to acute and chronic aquatic life standards (MT DEQ 2006). Results of the water quality monitoring effort are included in Appendix A.

As and Heavy Metal Samples and Analysis

Heavy metals and As samples were frequently collected at each of the 6 sampling locations, if sufficient flows permitted, from March 23 to September 14, 2007. Grab samples were collected in clean 250 ml plastic bottles from the center of flow in either the Alta tributary or Corbin Creek. Bottles were rinsed 3 times with stream water before a sample was collected on the 4th grab. Stream pH was measured directly with a handheld model IQ150 pH meter at the time of sample collection.

All samples were analyzed for total recoverable (TR) metals and As. A limited subset of samples was analyzed for total soluble (TS) metals and As. TR and TS samples were prepared by acidifying to pH<2 or by filtering (0.2 µm) and acidifying to pH<2, respectively.

Hardness

Hardness was measured exclusively at each of the two monitoring sites in Corbin Creek in order to draw comparison with acute and chronic aquatic life standards (ALS) for Cd, Cu, Pb, and Zn instituted by MT DEQ (2006). Toxicity of heavy metals and subsequent standards for aquatic life are a function of hardness, (Table 4), due to competition of benign calcium (Ca) and magnesium (Mg) cations with toxic heavy metal cations. In general, as hardness increases, toxicity of heavy metals decreases. If hardness is <25mg L⁻¹ as CaCO₃, the number 25 is used in the relationships; likewise, 400 is used in the relationships for hardness >400 mg L⁻¹ as CaCO₃ (MT DEQ 2006).

Table 3. Hardness Relationships and Coefficients for Acute and Chronic Aquatic Life Standards (MT DEQ 2006)

Hardness relationships				
	Acute ALS = e ^{ma[ln(hardness)]+ba}			
	Chronic ALS = e ^{mc[ln(hardness)]+bc}			
Coefficients				
	ma	ba	mc	bc
Cadmium	1.0166	-3.924	0.7409	-4.719
Copper	0.9422	-1.7	0.8545	-1.702
Lead	1.273	-1.46	1.273	-4.705
Zinc	0.8473	0.884	0.8473	0.884

Hardness (as CaCO_3) was determined by analysis of water samples for both Ca and Mg cations by ICPMS. A single sample per month of study was randomly selected for hardness determination and considered representative of hardness for the stream until subsequent samples were taken.

Stream Gaging

The height of the water column was gaged at all surface water sampling locations except for the #8 shaft and Corbin Creek above the Alta tributary. These sites were excluded due to a limited number of gaging instruments and because the #8 shaft was not a suitable location for instrumentation. Gage height was read with Ecotone WM water level monitors at 15 minute intervals during the summer of 2007.

Discharge (Q) was determined at each monitoring location by 1 of 2 methods: 1) a calibrated bucket and stopwatch; or 2) the continuity method and a Swoffer 3000 stream velocity meter. As a rule, Q was determined by calibrated bucket at monitoring locations at the lower Alta reclaimed site; and the velocity area method was used for sites lower in the watershed. Sedimentation dams constructed at the lower Alta site in 1999 provided confined flows over spillways that were easily sampled by calibrated bucket; further, rip rap placed in the channel during the reclamation effort negated our ability to use a velocity meter there. Monitoring locations at lower sites had no such spillways but were free of large rocks that would preclude usage of a velocity meter. Gage heights were related to stream flow by power function rating curves.

Suspended Sediment Samples and Analysis

Suspended sediment concentrations were monitored at each location except for the #8 shaft. The height of the water column in both the Alta tributary and Corbin Creek was insufficiently high to accommodate the use of standard USGS sampling equipment, US DH-48 and US U-59 samplers. Instead, suspended sediment samples were collected in an open bottle (US DH-48 variety), as suggested by Edwards and Glysson (1999). Samples were analyzed according to standard methods (American Public Health Association 1989) for Total Suspended Solids.

Precipitation

A tipping bucket rain gage with a Hobo® event recorder was deployed on northeast corner of the lower Alta reclaimed site at approximately 1,710 m amsl. The gage was situated on a level plane away from objects that would obstruct rain and wind. The gage was used to record cumulative precipitation, event frequencies, and durations from March 23 to October 1, 2007.

Snow Water Equivalent

Snow water equivalent was estimated in bi-weekly snow course measurements from January 22 to April 15, 2007. Measurements were made according to Colbeck et al. (1990) on a snow course established on the lower Alta reclaimed area. Slopes of south and north aspect were represented in 10 established measuring locations within the snow

course. The snow course was established on the lower Alta reclaimed area because the site was not covered with tree canopy; but trees nearby provides some resistance to wind. Also, the lower Alta site was situated at a moderate elevation in the Alta subwatershed.

Groundwater

Shallow groundwater on site was characterized for heavy metal and As concentrations by installing and sampling a network of shallow monitoring wells (Figure 8). The wells were systematically located near seeps and abandoned mine features that had the appearance of potential groundwater movement and on the flanks of the Alta tributary, where hyporheic mixing was possible. Aside from the #8 shaft, the most notable sources of water at the lower Alta reclaimed area were the portal, a horizontal adit south of the #8 shaft, and the bathtub springs, a small spring to the north of the #8 shaft that was not impacted by mining activity. In the absence of a seep or leaky mine feature, most of the slopes of the Alta subwatershed were unsaturated to depths below that which could be reached by shallow monitoring wells. Shallow wells were installed near each of the 3 surface water monitoring sites near the confluence of the Alta tributary and Corbin Creek.

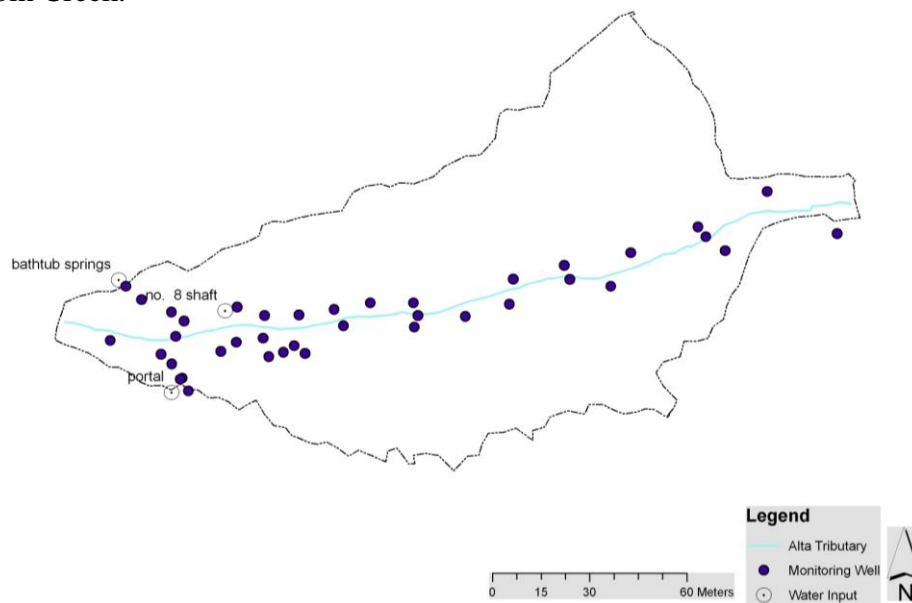


Figure 7. Network of Shallow Monitoring Wells at Lower Alta Reclaimed Area.

Well Construction. Holes used in well construction were made with a 5 cm diameter conical tipped steel pipe. The pipe was driven into the ground with a post driver and extracted with a hi-lift jack. Wells were cased with 2.54 cm diameter PVC pipe screened over an approximate 30 cm interval from completed depth. PVC pipe was capped at the bottom and lowered into completed holes. Annular space around the casing was filled with 2 mm silica sand to the top of the screened interval. A 25 cm bentonite

clay seal was layered over the sand in each well. Soils found on site were used to fill the remainder of the annular space. Each well was capped with a 3.8 cm PVC sleeve to prevent rainfall from entering the casing. Completed depths of the shallow wells ranged from 114 cm to 200 cm below the ground surface.

Groundwater Sample Collection and Analysis. Shallow groundwater was drawn from 12 of the monitoring wells in the summer of 2007. First, each well was purged with a peristaltic pump to confirm a hydraulic connection with groundwater. Approximately 1 hour after purging, samples were pumped into clean 250 ml bottles from wells that exhibited adequate recovery. The pH of each sample was measured with a handheld Model IQ150 pH meter and recorded at the time of collection. Samples were filtered (0.2 μm), transferred to a separate clean sample bottle, and acidified to $\text{pH} < 2$. Samples were analyzed by Energy Laboratories, Inc. of Billings, MT with inductively coupled plasma mass spectroscopy (ICPMS).

Static Water Level Measurements. A Solinst® water level monitor was used to establish groundwater depths below the ground surface. Water level measurements were used to indicate water level recovery during groundwater sampling events. Also, bi-monthly measurements were made throughout the summer of 2007.

Statistical Methods

Z* test Statistic

Existing soil As and Pb concentrations in the 0 – 15 cm interval were compared to soil screening levels used in the 1999 reclamation project. The null hypothesis (H_0) was that observed mean soil As and Pb levels were equivalent to targeted screening levels. The alternative hypothesis (H_a) being that soil As and Pb concentrations in 2006 were indeed higher than the screening levels. The hypothesis was tested on the basis of a Z statistic (Devore and Farnum 2005). Prior to analysis, normal probability plots of the data were examined and a logarithmic data transformation was made to normalize the data.

ANOVA Approach to Linear Regression

Single and multifactor linear regression models were constructed in R 2.5.1 to determine any correlation between soil physical and chemical properties and vegetation on site. Vegetative cover was used as the dependent variable; and independent variables included aspect, pH, ABP, OM, nutrients, heavy metals, and arsenic. Association between dependent and independent variables was measured with the coefficient of correlation (r); and regression models were considered significant at $p < 0.1$. The aptness of linear regression models was diagnosed with normal probability plots and plots of residuals against fitted values. Significant single and restricted variable regression models were compared to multifactor models by Analysis of Variance (ANOVA), using

R version 2.5.1 (2007), to account for variability in vegetation due to cumulative factor effects. Like regression models, ANOVA models were considered significant at $p < 0.1$.

Wilcoxon Rank Sum Test

The Wilcoxon Rank Sum Test was used to compare the relative quality of soil in the 0 – 15 cm interval to that of soil in the 60 – 75 cm interval for each of the 30 soil pits. The comparison was made on the basis of total Pb, As, Zn, OM, ABP, N, P, K, and pH. It was expected that the test would establish patterns of incomplete waste removal, upward movement of contaminants, or erosion of topsoil cover material.

The Wilcoxon Rank Sum Test was also used to compare lime and compost treatment effectiveness at increasing pH, decreasing EC, increasing vegetative cover, and decreasing available heavy metals and As. The test was used because the assumption of normality was not appropriate with only 4 replicates of each treatment type. R 2.5.1 was used to perform statistical computation.

RESULTS AND DISCUSSION

Water Quality Monitoring

Hydrograph

Stream flow in the Alta tributary and Corbin Creek was gaged and discharge hydrographs for summer 2007 were approximated at three locations: at the lower Alta reclaimed site, in the Alta tributary above Corbin Creek, and in Corbin Creek below the Alta tributary (Figure 9). Low intermittent flows at the monitoring site between the upper Alta waste rock dump and lower Alta reclaimed area prevented the establishment of a hydrograph and limited the monitoring effort at that location. A discharge hydrograph was not established for the #8 shaft, due to diffuse flows that were not measurable by a calibrated bucket, stream velocity meter, or Ecotone® water level monitor. As such, flows recorded at a confined overflow point 50 m downstream were considered representative of #8 shaft discharge. Corbin creek above the Alta tributary was not gaged; although, stream flow measurements were made as surface water samples were collected. Surface water flows were not observed above the confluence with the Alta tributary from 6/9/2007 to 9/14/2007.

Flow patterns in the Alta tributary immediately above Corbin Creek and in Corbin Creek immediately below the tributary were typical of low order mountain streams. Peak discharge at both sites corresponded to spring rain and snowmelt. Seasonal snow accumulation had completely disappeared from the lower Alta snow course by early April. Snow water equivalent accounted for 3.5 cm of the total 25.5 cm of precipitation received in the Alta sub-watershed. At the lower Alta reclaimed site, discharge was highly variable; and flow patterns were controlled more by mine shaft discharge than by surface hydrologic processes. Discharge at all locations was low and easily quantified in L min^{-1} . Peak flow at all sites occurred on May 22, as the result of an extended late spring rainfall event. Peak flows were estimated as 239, 137, and 91 L min^{-1} , respectively, at Corbin Creek below Alta, the Alta tributary above Corbin Creek, and at the lower Alta reclaimed site.

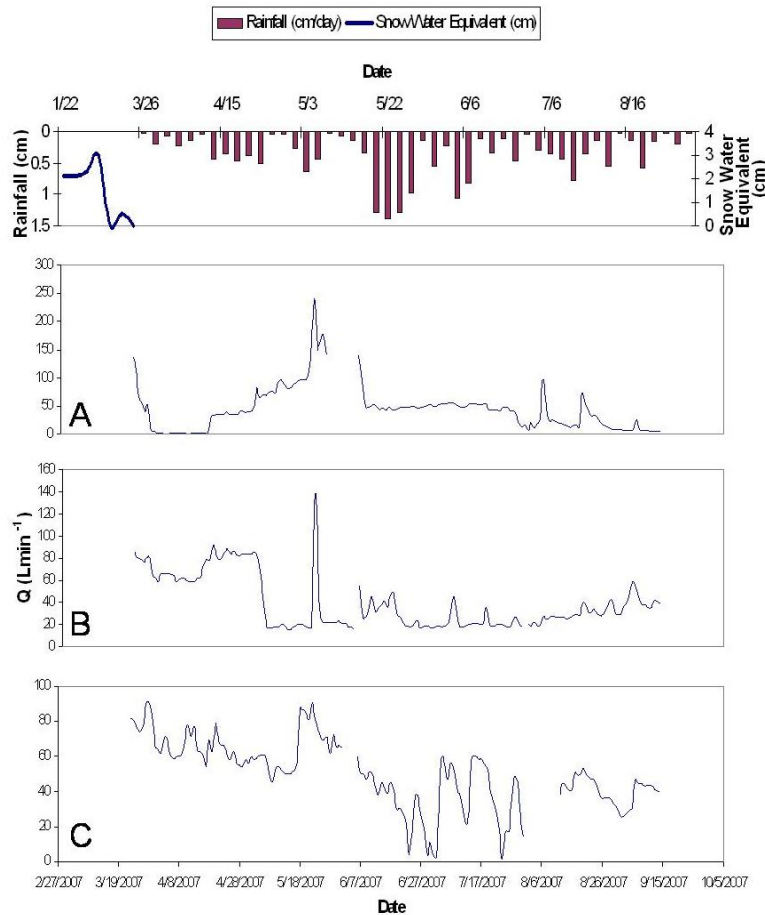


Figure 8. Rainfall Hyetograph, Snow Water Equivalent, and Mean Daily Discharge for A.) Corbin Creek Below the Alta Tributary, B.) Alta Tributary Above Corbin Creek, C.) Alta Tributary Below Lower Alta Reclaimed Area.

Surface Water pH

Each monitoring location had a distinct pH signature. Generally, pH was greatest in surface flows of Corbin Creek above the confluence with the Alta tributary. Measurements made at the upper Corbin Creek monitoring location ranged from 7.16 – 8.0 before the stream dried up in early June 2007. Neutral pH at this site might be the result of lime applied to soils and limestone rip-rap used in the stream channel during the reclamation of the Bertha tailings. This is a crude indicator that removal of the acidic tailings (pH < 3.0, Deckler 1982) may have mitigated water quality impacts in Corbin Creek above the contribution of the Alta tributary.

Stream flow at all other monitoring locations exhibited pH that was well below neutral. A single pH measurement of the intermittent surface flow between the upper Alta waste rock pile and lower Alta reclaimed site was 3.5. Trends in pH followed the

hydrograph at the remainder of the monitoring locations (Figure 10). Generally, pH was highest for observations made in the spring and during precipitation events. When peak hydrograph conditions subsided in early June, a distinct drop in pH was observed at all locations. The pH drop was likely attributable to less mixing with neutral snow-melt and shallow meteoric waters.

Decreased pH was nowhere more noticeable than in Corbin Creek below Alta, where pH dropped by more than 1 unit (from 3.7 to 2.5). The decrease in pH at this location was due to vanished or reduced mixing with neutral surface waters from above. Discharge from the #8 shaft had the highest pH (as high as 4.63) of the monitoring locations in the Alta tributary; but it decreased rapidly in the downstream direction. The rapid decrease was probably due to sulfide oxidation or the precipitation of Fe-hydroxides. The stream channel immediately below the #8 shaft was blanketed with ferric hydroxide precipitates. It was common for pH to have dropped more than 1 unit by the time flows exited the lower Alta reclaimed site, roughly 180 m downstream. Further reductions in pH occurred in the downstream direction. Surface flows with the lowest pH were generally found in the Alta tributary immediately above Corbin Creek.

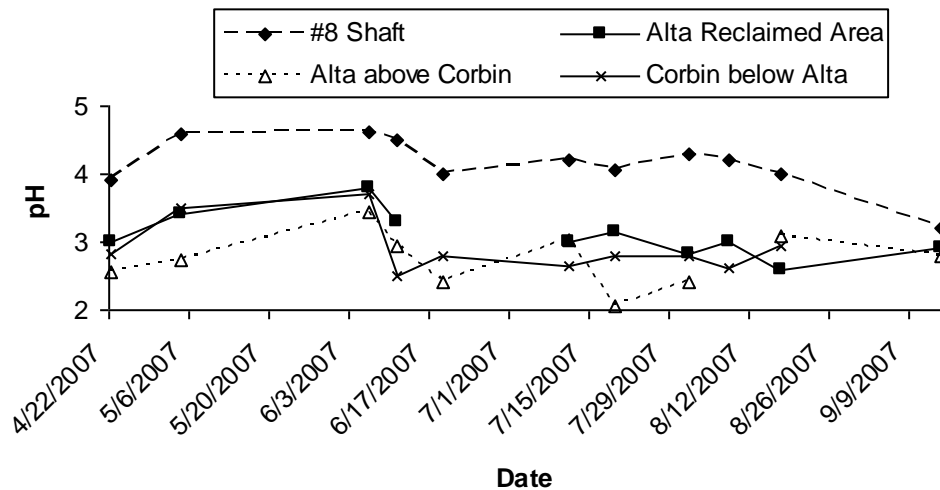


Figure 9. Temporal Trends in Alta Sub-Watershed pH by Site.

Heavy Metals and As.

Sources of heavy metal and arsenic varied by element and were controlled by pH, stream flow patterns, and apparent reactive processes. Heavy metal and As monitoring was only meaningful at or below the #8 shaft. Intermittent stream flow between the upper Alta waste rock pile and lower Alta reclaimed area was minimal during visits to the site. Before the flows ceased in early June 2007, two (2) observations of paired flow and heavy metal and As concentrations were made at the monitoring location between the upper and lower Alta (Table 5). Loads greater than those observed were likely to have occurred during peak runoff and high intensity rainfall events; but low aqueous metal and

As concentrations would still result in significantly lower transport rates than those measured at downstream monitoring locations.

Table 4. Heavy Metal and Arsenic Loads From Upper Alta Waste Rock Pile.

Date	Time	Flow L min ⁻¹	Element Load kg day ⁻¹				
			As	Cd	Cu	Pb	Zn
23-Mar	16:00	8.18	ND*	ND*	0.12	0.04	0.62
22-Apr	13:00	1.57	0.07	0.005	0.18	0.33	5.04

*ND=Element not detectable by ICPMS

Arsenic was predominately discharged from the #8 shaft and was naturally attenuated in the downstream direction (Figure 11). As concentrations observed in the #8 shaft discharge ranged from 4.37 – 10.5 mg L⁻¹ but decreased by an average of 73% at the monitoring location approximately 180 m downstream. Enriched As concentrations in #8 shaft discharge resulted in the highest loads of any site in the Alta tributary. Stream flow increased in the downstream direction from March to June; so dilution may have accounted for some of the decrease in As concentration. However, the decline in As load was likely due to co-precipitation with noticeable Fe-hydroxides in the channel of the lower Alta reclaimed site. No measures of Fe-hydroxide production or As sorption were made in the monitoring effort.

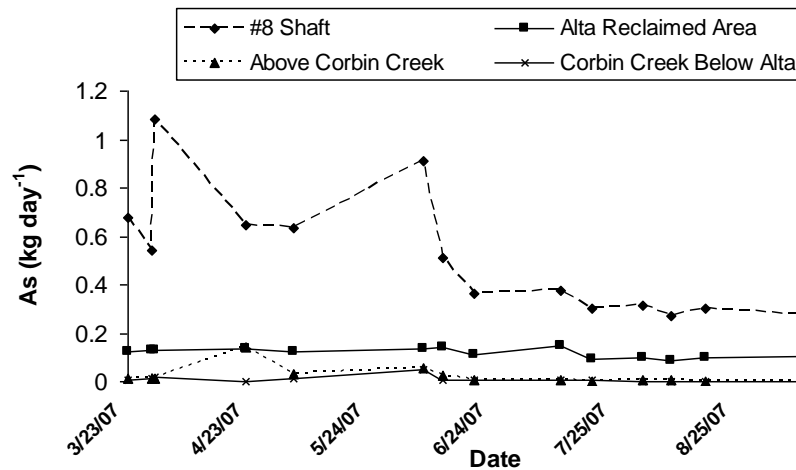


Figure 10. Temporal Trend in Alta Sub-Watershed As Loads by Site.

Cu load in the tributary was similar in magnitude to As load; but it exhibited an opposite trend (Figure 12). Concentrations emerging from the #8 shaft were 0.1 – 0.3 mg Cu L⁻¹ during spring and early summer and no Cu was observed in shaft discharge (by ICPMS) from June 11 to September 14, 2007. Cu load increased in the downstream direction, which implicated an input of leachate from Alta mine soils or waste rock in the lower reach of the tributary. The highest Cu loads were typically measured at the Alta

tributary above Corbin Creek monitoring site; however, the observed peak Cu load for all monitoring locations and all sampled times occurred in Corbin Creek below the Alta tributary during a June 6th precipitation event. Peak loads measured at upper monitoring locations (#8 shaft, and Below Reclaimed Area) were also at times of hydrologic input of either snowmelt or rainfall. The response of Cu transport to hydrologic input further suggests that it is flushed to the Alta tributary in soil pore water.

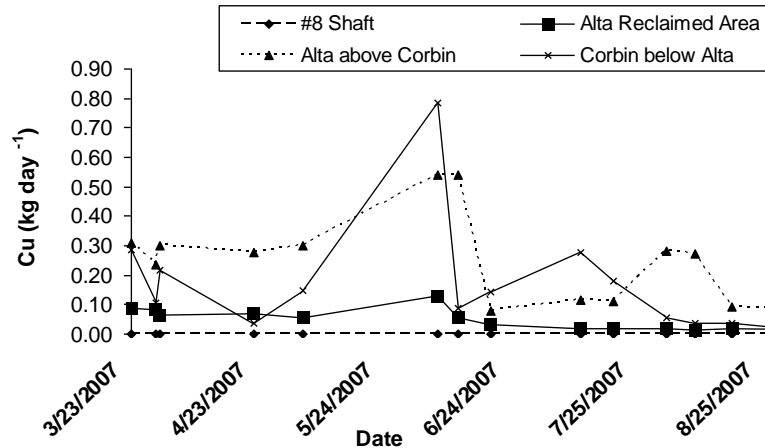


Figure 11. Temporal Trend in Alta Sub-Watershed Cu Loads by Site.

Maximum Cd and Pb loads observed at any location in the Alta tributary were an order of 10x less than those of Cu and As. Higher Pb loads were observed at the #8 shaft; while, Cd accumulated in stream flows throughout the lower reach of the Alta tributary (Figure 13). Both metals, however, appeared to originate from point source deep underground mine workings and diffuse landscape contributions. Cd loads observed at both the #8 shaft and below the lower Alta reclaimed area remained relatively constant over all hydrologic conditions monitored. Cd loads at lower monitoring locations followed trends similar to Cu and Pb, in that they varied with hydrologic input.

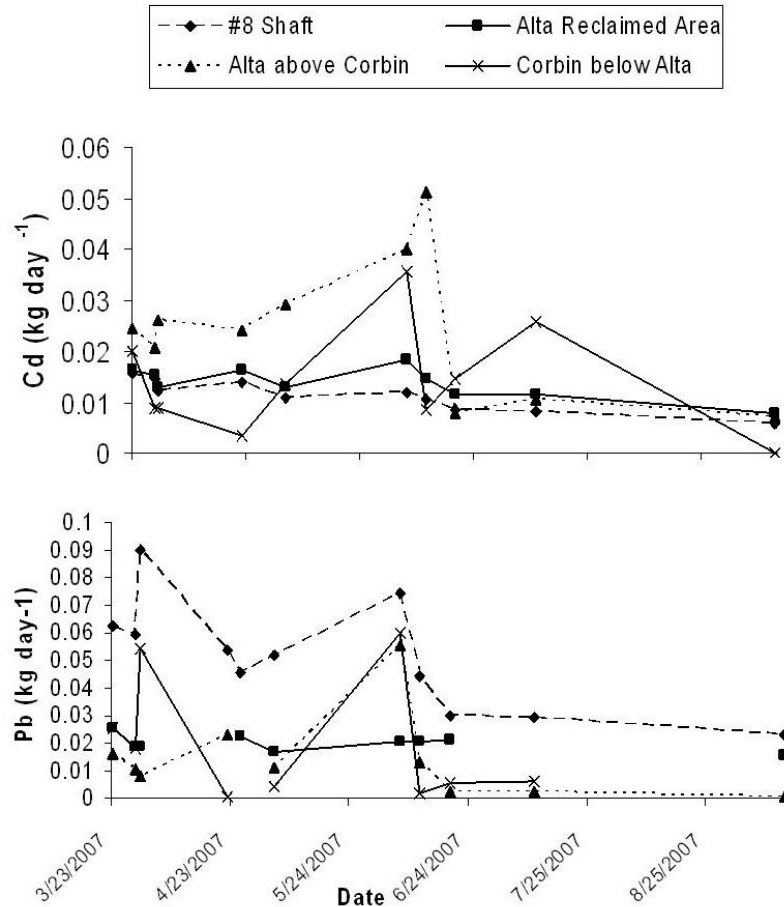


Figure 12. Temporal Trends in Alta Sub-Watershed A.) Cd Load and B.) Pb Load by Site.

By suspected co-precipitation with Fe-hydroxide or other chemical transformations, #8 shaft Pb loads were mitigated by an average of 60% by the time they reached the monitoring location below the lower Alta reclaimed site; however, Pb loads at downstream monitoring locations did not appear to be controlled by loads sourced from above. Pb loads more closely followed hydrologic patterns. During a freeze thaw cycle that occurred in late April, Pb loads were as low as $7 \times 10^{-4} \text{ kg day}^{-1}$ in the Alta tributary above Corbin Creek. At the same monitoring location, Late spring rains elevated Pb loads to $5.6 \times 10^{-2} \text{ kg day}^{-1}$, despite a near constant Pb discharge from the lower Alta reclaimed area.

Zn loading rates in the Alta sub-watershed were far greater than that of any other element under study. Loads as high as 45 kg day^{-1} were observed from the #8 shaft (Figure 14). The shaft generally transported the highest rates of Zn; but concentrated discharge that occurred during spring rains also led to elevated Zn loads at lower monitoring locations. Zn loads from the #8 shaft responded only mildly to hydrologic inputs and decreased continually throughout the monitored interval. Zn loads below the

lower Alta reclaimed area were relatively constant throughout the study and did not decrease with decreasing Zn input from the #8 shaft above.

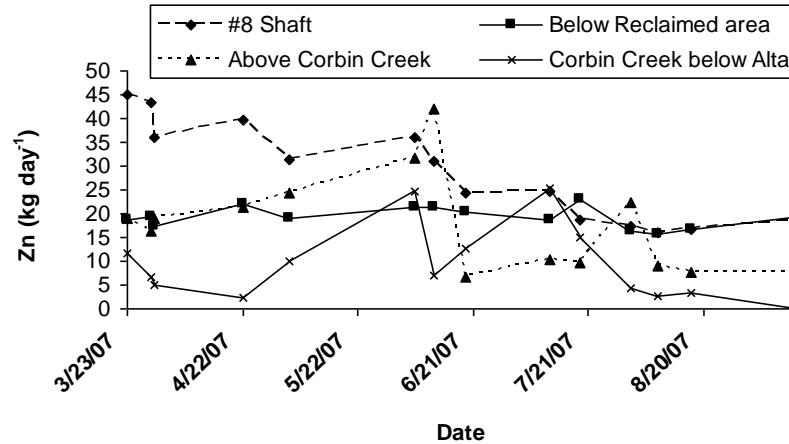


Figure 13. Temporal Trends in Alta Sub-Watershed Zn Load by Site.

Heavy Metals and As in Soil-Water and Groundwater.

Concentrations of As, Cu, and Zn were determined in both soil-water and in shallow groundwater for a random sub-sample of soil pits and monitoring wells, respectively, on the lower Alta reclaimed area in order to determine the contribution of the elements from the mine-impacted landscape. Groundwater samples were collected on August 17th and limited to wells constructed at the lower Alta reclaimed area because wells at the Corbin Creek and Alta tributary above Corbin Creek monitoring locations were dry at the time of sampling. Soil and groundwater source determination was particularly important in the case of Cu loading to the Alta tributary, as the #8 shaft was found to be a minimal source of that element. By examination of surface water concentrations of other heavy metals, it appeared that Cd, Pb, and Zn came from both deep underground sources and landscape sources. Zn was the only of the three metals measured in soils and groundwater; and its behavior was treated as a surrogate for Cd and Pb behavior. As concentrations in soil and shallow groundwater were determined to test the assumption that As was primarily discharged from the #8 shaft and because As behaves markedly different in soil and aqueous systems than heavy metals (Inskeep et al. 2002).

Patterns of soil-water and shallow groundwater As, Cu, and Zn concentrations differed greatly by element (Figure 15). Maximum water extractable Zn concentrations in soil were lower than groundwater concentrations or surface water quantities at either the #8 shaft or below the lower Alta reclaimed area; but considerably higher than soil water concentrations of the other elements. On the date sampled, Zn concentrations at the shaft and below the reclaimed area were nearly equal. Shallow groundwater Zn concentrations in wells immediately adjacent to the Alta tributary were indicative of concentrated surface waters mixing with dilute soil leachate that had accumulated in the

saturated hyporheic zone. The connection of surface water and shallow groundwater is further evidenced by Cu concentrations in soil-water and shallow groundwater.

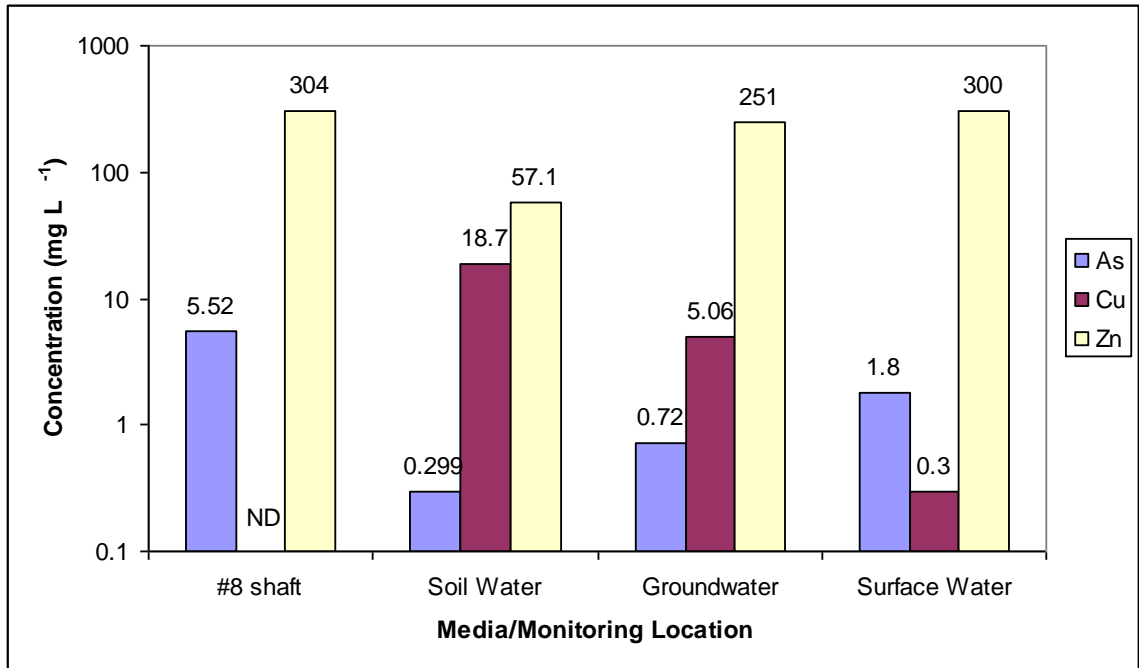


Figure 14. Peak As, Cu, and Zn Concentrations in Soil-Water, Shallow Groundwater, and Surface Water at the Lower Alta Reclaimed Area (August 17, 2007).

An apparent gradient of peak Cu concentrations from soil to shallow groundwater and ultimately to Alta tributary surface flow was identified. The peak soil water-extractable Cu concentration (18.7 mg L^{-1}) was determined in a soil pit on the south facing slope of the Alta reclaimed area near where Becraft (1963) described an exploratory mining effort of a Cu-rich vein that resulted in waste deposits on the lower Alta dump. Cu on the landscape of the lower Alta reclaimed area is likely the result of residual Cu-bearing minerals left during the 1999 reclamation project; or it is leached from the collapsed exploratory adit. The average Cu concentration in shallow groundwater of 6 monitoring wells was $2.04 \pm 1.53 \text{ mg L}^{-1}$. The relatively dilute Cu concentrations in the saturated subsurface near the Alta tributary were the result of mixing with Cu-deficient waters discharged from the #8 shaft. During the August 17th sampling effort, the #8 shaft Cu concentration was not detectable by ICPMS and the in stream concentration of discharge below the lower Alta reclaimed area was 0.3 mg L^{-1} .

Water extractable As concentrations in soil were low, averaging $0.06 \pm 0.08 \text{ mg L}^{-1}$ and peaking at 0.299 mg L^{-1} . Low As mobility was expected in Alta soils because As is highly sorbed to soils and metal hydroxide solid phases in low pH systems (Manning and Goldberg 1997, Goldberg 2002). Concentrations of As in shallow groundwater were slightly more elevated ($0.14 \pm 0.22 \text{ mg L}^{-1}$) than soil-water concentrations, likely due to mixing with surface waters. Consistent with observations made at surface water monitoring locations, the #8 shaft appears to be the prominent source of As in the Alta tributary.

Alta Contribution to Corbin Creek Loads

In order to directly address the hypothesis that the Alta tributary is the significant source of As and heavy metals to Corbin Creek, tributary loads were compared to background concentrations in the stream. Heavy metal and As loads carried by Corbin Creek above the Alta tributary and by the Alta tributary above Corbin Creek were not conservative beyond the confluence of the 2 streams; instead, co-precipitation of the elements with Fe-hydroxide precipitation in the mixing zone resulted in decreased transport of the elements. Background loads of each element in Corbin Creek and loads delivered to Corbin Creek by the Alta tributary were expressed as the mean fraction of the total load in Corbin Creek below the confluence with the Alta tributary. Fractionation normalized the data to account for changes in hydrologic regime throughout the monitoring period. Loads in Corbin Creek above the confluence with the Alta tributary were only 3.8% - 36% of the load in Corbin Creek below the mixing zone with the Alta tributary, depending on element (Figure 17). In contrast, Alta tributary loads ranged from 286% to 1,492% of the total As, Cd, Cu, Pb, and Zn in Corbin Creek. This result provided compelling evidence that the Alta tributary accounts for a significant fraction of the total As and heavy metals in Corbin Creek.

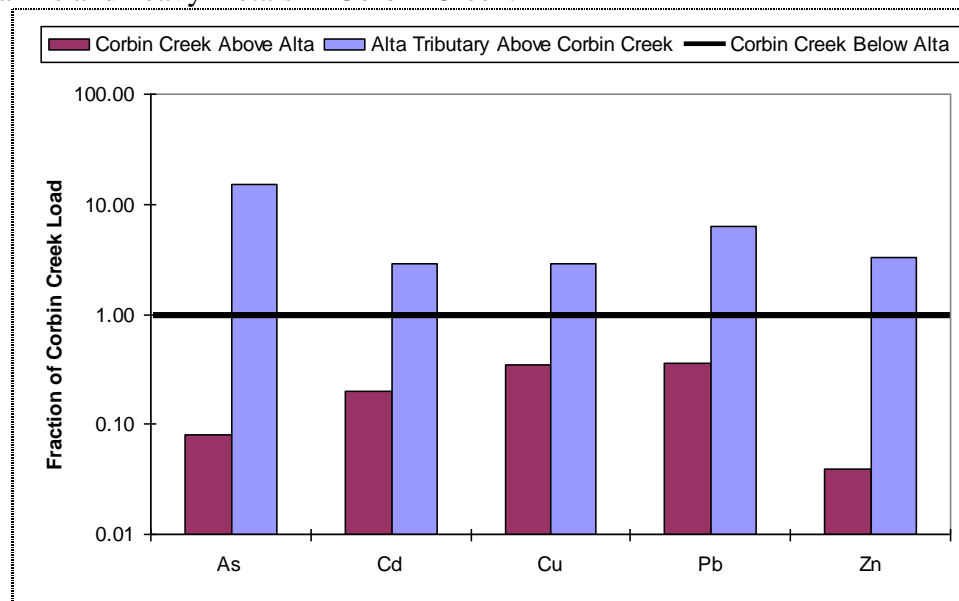


Figure 15. Alta Tributary and Corbin Creek above Alta Tributary Heavy Metal and As Loads as Fraction of Total Corbin Creek Below Alta Tributary Load.

Alta Contribution to Aquatic Life Standard Exceedences

Above the Alta tributary, hardness ranged from 347 – 392 mg L⁻¹ CaCO₃. These values were within the range of 25 – 400 mg L⁻¹ CaCO₃ and were used to determine acute and chronic ALS in Corbin Creek above the Alta tributary. Below the Alta tributary, hardness ranged from 556 – 1,330 mg L⁻¹ CaCO₃. The maximum value (400 mg L⁻¹ CaCO₃) was used to determine ALS below the Alta tributary. Heavy metal and As

concentrations measured in the summer of 2007 were compared to ALS established for each element (Figure 18).

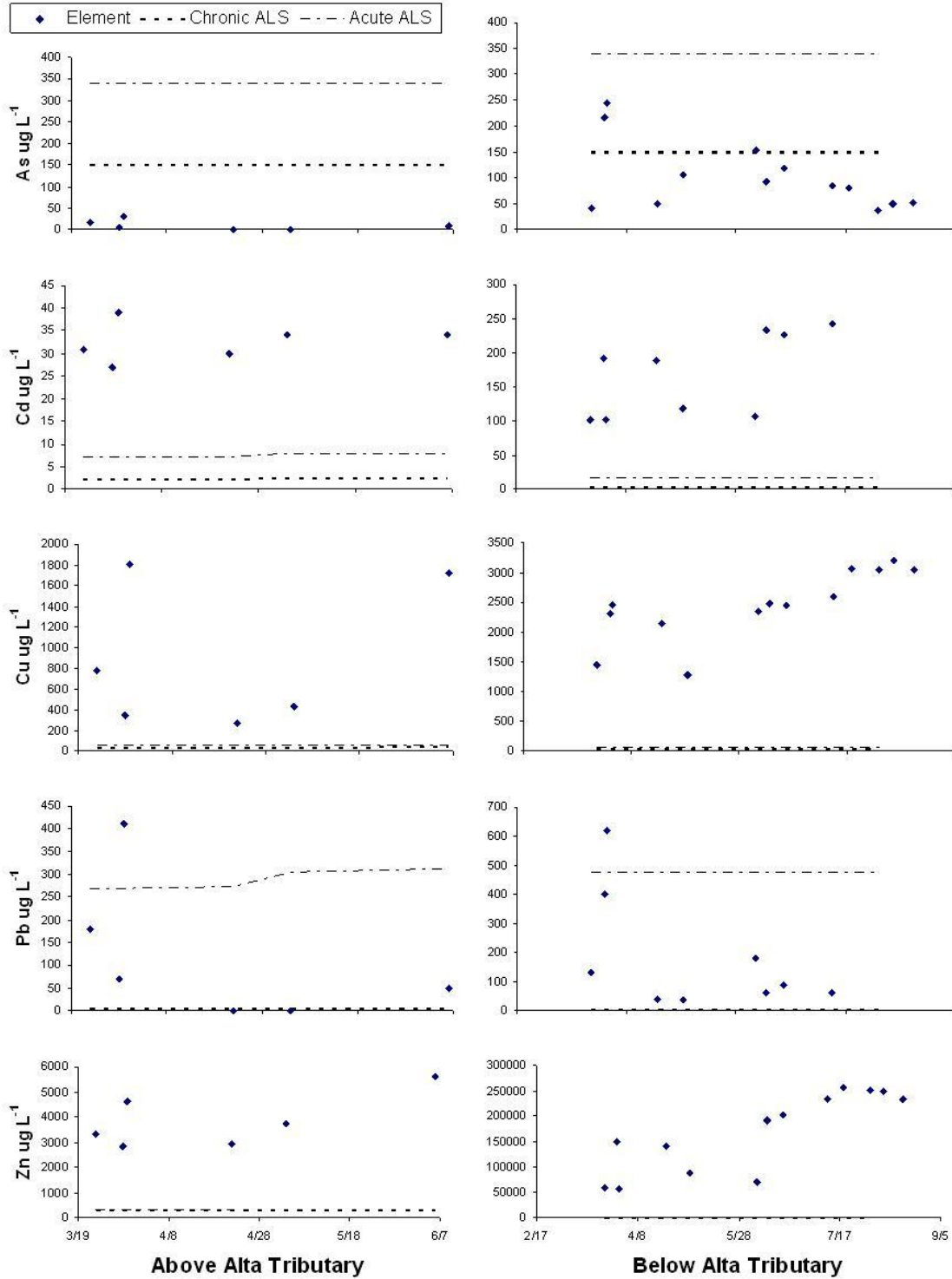


Figure 16. Heavy Metal and As Concentrations in Corbin Creek Above and Below the Alta Tributary Compared to Aquatic Life Standards in Summer of 2007.

Trace element concentrations that exceeded acute and chronic ALS were common at both monitoring locations in Corbin Creek for all elements with the exception of As. Only below the confluence with the Alta tributary were exceedances of ALS observed in the summer of 2007. Exceedances of only the chronic ALS, which is the lower standard, were observed at the monitoring location in Corbin Creek below the Alta tributary. This result suggests that of all of the elements considered in this study, As may have the least amount of impact on the health of aquatic life.

All observed heavy metal concentrations in Corbin Creek at monitoring locations above and below the Alta tributary exceeded at least the chronic ALS. Pb was the only metal not concentrated at levels above the acute ALS for all observations made. Even so, Pb was concentrated to levels above the acute ALS during early spring runoff. The level of exceedance for Cd, Cu, Pb, and Zn was far greater below the Alta tributary than in Corbin Creek above, as evidenced by the y-axes in the plot above. Again, the greater exceedances can be attributed to the disproportionately large loads contributed by the Alta tributary.

Alta Contribution to TMDL Exceedances

As and heavy metal loading rates measured in Corbin Creek above and below the Alta tributary were also compared directly to Corbin Creek TMDLs. Loads measured in the summer of 2007 at both of the Corbin Creek monitoring sites were plotted with the envelope of TMDL goals and previously estimated maximum daily loads (US EPA 2006) (Figure 19). Patterns of TMDL exceedances varied by element; but more and greater exceedances were observed in Corbin Creek below the Alta tributary. Pb and As loads exceeded the TMDL only during observed periods of high flow and only in Corbin Creek below the Alta tributary; although, Pb loads in Corbin Creek above the Alta tributary were very near the TMDL during periods of high flow. Like Pb and As, Zn loads only exceeded the TMDL in Corbin Creek below the Alta tributary. There, Zn loads routinely, almost daily, exceeded the TMDL under all hydrologic conditions.

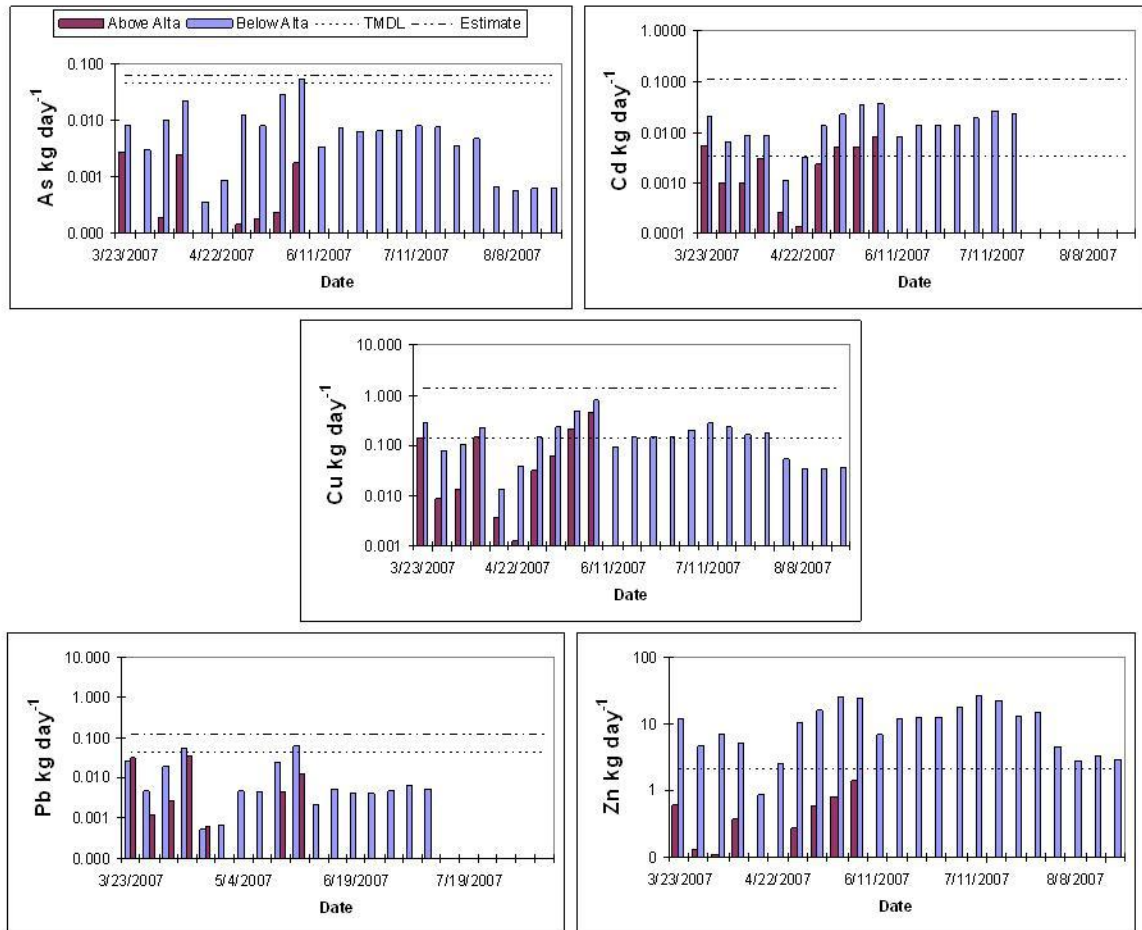


Figure 17. Corbin Creek Heavy Metal and As Loads Above and Below the Alta Tributary Compared to TMDL Goals and EPA Estimated Maximum Loads (US EPA 2006).

The plots provide evidence that TMDLs were not often exceeded by Corbin Creek background As and heavy metal concentrations alone; but that the Alta tributary contribution to Corbin Creek resulted in loads that exceeded TMDLs during some or all hydrologic conditions. Cu and Cd loads measured above the Alta tributary during the greatest observed flow events were the only exceptions. The combined results of the Alta tributary load to Corbin Creek background load comparison, ALS comparison, and TMDL comparison provide evidence to accept the hypothesis that the Alta tributary is not only the significant source of heavy metals and As but that it hinders attainment of TMDLs.

Sediment

Sediment transport, estimated by total suspended solids (TSS), was lower than estimated daily maxima for Corbin Creek (US EPA 2006) throughout the summer at all monitoring locations. The highest sediment loading rates observed came during the June

6, 2007 rainfall event or early spring runoff measured on March 30, 2007 (Table 6). Concentrations of TSS measured during low flow or baseflow conditions were often below the detectable limit of the analytical method (APHA 2001). Difficulties in determining suspended sediment concentrations below the lower Alta reclaimed area arose because Fe rapidly precipitated in sample bottles before samples could be transported to the lab; thus, the analysis of suspended sediment was restricted to the Alta tributary above Corbin Creek and Corbin Creek above and below the Alta tributary. Table 5. Summer 2007 Alta Tributary and Corbin Creek Sediment Loads and TMDLs.

Monitoring Location	TMDL kg day ⁻¹	EPA Estimated Maximum kg day ⁻¹	Measured Maximum kg day ⁻¹
Corbin Creek Below Alta	0.45	0.59	0.065
Corbin Creek Above Alta	0.45	0.59	0.037
Alta Tributary Above Corbin Creek	--	--	0.018

No TMDL exceedances were measured at either of the Corbin Creek monitoring locations. Also, the maximum observed sediment load carried by the Alta tributary was not above the TMDL established for Corbin Creek. During the monitoring effort, substantial accumulation of sediment was observed behind each of the sediment traps installed during the 1999 Alta reclamation project and the 2002 Bertha tailings removal. It is likely that sediment aggradation is the result of debris flows from low frequency high intensity rainfall events (Benda 1990) that occurred without observation or prior to the study. More monitoring data that includes these events are needed to construct a new sediment transport model or to validate the existing one (US EPA 2006) in Corbin Creek below the Confluence with the Alta tributary.

Soil Characterization

Soil physical and chemical factors were successfully analyzed as outlined in methods and materials. A summary of the results of the soil survey are presented below. Complete results are listed in Appendix B. Where applicable, soil parameters in subsoil were compared to parameters in topsoil on the basis of the Wilcoxon Rank Sum Test.

Soil Texture

All soils analyzed for texture, from both the surface and at depth, were found to be either sandy loam or loamy sand. Sand, silt, and clay fractions ranged from 56.1 – 84 %, 8 – 42.5 %, and 0 – 15.6 %, respectively. Rock fragments (> 2 mm) ranged from 24 – 70 % by mass of each sample. The texture, rock content, elevation, and appearance of Alta soils are consistent with the *Comad series* (Veseth and Montagne 1980) of well-drained, weak-structured, granitic soils. Soils of this type may be limiting to a revegetation effort because of their high erodability and inability to hold moisture.

Soil Nutrients and Organic Matter

Soil fertility on the basis of N was typically low on the Alta reclaimed site; and P levels were low to medium (Table 7). K concentrations were near or below the range for disturbed soils ($150 \text{ mg kg}^{-1} - 500 \text{ mg kg}^{-1}$); and OM was found to be in the low (2.1 – 3.5 %) to very low (<2 %) range (Munshower 1994). The lack of N and P in Alta soils may be explained conceptually by a cumulative effect of their low OM and coarse texture. Nutrients are leached from the well-drained soils when there is not sufficient OM to bind them. Sterile soils will not support vegetation; thus, they will not receive input of additional OM due to natural plant decay. Eventually, the structureless bare soils will erode. Merely through the textural and nutrient analyses of Alta soils, there was impetus for soil amendment with OM.

Table 6. Nutrient (mg kg^{-1}) concentrations and OM (%) in Alta mine soils

Interval	Macronutrient			OM
	Nitrate (N)	P-Olsen	K-extractable	
0 - 15 cm	$2.6 \pm 1.07 \text{ a}$	$11.1 \pm 5.7 \text{ a}$	$107.3 \pm 41.2 \text{ a}$	$2.046 \pm 0.84 \text{ a}$
60 - 75 cm	$2 \pm 1.6 \text{ a}$	$14.7 \pm 7.8 \text{ a}$	$63.7 \pm 26.4 \text{ b}$	$1.33 \pm 0.5 \text{ b}$

Values followed by same letter within columns are not significantly different ($p < 0.1$).

pH and EC

The pH of Alta soils ranged from 2.32 – 7.23 in the 0-15 cm interval and from 2.53 – 6.21 in the 65 – 70 cm interval. More instances of near neutral pH occurred in the upper interval, which is indicative of remnants of topsoil from the 1999 reclamation effort. Overall, pH of surface soils was significantly greater than that of subsoils (Table 8); however, many soil samples in both intervals were in the range of acute toxicity to plants (Rengel 2002).

Table 7. pH (standard units) and EC ($\mu\text{S cm}^{-1}$) of Alta mine soils.

Interval	pH	EC
0 - 15 cm	$4.45 \pm 1.2 \text{ a}$	$535.8 \pm 491.1 \text{ a}$
60 - 75 cm	$3.45 \pm 0.9 \text{ b}$	$854 \pm 546.7 \text{ b}$

Values followed by same letter within columns are not significantly different ($p < 0.1$).

By EC measurement, salinity of Alta soils was found to be sufficiently lower than published inhibitory thresholds. Depending on species, salinity is not expected to cause a reduction in yield of grass or other forage except at levels $> 2,300 \mu\text{S/cm}$ (Cardon et al 2003). EC was lower in surface samples than at depth, which suggested that plant exposure to salts is limited. The low level of available salts may only prove to be significant if they contain phytotoxic trace elements. Salts of CdCl^+ were increasingly taken up by wheat and Swiss chard (*Beta vulgaris*) when dissolved NaCl salts were added to soil solution (Weggler-Beaton et al. 2000).

Heavy Metals and Arsenic

Total Metals and Arsenic. Prior to reclamation in 1999, mean Pb and As concentrations in the top 75 cm of waste were 3,238 mg kg⁻¹ and 1,063 mg kg⁻¹, respectively (PRC EMI 1997). In the reclaimed condition, respective mean concentrations over the entire 75 cm interval were reduced to 373 mg Pb kg⁻¹ and 337 mg As kg⁻¹. The mean Zn concentration of Alta waste from 3 samples taken in 1993 was 300 mg kg⁻¹ (Pioneer 1994), which was actually lower than mean Zn concentrations found in 30 soil pits in summer of 2006. Concentrations of total metals and As in Alta mine surface soils were not significantly different than concentrations at depth (Table 9). It is possible that metals have either migrated from mine impacted subsoils into the more recently applied topsoil by capillarity or that topsoil cover has been removed by erosion. Table 8. Heavy metals and As (mg kg⁻¹) in Alta mine soils.

Interval	Heavy Metals and As			
	As	Pb	Zn	Total
0 - 15 cm	316.8 ± 473.8 a	355.7 ± 304.9 a	391.9 ± 120.6 a	1,064.4 ± 756 a
60 - 75 cm	357 ± 336.3 a	390.6 ± 398.3 a	440.3 ± 234 a	1187.9 ± 614 a

Values followed by same letter within columns are not significantly different (p<0.1).

Target removal concentrations of Pb and As used in the 1999 reclamation effort were 235 mg kg⁻¹ and 323 mg kg⁻¹, respectively (PRC-EMI 1997). This means that the waste rock pile was removed until surface concentrations were routinely at or below targets. Once target levels were reached, removal ceased. Current soil As and Pb concentrations in the 0 – 15 cm interval were tested against reclamation targets, assuming a lognormal distribution and a Z* test statistic. The null hypothesis of the test was that mean soil concentrations were equal to target concentrations; conversely, the alternative hypothesis was that surface soil concentrations were higher than targets. Though Pb and As levels in surface soils were indicative of mine impacted materials, neither element was significantly (p<0.1) concentrated above target levels (Table 10).

Table 9. Recreational clean up levels and current Pb and As in Alta mine soils.

Element	Comparison to Reclamation Targets			
	Target mg kg ⁻¹	mean ± standard deviation mg kg ⁻¹	Z*	p
As	323	316.8 ± 473.8	-3.474	0.9997
Pb	235	355.7 ± 304.9	0.694	0.25

Soluble Metals and Arsenic. Water extractable Cu, As, and Zn concentrations were determined for a random subset of soils in the 0 – 15 cm interval, as this was the primary rooting depth observed during soil pit excavation. The soluble fraction of these constituents is not only indicative of bioavailability but also of the amount of potentially toxic trace elements that may migrate from soil to surface and ground water. Concentrations were variable but higher for Cu and Zn than for As. Concentrations

ranged from 0.07 – 18.7 mg L⁻¹ and 0.01 – 57.1 mg L⁻¹ for Cu and Zn, respectively. Water soluble As concentrations ranged from non detectable by ICPMS to 0.299 mg L⁻¹.

Acid-Base Potential

ABP was measured in the 0 – 15 cm interval for all 30 soil pits and in the 60 – 75 cm interval for 7 soil pits. The Wilcoxon Rank Sum Test was used to draw comparison between intervals. There was not a significant difference ($p < 0.1$) between ABP in surface soils and ABP at depth. In the 0 -15 cm depth interval, ABP ranged from net acid neutralizing (13 T-CaCO₃ 1kT-soil-1⁻¹) to net acid producing (-57 T-CaCO₃ 1kT-soil⁻¹), with a mean value of -4.23 T-CaCO₃ kT-soil⁻¹. ABP from 8 T-CaCO₃ kT-soil⁻¹ to -45 T-CaCO₃ kT-soil⁻¹ were found in the 60 – 75 cm soil interval. Prior to waste rock removal in 1999, the top 75 cm of waste rock had ABP ranging from -12 T-CaCO₃ 1kT-soil-1⁻¹ to -196 T-CaCO₃ 1kT-soil-1⁻¹ (PRC EMI 1997). Though soils at the Alta mine appeared to have less acid generating potential than extreme values present in pre-reclamation substrates, net acid producing values of ABP indicated that low soil pH at the Alta mine may yet be the result of active sulfide mineral weathering.

Vegetation Survey

Vegetative cover on the Alta reclaimed site was generally sparse. Mean vegetative cover determined from all sample frames was 11.7 %; yet, it ranged from 0 – 67.5 %. On the slope of north aspect, mean vegetative cover was 21.6 %, as compared to only 6.1 % on south facing slopes. Bare ground, rocks, and litter were abundant on site. Together, they accounted for a minimum of 40 % or 45 % of the total area in any given sample frame on the north or south facing slope, respectively. Much of the sampled area on the south facing slope was 95 – 100 % bare. Despite having minimal vegetative cover, 31 different plant species were identified on site (Table 11).

The Alta reclaimed area, with relatively high species richness and low vegetative cover, does not correspond with patterns of vegetative establishment on 3 reclaimed mines nearby. Tafi (2006) found only 12 species on a reclaimed site with 38.1 % cover and 37 species in an area with 70.9 % cover. Of the 31 species found at Alta, 20 were native and only 12 were seeded during the 1999 reclamation effort. Complete results of the vegetation survey are tabulated in Appendix B.

Table 10. Plant Species Found 7 Years After Reclamation of Alta Mine.

Common Name	Scientific Name	Native Y/N	1999 Seed Mix Y/N
Western Yarrow	<i>Achillea millifolium</i>	Y	Y
Thickspike wheatgrass	<i>Agropyron dasystachyum</i>	Y	Y
Intermediate wheatgrass	<i>Agropyron intermedium</i>	N	N
Western wheatgrass	<i>Agropyron smithii</i>	Y	N
Slender wheatgrass	<i>Agropyron trachycaulum</i>	Y	N
Redtop	<i>Agrostis alba</i>	N	Y
Ticklegrass	<i>Agrostis scabra</i>	N	N
Fringed sagewort	<i>Artemesia frigeria</i>	Y	N
Aster	<i>Aster spp</i>	Y	N
Cheatgrass	<i>Bromus tectorum</i>	N	N
Wavyleaf thistle	<i>Cirsium undulatum</i>	Y	N
Idaho fescue	<i>Festuca idahoensis</i>	Y	Y
Sheep fescue	<i>Festuca ovina</i>	Y	N
Rough fescue	<i>Festuca scabrella</i>	Y	Y
Hawk's beard	<i>Hierceulum</i>	Y	N
Dalmation toadflax	<i>Linaria dalmatica</i>	N	N
Lewis flax	<i>Linaria lewisii</i>	Y	Y
Annual ryegrass	<i>Lolium multiflorum</i>	N	Y
Silky Lupine	<i>Lupinus sericeus</i>	Y	N
Alfalfa	<i>Medicago sativa</i>	N	Y
Canada bluegrass	<i>Poa compressa</i>	N	Y
Kentucky bluegrass	<i>Poa pratensis</i>	N	N
Sandberg bluegrass	<i>Poa sandbergii</i>	Y	Y
American bistort	<i>Polygonum bistortoides</i>	Y	N
Quaking aspen	<i>Populus tremuloides</i>	Y	N
Bluebunch wheatgrass	<i>Pseudoroegneria spicatum</i>	Y	Y
Raspberry	<i>Rubus</i>	Y	N
Columbia needlegrass	<i>Stipa columbiana</i>	Y	Y
Green needlegrass	<i>Stipa viridula</i>	Y	N
Western salsify	<i>Tragopogon dubius</i>	N	N
Mullen	<i>Verbascum thapsus</i>	N	N

Correlation between Soil and Vegetative Cover

Univariate and multifactor linear regression models were constructed in R 2.5.1 to determine correlation between soil physical and chemical properties and vegetative cover. Results of all linear regression models, including correlation coefficients, p-values, and diagnostics plots are included in Appendix B.

Univariate Models

Single variable models found significantly correlated with vegetative cover were pH (0 – 15 cm), EC (60 – 75 cm), P (60 – 75 cm), soluble As (0 – 15 cm), and aspect (Table 12). EC and aspect were negatively correlated; while, pH, P, and As were positively correlated with vegetative cover.

Table 11. Significant Models for Vegetative Cover on Lower Alta Reclaimed Site.

Model	Results			
	Coefficient	Intercept	r	p
Cover ~ As, soluble (0-15cm interval)	108.193	6.145	0.84	0.00058
Cover ~ Aspect	-9.36	16.071	-0.49	0.05434
Cover ~ EC (60-75cm interval)	-0.01183	18.587	-0.54	0.02987
Cover ~ P (60-75cm interval)	0.41313	0.057	0.6	0.0694
Cover ~ pH (0-15cm interval)	3.775	-6.948	0.48	0.0594

The most unexpected of the single variable regression models was the strong positive correlation between vegetative cover and soluble As. Plant yield reduction is expected when levels of bioavailable As are high, as it is a metabolic inhibitor (Kabata-Penias 2001). At low levels of soluble As, such as those found at Alta, As may not have any damaging effects on plant growth. Abedin and Meharg (2002) found rice seed germination to be unaffected by As(V) and As(III) at concentrations up to 2 mg L⁻¹ in soil solution. Further, root growth was only inhibited by 17% when arsenic was added to soil solution at 0.5 mg L⁻¹. Recall that concentrations of As in Alta soil solution ranged from non-detectable to 0.299 mg L⁻¹. A possible explanation for the positive correlation between As and vegetative cover is competition for soil sorption sites between As (V) and phosphate. As (V) was found to be more strongly sorbed than phosphate over a range of pH from 3 – 10 when the anions were tested at equimolar concentrations in a ferrihydrite suspension (Jain and Loeppert 2000). If As (V) has a competitive advantage for adsorption sites over phosphate, more phosphate may be available to plants. There was a positive correlation between vegetative cover and P (phosphate), though it was with P in the 60 – 75 cm depth interval. An equally plausible explanation for the strong positive correlation between As and vegetative cover is the presence of a single influential point. The influential point (soil pit 16) had the highest observed vegetative cover (38.2%), near the highest soil pH (pH=6.46), and the greatest soluble As concentration (0.299 mg As L⁻¹). Near neutral pH at the influential point may have resulted in both higher vegetative cover and soluble As. As noted, however, the enriched level of soluble As was likely not phytotoxic.

EC (dissolved solids) in the 60 – 75 cm interval were likely not available to plants growing at the Alta mine; however, EC was negatively correlated with vegetative cover. As noted above, plant growth would be most heavily dependent on EC when potentially toxic trace elements account for a portion of the dissolved salts. The relationship of EC at depth and vegetative cover was considered further in multivariate models.

Vegetative cover was significantly correlated with aspect, as a binomial factor. Slopes were considered as either north (1) or south (0) of the Alta tributary. Slopes south

of the Alta tributary (north aspect) were shaded by trees, held increased snow in the winter, and were likely exposed to less solar radiation in summer. Increased vegetative cover on the north facing slope is apparent in aerial photography of the lower Alta mine (Figure 5). Slope aspect control on vegetation in this study is consistent with Martinez-Ruiz (2005), who found that vegetative succession at a reclaimed uranium mine in an arid climate was expedited on slopes of north aspect.

Soil pH in the rooting zone at the reclaimed Alta mine was significantly correlated ($p < 0.1$) with vegetative cover. This result was not surprising, given the low pH values found on site. Many of the variables tested, however, were not correlated with vegetative cover. These included nutrients (N, P, and K), OM, ABP, total trace elements (As, Pb and Zn), and soluble trace elements (Cu and Zn). Though not found to be correlated with vegetative cover, many of these parameters were within ranges found to be limiting to plant growth by other researchers. For example, total As, Pb and Zn concentrations were well above the 10% yield reduction toxicity threshold for assumed transfer coefficients (Munshower 1994, Alloway 1995, Kabata-Pendias 2001). Factors that were insignificant alone were applied to multivariate models so that cumulative factor effects could be identified.

Multivariate Models

Cumulative factor effects on vegetative cover were considered in multifactor linear regression models. Then, by ANOVA, restricted models (models which accounted for fewer variables) were compared to unrestricted models (models that included more variables). Similar to univariate regression models, unrestricted models found to be significant ($p < 0.1$) by the ANOVA approach to linear regression included pH (0 -15 cm interval) and aspect as variables (Table 13). ABP (0-15 cm interval) was also found to be significant when considered with pH or pH and aspect.

The model that considered both pH and ABP was significantly stronger ($p < 0.1$) than the model with pH alone. Intuitively, pH is likely to be low in substrates with net acid generating potential. Schippers (2000) examined vegetation death on tailings that ranged in pH and acid generating potential. Mortality was resoundingly higher on tailings with low pH and net acid generating potential. However, these tailings had mean concentrations of water extractable Cu and Zn (mg L^{-1}) that were twice as high as Alta concentrations and mean water extractable As concentrations (mg L^{-1}) that were nearly 200 times greater than those found at Alta. The pH + ABP model indicates that acid generating potential and pH significantly control vegetative succession even in the absence of enriched levels of phytotoxic elements.

Table 12. Significant Multivariate Regression and ANOVA Models for Vegetative Cover on Lower Alta Reclaimed Site.

<i>Regression Models</i>	<i>r</i>	<i>p</i>
pH	0.23	0.059
Aspect	0.24	0.054
pH + Aspect	0.39	0.041

pH + ABP	0.49	0.013
pH + ABP + Aspect	0.57	0.014
<i>ANOVA, (model 1, model 2)</i>	F*	p
pH, (pH + ABP)	6.540	0.024
pH, (pH + Aspect)	3.360	0.090
pH, (pH + ABP + Aspect)	4.780	0.030
Aspect, (pH, Aspect, ABP)	4.67	0.032
(pH + Aspect), (pH + ABP + Aspect)	5.142	0.043
(pH + ABP), (pH + ABP + Aspect)	2.350	0.150

Aspect was correlated with vegetative cover when paired with pH and ABP or pH alone. This statistical outcome indicated that harsher environmental conditions present on the south facing slope and soil acidity had a cumulative effect on vegetative cover. The model that included ABP, pH, and aspect, however, did not significantly ($p < 0.1$) account for more variability in cover than a model restricted to just pH and ABP as independent variables.

Several other multivariate models were found to be significant by linear regression; however, they did not account for more variability in vegetative cover than restricted models. As an example, regression models that considered EC (60 – 75 cm interval) and several other variables were significant; but ANOVA comparisons between these and restricted models were not.

Soil Amendments and Revegetation

Treated Soils

Changes in soil productivity with respect to pH, OM, and heavy metal and As availability were variably induced by lime and compost amendments. Each of the three treatments, lime alone, compost alone, and lime and compost, resulted in at least an apparent positive effect on 1 or all of the soil parameters analyzed.

The pH of soils collected from all 3 treatments was ostensibly greater than that of control soils; but the only statistically significant increases in soil pH were induced by compost alone or by compost and lime amendment (Table 14). Soil pH ranged from 6.15 – 8.07 over both the compost alone and compost and lime plots. Plots treated with lime alone had pH ranging from 5.03 – 6.2. At the applied rate, lime alone was not enough to raise pH to the target level of 6.5. Though this was the case, Ryan (1986) has shown plant growth was significantly less inhibited at pH of 4.8 than at 3.0. All treatments raised pH from the level of acute toxicity (3.5 – 4.0) published by Rengel (2002). Soil pH of control plots ranged from 3.43 – 3.92.

All plots that received compost were within the targeted range of 2 – 6% OM at the end of the growing season. Control and lime plots, which received no compost, were below or at the lower end of the targeted range. Soil OM for these plots ranged from 1.8 – 3.0%. The resulting increase in OM was significant for compost and lime treatments but not for the compost alone treatment; although OM in soils of the compost treatment was noticeably higher than non-compost plots (Table 14).

Table 13. Soil pH and OM in Treated Soils

Treatment	Soil pH and OM expressed as mean of 4 replicates		
	No. of treatments	pH	OM (%)
Control	4	3.68 b	2.15 b
Lime	4	5.73 b	2.38 b
Compost	4	7.08 a	4.28 a,b
Compost & Lime	4	7.27 a	5.1 a

Values followed by same letter within columns are not significantly different ($p < 0.1$).

Water extractable metal levels in soils of both the compost and lime and compost plots were not detectable by 10:1 extraction and ICPMS (Table 15). Pb was not detectable for all soils tested. Zn in the control soil and lime amended soils appeared higher than Zn in compost and lime and composted soils; but significant statistical differences were not found due to non detected (ND) values. Lime treatment resulted in a significant ($p < 0.1$) difference in extractable As concentration. Relatively low values of each element were likely not significant inhibitors to plant growth.

Table 14. Water Extractable As and Heavy Metals (mg kg^{-1}) in Treated Soils.

Treatment	Extractable Heavy Metals and As				
	As	Cd	Cu	Pb	Zn
Control	0.22 ± 0.29 a	ND - 2.0	13 ± 12.7	ND	84.25 ± 77.3
Lime	0.035 ± 0.01 b	ND - 1.0	ND - 12	ND	38 ± 65.8
Compost	0.74 ± 0.72 a	ND	ND	ND	ND
Compost & Lime	0.32 ± 0.037 a	ND	ND	ND	ND

Values followed by same letter within columns are not significantly different. ($p < 0.1$)

Vegetative Cover

Despite apparent and statistically significant improvements in the relative soil productivity of treated soils, canopy cover estimates performed at the end of the growing season indicated that none of the treatments resulted in vegetation establishment indicative of rehabilitated lands. Mean canopy cover was 1.48%, 3.38%, 5.53%, and 8.65% on control, lime, compost, and lime and compost treatments, correspondingly. Neuman (2005) achieved a median canopy cover of 62.5% on plots treated with lime and compost; and Tafi (2006) classified cover less than 25% as poor in her assessment of 3

abandoned mines near Alta. Emergence of plant varieties in the seed mix was minimal on treated plots. Of the grasses seeded, only Bluebunch wheatgrass (*Pseudoroegneria spicata*) was counted in Daubenmire frames on any of the 3 treatments; however, it was present on plots of all 3 treatments and the control. The lone seeded forb, Lewis flax (*Linaria lewisii*), was counted on 1 lime plot and on 1 compost plot but on none of the control or lime and compost plots. None of the seeded grasses, forbs, or cover crops accounted for more than 1% of the total canopy cover for a given treatment type.

A total of 11 species were counted on the treated area of the lower Alta site (Table 16). Seven (7) volunteer plant varieties were counted in addition to 4 seeded species. With only 1 exception, the total cover of any given species for all treatments was <1%; thus, vegetation has not been broken down into treatment type. The notable exception was the presence of Kochia on treatments amended with compost. Kochia canopy cover was 1.92% and 2.27% on compost alone and lime and compost treatments, respectively. It was suspected that Kochia seeds were present in some element of the compost and not destroyed during the composting process.

Table 15. Plant Species on Treated Plots.

Common Name	Scientific Name	Seeded (Y/N)
Western wheatgrass	<i>Agropyron smithii</i>	N
Wavyleaf thistle	<i>Cirsium undulatum</i>	N
forb	<i>Forb spp.</i>	N
Kochia	<i>Kochia spp.</i>	N
Lewis flax	<i>Linaria lewisii</i>	Y
Alfalfa	<i>Medicago sativa</i>	Y
Sandberg bluegrass	<i>Poa secunda</i>	N
Bluebunch wheatgrass	<i>Pseudoroegneria spicata</i>	Y
Russian thistle	<i>Salsola kali</i>	N
Green needlegrass	<i>Stipa viridula</i>	N
Spring wheat	<i>Triticum spp.</i>	Y

Because of the apparent gross introduction of a weedy species, no significant statistical analyses were performed in regard to treatment effectiveness at increasing vegetative cover. The low emergence of alfalfa and other seeded species also negated any relevant comparison between the alfalfa block and the trees block.

Aspen planted below treatment plots near the Alta tributary had a 100% mortality rate. The absolute toxicity of Alta mine soils to aspen saplings may explain the apparent lack of acid mine revegetation trials with this species (Pulford and Watson 2003).

Douglas fir and Limber pine mortality, however, was only 40% at the end of the first growing season. Though coniferous tree mortality was higher than that found by Ryan et al. (1986) in a controlled laboratory, results were consistent with transplanted shrub mortality observed on steep mine waste dumps (Leavitt et al. 2000). If the pattern of mortality observed by Leavitt et al. (2000) is representative of Alta mine conditions,

transplant survivorship may be as low as 25% in 3 years. In which case, more than 12 of the original 50 coniferous trees will remain alive on site. Results of both the soil productivity analyses and end of growing season vegetation survey are included in Appendix C.

Downslope Migration of Seed Bank

Soil erosion was expected ensuing treatment plot construction; thus, silt fence was installed below plots as a best management practice. The silt fence collected a noticeable but inestimable amount of soil by the end of summer 2007. Soil loss by erosion, and the subsequent mobilization of the seed bed, was a likely cause for vegetation failure. Though our experimental design did not include a direct measure of either erosion or seed bank removal, a spatial trend in vegetative cover was recognized during analysis (Figure 21).

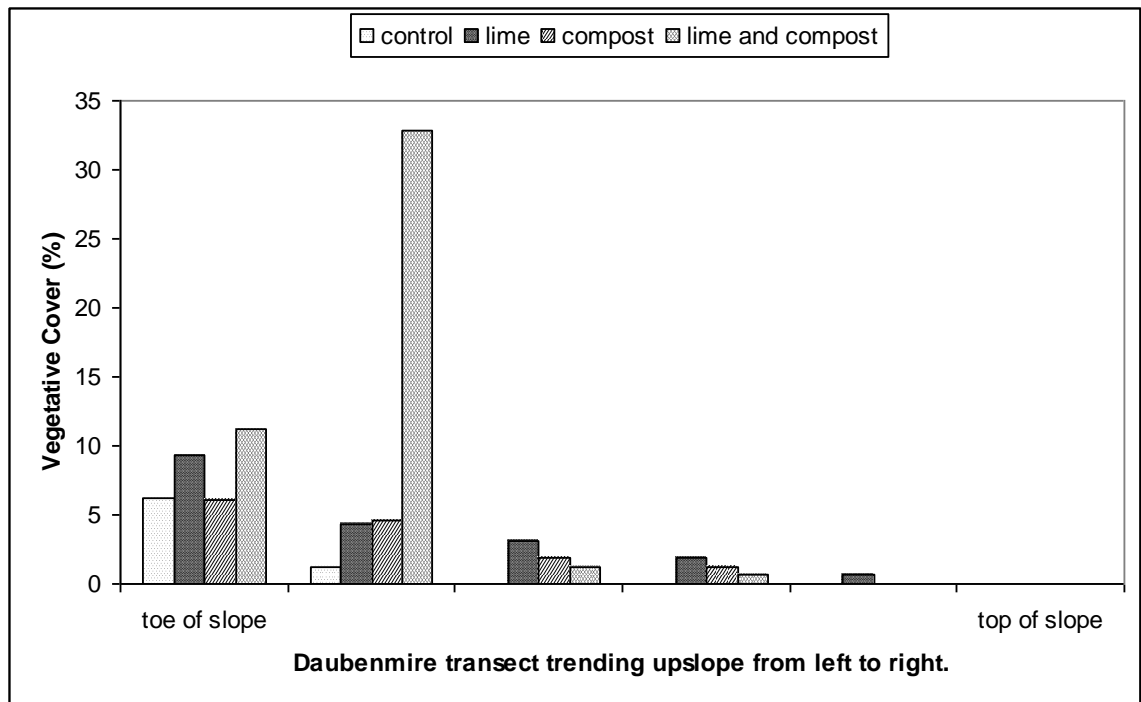


Figure 18. Apparent Trend in Vegetative Cover and Slope on Experimental Treatment Plots.

A greater vegetative cover was established at or near the toe of each treatment plot. Soil, soil amendments, and seed were likely displaced by erosion to the toe of the slope; there, seeds that were not deeply buried had the greatest success of emergence.

Soil loss (sediment yield) is controlled by the collateral relationship between vegetative cover and precipitation (Langbein and Schumm 1958). Sediment yield reaches a maximum when annual effective precipitation is between 30 and 35 cm. Precipitation greater than 30 cm stimulates the growth of vegetation; thus, less erosion occurs. Precipitation <30 cm does not provide enough erosive energy to move soil down slope. Annual precipitation at the Alta mine site is 28.7 cm (29.3 in 2006), which is in

the range that limits vegetation and practically in the range suggested to yield increased erosion. In unamended soils, the amount of soil loss is compounded by other controlling variables like acidity, which has already been shown to effect plant growth.

CONCLUSIONS AND RECOMMENDATIONS

Three (3) hypotheses were tested in 2 years (2006 – 2007) of study at the abandoned reclaimed Alta mine complex: 1) Waters that drain the site are the significant source of impairment to downstream water quality in terms of total maximum As, Cd, Cu, Pb, Zn, and sediment load; 2) Alta mine soils are still impacted by chemical or physical influences that preclude vegetative cover; and 3) Lime and compost amendments applied to experimental plots would improve soil productivity and vegetative cover. Each hypothesis was accepted or rejected based on results of field measurements and monitoring activities, laboratory analyses, and statistical inference.

Water Quality

Results of the 2006 – 2007 monitoring effort indicate that abandoned underground mine workings, shallow subsurface flow, and soil leachate were all sources of As and heavy metals in the Alta tributary. The Alta mine sub-watershed is not unlike numerous other mined watersheds that have been found to discharge As and heavy metals from various sources and media (Brooks et al. 2001, Sullivan et al. 2001, Kimball et al. 2002). The primary source of individual elements varied; but the source with the highest overall discharge of As and heavy metals was the 180-m deep #8 shaft. The significant contribution of AMD discharge from point source abandoned mine features such as adits, shafts, and portals has been resoundingly confirmed by other researchers (Runkel and Kimball 2002, Kimball et al. 2002, Caruso 2003, and Herr et al. 2003).

Patterns of As and heavy metal discharge along the longitudinal profile of the Alta tributary downstream from the #8 shaft revealed that the Alta sub-watershed stores a portion of the As and heavy metals loads; and solutes that do reach Corbin Creek likely undergo chemical transformation and attenuate in the mixing zone. Decreases of metal and As load are common in mixing zones with neutral streams (Runkel and Kimball 2002, Butler II 2006). Nonetheless, loads that remain mobile in Corbin Creek are attributable to significant water quality impairment and hindrance to TMDL attainment. During periods of low flow, the Alta tributary is the only source of heavy metals and As in Corbin Creek. It was observed that flow above the Alta tributary had stopped by June 9, 2007. During flow regimes where background loads are contributed from Corbin Creek above the Alta tributary, they equal less than 40% of the total load in Corbin Creek below the confluence. In contrast, Alta tributary loads ranged from 286% to 1,492% of the total As, Cd, Cu, Pb, and Zn in Corbin Creek. These results support the hypothesis that the Alta tributary is the major source of As, Cd, Cu, Pb, and Zn in Corbin Creek.

Significantly lower loads in Corbin Creek above the Alta tributary suggest that reclamation activities performed in the Corbin Creek watershed, namely the removal of the Bertha tailings pile, were effective at mitigating water quality impairments. The pH of Corbin Creek above the Alta tributary was neutral, as compared to Alta tributary pH that ranged from 2.06 to 4.63. Removal of the Bertha tailings pile had positive effects on

water quality because no additional source of AMD, like the #8 shaft, was present. However, AMD products were not the only indices of impaired water quality in the Alta tributary.

The abundance of bare ground and uncovered waste rock still present in the Alta sub-watershed has the potential to cause water quality impacts due to sedimentation. Sediment accumulation in both the Alta tributary and Corbin Creek channels was evident during the course of the study. It is likely that the sediment is carried by debris flows during low frequency, high intensity rainfall events. These events were not monitored during the summer of 2007; thus, further sediment samples taken during thundershowers, such as those measured by our rain gage in August 2007, are needed to accurately quantify the Alta tributary sediment load. For this reason, the hypothesis that the Alta tributary is the major source of sediment in Corbin Creek could neither be accepted nor rejected. Ideally, however, sediment load reductions could be achieved by revegetation.

Limitations on Revegetation

The physical character of soils at the reclaimed Alta mine was consistent with soils found naturally around the Boulder Batholith (Deckler 1982, and Veseth and Montagne 1980); however, the chemical characteristics, in terms of elevated heavy metals, ABP, and low pH, were consistent with mine waste rock (Pioneer 1994). Acid base accounting performed on Alta soils proved that much of the substrate was moderately to highly net acid generating in 2006, seven years after the 1999 reclamation effort. Soil pH was also indicative of acidic conditions. Vegetative cover was significantly ($p < 0.1$) controlled by net acid generating potential and low pH in soils. Cover was also significantly ($p < 0.1$) influenced by slope aspect. Dry conditions compounded acid toxicity, especially on the south facing slope. The south facing slope at the reclaimed Alta mine was generally devoid of vegetation and had numerous eroding rills. The hypothesis that chemical (soil pH and ABP) and physical (aspect) variables precluded vegetation on the reclaimed Alta mine site was accepted based on statistical significance determined by the ANOVA approach to linear regression. Other suspected variables (i.e. heavy metals and As) were not found to significantly impact vegetative cover.

Lime and compost amendments used to increase soil productivity on treated plots on the south facing slope of the Alta mine had marginal success. Lime treatment alone did not significantly ($p < 0.1$) raise soil pH above control levels or, to the target of 6.5. Compost alone and compost and lime treatments both resulted in soil pH that was significantly ($p < 0.1$) better than controls. OM content was also significantly ($p < 0.1$) greater in compost treated plots, with or without lime, than in control plots. Despite increased soil productivity, none of the treated plots resulted in vegetative cover that was indicative of successful land rehabilitation. The hypothesis that lime and compost amendments would raise both soil productivity and vegetative cover was only partially accepted. Lime and compost improved soil quality; but vegetation establishment at the Alta mine was still limited.

The precipitation regime in southwest Montana is consistent with a level of effective annual precipitation that does not support enough vegetation to overcome the erosion that it creates. Sandy soils on steep south facing slopes were particularly susceptible to erosion at the Alta mine; thus, experimental plots built during the current revegetation effort, on the approximate original hill contour, were subject to seed loss. Seed loss due to unstable topsoil has been the unfortunate outcome of previous attempts to revegetate steep slopes (Leavitt 2000). Slopes at the Alta site must be significantly stabilized, by means other than terraces, before vegetation can be established. It cannot be assumed that a vegetative cover alone will stabilize the slopes.

Bluebunch wheatgrass (*Pseudoroegneria spicata*) was the lone seeded grass species that had any apparent success during the revegetation trial. It appeared in all of the treatment plots and on the unamended controls. Aspen (*Populus tremuloides*) establishment was entirely unsuccessful in the acidic soils of the Alta mine, despite the tree's presence nearby. Douglas fir (*Pseudotsuga menziesii*) and limber pine (*Pinus flexilis*) exhibited some tolerance to acidic conditions, as predicated by Ryan (1986); but 40% mortality of conifers still occurred.

Abandoned Mines and Watershed Restoration

This study successfully linked abandoned, acid-producing, heavy metal mines to major downstream water quality impairments. The Alta mine, specifically, is the major contributing source of contaminants in Corbin Creek. Other mines of similar size, which are abundant in southwest Montana, may need to be considered for their impact on surface water quality and TMDL attainment status. Ineffective land rehabilitation may have a substantial impact on water quality impairments through sediment or As and heavy metals leached from soils. This may be true of Cu at the Alta mine, since soil-water extractable concentrations were higher than concentrations in #8 shaft discharge. However, deep underground mine workings were the most abundant source of other heavy metals and As discharge at the study site. Consequently, any level of successful land treatment will have little effect on Corbin Creek heavy metal and As TMDL attainment status.

Recommendations

Sufficient amounts of waste rock were removed by MT DEQ in 1999 in order to obtain surface soils at the Alta mine with As and Pb concentrations below a recreational risk-based standard. These standards appeared to have been met; however, minimal top soil and fertilizer application did not prevent acid generating substrates from inhibiting plant growth. It is recommended that more emphasis be placed on soil productivity than on arbitrary or risk-based soil metal action levels if successful revegetation is an expected outcome of further reclamation activities at the Alta Mine. In this study, soil productivity was increased on the south-facing slopes of the Alta reclaimed area with modest amounts of lime and compost; yet vegetation failure resulted because of unstable slopes. It is

recommended that the slopes be stabilized with tackifier or erosion control fabric in addition to soil amendment. .

It is not expected that more waste will be removed from the Alta sub-watershed; however, residential real-estate development in the immediate vicinity may provide the impetus for aesthetic enhancement of the landscape. In the event of further waste removal, it is recommended that the effort be focused on sediment accumulation in the Alta tributary channel. This research has shown the channel to be a sink for As and heavy metals that are suspected to have coprecipitated with Fe-hydroxides in the stream bed. The stored sediment and heavy metals have the potential to result in downstream exceedances of aquatic life standards, TMDLs, and other water quality standards if they are flushed during high magnitude storm events.

It is entirely meaningless to remove the heavy metal and As laden sediment if the source of heavy metals and As is not addressed. This research identified the #8 shaft as the most significant source of heavy metals and As in the Alta tributary; thus, the most progressive action that could be taken at the Alta mine would be the direct treatment of AMD discharged from the shaft. It was beyond the scope of this research to address feasible treatment options for shaft discharge. Further research is needed to identify applicable and cost effective water treatment options.

REFERENCES CITED

- Abedin, M.J. Meharg, A.A. 2002. Relative toxicity of arsenite and arsenate on germination and early seedling growth of rice (*Oryza sativa* L.). *Plant and Soil*. 243:57 – 66.
- Adu-Wusu, C. Yanful, E.K. 2006. Performance of engineered test covers on acid-generating waste rock at Whistle mine, Ontario. *Canadian Geotechnical Journal*. 43:1 – 18.
- Alloway, B.J. 1995. The origin of heavy metals in soils. *In Heavy Metals in Soils 2nd edition* [Alloway, B.J. editor]. Glasgow, UK. Blackie academic and professional. 368 p.
- American Public Health Association (APHA). 2001. Standard methods for the examination of water and wastewater: including bottom sediment.
- American Society of Agronomy, Inc., Soil Science Society of America, Inc. (ASA, SSSA). 1982. Methods of soil analysis part 2-chemical and microbiological properties, 2nd edition. Madison, WI.
- Baker, A.J.M. 1987. Metal Tolerance. *New Phytologist*. 106:93 – 111.
- Ballen, K.G. Graham, P.H. 2002. Regulation of microbial processes by soil pH. *In Handbook of plant growth: pH the master variable* [Rengel, Z. editor]. New York, NY. Marcel Dekker, Inc. 446 p.
- Basta, N.T. Ryan, J.A. Chaney, R.L. 2005. Trace element chemistry in residual-treated soils: key concepts and metal bioavailability. *Journal of Environmental Quality*. 34:49- 63.
- Becraft, G.E. Pinckney, D.M. Rosenblum, S. 1963. Geology and mineral deposits of the Jefferson City quadrangle, Jefferson and Lewis and Clark Counties, Montana. USGS Professional Paper 428.
- Benda, L. 1990. Influence of debris flows on channels and valley floors in the Oregon Coast Range, U.S.A. *Earth Surface Processes and Landforms*. 15(5):457 – 466.
- Bonta, J.V. 2000. Impact of coal surface mining and reclamation on suspended sediment in three Ohio watersheds. *Journal of the American Water Resources Association*. 36(4):869 – 887.

- Borgegard, S.O. Rydin, H. 1989. Biomass, root penetration and heavy metal uptake in birch in a soil cover over copper tailings. *The Journal of Applied Ecology*. 26: 585 - 595.
- Brooks, P.D. McKnight, D.M. Bencala, K.E. 2001. Annual maxima in Zn concentrations during spring snowmelt in streams impacted by mine drainage. *Environmental Geology*. 40:1447 – 1454.
- Broshears, R.E. 1996. Reactive solute transport in acidic streams. *Water, Air and Soil Pollution*. 90:195 – 204.
- Butler II, T.W. 2006. Geochemical and biological controls on trace metal transport. *Environmental Geochemistry and Health*. 28:231 – 241.
- Cardon, G.E. Davis, J.G. Bauder, T.A. Waskom, R.M. 2003. Salt-affected soils. Colorado State University Extension Publication no. 0.503.
- Caruso, B.S. 2003. Water quality simulation for planning restoration of mined watersheds. *Water, Air, and Soil Pollution*. 150:359 -382.
- Cela, S. Sumner, M.E. 2002a. Critical concentrations of copper, nickel, lead, and cadmium in soils based on nitrification. *Communications in Soil Science and Plant Analysis*. 33(1):19 – 30.
- Cela, S. Sumner, M.E. 2002b. Soil zinc fractions determine inhibition of nitrification. *Water, Air, and Soil Pollution*. 141:91 - 104.
- Christensen, T.H. 1984. Cadmium soil sorption at low concentrations: I. effect of time, cadmium load, pH, and calcium. *Water, Air, and Soil Pollution*. 21:105 – 114.
- Colbeck, S., Akitaya, E., Armstrong, R., Gubler, H., Lafeuille, J, Lied, K., McClung, D., Morris, E. 1990. The international classification for seasonal snow on the ground: International Association of Scientific Hydrology. 23 p.
- Crowley, D.E. Alvey, S.A. 2002. Regulation of microbial processes by soil pH. *In Handbook of plant growth: pH the master variable* [Rengel, Z. editor]. New York, NY. Marcel Dekker, Inc. 446 p.
- Datta, R. Sarkar, D. 2004. Effective integration of soil chemistry and plant molecular biology in phytoremediation of metals: an overview. *Environmental Geosciences*. 11: 53 – 63.
- Daubenmire, R. 1959. A canopy coverage method of vegetational analysis. *Northwest Science*. 33:43-64.

- Deckler, J.H. 1982. Characterization of four inactive hard rock mines in western Montana. M.S. thesis, Land Rehabilitation. Montana State University. Bozeman, MT.
- Devore, J. Farnum, N. 2005. Applied statistics for engineers and scientists 2nd edition. Belmont, CA: Thomson Brooks/Cole. 605p.
- Edwards, T.K. Glysson, D.G. 1999. Field Methods for Measurement of fluvial sediment. U.S. Geological Survey Techniques of Water Resources Investigations, Book 3, Chapter C2.
- Evangelou, V.P. 1995. Pyrite oxidation and its control. Boca Raton, FL: CRC Press. 293 p.
- Foth, H.D. Ellis, B.G. 1997. Soil Fertility 2nd Edition. Boca Raton, FL: CRC Press. 290 p.
- Friesl, W. Lombi, E. Horak, O. Wenzel, W.W. 2003. Immobilization of heavy metals in soils using inorganic amendments in a greenhouse study. Journal of Plant Nutrition Soil Science. 166:191 – 196.
- Gallagher, L.M. 2001. Clean water act. In *Environmental law handbook* [Sullivan T.F.P. editor]. Rockville, MD. Government Institutes, Inc. 811p.
- Gilbert, G.K. 1917. Hydraulic mining debris in the Sierra Nevada. USGS Professional Paper 105. Wasington D.C. Government Printing Office. 154 p.
- Goldberg, S. 2002. Competitive adsorption of arsenate and arsenite on oxides and clay minerals. Soil Science Society of America Journal. 66:413 – 421.
- Henry, T.B. Irwin, E.R. Grizzle, J.M. Wildhaber, M.L. Brunbaugh, W.G. 1999. Acute toxicity of an acid mine drainage mixing zone to juvenile bluegill and largemouth bass. Transactions of the American Fisheries Society. 128: 919-928.
- Herr, J.W. Chen, C.W. Goldstein, R.A. Herd, R. Brown, M.J. 2003. Modeling acid mine drainage on a watershed scale for TMDL calculations. Journal of the American Water Resources Association. 39(2):289 – 300.
- Inskip, W.P. McDermott, T.R. Fendorf, S. 2002. Arsenic cycling in soils and natural waters: chemical and microbiological processes. In *Environmental Chemistry of Arsenic* [Frankenberger Jr., W.T. editor]. New York, NY. Marcel Dekker, Inc. 391p.
- Jain, A. Raven, K.P. Loeppert, R.H. 1999. Arsenite and arsenate adsorption on ferrihydrite: surface charge reduction and net OH⁻ release stoichiometry. Environmental Science and Technology. 33(8):1179 – 1184.

- Jain, A. Loeppert, R.H. 2000. Effect of competing anions on the adsorption of arsenate and arsenite by ferrihydrite. *Journal of Environmental Quality*. 29:1422 – 1430.
- Jennings, S.R., Dollhopf, D.J. 1995. Geochemical characterization of sulfide mineral weathering for remediation of acid producing mine wastes. Reclamation Research Unit, Montana State University, Bozeman, MT. Reclamation Research Publ. No. 9502.
- Jiang, Q.Q. Singh, B.R. 2004. Effect of different forms and sources of arsenic on crop yield and arsenic concentration. *Water, Air, and Soil Pollution*. 74 (3-4):321 – 343.
- Jones, C.A. Inskeep, W.P. Neuman, D.R. 1997. Arsenic transport in contaminated tailings following liming. *Journal of Environmental Quality*. 26: 433 – 439.
- Kabata-Pendias, A. 2001. Trace elements in soils and plants 3rd edition. Boca Raton,FL: CRC Press. 413p.
- Khan, D.H. Frankland, B. 1983. Plant and Soil. Effects of cadmium and lead on radish plants with particular reference to movement of metals through soil profile and plant. *Plant and Soil*. 70:335 – 345.
- Kimball, B.A. Runkel, R.L. Walton-Day, K. Bencala, K.E. 2002. Assessment of metal loads in watersheds affected by acid mine drainage by using tracer injection and synoptic sampling: Cement Creek, Colorado, USA. *Applied Geochemistry*. 17:1183 – 1207.
- Kramer, P.A. Zabowski, D. Scherer, G. Everett, G.L. 2000. Native plant restoration of copper mine tailings: I. substrate effect on growth and nutritional status in a greenhouse study. *Journal of Environmental Quality*. 29:1762 – 1769.
- Langbein, W.B. Schumm, S.A. 1958. Yield of sediment in relation to mean annual precipitation. *Transactions of the American Geophysical Union*.
- Leavitt, K.J. Fernandez, G.C.J. Nowak, R.S. 2000. Plant establishment on angle of repose mine waste dumps. *Journal of Range Management*. 53:442 – 452.
- Lefebvre, R. Hockley, D. Smolensky, J. Gelinis, P. 2001. Multiphase transfer processes in waste rock piles producing acid mine drainage 1: conceptual model and system characteristics. *Journal of Contaminant Hydrology*. 52:1-4, 137 – 164.
- Ma, L.Q. Rao, G.N. 1997. Chemical fractionation of cadmium, copper, nickel, and zinc in contaminated soils. *Journal of Environmental Quality*. 26:259 – 264.

- Macdonald, B. 1986. Practical woody plant propagation for nursery growers. Portland, OR. Timber Press. 669p.
- Macdonald, B.C.T. White, I. Astrom, M.E. Keene, A.F. Melville, M.D. Reynolds, J.K. 2007. Discharge of weathering products from acid sulfate soils after a rainfall event, Tweed River, eastern Australia. *Applied Geochemistry*. 22: 2695 – 2705,
- Manning, B.A. Goldberg, S. 1997. Arsenic(III) and arsenic(V) adsorption on three California soils. *Soil Science*. 162(12):886 – 895.
- Manning, B.A. Suarez, D.L. 2000. Modeling arsenic(III) adsorption and heterogenous oxidation kinetics in soils. *Soil Science Society of America Journal*. 64:128 – 137.
- Marin, A.R. Masscheyleyn, P.H. Patrick Jr., W.H. 1993. Soil redox-pH stability of arsenic species and its uptake on arsenic uptake by rice. *Plant and Soil*. 152(2):245 - 253
- Martinez, C.E. Motto, H.L. 2000. Solubility of lead, zinc, and copper added to mineral soils. *Environmental Pollution*. 107: 153 – 158.
- Marcus, A.W. Meyer, G.A. Nimmo, D.R. 2001. Geomorphic control of persistent mine impacts in a Yellowstone Park stream and implications for the recovery of a fluvial system. *Geology*. 29(4):355- 358.
- Montana Department of Environmental Quality (MT DEQ). 2005. A guide to abandoned mine reclamation. Published online at: <http://www.deq.state.mt.us/abandonedmines/bluebook.asp>. Accessed January 2008.
- Montana Department of Environmental Quality (MT DEQ). 2006. Montana numeric water quality standards. Circular DEQ-7. Helena, MT. 40p.
- Montana Department of Environmental Quality (MT DEQ). 2008. Priority mine sites. Published online at: <http://www.deq.state.mt.us/abandonedmines/priority.asp>. Accessed January 2008.
- Nelson, D.W. Sommers, L.E. 1996. Total carbon, organic carbon, and organic matter. *In Methods of soil analysis part 3 – chemical methods* [Sparks, D.L. editor]. Madison, WI. Soil Science Society of America. 1390p.
- Neuman, D. R. Vandenberg, G.S. Blicher, P.B. Jennings, S.R., Ford, K. 2005. Phytostabilization of acid metalliferous mine tailings at the Keating sing in Montana. Presented at the National Meeting of the American Society of Mining and Reclamation. ASMR.

- Niyogi, D.K. Lewis, Jr., W.M. McKnight, D.M. 2001. Litter breakdown in mountain streams affected by mine drainage: biotic mediation of abiotic controls. *Ecological Applications*. 11: 506 – 516.
- Niyogi, D.K. Lewis, Jr., W.M. McKnight, D.M. 2002. Effects of stress from mine drainage on diversity, biomass, and function of primary producers in mountain streams. *Ecosystems*. 5:554 – 567.
- O'Dell, R. Silk, W. Green, P. Claassen, V. 2007. Compost amendment of Cu-Zn minespoil reduces toxic bioavailable heavy metal concentrations and promotes establishment and biomass production of *Bromus carinatus* (Hook and Arn.). *Environmental Pollution*. 148:115 – 124.
- Ohio State University Research Foundation. 1971. Acid mine drainage formation and abatement. EPA 14010 FPR 04/71.
- O'Neill, P. 1995. Arsenic. *In Heavy metals in soils 2nd edition* [Alloway, B.J. editor]. Glasgow, UK. Blackie academic and professional. 368 p.
- Peppas, A. Komnitsas, K. Halikia, I. 2000. Use of organic covers for acid mine drainage control. *Minerals Engineering*. 13:563 – 574.
- Pioneer Technical Services, Inc. 1994. Abandoned hardrock mines priority sites: summary report. Montana Department of State Lands-Abandoned Mine Reclamation Bureau.
- PRC Environmental Management, Inc. (PRC EMI). 1997. Expanded engineering evaluation/cost analysis for the Alta Mine Jefferson County, MT. Prepared for Montana DEQ.
- Pulford, I.D. Watson, C. 2003. Phytoremediation of heavy metal-contaminated land by trees—a review. *Environmental Pollution*. 29:529 – 540.
- R version 2.5.1. (2007). The R foundation for statistical computing. Copyright © 2007.
- Reclamation Research Unit. Bitterroot Restoration, Inc. (RRU-BRI). 2004. Clark Fork River riparian evaluation system a remedial design tool. Prepared for US EPA, region 8. Montana office.
- Reddy, K.J. Wang, L. Gloss, S.P. 1995. Solubility and mobility of copper, zinc, and lead in acidic environments. *Plant and Soil*. 171:53 – 58.

- Rengel, Z. 2002. Role of pH in availability of ions in soil. *In Handbook of plant growth: pH the master variable* [Rengel, Z. editor]. New York, NY. Marcel Dekker, Inc. 446 p.
- Runkel, R.T. Kimball, B.A. 2002. Evaluating remedial alternatives for an acid drainage stream: application of a reactive transport model. *Environmental Science and Technology*. 36:1093 – 1101.
- Ryan, P.J. Gessel, S.P. Zasoski, R.J. 1986. Acid tolerance of pacific northwest conifers in solution culture. *Plant and Soil*. 96:239 – 257.
- Schippers, A. Jozsa, P.G. Sand, W. Kovacs, Z.M. Marian, M. 2000. Microbiological pyrite oxidation in a mine tailings heap and its relevance to the death of vegetation. *Geomicrobiology Journal*. 17:2, 151 – 162.
- Schroth, A.W. 2001. Geochemical pathways and processes in an acid mine drainage system, Alta mine, MT. M.S. thesis, Geology. Northern Arizona University. Flagstaff, AZ.
- Schroth, A.W. Parnell Jr., R.A. 2005. Trace metal retention through the schwertmannite to goethite transformation as observed in a field setting, Alta mine, MT. *Applied Geochemistry*. 20:907 – 917.
- Sobek, A.A. Schuller, W.A. Freeman, J.R. Smith, R.M. 1978. Field and laboratory methods applicable to overburdens and minesoils. U.S. Environmental Protection Agency Environmental Protection Technology. Cincinnati, OH: EPA-600/2-78-054.
- Soucek, D.J. Cherry, D.S. Currie, R.J. Latimer, H.A. Trent, C.G. 2000a. Laboratory to field validation in an integrative assessment of an acid mine drainage-impacted watershed. *Environmental Technology and Chemistry*. 19: 1036 -1043.
- Soucek, D.J. Cherry, D.S. Trent, C.G. 2000b. Relative acute toxicity of acid mine drainage water column and sediments to *Daphnia magna* in Puckett's Creek watershed, Virginia, USA. *Archives of Environmental Contamination and Toxicology*. 38: 305 – 310.
- Stracek, O. Choquett, M. Gelin, P. Lefebvre, R. Nicholson, R.V. 2004. Geochemical characterization of acid mine drainage from a waste rock pile, Mine Doyon, Quebec, Canada. *Journal of Contaminant Hydrology*. 69: 45 – 71.
- Sullivan, A.B. Drever, J.I. 2001. Spatiotemporal variability in stream chemistry in a high-elevation catchment affected by mine drainage. *Journal of Hydrology*. 252: 237 – 250.

- Tafi, T.C. 2006. Reclamation effectiveness at three reclaimed abandoned mine sites in Jefferson County, Montana. M.S. Thesis, Land Rehabilitation. Montana State University. Bozeman, MT.
- Tan, K.H. 2005. Soil sampling, preparation, and analysis 2nd edition. Boca Raton, FL: CRC Press. 623 p.
- Temminghoff, E.J.M. Van Der Zee, S.E.A.T.M. De Haan, F.A.M. 1997. Copper mobility in a copper contaminated sandy soil as affected by pH and solid and dissolved organic matter. *Environmental Science and Technology*. 31:1109 – 1115.
- Tetra Tech 1997. Hydrogeologic evaluation of the Alta mine site, Jefferson County, MT. Prepared for MTDEQ.
- Tetra Tech. 2002. Construction report for the Alta lower waste rock dump reclamation project, Jefferson County, MT. Prepared for MT-DEQ.
- Thomann, R.V. Mueller, J.A. 1987. Principles of surface water quality modeling and control. New York, NY. Harper Collins Publishers. 644p.
- Tordoff, G.M. Baker, A.J.M. Willis, A.J. 2000. Current approaches to the revegetation of metalliferous mine wastes. *Chemosphere*. 41, 219 – 228.
- U.S. Department of Agriculture, Natural Resources Conservation Service (USDA, NRCS). 2007. National Soil Survey Handbook, title 430-VI. [Online] Available: <http://soils.usda.gov/technical/handbook/>
- U.S. EPA. 1995. In test methods for evaluating solid waste, 3rd edition, 3rd update. Washington, D.C.
- U.S. EPA. 2006. Framework water quality restoration plan and total maximum daily loads (TMDLs) for the Lake Helena Watershed Planning Area: volume II final report. Prepared for the MT-DEQ.
- U.S. Environmental Protection Agency National Research Laboratory (US EPA, NERL). 1993. Methods for the determination of inorganic substances in environmental samples. EPA/600/R-93/100.
- Weggler-Beaton, K. McLaughlin, M.J. Graham, R.D. 2000. Salinity increases cadmium uptake by wheat and Swiss chard from soil amended with biosolids. *Australian Journal of Soil Research*. 38(1): 37 – 47.
- Whitney, D.A. Lamond, R.E. 1993. Liming acid soils. Kansas State University Agricultural Experiment Station and Cooperative Extension Service. MF-1065.

- Wu, L. Antonovics, J. 1975. Zinc and copper uptake by *Agrostis stolonifera*, tolerant to both zinc and copper. *New Phytologist*. 75:231 – 237.
- Xian, X. 1989. Effect of chemical forms of cadmium, zinc, and lead in polluted soils on their uptake by cabbage plants. *Plant and Soil*. 113: 257 – 264.
- Ye, Z.H. Wong, J.W.C. Wong, M.H. 2000. Vegetation response to lime and manure compost amendments on lead/zinc mine tailings: a greenhouse study. *Restoration Ecology*. 8:3, 289 – 295.
- Zhixun, L. Herbert Jr., R.B. 1996. Heavy metal retention in secondary precipitates from a mine rock dump and underlying soil, Dalarna, Sweden. *Environmental Geology*. 33:1 – 12.

The Importance of Ecologically Connected Streams to the Biological Diversity of Watersheds: a case study in the St. Regis River subbasin, Montana

Basic Information

Title:	The Importance of Ecologically Connected Streams to the Biological Diversity of Watersheds: a case study in the St. Regis River subbasin, Montana
Project Number:	2008MT165B
Start Date:	3/1/2008
End Date:	2/28/2010
Funding Source:	104B
Congressional District:	At-Large
Research Category:	Biological Sciences
Focus Category:	Conservation, Management and Planning, Ecology
Descriptors:	
Principal Investigators:	Winsor Lowe

Publication

The Importance of Ecologically Connected Streams to the Biological Diversity of Watersheds: a case study in the St. Regis River subbasin, Montana

Montana Water Center USGS grant
Interim Report

by

Winsor Lowe, PhD
Assistant Professor Division of Biological Sciences
University of Montana – Missoula

Overview: For this grant, we proposed to (1) identify variables that influence patterns of IGS distribution and abundance, (2) to use genetics (microsatellite DNA markers) and (3) mark-capture-recapture (MCR) to assess the importance of connected stream networks to IGS population persistence and (4) to determine the affect of human disturbance on stream connectivity. To date, we have completed objectives 2 and 3. This summer, we will complete our surveys in the St. Regis basin in order to identify variables associated with IGS distribution and abundance. We will then summarize all of our data to complete objective 4. Below, we share the results to date on objectives 1 – 3.

Objective 1: To identify variables that influence patterns of IGS distribution and abundance

Abstract: Stream substrate disturbance is an important driver of community composition. Substrate moves when the driving forces of water on the stream bed exceed the resisting forces holding the substrate. Channel morphology can mitigate disturbance by shifting the balance between driving and resisting forces. We assessed the importance of high flow disturbance and channel morphology on the occurrence and density of a stream salamander, *Dicamptodon aterrimus* (Idaho Giant salamander) in 30 streams in the St. Regis basin of Montana. We compared support for models that describe *D. aterrimus* occurrence and density as a function of channel confinement (bankfull width: valley width) and the ratio of bankfull flow competence (τ^*) to the shear stress required to set a particle into motion (τ_c^*). These models were compared to the top-ranked models that described salamander occupancy and density as functions of habitat quality, connectivity, and fragmentation in a previous study (Sepulveda and Lowe, *in press*). We hypothesized that channel geomorphology influences *D. aterrimus* occupancy and density during high flow and predicted that streams with low confinement and low $\tau^* : \tau_c^*$ would have greater occupancy and density. Support for channel confinement's influence on salamander occupancy and density was plausible, but had less support than models from the previous study. Probability of occurrence and density increased as channel confinement decreased, but $\tau^* : \tau_c^*$ had little effect. Results suggest that salamanders are (1) resistant to high flow disturbance and/or that (2) that disturbance has low intensity because high flows do not mobilize the entire stream bed. Experimental studies are needed to better understand how channel morphology and high flows interact to affect stream organisms.

Methods: In 2006 and 2007, I surveyed 30 headwater streams in the St. Regis River basin. Within each stream, I surveyed two 50-m reaches separated by 200 m for *D. aterrimus* occurrence and density. The lower reach began 25 m upstream of the confluence with a similar or higher-order stream. I used a backpack electrofisher to search for salamanders within the stream. To determine detection probability, all reaches were surveyed three times within one season. I used *D. aterrimus* occurrence (presence/absence) and density within a stream as response variables. *Dicamptodon aterrimus* were declared present in a headwater stream if they were detected in at least one 50-m reach in at least one of the three surveys. I calculated density for each headwater stream as the mean number of salamanders per m² captured in the lower and upper stream reaches over the three surveys.

Channel geomorphology variables: I used channel confinement and the ratio of bankfull flow competence (τ^*) to the shear stress required to set a particle into motion (τ_c^*) as predictor variables (Table 1). Channel confinement was calculated as the ratio of valley width to channel width such that high values describe low confinement. Competence is a dimension-free measure of the shear stress exerted by the flow on the bed and was calculated as

$$\tau^* = \frac{\rho g d S}{g(\rho_s - \rho)D},$$

where ρ_s and ρ are the sediment and fluid densities, respectively; g is the acceleration of gravity, d is maximum flow depth, and D is the median particle size (Church 2006). Because τ_c^* values range from 0.03 to 0.06 in most streams, I set $\tau_c^* = 0.045$ for all stream reaches.

To estimate channel confinement and $\tau^*:\tau_c^*$, I measured valley width using USGS digital elevation maps. In the field, I measured bankfull width at four random, 1-m wide transects that extended between bank-full channel edges within each reach. At six random points along each transect, I recorded stream depth and substrate particle diameter. Stream slope was estimated as the difference in elevation between the upstream and downstream ends of each plot divided by the distance between these points. Abiotic variables were averaged across the two study reaches within each headwater stream.

Top-ranked variables: I also estimated variables associated with the top-ranked models from Sepulveda and Lowe (*in press*). The top-ranked occupancy model included habitat connectivity, fragmentation, and alteration and the top-ranked density model included the proportion of fine and embedded substrate (Table 1). I measured habitat connectivity as the minimum distance along the stream corridor from the mouth of the sampled headwater drainage to the mouth of the nearest headwater drainage. I characterized habitat fragmentation and alteration by road density and forest structure. I quantified road density as length of roads standardized by headwater drainage area (km of road per km²) using the 2001 Inventoried Roadless Area data layer for the Clearwater National Forest. I described forest structure as the density of old-growth trees (trees per km²). I also recorded the proportion of fine substrate (< 2 mm) and substrate that was embedded, defined as having visible vertical surfaces buried in either silt or sand (Welsh et al., 1997)

at 6 points along each transect within each study reach. Proportions of embedded and fine substrate were positively correlated, so I used principle components analysis (PCA) to produce one axis that accounted for 75% of this variation (coefficients of the first eigenvector: embedded substrate = 0.71, proportion of fines substrate = 0.71).

Statistical analysis and model selection: To identify predictors of *D. aterrimus* occupancy, I compared two sets of models: (1) all possible combinations of the three channel geomorphology variables and, (2) the top-ranked model from Sepulveda and Lowe (*in press*), which included habitat connectivity, fragmentation, and alteration. To identify predictors of *D. aterrimus* density, I compared two sets of models: (1) all possible combinations of the three channel geomorphology variables and, (2) the top-ranked model from Sepulveda and Lowe (*in press*), which included the proportion of fine-embedded substrate. I then used model selection to identify the most plausible statistical models for predicting *D. aterrimus* and probability of occurrence and density when present. Prior to this analysis, I tested for highly correlated pairs of variables (those with $r \geq 0.7$) and used PCA to reduce collinearity among these variables. Logistic regression was used to determine the relative likelihood of each candidate occupancy model and multiple linear regression was used to determine the relative likelihood of each candidate density model. Finally, I used Akaike's Information Criterion for small samples (AIC_c) based methods to select the best models of occurrence and density from sets of candidate models (Burnham and Anderson, 2002).

I determined strength of support for the model using ΔAIC_c values and AIC_c weights (ω). Models with $\Delta AIC_c \leq 4$ for small sample size ($n/K < 40$; where n = sample size and K = number of parameters) have empirical support as being plausible (Burnham and Anderson, 2002). To assess the importance of individual parameters within the presented models, I calculated importance weights by summing ω values of all models in which the parameter occurs (Burnham and Anderson, 2002). Parameters with importance weights > 0.20 are considered to be significant (Stoddard and Hayes, 2005). Finally, coefficients (β) of local and landscape habitat covariates for *D. aterrimus* occurrence and relative density were obtained by averaging across all models weighted by ω (i.e., model averaging; Burnham and Anderson, 2002). Odds ratios were calculated from *D. aterrimus* occurrence coefficient estimates as $\exp(\beta)$. An odds ratio of 1.0 indicates no difference between the proportion of sample points with or without salamanders, while odds ratios close to zero or substantially >1.0 indicates a large difference. Odds ratios less than 1.0 indicate a negative effect while ratios greater than 1.0 indicate a positive effect (Keating and Cherry, 2004).

Obj. 2: To use genetics (microsatellite DNA markers) to assess the importance of connected stream networks to IGS population persistence.

Abstract: The dendritic structure of stream networks provides constraints on the movement of freshwater organisms with individual, population and community level consequences. This consistent structural foundation provides a system in which

examination of life-history influences on population genetic structure may reveal general insight on dispersal in stream networks. We examined the interaction of stream network structure with life-history and dispersal on population genetic structure of the facultatively paedomorphic Idaho Giant salamander, *Dicamptodon aterrimus* in stream networks of Idaho and Montana. We tested microsatellite data for support of population structure models by (i) examining hierarchical partitioning of genetic variation in river networks and (ii) testing for isolation by distance (along stream corridors and overland) to examine the importance of within-stream and overland gene flow on population structure. Systematic and controlled sampling within stream network scales revealed that hierarchical structure of stream networks has a strong effect on gene flow and genetic structure of *D. aterrimus*. Analysis of molecular variance (AMOVA) identified significant structure due to differences among all hierarchical levels (among sub-basin, among networks, among streams), where the “among network” level was responsible for the greatest structural influence. Significant isolation by distance was detected within networks, and in-stream distance was a strong predictor of genetic distance. Genetic differentiation among streams within networks is driven by limited migration, but divergence among networks and among sub-basins is driven by genetic drift. These results identify the influence of stream network structure on evolution of a freshwater salamander, and show that large spatial scales are important and influenced by stream network structure. High genetic divergence over small geographic distance accompanied by drift of adjacent stream networks may have negative effects on the ability of *D. aterrimus* to respond to climate change.

Methods: To examine the spatial extent of gene flow and population structure in *D. aterrimus*, I collected individuals in a systematic nested hierarchical design. I sampled individuals in 1st-order streams that were nested within networks of confluent streams draining into a mainstem river. Stream networks were nested within sub-basins of three major rivers: the Lochsa (four networks), St. Joe (two networks) and St. Regis (two networks). I collected 15 *D. aterrimus* from three 1st-order streams within each network. Stream networks were selected in sub-basins such that they were separated by a common ridge running approximately perpendicular to the mainstem river. This orientation allowed me to test for in-stream and overland gene flow within and among adjacent networks.

In each stream, I used an LR-20 backpack electrofisher (Smith-Root Inc., Vancouver WA) to collect salamanders from reaches beginning at least 25 m upstream of the confluence with a higher-order stream. Survey reaches ranged from 200-391 m in length (mean survey length \pm 1 SD: 220 m \pm 72.7). Two streams (LWWF and LPEF; Table 1) were sampled with three 30-m reaches separated by approximately 15 m. I clipped a small section of tail tissue from captured salamanders and stored it in 95% ethanol. Both juveniles and adult salamanders were sampled. Snout-vent lengths of sampled animals ranged from 22 mm-160 mm and weights ranged from <1 g to 130 g. All sampling took place in July – October of 2008, except for five samples from one stream that were collected on July of 2007 (LSSP).

Microsatellite amplification and scoring: Fifteen salamanders from each stream were genotyped at 14 microsatellite loci developed for *Dicamptodon tenebrosus* and *D. copei*

(Curtis and Taylor, 2000; Steele et al., 2008). To extract DNA, I digested tissues with protease in a detergent based cell lysis buffer, then precipitated proteins with an ammonium acetate solution and DNA with isopropyl alcohol. Isolated DNA was re-suspended in 100 μ l TE buffer and diluted 1:10 for polymerase chain reaction (PCR) amplification in a PTC-100 thermocycler (MJ Research Inc., Waltham, MA) with a total volume of 10 μ L. Multiplex reactions followed the QIAGEN microsatellite protocol with a single PCR touchdown profile: primer annealing started at 67°C and dropped 0.5°C for 20 cycles, followed by 25 cycles with a 57°C annealing temperature. Microsatellite markers Dte5, D04, D24, and D18 were PCR amplified individually following QIAGEN microsatellite protocols with separate PCR annealing temperatures. Following individual PCRs, these markers were pooled with multiplexed markers for fragment analysis. PCR products were visualized on an ABI3130xl Genetic Analyzer (Applied Biosystems Inc., Foster City, CA) in the Murdock DNA Sequencing Facility at the University of Montana, Missoula, USA. Allele sizes were determined using the ABI GS600LIZ ladder (Applied Biosystems Inc.) and allele sizes were called with GeneMapper version 3.7 (Applied Biosystems Inc.).

Genetic Analyses: Using exact tests implemented in GENEPOP version 4.0 (Raymond and Rousset, 1995), I tested for significant departures from Hardy-Weinberg proportions and for non-random association of pairs of loci across populations (linkage disequilibrium). Loci that deviated from HW proportions in each population were removed from further analyses. After removal of a single locus that deviated from HW proportions in all populations where it was not fixed for a particular allele, I calculated genetic diversity within-streams and examined subdivision among hierarchical levels.

Intra-population genetic diversity was calculated as allelic richness (A_S), the number of alleles observed in populations (N_A), and expected and observed heterozygosity (H_E , H_O) of streams. I then tested for population differentiation and the extent of gene flow with pairwise F_{ST} , a measure of genetic divergence based on the number of different alleles calculated in Arlequin version 3.1 (Excoffier et al., 2005). The inbreeding coefficient, F_{IS} was calculated for every locus in each stream to detect significant heterozygote deficit or excess in streams (GENEPOP; (Raymond and Rousset, 1995).

For a qualitative sense of genetic structure within the data set, I examined pairwise F_{ST} s to assess levels of divergence occurring among streams within networks and sub-basins. Furthermore, I used a hierarchical analysis of genetic variation (AMOVA implemented in the hierfstat package in R v 2.8.1, Goudet, 2005) to partition genetic variance within and among hierarchical scales. I first used the entire data set to assess patterns of genetic variance throughout the entire sampling area. Specifically, I tested for structure at four levels: among-subbasins, among networks within subbasins, among streams within networks, and within streams. To test for influence of local genetic structure on overall structure, I performed two additional AMOVAs, (i) within the Lochsa sub-basin, and (ii) within and among the St. Joe and St. Regis sub-basins. The AMOVAs generated hierarchical F-statistics (Yang, 1998) in which F_{SB} is divergence among sub-basins, F_{AN} is divergence among networks within sub-basins, F_{AS} is divergence among streams within networks, F_{IS} is the inbreeding coefficient within streams, and F_{ST} is the global divergence among streams.

Genetic structure was also visually interpreted using principal components analysis (PCA) which reduces dimensions in a multivariate dataset such that the 1st principal component (PC1) explains as much of the variance in allele frequencies as possible (Reich et al., 2008). To maintain quasi-independence of the data set, I removed the highest frequency allele of each microsatellite locus and performed the PCA on remaining allele frequencies (Leary et al., 1993). Plots of PC 1 against PC2 were examined to assess the similarity of allele frequencies among streams within networks, among networks within sub-basins and among sub-basins.

I used partial Bayesian individual assignment tests (Rannala and Mountain, 1997) to assign individuals to populations based on the expected probability of multilocus genotypes occurring in potential sources (GENECLASS2; (Piry et al., 2004). This method can accurately identify migrants especially when genetic differentiation is substantial and many loci are used (Berry et al., 2004). I used Monte Carlo resampling for 10,000 simulations of reference populations with the same allele frequencies and number of individuals as sampled populations (Paetkau et al., 2004). Salamanders were excluded from their sample stream with $\geq 99\%$ confidence of exclusion ($p \leq 0.01$) and conservatively included in another stream when $p > 0.33$ (Pruett et al., 2008). Individuals excluded from their stream origin but not included in another stream were considered potential immigrants or descendents of immigrants from populations not sampled. I performed three assignment tests with the above standards: (i) assignment of individuals to sub-basins, (ii) assignment of individuals to networks, and (iii) assignment of individuals to streams.

To understand the role of gene flow by in-stream dispersal v. overland pathways, I tested alternative hypotheses of *D. aterrimus* gene flow resulting in isolation by distance (IBD). IBD is detected by testing for correlations among matrices of genetic distance (F_{ST}) and geographic distance with Mantel tests that correct non-independence of pairwise points (Manly, 1997). I used two measures of pairwise distance between midpoints of survey reaches to test alternate pathways of gene flow with FSTAT version 2.9.3.2 (Goudet, 1995).

To test the hypothesis that *D. aterrimus* gene flow occurs primarily along stream corridors, I estimated the correlation between F_{ST} and stream distance in each sub-basin. Stream distance was the shortest pathway along streams connecting two points (ArcGIS 9.2, ESRI, Redlands, CA). Second, I tested the hypothesis that gene flow in *D. aterrimus* occurs primarily overland by estimating the correlation between F_{ST} and surface distance in each sub-basin. Surface distance is a straight line distance connecting two points that corrects for changes in elevation along the path (ArcGIS 9.2, ESRI, Redlands, CA).

Sub-basins were tested separately for IBD to detect regional differences in the scale and strength of IBD due to in-stream v. overland gene flow. Pairwise stream and surface distances were significantly correlated ($r = 0.88$, $p < 0.001$). Therefore, the strength of correlations of genetic distance with stream distance v. surface distance were used to assess in-stream v. overland gene flow.

Obj. 3: To use mark-capture-recapture to assess the importance of connected stream networks to IGS population persistence.

Abstract: Understanding how dispersal affects community dynamics and emergent patterns of species diversity is a major goal in stream ecology because dispersal is a phenomenon occurring in most species and because habitat fragmentation, riparian land use, and climate change have altered dispersal rates for many freshwater organisms. We examined the relative contributions of dispersal between stream reaches and local ecological and evolutionary processes within stream reaches to stream salamander persistence and coexistence with fish. Empirical data and lab experiments suggest that salamander and fish interactions in headwater streams are unstable because fish are predators and superior competitors of salamanders. These data are consistent with observations across North America that salamanders are largely limited to fishless stream reaches. However, my data show not only that salamanders persist with fish, but also that salamanders in reaches with fish have downstream-biased dispersal. These results call into question the mechanisms allowing for species coexistence and lead to the hypothesis: dispersal from upper reaches offsets negative effects of fish predation and competition in lower reaches. In this study, we used mark-recapture methods in multiple headwater streams to test whether dispersal could foster coexistence between the stream salamander, *Dicamptodon aterrimus* (the Idaho giant salamander), and salmonid fish. We estimated net dispersal rates, apparent survival, recruitment, and realized rate of population growth of *D. aterrimus* in upstream reaches without fish and downstream reaches with fish from multiple streams. Our results suggest that dispersal did not influence population growth rates or coexistence with fish, and that salamander dispersal between stream reaches is not the primary mechanism for *D. aterrimus* × fish coexistence. Apparent survival, recruitment, and population growth rate did not differ between reaches within a stream. Population growth was a function of local survival and recruitment, but not of dispersal because there was no evident difference in net emigration between upstream and downstream reaches. We did find that *D. aterrimus* movement within and between stream reaches was common. These results suggest that local processes within stream reaches, and not spatial processes between stream reaches, promote *D. aterrimus* × fish coexistence.

Methods: To sample salamanders, we used Pollock's robust design with five primary sampling periods in each stream (Pollock 1982). During each primary sampling period, secondary samples occurred 24 hours apart. All unmarked salamanders were individually marked using fluorescent elastomer (Northwest Marine Technologies, Shaw Island, Washington, USA) and marked individuals were recorded. The longitudinal position (distance from the confluence, m), snout-vent length (SVL, mm), and mass (mg) of all individuals encountered were recorded. To test the retention of fluorescent elastomer, we clipped tails of all marked salamanders and noted individuals with a clipped tail and no elastomer mark recaptured in the subsequent secondary period (24 hours later) and primary period (1 month later).

Movement direction.— To test if net dispersal of *D. aterrimus* in upstream reaches was downstream biased and greater than net dispersal in downstream reaches with fish, we described *D. aterrimus* movement across all primary sampling periods. Movement of recaptured individuals was measured as distance along the stream (meters) from the position of last capture. To quantify movement, we used the frequency distributions of

distances moved, assigning negative values to downstream moves and positive values to upstream moves, to quantify movement (Skalksi and Gilliam 2000, Lowe 2003). To determine if salamander movement distributions were consistent within each stream, we tested for differences in the movement distribution of the two study reaches using a Kolmogorov-Smirnov test. We assessed directional bias by testing for skewness of the movement distribution (Zar 1984). To better understand if salamander \times fish coexistence in downstream reaches was influenced by size-biased dispersal rather than dispersal rate, we also tested if distance moved and directional bias were linked to salamander size using parametric (t -test) and non-parametric (Spearman Rank correlation and Mann-Whitney) tests.

To examine if movement distance and direction bias were influenced by our sampling protocol, seasonal flow pulses, or seasonal breeding migrations, we tested the hypothesis that the variance of distance moved increased linearly with time, a characteristic of movement by simple diffusion (Skellam 1951, Turchin 1998, Skalski and Gilliam 2000, Lowe 2003). We regressed the estimated variance of distance moved (weighted by sample size) on time (months) using the polynomial equation $y = c_0 + c_1t + c_2t^2$, where y is the variance and t is time. The hypothesis predicts $c_0 = 0$, $c_1 > 0$, and $c_2 = 0$. Any temporal pulses in movement caused by sampling, discharge, or behavior would lead to non-diffusive movement.

Apparent survival, population growth rate, and recruitment.— To assess how fish affected local population dynamics of *D. aterrimus*, we used the Robust design Pradel (Huggins closed capture) model in program MARK to model variability in apparent survival (Φ) and realized population growth rate (λ) by stream reach and time (Pollock and Otto 1983, Pradel 1996, White and Burnham 1999). Because Pradel models assume demographic closure and therefore cannot incorporate transitions between populations, individuals that dispersed between reaches had two recapture histories, each specific to a reach (Lowe et al. 2003).

The primary parameters of interest were Φ and λ , so we first evaluated models of capture probability (p) and recapture probability (c) to avoid unnecessary bias and imprecision in the Φ and λ estimates (Lebreton *et al.* 1992). We identified the best model of p and c for each stream by pairing the global model for Φ and λ (reach \times primary sampling period \times time) with all possible combinations of $p \neq c$ (reach \times primary sampling period \times time) and $p = c$ (reach \times primary sampling period \times time). We treated p and c as nuisance variables and they were not constrained in models that compared Φ and λ by reach and time (Barker and White 2004, Barker et al. 2005).

To test the prediction that apparent survival was lower in reaches with fish than in fishless reaches and that realized population growth rate did not differ between reaches with and without fish, we modeled variability in Φ and λ by stream reach (r) and primary sampling period. Apparent survival and λ were assumed to vary across primary sampling periods, but be constant over secondary samples. We used Program MARK to compare the following five models

Model 1 and 2.— Apparent survival varies by reach ($\Phi(r)$) (Model 1), and apparent survival is constant between reaches ($\Phi(.)$) (Model 2). Realized population growth is constant between reaches ($\lambda(.)$).

Model 3 and 4.— Apparent survival is constant between reaches ($\Phi(\cdot)$). Realized population growth rate varies by reach ($\lambda(r)$) (Model 3), and realized population growth rate is constant between reaches ($\lambda(\cdot)$) (Model 4).

Model 5.— For Models 1 – 4, we assumed Φ and λ varied across primary sampling periods because of variation in stream discharge and temperature. For Model 5, we compared the top-ranked model from Models 1 – 4 to the same model with no variation across primary sampling periods.

Estimation of Φ and λ allowed for the estimation of recruitment (f) because

$$f_t = \lambda_t - \Phi_t$$

in the Pradel model (Franklin 2001, Williams et al. 2002), where f_t is the number of new individuals entering the population in year $t + 1$ per individual in the population in year t .

We ranked competing models according to how well they were supported by the capture data using AIC_c , AIC_c weights, and evidence ratios (a multiplicative factor for the likelihood of the best model compared to an alternative model) (Burnham and Anderson 2002). Parameter estimates were calculated using model averaging (Burnham and Anderson 2002). Goodness-of-fit tests are not currently possible for the Robust design Pradel model in program MARK, so we assessed the rank stability of the best-fitting models by entering \hat{c} values between 1.0 and 6.0 (e.g., Lebreton et al. 1992, Cooch and White 2001, Lowe 2003).

To assess if *D. aterrimus* movement was a function of *D. aterrimus* density, we regressed proportion of *D. aterrimus* individuals that moved greater than 1 m, 5 m, and 10 m against the average density of salamanders (individuals/m²) within each stream reach across all primary sampling sessions. To be conservative, we used multiple movement distances (i.e., 1 m, 5 m, and 10 m) because the distance threshold that delineates dispersal from local movement is not known for *D. aterrimus*. We transformed proportional data using the arcsine square root. Estimates of salamander abundance were taken from our most supported Robust-design Pradel models from each stream. Stream area was based on field measurements in August 2006 and 2008.

Summary: For this grant, we proposed to identify variables that influence patterns of IGS distribution and abundance, to use genetics (microsatellite DNA markers) and mark-capture-recapture (MCR) to assess the importance of connected stream networks to IGS population persistence and to determine the affect of human disturbance on stream connectivity. This summer, we will complete our surveys in the St. Regis basin in order to identify variables associated with IGS distribution and abundance. We have completed work on genetics.

Modeling the Potential for Transport of Contaminated Sediment

Basic Information

Title:	Modeling the Potential for Transport of Contaminated Sediment
Project Number:	2008MT166B
Start Date:	3/1/2008
End Date:	2/28/2009
Funding Source:	104B
Congressional District:	At-Large
Research Category:	Climate and Hydrologic Processes
Focus Category:	Wetlands, Floods, Models
Descriptors:	
Principal Investigators:	Joel E. Cahoon

Publication

Assessing the Potential for Contaminated Sediment Resuspension from a Mine Impacted Wetland

Jessica Mason¹, Joel Cahoon², Matthew Blank³, Denine Schmitz⁴

¹Department of Civil Engineering, Montana State University
Bozeman, Montana 59717

²Department of Civil Engineering, Montana State University
Bozeman, Montana 59717

³Western Transportation Institute, Department of Civil Engineering, Montana State University
Bozeman, Montana 59717

⁴Department of Land Resources and Environmental Sciences, Montana State University
Bozeman, Montana 59717

ABSTRACT

Wetlands associated with Montana hard rock mines play a paradoxical role. The benefit of attenuating flood water and sediment has led to wetlands serving as sinks for metal precipitates and contaminated sediment. However, during high spring runoff or storm events these wetlands may become significant sources of resuspended contaminated sediments and generate potential impacts to downstream recipients. Using a loosely coupled hydraulic model (HEC-RAS) and a GIS, we explored the influence of flood events of varying magnitude on stream hydraulics and sediment mobilization across a wetland complex located in the Blackfoot River near Lincoln, MT. Field survey data provided a topographic template for running the hydraulic model. Spatial interpolation and geostatistical methods were used to create spatially continuous data surfaces for model input parameters (i.e. roughness coefficient, D_{50}), measured contaminant concentrations (As, Cu, Zn, Cd, Pb) for the upper 2 inches of soil, model output parameters (i.e. velocity, water depth), and critical velocity. Combining critical velocity data layers with modeled velocity and contaminant concentration data layers allowed us to identify zones with high contaminant concentrations and a high potential for sediment mobilization in a spatially explicit manner. Sensitivity analysis showed the one-dimensional hydraulic model to be increasingly sensitive to roughness coefficients with increasing discharge. Comparison of modeled stream velocity distributions to measured velocity distributions showed deviations from observed data in shallow near-bank and over-bank areas. Thorough investigation of differences between modeled and measured velocity distributions at a range of flows and across several transects at a given site will help practitioners decide whether or not this approach will be useful and provides an avenue for future flood risk assessment. We conclude that when carefully applied, this approach may be a valuable tool for assessing contaminated sediment mobilization risk in areas where data is limited and/or development of more data intensive models is not feasible.

1.0 INTRODUCTION

1.1 EXECUTIVE SUMMARY

Hydrologic and hydraulic analyses are used by scientists and engineers for environmental and regulatory decisions. The integration of spatial analysis and hydrological modeling by way of geographic information systems (GIS) is becoming an integral component of flood assessment practices. The potential environmental impacts to downstream groundwater, surface water, and sediment quality affect human, aquatic, and riparian resources (Werner 2001). Flood risk assessment calls for a thorough spatial evaluation of a flood event, where risk is defined as the relationship between hazards in the area and the area's vulnerability, and GIS provides a tool for this type of analysis. This study models the effect of discharge events with varying return intervals in order to assess the potential for sediment transport from a mine-impacted wetland in the Upper Blackfoot Mining Complex (UBMC). There has been substantial work to assess and remediate the impact of the UBMC on aquatic resources by Helena National Forest (HNF), Montana Department of Environmental Quality (MTDEQ), and the mining company, ASARCO. Until recently, however, the wetland complex has largely been omitted from environmental assessments.

The benefit of attenuating flood water and sediment has led to some wetlands serving as sinks for metal precipitates and contaminated sediment. However, during high spring runoff or storm events these wetlands may become significant sources of resuspended contaminated sediment. An essential step for mine-impacted wetland and water resource management and conservation is the capability to predict the impacts of floods on wetlands (Thompson et al. 2004b). Combining surface water hydrology and hydraulic modeling with a GIS provides a method for assessing the potential for resuspension of metals from mine-impacted wetlands currently serving as contaminant sinks. This proof-of-concept report details a methodology that authorities may use to judiciously apply remediation efforts to impacted wetlands.

Identifying critical shear stresses for channel and floodplain areas for several flood frequencies provides a relatively straightforward method for assessing the probability of sediment erosion and transport in contaminated floodplain zones. Erosion is a result of increased shear stresses on soil particles on the channel bed and overbank surfaces. Large storm events may cause sediments, typically smaller sediment particles, within a wetland to erode when the

critical shear stress is surpassed. Critical shear stress is the maximum unit tractive force a particle can withstand. Metals that are resuspended, adsorbed to sediments, or precipitated behave as any other sediment in a fluvial environment (Gibbs 1973). Therefore, improved understanding and simulation of flood risk analysis will assist water resource managers and restoration practitioners in future remediation efforts. It is hoped that incorporation of the methodology presented in this report into current remediation strategies will benefit downstream recipients of water from the mine-impacted wetland as well as researchers, and state and local organizations concerned with flood prediction, mapping, and risk assessment.

This report evaluated a method for assessing potential contaminant resuspension given a data set that included topography, flow, and sediment parameters. Remediation requires knowledge of the metals distribution and an understanding of the potential for resuspension. We utilized a loosely coupled modeling technique that integrates a one-dimensional hydraulic model (HEC-RAS) and a GIS via an extension, HEC-geoRAS. The selected hydraulic model—HEC-RAS (developed by the U.S. Army Corps of Engineers)—is a widely used model and requires relatively little input data, especially when coupled with digital elevation models (DEM) in a GIS. Due to its relative simplicity and low data requirements when compared to more complicated 2D or 3D hydraulic models, it is believed that this approach is a viable option for assessment of sediment suspension risk. This is an especially attractive approach for large sites where costs prohibit the collection of fine scale spatial data needed to accurately parameterize complex models. The methodology described in this report aims to determine the potential for resuspension of sediments within inundated areas corresponding to various extreme discharge events. Locations in the study area that warrant attention from governing agencies and consultants for possible removal from the dynamic fluvial system are identified.

1.2 BACKGROUND

Risk and mine impacted wetlands

The legacy and future of mining in Montana will likely impact wetlands located downstream from mine adits and tailings piles for generations. The wetland downstream of the McLaren Mine in the Stillwater basin is a prime example. The Stillwater wetland has been assessed for metals distribution and the origin of those metals (Cook 2007; Furniss et al. 1999; Gurrieri 1998). Cook (2007) found that metals concentrations increased with depth in the

floodplain due to sediment trapping and decreased with depth in the channel due to annual flushing. August et al. (2002) studied a mine-impacted wetland near Leadville, Colorado and found the wetlands have a finite ability to retain metals and predict they will eventually shift from being a contamination sink to a source. Despite these risks, no hazard assessments of metals-laden wetlands have been conducted to date. Instead, most studies point to these wetlands as sinks that should not be disturbed (e.g. Moore 1992).

The Upper Blackfoot wetland has been studied for several decades. The impact of more than a century of silver, lead, and zinc mining has drawn attention from federal and state officials and research scientists. Spence (1975) inventoried the aquatic biota and water quality before and after a 1975 dam breach that drastically altered water quality in the drainage. The role of the wetlands in attenuating the impact of mine tailings transport during the flood was considered limited. Moore (1992) evaluated aquatic biota upstream and downstream of the wetland ten years later and found that contaminated sediment is transported downstream of the wetland during high flows. This impacts the food web of the drainage through bioaccumulation. Dolhopf, et al. (1988) evaluated the wetland for its ability to remove water borne contamination carried from upstream sources. They estimated that approximately 550 metric tons of iron is deposited in the wetland. The DEQ recently embarked on a damages assessment that includes the wetland (TetraTech 2007). This study will map the distribution of contaminants deposited during the dam breach flood of 1975. Currently, the potential for these contaminants to be resuspended has not been evaluated.

Most of the focus on mine impacted wetlands has been to identify the source of contamination and assign responsibility for damages. Most often these wetlands are sinks for contamination and left in place to protect downstream resources. However, August et al. (2002) showed that mine impacted wetlands are finite sinks that may eventually become contaminate sources. Helena National Forest (HNF) is currently removing a major source of metals-laden sediment upstream of the wetland (an impoundment and tailings dam); however, there remains a second significant source of surface flow from the Mike Horse Mine adit. Any disturbance to contaminated sediment (natural, remedial, or constructive) will cause metals resuspension as well as alter the biogeochemical environment with an increase in metals mobilization.

Modeling floods and erosion

Extensive research and risk assessment of sites with contaminated sediment typically involves chemical identification and an evaluation of the quantities and location of pollutants. The inherent risk of erosion of contaminated sediment which eventually leads to transport and deposition further downstream requires knowledge of sediment behavior and the hydraulic forces acting on the riverbed (Haag et al. 2001). When contaminated sediments are suspended into the water during erosion, the bioavailability and toxicity levels usually increase generating hazardous conditions for aquatic life and downstream recipients. Forstner (2004) suggests a model for evaluating the mobility of contaminated sediment that incorporates measurements of sediment regions, shear stress, and critical shear stress. Therefore, assessing the environmental impacts of contaminated sediment involves an evaluation of the risk of erosion due to hydraulic forces and potential transport during a flood event.

Intricate analysis and simulation capabilities are available with both hydrologic/hydraulic models and GIS, and the integration of the two provides a powerful tool for scientific researchers and policy makers. The widespread availability of spatially distributed data through GIS has made physically based hydrologic models more useable and spurred the development of hydrologic models that take advantage of these new data. Engineering hydrology has time-tested empirical approaches for hydrologic modeling, and the development of hydrologic models that can better simulate spatially varied hydrology involves a combination of these practices with the data-handling capabilities of GIS and enhanced processing involved with GIS modules (Sui and Maggio 1999). Further development of scaling relationships for spatially distributed hydrologic variables will lead to improved performance of the integrated models. Hydrologic and GIS models, however, have inherently different temporal data representation schemes. The input, storage, and management of time varying data are not adequately facilitated by GIS technology to date. GIS has a rigid spatial-temporal framework that restricts complex hydrological processes; therefore, coupling hydraulic modeling results and GIS becomes an interactive process incorporating uncertainty during information exchange (Ogden et al. 2001; Sui and Maggio 1999).

A variety of software is available that attempts to integrate GIS and hydrologic/hydraulic models. Loose coupling is the most widely used practice by GIS and hydrologic/hydraulic modelers. This technique combines a GIS package and hydrologic/hydraulic modeling programs,

such as HEC-1, HEC-2, or STORM, and statistical packages, such as SAS or SPSS. Without a common user interface, data is exchanged between the three packages via a common language or format (ASCII or binary data format) and requires extensive data development, which can be labor intensive and error prone (Ogden et al. 2001; Sui and Maggio 1999).

The majority of robust hydraulic engineering models, including HEC, MIKE 11, and ISIS, incorporate one-dimensional flow routing approaches. Additional flood simulation approaches that accommodate more realistic physical and hydrodynamic conditions in river processes require two- and three-dimensional analysis. One-, two-, and three-dimensional hydraulic modeling approaches incorporate terrain analysis and the calculation of flood extents and depth by means of GIS, and each has advantages and disadvantages for use in flood risk estimates.

Exercising a loosely coupled modeling technique, the one-dimensional HEC-RAS model (U.S. Army Corps of Engineers) has the capability to incorporate georeferenced cross-section data into its model coordinate system for hydraulic analysis through modeling software, such as HEC-geoRAS. Techniques for coupling the results from one-dimensional flow models with a GIS involve geostatistical interpolation, neighborhood analysis, and calculating interception points of water levels in the cross section profile (Werner 2001). For hydraulic modeling of river channels, high resolution digital terrain models (DTM) provide detailed cross-sections for analysis and the location of the channel thalweg, but these are typically only available through land survey data or remote sensing.

One-, two-, and three-dimensional models each have advantages and disadvantages for use in a flood risk assessment. One-dimensional models require cross-sections which do not accurately model topographic changes in water surface elevations between transects. Two- and three-dimensional modeling incorporates a continuous surface to represent complicated river systems and to generate a finite element mesh. Quality point data and information about channel morphology for interpolation of points from cross sections is important where unrealistic surfaces could result from cross section location and spacing, inclusion of points outside the main channel, and interpolations that do not capture the true thalweg. Merwade, Cook et al. (2008) recommend anisotropic techniques that define search neighborhoods and assign weights according to flow direction when working with point measurements. They also propose a method for linear interpolation between cross sections to incorporate information about unmeasured

locations. The merging of intricate and accurate channel and floodplain topography produce an accurate terrain model for flood modeling and groundwater/surface water interaction investigations. However, the time and expense involved in collecting such high resolution spatial data may be beyond the scope and budget of many remediation strategies.

Although two- and three-dimensional hydraulic flow models produce descriptive results for flood analysis, they have high computational requirements and labor-intensive data input making them difficult to use for decision support systems. The incorporation of higher dimensions into a hydraulic analysis introduces more uncertainty as the number of assumptions increases. Rapid assessment of flood impacts is most easily completed with a one-dimensional hydraulic model, as two- and three-dimensional models require comprehensive data that may not be readily available for the area of study.

GIS based hydrologic models will likely advance current practices in flood control, flood mitigation, floodplain mapping, and flood insurance studies. A fully integrated hydrologic and GIS based system would apply robust modeling techniques and concepts representing spatial and temporal processes at the same level. GIS provides a powerful tool when coupled with hydrologic/hydraulic models not only for visualization of flood extents and depths but for further analysis of flood damage and risk estimates.

1.3 SITE DESCRIPTION

Location

The UBMC is east of Lincoln, Montana in Lewis and Clark County and is located at the headwaters of the Blackfoot River. The area encompasses several abandoned mines on private property and the National Forest Service (see Figure 1.1). Once mined for silver, zinc, and lead, the mines continue to be a source of contamination to local water-ways. The major individual mines include the Mike Horse Mine, the Anaconda Mine, the Edith Mine, the Paymaster Mine, and the Carbonate Mine. Smaller mines are located within the Blackfoot River drainage. In conjunction with a plugged spillway pipe, a 1975 rain-on-snow event lead to a breach in the Mike Horse tailings impoundment below the Mike Horse Mine. The resulting flood wave washed tailings down the headwaters of the Blackfoot River (Tate et al. 2002). Combined effects from the breach and continuous leaching of acid mine drainage from historic mine sites along tributaries acidified sediments along the floodplain and within a downstream wetland. Within the

drainage area, elevations range from 5,200 feet above mean sea level (AMSL) at the marsh system to 7,500 feet AMSL along the continental divide (Figure 1.1).

Hydrology

Several tributaries contribute runoff to the Blackfoot within the UBMC. The confluence of Beartrap Creek and Anaconda Creek form the Blackfoot River. Further downstream, the wetland receives flow from five additional streams (three perennial, two intermittent) during spring runoff, Shaue Creek, Stevens Gulch, Paymaster Creek, Pass Creek, and Meadow Creek. The wetland system initiates just upstream of the confluence of the Blackfoot River and Pass Creek and continues for several miles downstream of the confluence. The total drainage area to the wetland is 14 square miles. Figure 1.1 denotes drainage areas to the study area.

Climatic data is recorded at the nearby Rogers Pass Station and Lincoln Ranger Station. Annual precipitation averages are 17.99 inches. The highest annual precipitation in the area was recorded in 1975 (31.4 inches), the year of the tailings impoundment breach. Until the recent draining of the reservoir behind the tailings impoundment, water seeped through the earthen dam and flowed through the overflow pipe during runoff periods maintaining a supply of heavy metals to downstream tributaries.

Vegetation

The vegetation of the UBMC is characteristic of the Rocky Mountains with some alterations due to mining activity. The majority of the slopes and transition areas into floodplains are composed of coniferous forest with lodgepole pine, spruce, and Douglas fir. Mountain big sagebrush and fescue grassland dominate drier slopes. Wetland and riparian areas within the study area encompass coniferous and deciduous tree communities as well as shrubs and herbaceous species. The photos represent vegetation coverage in the marsh study area and surrounding drainage areas.

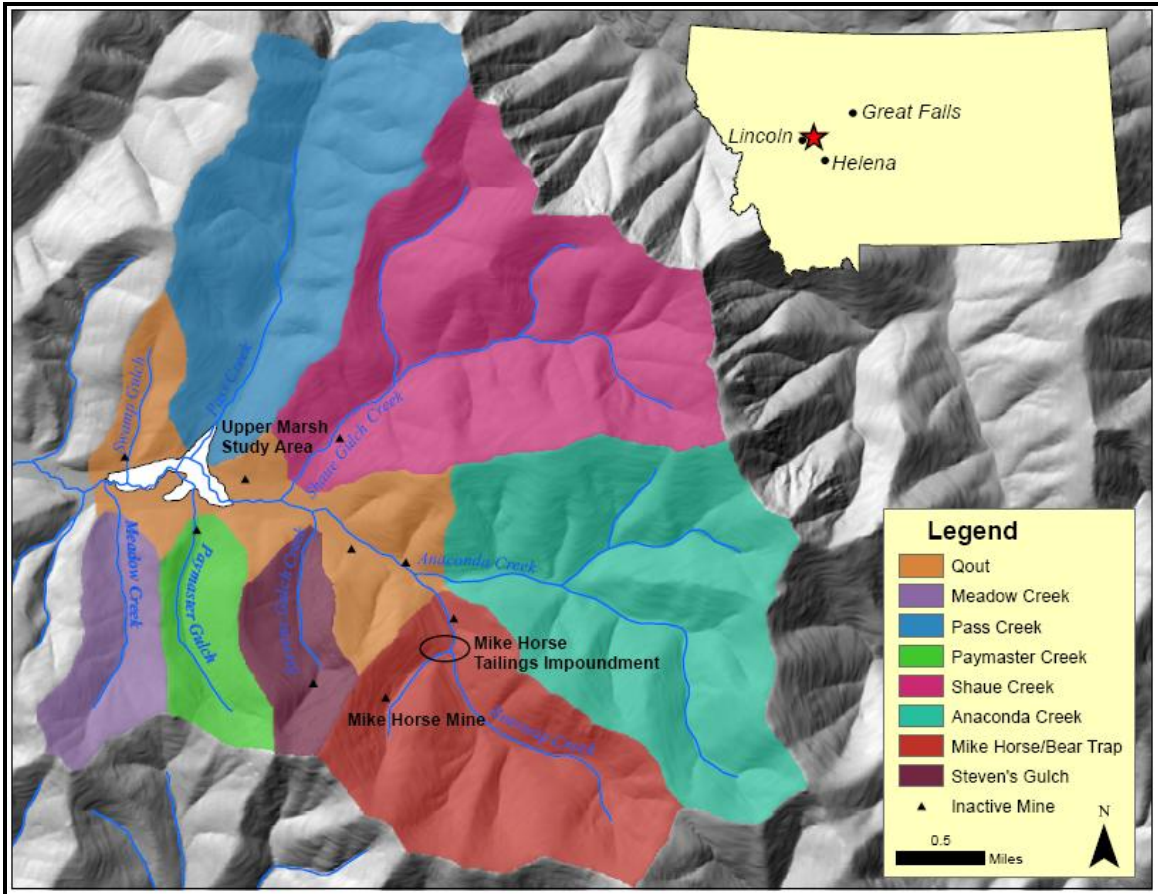
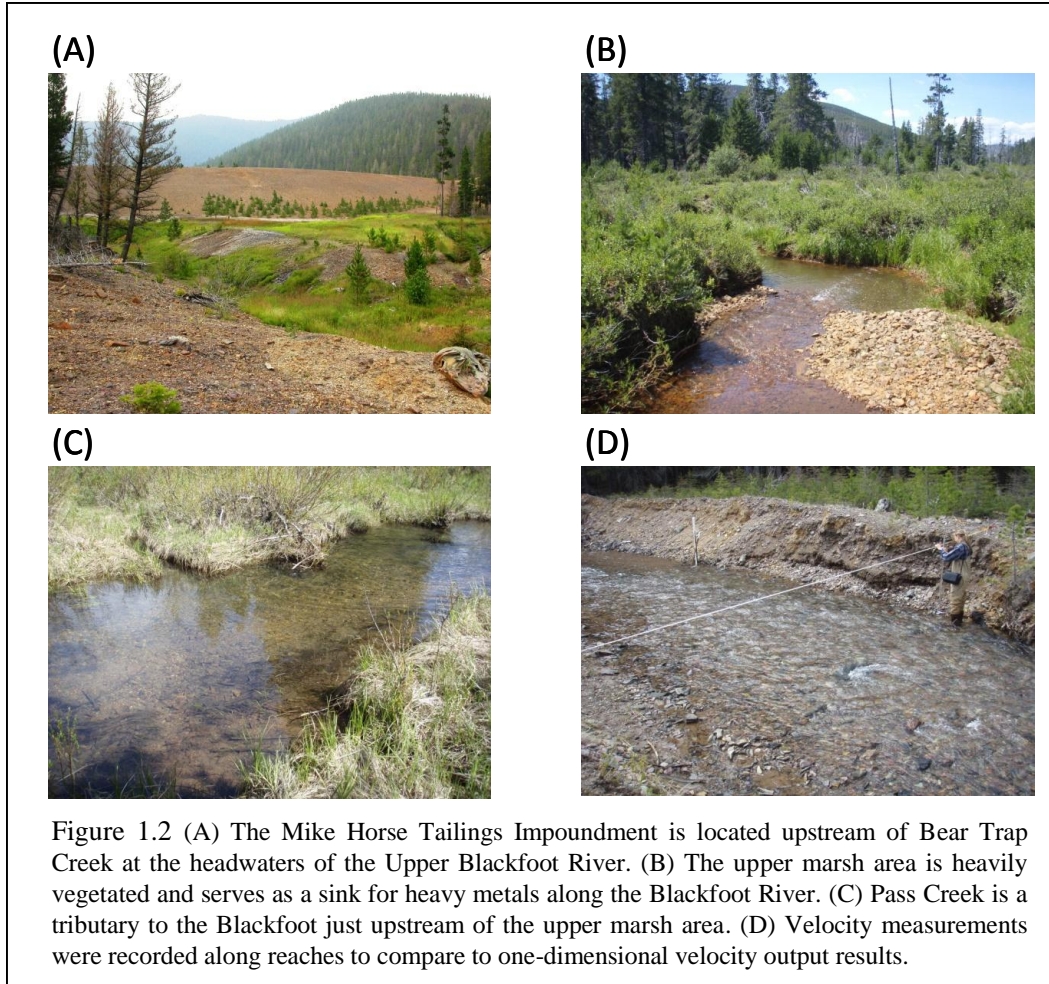


Figure 1.1. The Upper Marsh Study Area (denoted in white above) is located along the Blackfoot River with several upstream abandoned mines acting as sources of heavy metals (Data Source: NRIS, MT DEQ)

Geology and Hydrogeology

A mixture of bedrock units are identified within the UBMC, including the Belt Series Spokane Formation, a diorite sill, and Tertiary-age intrusive bodies. Based on well yield tests, low bedrock permeability characterizes the site. Permeability is also restricted due to low recharge areas near the continental divide. Groundwater flows are recharged primarily from snowmelt from higher elevations to alluvial groundwater systems and tributaries. Major flowpaths include secondary fractures, joints, and fault zones.



2.0 METHODS AND DATA COLLECTION

The goal of this study was the evaluation of a one-dimensional hydraulic model and the production of a hazard probability map that encompassed the potential erosive surfaces for the 10, 25, and 100 year recurrence intervals. The identification of drainage areas assisted with the estimation of flood event discharge values necessary for the hydraulic analysis. A detailed topographic survey provided the foundational data for the hydraulic model. Soil samples collected from various points in the wetland by MT DEQ and during field campaigns provided information on surface roughness and contaminant distributions.

Discharge

Drainage areas (Figure 1.1) for each reach were determined with a GIS. Using the methods described by Parrett et al. (2004), the drainage area, basin characteristics, annual precipitation, and active channel width were determined for each reach to estimate discharge events with 2, 10, 25, 50, 100, 200 and 500 year recurrence intervals. Table 2.1 provides results from the regression analysis. Discharge estimates were used to parameterize the hydraulic model.

Velocity and stage measurements were taken in each tributary at the same cross section for thirteen weeks beginning in May and ending in July. Velocity measurements were recorded every 0.5 ft at a depth six tenths from the bed using a Marsh McBirney. Recorded velocity measurements across each surveyed cross section provided parameters for an evaluation of the one-dimensional hydraulic model performance.

Table 2.1 Drainage areas were estimated for each tributary in the study area and discharges for flood events were estimated.

Drainage Area ID	Drainage Area (sq. miles)	2-yr (cfs)	5-yr (cfs)	10-yr (cfs)	25-yr (cfs)	50-yr (cfs)	100-yr (cfs)	200-yr (cfs)	500-yr (cfs)
Anaconda Creek	2.90	13	36	64	129	212	344	538	966
MikeHorse/Bear Trap Creek	1.99	14	37	65	126	200	311	466	784
Shaue Creek	3.28	26	65	109	205	317	485	716	1180
Pass Creek	2.33	24	59	99	185	288	442	653	1080
Paymaster Gulch	0.58	8	21	38	76	122	194	295	506
Meadow Creek	0.64	5	13	24	51	84	135	207	358
Steven's Gulch	0.55	3	10	19	41	69	113	176	311
Qout	1.45	12	32	56	109	173	270	405	680

Topography and channel geometry

Detailed cross section geometries are necessary to predict flow characteristics in the wetland, and topographic land surveys were completed using a total station and a survey grade global positioning system (GPS) device. Variations in topography were also evaluated with an orthorectified aerial photo and aerial photographs. Using the Delunay triangulation method, an interpolated surface (TIN) was generated from land survey points and breaklines from the orthorectified aerial photo. The Delunay triangulation interpolation method had several advantages: 1) triangles created were as equi-angular as possible, 2) new node values were close to known observation points, and 3) interpolations were not affected by the sequence of input data (Hu 1995).

2.1 MODEL DESCRIPTION

The one-dimensional hydraulic model, HEC-RAS, incorporates several parameters to estimate water surface profiles for steady gradually varied flow. Discharge amounts for each

flood event along contributing reaches and locations of flow changes are required for the analysis. Surveyed cross section geometries provide detailed topography of the channel and floodplain areas. The selection of roughness coefficients based on photographs, sediment samples, and topography transitions is a critical component when incorporating Manning's equation to estimate water surface profiles.

One-dimensional hydraulic models are widely used for flood mapping and are typically simpler to use with minimal amounts of input data in comparison to two- and three-dimensional models. The U.S. Army Corps of Engineers' River Analysis System, HEC-RAS, is a robust, public domain, internationally used hydraulic modeling program. Numerous studies in a variety of environments, including surface flow through wetlands, have demonstrated HEC-RAS's effectiveness in estimating peak discharge (Auble et al. 2005; Johnson et al. 1999). HEC-RAS calculates one-dimensional, energy-balanced water surface profiles for subcritical and supercritical conditions. Using an estimated downstream water surface elevation for subcritical flow, HEC-RAS iteratively determines upstream or downstream water surface profiles. Several equations are available for calculating channel flow using mass, energy, and momentum conservation. HEC-RAS has the ability to model an entire network of channels, in either looped or dendritic configurations.

The model supports several options for incorporating friction equations depending on the flow regime and profile type. For gradually varied, steady flow estimates, the energy equation is balanced between successive cross sections. The uniform flow equation, Manning's equation, is used to estimate the energy slope at each cross section. To estimate discharges, the Manning equation combines channel geometry, slope, and an estimate of resistance to flow (roughness coefficient) to determine stream velocity for turbulent flow on a rough surface. When the velocity head is rapidly varied (hydraulic jumps, junctions between reaches), the momentum equation is employed. Further, HEC-RAS offers the capability of entering a roughness coefficient for each topographic break in a cross-section rather than a single integrated value, thereby, producing a more accurate representation of spatial variability of roughness across channel and overbank environments.

Using the energy equation, the robust model estimates water surface profiles between successive cross sections using the standard step method (Chow 1959). Calculations of flow depth are carried upstream for subcritical flow and downstream for supercritical flow. An

iterative solution calculates unknown water surface elevations at the cross section based on an assumed water surface elevation, the boundary condition. Total conveyance and velocity head are used to estimate the friction slope (S_f) and friction head loss (h_f).

The energy equation is given by:

$$y_1 + z_1 + \frac{\alpha_1 V_1^2}{2g} = y_2 + z_2 + \frac{\alpha_2 V_2^2}{2g} + h_e \quad (1)$$

where; y = the thalweg flow depth,
 z = the elevation of the channel invert,
 α = the velocity head weighting coefficient,
 V = the average cross section velocity,
 g = the gravitational acceleration, and
 h_e = the head loss.

The friction head loss is estimated through Manning's equation and accounts for boundary roughness conditions.

$$S_f \cdot \Delta x = \frac{\Delta x}{2} \left(\frac{V_1 n_1^2}{K_n^2 R_1^{4/3}} + \frac{V_2 n_2^2}{K_n^2 R_2^{4/3}} \right) \quad (2)$$

Δx = the distance between cross sections,
 n = Manning's n ,
 K_n = the unit correction factor for Manning's equation, and
 R = the hydraulic radius.

The standard step method has several advantages for modeling natural channels. Even if the water surface elevation is not known at the starting cross section, profile estimates converge closer to the correct elevation with every step. Therefore, if the elevation at the control section is unknown, estimates can be made for the initial elevation or computations can begin a few cross sections away from the desired location.

Manning's equation assumes uniform flow with consistent channel cross section and velocity where the energy gradient is equal to the slope of the water surface and stream bed (Chow 1959). Criticisms of the flow equation include Manning set the exponent of the wetted perimeter to 2/3 even though his and later research indicates that the value can range from 0.6175 to 0.8395. In addition, the flow equation is dimensionally inhomogeneous and represents uniform flow rather than non-uniform flow (Pappenberger et al. 2005). The square root of the slope tends to dampen the uncertainty from energy slopes based on water surface gradient surveyed in the field.

Selection of Manning's n Using a Component Method

The combination of calibrated roughness parameters and geometry affect the flood extent estimates as most hydraulic models are sensitive to these metrics (Marcus et al. 1992; Pappenberger et al. 2005). Uncertainty arises with approximations of geometry and selection of roughness values, and it is almost impossible to quantify every source of energy loss in a system. Roughness coefficients represent the resistance to flood flows in channels and floodplains. Flow resistance results from sediment size, sediment load, vegetation, sinuosity, contraction and expansion. Several methods have been developed to estimate values of n , including photographic comparisons, particle-size based techniques, combinations of roughness generating factors, direct measurement, and regime equations relating roughness to hydraulic variables (Chow 1959; Marcus et al. 1992; Pappenberger et al. 2005; Schneider and Arcement 1989).

Roughness coefficients were estimated using the method described by Arcement and Schneider (1989) for the stream channels and by Cowan (1956) for floodplains. We collected data for the following parameters: depth of water, sediment size, channel irregularities, changes in size of channel, channel meanders, obstructions, and vegetation density. Depth and velocity are two critical factors that will affect the evaluation of flow through the wetland (Kadlec 1990) and should be considered when selecting a roughness coefficient. Roughness coefficients are larger if flow depths are small in comparison to the sediment size and decrease with increasing flow depth if channel banks are not rougher than the bed or if dense vegetation does not intercept flow in the channel (Schneider and Arcement 1989). The Arcement and Schneider procedure incorporates the effects of several factors to estimate a roughness coefficient for channel and floodplain areas. The value of total roughness factor, n , may be computed by the following:

$$n = (n_b + n_1 + n_2 + n_3 + n_4)m \quad (3)$$

where; n_b = a base value of n ,

n_1 = a correction factor for the effect of surface irregularities,

n_2 = a value for variations in shape and size of the channel cross section,

n_3 = a value for obstructions,

n_4 = a value for vegetation and flow conditions, and

m = a correction factor for channel meandering.

Parameters n_1 through n_4 are determined through visual observations. Base roughness values (n_b) combine values from Chow (1959), Benson and Dalrymple (1967), and Aldridge and Garrett (1973). Selecting a base n_b value for a channel involves determining if the channel is a

stable or sand channel. If the bed consists of firm soil, gravel, cobbles, boulders, or bedrock, it is classified as stable, while an unlimited supply of sand characterizes a sand channel with grain sizes ranging from 0.062 to 2mm. Sand bed channel material is transported easily and creates a resistance to flow with varying bed forms. The movement of sand and the creation of different configurations is a result of flow velocity, sediment size, bed shear, and temperature.

Floodplain roughness coefficients are estimated with the Cowen method using a similar procedure for estimating channel roughness. The base roughness value (n_b) is selected for the underlying sediment composition. Adjustment factors for surface irregularities (n_1), obstructions (n_3), and vegetation density (n_4) are then incorporated into the floodplain roughness coefficient. The n values for the floodplains are estimated where abrupt changes in resistivity occur, including topographic breaks, vegetation density, and sediment size changes.

2.2 EROSION

Mine impacted natural wetlands exist in overbank areas throughout Montana, and evaluating floods for ecosystem impacts aids with making water resource management decisions (August et al. 2002). Because the mechanism for sediment resuspension in a wetland is erosion, the dominant controlling factors must be addressed in a model. Soil physical properties, vegetation, and geomorphology influence friction; therefore, shear stress differs across the wetland channel and overbank areas (Bendoricchio 2000; Kadlec and Knight 1996).

An essential step for mine-impacted wetland risk assessment is the capability to predict the impacts of flood events on wetlands (Thompson et al. 2004a). Erosion is a result of increased forces on soil particles within the channel bed and overbank surfaces and is a function of the magnitude of resisting channel forces and the hydraulic forces over time (Fischenich et al. 2001). Predictions of sediment transport and erosion potential depend on empirical equations for natural channels. Erosion characterization involves predictions of critical shear stress or critical velocity and is affected by the following parameters: flow properties, sediment composition, climate, subsurface conditions, channel geometry, biology, and anthropogenic factors. Velocity is a parameter measured within channel flow; while shear stress is calculated from flow parameters as a force per unit area. Metals that are resuspended, adsorbed to sediments, or precipitated, behave as any other sediment in a fluvial environment (Gibbs 1973); therefore, identifying

erosion potential for channel and overbank areas for several flood magnitudes may be a valuable tool to assist in remediation efforts of mine impacted wetlands.

Evaluating the threshold condition or incipient motion reached between erosion and sedimentation as the forces resisting motion become balanced with the forces acting on particles provides a critical parameter for evaluation of resuspension potential (Fischenich et al. 2001; Julien 1995a). Under uniform steady flow, the forces acting on a noncohesive particle are a resisting force, hydrodynamic drag force, hydrodynamic lift, and submerged weight. The resultant of each of these forces is zero at the threshold condition, and the initial movement of soil particles can be evaluated with either critical shear stress (λ_{cr}) or critical velocity (V_c).

The maximum unit tractive force a surface can withstand without eroding is termed the critical shear stress and is a measure of fluid force on a channel. This includes the flow-generated shear and gravitational forces acting on soil particles. Shear stress is a widely used method to quantify the potential for transport of material. Average bed shear stress estimates incorporate variations in roughness and velocity caused by fluctuations in turbulence and is defined by the following:

$$\lambda = \gamma R S_f \quad (4)$$

where; λ = the fluid shear stress,
 γ = the specific gravity of water,
 R = the hydraulic radius, and
 S_f = the frictional slope.

A particle's size relative to surrounding particle sizes, its orientation, and the degree it is embedded determine the amount of shear stress that particle will experience. By equating resisting forces to applied forces, critical shear stress estimates can be made. Approximations of critical shear stress can be made with widely used equations estimated by Shields (Brunner 2002), Lane, Julien (Julien 1995b), and Andrews (Andrews 1983). By equating resisting forces to applied forces, critical shear stress estimates can be made. Shields developed the following equation for critical shear stress (λ_{cr}) (at incipient motion) from flume experiments.

$$\lambda_{cr} = K_s \gamma_s - \gamma D \quad (5)$$

where; K_s = Shield's coefficient,
 γ_s = the specific weight of sediment, and
 D = the particle size.

The hydraulic model estimated average shear stress values for each cross section. Flow was modeled as subcritical using the normal depth as a boundary condition. Segmented roughness values across the cross sections in the wetland region and contributing tributaries were assigned based on sediment size, vegetation coverage, obstructions, and channel meanders. Shear values were a function of frictional slope, hydraulic radius, and the weight of water and, therefore, dependent on cross sectional area. Shear stress estimated in the one-dimensional model is an average shear stress; however, shear stress can also be calculated using log velocity profiles. The hydraulic radius, a ratio of area to wetted perimeter, heavily influences shear stress estimates in the hydraulic model. The von Karmen-Prandtl law of velocity distribution (Bergeron and Abrahams) is another method for estimating shear stress based on log-velocity profiles plotted as a function of velocity near the channel bed and the natural log of depth over roughness. Estimating the roughness parameter incorporates uncertainty into shear stress calculations, but with detailed vertical velocity profiles, the method provides another calibration estimate for the model.

Critical Velocity

The maximum velocity or critical velocity is the channel velocity that will not permit erosion, and surpassing the critical velocity results in the initiation of particle motion. An estimate for critical velocity, developed by Laursen (Akan 2006) is obtained by equating shear stress to critical shear stress and is based on the concept of tractive force:

$$V_c = \frac{K_n}{n} \sqrt{K_s (s-1) g}^{1/6} D^{1/2} \quad (6)$$

where: s is the specific gravity of particles (γ_s/γ). Typical values include 0.039 for K_s and median diameter (D_{50}) for particle size.

Empirical methods for evaluating velocity and shear stress were developed in flumes. Natural channels experience high levels of variability and may not experience uniform or steady flow. The amount of sediment in suspension minimizes turbulence and is not accounted for in the given estimates of velocity and shear stress. Variation in particle size influences stress in channels. Larger particles often inhibit smaller particles from motion until significant flows and higher stress are experienced. Application of this method to our data required the assumption that flow is steady and the use of an interpolated median particle size distribution.

Velocity distributions were calculated along each cross section in each hydraulic model. Dynamic segmentation provided a tool for assigning parameter values for velocity, depth, and roughness coefficients (n) across a cross section within segments. Continuous critical velocity data surfaces were created using Delaunay Triangulation to interpolate values between cross sections.

Soil Physical Properties

Field investigations provided several of the metrics required for the hydraulic model and for the velocity and critical velocity distribution analysis. Sediment size distributions were evaluated with samples extracted along each cross section (channel and floodplain) where sediment sizes varied. At each of these transition points, thirty sediment grain samples were selected from within a one square meter area and measured with a gravelometer. Additional samples with an abundance of fine material (less than 2mm) were analyzed with sediment sieves in the lab. Each sampled location was recorded, and sediment size distributions (e.g. D_{50}) were used in the selection of appropriate roughness coefficients. We used inverse distance weighting to spatially interpolate sediment sizes across the study site. Through this method, the value at an unknown point is estimated by surrounding known-point values which are weighted according to their respective distances. Therefore, the closer a point is to the center of the estimated cell, the more influence it has on the estimated value. For example, sediment sample points in the steep terrain beyond the floodplain did not significantly influence interpolated sediment size cells within the channel. Sediment particle distributions in the study area resulted from erosion and deposition and varied significantly between the channel and floodplain areas.

The MT DEQ provided the metal concentration levels sampled along a 250 foot square grid and some intermittent points within and surrounding the wetland area. Concentrations of aluminum (Al), arsenic (As), cadmium (Cd), copper (Cu), iron (Fe), lead (Pb), manganese (Mn), mercury (Hg), and zinc (Zn) within 0-2, 2-6, and 6-12 inches of the surface were sampled. We selected a subset of this data for analysis. Concentrations in the top two inches of soil were deemed most relevant to our analysis and were therefore used exclusively. Distribution surfaces were not interpolated for aluminum, manganese, and mercury due to lower concentration levels and an insufficient data set for spatial interpolation.

Kriging was selected as the spatial interpolation method for metal contamination and involved preliminary investigations of the spatial correlation of data. Each known point for

individual parameter data sets was employed in the spatial interpolation to distribute values to unknown cells in the raster data set. The kriging interpolation involved a weighted moving average method derived from regionalized variable theory where similar patterns of variation occur at every location on the surface. These patterns were observed in a semivariogram, which measured the degree of spatial correlation among the metals concentration data points in the grid as a function of the distance and direction between observational data points (Hu 1995; Kitanidis 1997; Marx 1987; McCoy and Johnston 2001). The model fit to the semivariogram controlled kriging weights assigned to the interpolated data points. Kriging resulted in the creation of continuous data surfaces for metal concentrations across the study site. Metal distributions resulted from resuspension and deposition during larger storm events and did not display abrupt spatial changes or spikes. Higher concentrations were observed in the entrance to the wetland and decreased toward the outlet.

Vegetation

The presence of barriers, including vegetation and litter mats, inhibits wetland sediment resuspension. A greater force is required to displace particles within vegetated areas. With the presence of vegetation, the probability of erosion is dampened as the velocity decreases and the forces that initiate movement diminish. Along each cross section, locations where changes in vegetation density and type occurred were recorded with a GPS. Obstructions, vegetation density, and vegetation species were documented and photographed. This assessment assisted with the selection of appropriate roughness coefficients during hydraulic model parameterization.

2.3 HAZARD MAPPING

Hazard potential maps were created by analyzing sediment characteristics, metals distributions, and hydraulic metrics, such as velocity distributions and inundation surfaces for the 10, 25 and 100 year flood events. The flow chart in Figure 2.1 summarizes the processes for the hazard probability map analysis completed for each flood event. Using water surface elevations and locations of the water surface extents generated from each hydraulic model, an inundation surface was mapped in the GIS. Terrain elevations subtracted from the water surface created the spatial extent of flood inundation and flood depth, and this layer provided a bounding layer for the data sets investigated in the hazard analysis. Using equation (7) continuous data surfaces for

water depth, flow velocity, and sediment size for each of the flood events of interest were combined to produce spatially continuous critical velocity layers. These layers were then overlaid by modeled velocity distributions to obtain a percent exceedance value. For any given cell on the hazard potential map, percent exceedance was calculated as follows:

$$(V_m / V_c) * 100 \quad (7)$$

where; V_m = modeled velocity
 V_c = critical velocity

Results of the percent exceedance map suggest areas where the modeled flood velocity is likely to exceed the threshold condition at which sediment is mobilized. Combining the percent exceedance data with data surfaces for contaminant distributions of arsenic (As), copper (Cu), cadmium (Cd), lead (Pb), and zinc (Zn) allows for the creation of hazard potential maps. These maps provide a qualitative visual tool for assessing the spatial distribution of sediment contamination and the estimated percent velocity exceedance simultaneously.

2.4 SENSITIVITY ANALYSIS AND ERROR CHECKING

Evaluation of the hydrologic and hydraulic performance of the model within a dynamic wetland situation was conducted by testing the accuracy and stability of the output in a sensitivity analysis. In particular, alterations to roughness coefficients, contraction/expansion coefficients, and spacing of cross-sections addressed the dependence of the output on specific input variables communicates the model's limitations. Manning's roughness coefficients were globally altered by 10%, -10%, 25%, and -25%. Contraction/expansion coefficients were adjusted from 0.1/0.3 to 0/0.5, 0/0, and 0.3/0.7. By adjusting the spacing of cross-sections through interpolation or removal, shortcomings in our topographic survey were identified. Velocity distribution results from the hydraulic model for selected cross sections were compared to field velocity measurements.

Metal concentration distributions were spatially interpolated with ordinary kriging and spherical models. The spherical models were fit using a Monte Carlo analysis which provided parameter sets that minimized the sum of squared errors. Kriging provides estimates of error variance for the interpolated contamination levels within the wetland.

3.0 RESULTS AND DISCUSSION

3.1 HYDRAULIC ANALYSIS

The one-dimensional model estimated water surface elevations and hydraulic parameters for calculations of critical velocity. Detailed roughness parameters based on sediment size and vegetation were used to estimate flow across cross sections and, therefore, water surface elevations and velocity distributions. Some cross sections required critical depth determination when the energy equation failed to balance within a specific number of iterations.

Estimates of water surface elevations within the natural channel in the one-dimensional hydraulic model involve several assumptions. Flow was assumed to be steady throughout the reach and to be gradually varied between cross sections as the energy equation is based on the theory of a hydrostatic pressure distribution across each cross section. Cross sections were located along a given reach and satisfied the gradually varied flow assumption. Flow was considered to be one-dimensional and in the dominant flow direction without considering velocity in any other direction. The total energy head was assumed to be the same at every point along a cross section. The energy slope was assumed to be uniform across any given cross section and between consecutive cross sections.

Table 3.1. Nine reaches within the study area were modeled with at least five cross sections to estimate water surface elevations.

Drainage Area ID	Reach Length (ft)	Number of Cross Sections
Anaconda Creek	2223	16
Blackfoot Reach 1 (MikeHorse/Bear Trap Creek)	3641	35
Blackfoot Reach 2	4993	70
Shaue Creek	1392	8
Blackfoot Reach 3	4724	28
Pass Creek	1563	8
Blackfoot Reach 4	4487	17
Meadow Creek	1878	5
Blackfoot Reach 5	2448	11

Velocity distributions in HEC-RAS calculated for a set number of divisions across a cross section are a function of conveyance and area for each subdivision. Velocity in a natural channel varies vertically and horizontally, and output from the one-dimensional model is an average velocity for each segmented area within the channel. Velocity distributions typically

increase the conveyance within each segment. Therefore, the sum of the conveyances from the segments does not equal the total conveyance from the original modeling technique, and a ratio of the total conveyance to the segmented conveyance is applied to the segments before estimating the average velocity.

Velocities were compared for thirteen cross sections in the marsh area. Table 3.2 notes the absolute relative error between the averaged measured velocity in the channel and the averaged HEC calculated velocity in the channel. Absolute relative error describes the difference between the measured velocity and the predicted velocity relative to the measured velocity. The averaged HEC velocity distributions create smooth velocity transitions between banks and do not capture variations in velocity due to eddies and bed topography. The relative error for cross sections within a defined channel was lower than cross sections in wider flow areas. Velocity predictions within cross sections with defined channels closely matched the measured velocity values near the thalweg. Ground water interactions, vegetation, beaver dams, and mild gradients likely affected flow characteristics in the wetland and cannot be accounted for by one-dimensional models. These results suggest that in a low gradient wetland with large inundated areas and sinuous flow, our method may produce erroneous velocity estimates in near-bank or shallow over-bank zones. Future studies that include more extensive comparisons between modeled and observed velocity distributions on multiple cross sections over a variety of flow conditions may help quantify the degree and extent of this error. Assessment strategies similar to that outlined above may need to be implemented by practitioners on a case-by-case basis to determine the appropriateness of our method at a given site.

Contraction and expansion coefficients and roughness coefficients were selected parameters for the sensitivity analysis, and comparison plots between predicted models and those with altered parameters identified the significance of the selected parameters. Changes in contraction and expansion coefficients had little effect on the performance of the one-dimensional model. Figure 3.2 is a representative example of changes in contraction and expansion coefficients where the initial velocity and shear stress values follow the linear 1:1 line in the graphs. Altering contraction and expansion coefficients to 0.3/0.7 respectively had the greatest effect on velocity and shear stress estimates. When the channel flowed from a wide area to a constricted section, such as the junction between Anaconda Creek and the Blackfoot River,

shear stress values increased. Error estimates for the flood events indicate that larger flood events are less affected by changes in contraction and expansion coefficients.

Table 3.2. Absolute relative error between average measured velocities and HEC average velocity output vary at thirteen locations in the wetland.

Cross Section	Absolute Relative Error (%)	Average Measured Velocity in Channel (ft/s)	Average HEC Calculated Velocity in Channel (ft/s)
11943	60	0.89	1.43
11633	386	0.40	1.96
10889	8	1.75	1.61
10184	24	1.15	0.87
9762	2	1.03	1.05
9566	151	0.59	1.49
9399	23	0.82	1.01
8594	6	0.74	0.79
7844	35	1.18	0.77
5674	412	0.41	2.12
5387	434	0.39	2.07
4463	13	0.69	0.60
2821	59	0.18	0.29

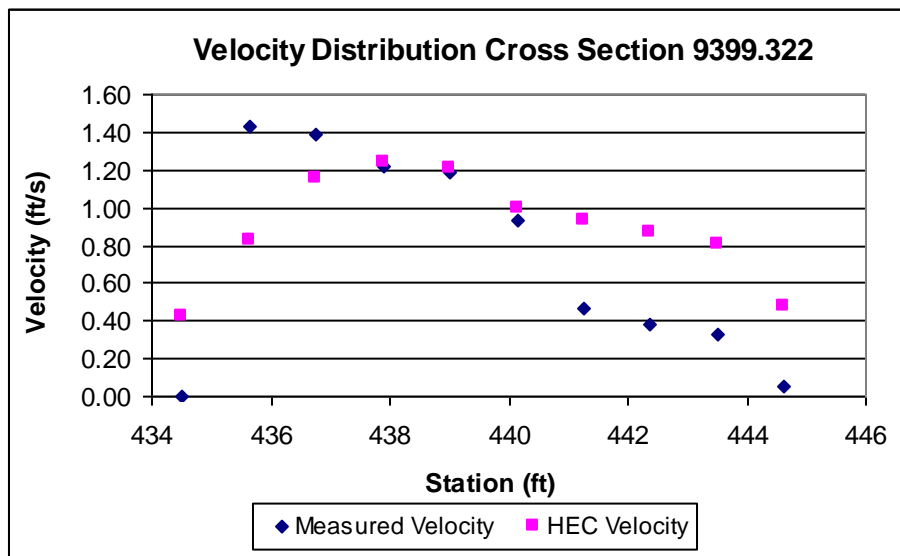


Figure 3.1. Velocity distributions at one foot increments across a defined cross section are similar near the thalweg (Station 438) but differ at the edges of the channel water surface.

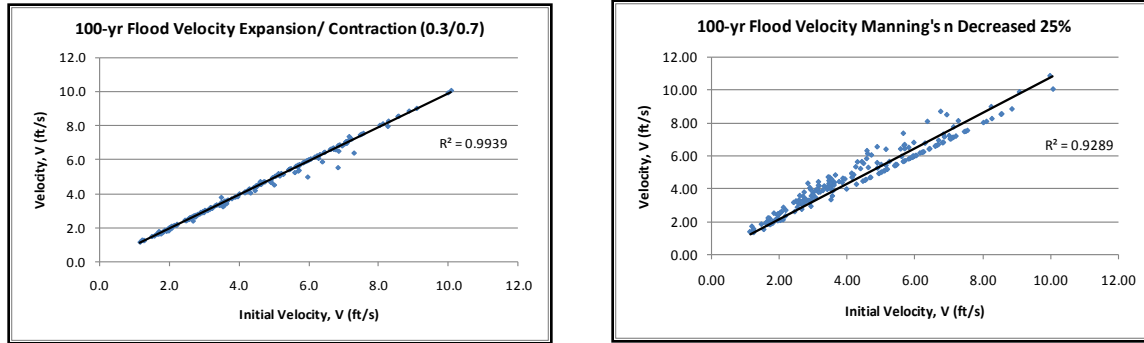


Figure 3.2. Changes in contraction and expansion coefficients from 0.1/0.3 to 0.3/0.7 had little effect on model velocity output. Decreasing the roughness coefficients by 25 percent caused an increase in velocity at cross sections that were near junctions and in constricted channel areas with steeper stream bed gradients.

Changes in velocity and shear stress were greater for global changes in Manning's n by 25% and -25% than those modified by 10% and -10%, shown in Tables 3.3 and 3.4. Evaluation of the results revealed a decrease in velocity and shear stress with increasing roughness and an increase in velocity and shear stress with decreasing roughness. We utilized root mean square error (RMSE) to assess how closely the velocity and shear stress values for models with altered parameters are to the original model output. Both velocity and shear stress estimates for the flood events indicate that smaller events (2-year through 50-year) were affected less by changes in roughness parameters than the larger events (100-year through 500-year). As the magnitude of the flood events increased, the error estimate increased. Roughness depends not only on vegetation, sediment size, and channel characteristics but on flow depth. The larger flow depth associated with larger flood events may require a change in roughness coefficient. Significant changes in velocity and shear stress were observed for cross section points that varied from the linear 1:1 line and were located at cross sections near junction locations, near flow change locations, and along reaches with significant bed slope changes. Cross sections upstream of culverts also displayed more error.

From the sensitivity analysis, one dimensional modeling is dependent on the selection of Manning's n coefficients which account for energy losses associated with vegetation and sediment roughness. Therefore, erroneous estimates of these parameters negatively affect model output. The detailed roughness coefficient evaluation incorporated in our approach affords confidence in the model output.

Table 3.3. The velocity root mean squared errors (ft/s) increase with higher magnitude flood events with changes in roughness and contraction and expansion coefficients.

Flood Event (year)	Increase Manning's n 10%	Decrease Manning's n 10%	Increase Manning's n 25%	Decrease Manning's n 25%	Contraction/ Expansion (0/0.5)	Contraction/ Expansion (0/0)	Contraction/ Expansion (0.3/0.7)
	RMSE (ft/s)	RMSE (ft/s)	RMSE (ft/s)	RMSE (ft/s)	RMSE (ft/s)	RMSE (ft/s)	RMSE (ft/s)
2	0.1226	0.1812	0.2676	0.3589	0.0361	0.0259	0.0909
10	0.2338	0.2695	0.4218	0.6242	0.1411	0.1555	0.1524
25	0.2173	0.2655	0.4874	0.6419	0.0800	0.0995	0.1213
50	0.2417	0.8297	0.5053	0.6688	0.0590	0.0888	0.1047
100	0.2734	0.2887	0.5914	0.6444	0.0755	0.1103	0.1674
200	0.5948	0.3145	0.5929	0.6942	0.0902	0.0947	0.1991
500	0.6478	0.2997	0.6428	0.7144	0.0870	0.1148	0.6478

Table 3.4. The shear stress root mean squared errors (lb/ft²) increase with higher magnitude flood events with changes in roughness and contraction and expansion coefficients.

Flood Event (year)	Increase Manning's n 10%	Decrease Manning's n 10%	Increase Manning's n 25%	Decrease Manning's n 25%	Contraction/ Expansion (0/0.5)	Contraction/ Expansion (0/0)	Contraction/ Expansion (0.3/0.7)
	RMSE (lb/ft ²)	RMSE (lb/ft ²)	RMSE (lb/ft ²)				
2	0.1578	0.1824	0.4064	0.3371	0.0165	0.0199	0.0753
10	0.3623	0.2742	0.6102	0.5259	0.2240	0.2388	0.2279
25	0.2564	0.2555	0.6390	0.5916	0.0725	0.1003	0.0937
50	0.3554	0.8774	0.8733	0.7622	0.0483	0.0825	0.0822
100	0.2960	0.2952	0.7019	0.7216	0.0812	0.1042	0.1721
200	1.0109	0.2683	0.6574	0.6213	0.0820	0.0905	0.1718
500	1.1335	0.2927	0.7127	0.6772	0.0688	0.0969	1.1335

The disconnected inundation surfaces in some areas of the study site result from cross section locations at junctions and areas of abrupt bed slope gradient change. Many of the reach junctions occurred in wide flat regions and restricted the number of cross sections that could be incorporated into the model. Balancing the momentum equation across large gaps with minimal cross sections is not recommended. The limited number of cross sections produced a disconnected inundation surface. A possible solution to the disconnected surface would be to model the Blackfoot network as a single reach with flow change locations where tributaries connect. The model also had difficulty creating an inundation surface at road intersections. Water surface elevations in the inundation map were based on interpolations between cross section water surface elevations. Changes in topography between cross sections were not accounted for in a one-dimensional model, which also could have produced error in the inundation surface. Smaller cell sizes in the inundation surface resulted in greater connectivity, but cell size selection was based on the accuracy of the survey data. These errors are acceptable because the inundation surface captured the critical areas of concern for the flood risk analysis.

Channel geometry was likely a source of error in the model output. The combination of several survey data sets to create a topographic TIN resulted in a highly variable elevation surface. Cross sections cut at locations with detailed survey data were located at elevations lower than those cut at interpolated locations without detailed survey data. The geometry of cross sections at interpolated locations was modified to fit the same slope as the surveyed cross sections while maintaining channel geometry across the cross section. However, this adjustment resulted in water surface elevations that did not match the TIN used to estimate the inundation surface and created gaps in the inundation surface. Future approaches should include a single detailed survey to avoid abrupt changes in geometry within the interpolated surface.

Initiation of motion using the Shields relation requires a dimensionless shear variable, which is dependent on the size and gradation of sediment, channel characteristics, and discharge. Even though the dimensionless shear varies, this parameter is often assumed to be constant for a range of sediment particle sizes (Simons and Sentürk 1992). Limitations exist with initiation of motion and sediment transport relations. Most transport relations, developed in sand-bed flumes and channels, rely on tests completed in flumes under steady and uniform conditions. The sediment transport relations also attribute measured variable deviations as errors in measurement and decrease the reliability of the estimates (Simons and Sentürk 1992).

Sediment sampled with a gravelometer provided data for sediment distributions across cross sections and provided parameters for roughness coefficient estimates and critical velocity calculations. Sediment distributions estimated with sieved samples introduces bias for smaller sediment sizes but provided data for fine sediment distributions which are generally mobilized first during a flood event. An in-depth investigation of sediment critical shear stress might involve flume tests with sediment samples but does not capture dynamic flow characteristics likely present in the system.

3.2 MODEL COUPLING AND MAPPING

The analysis method presented here incorporates resuspension risk assessment variables with collected data and modeling techniques accepted within the practice. The topographic TIN generated from land surveys and an orthorectified aerial photo captured detailed topography for cross sections used in the hydraulic model. The velocity distribution TIN, generated from cross sections and associated velocity values, interpolated planar surfaces appropriate for the one-

dimensional hydraulic model output. Since velocity values at cross sections vary significantly due to changes in channel slope, cross section geometry, and roughness factors, the planar surfaces of velocity values between the cross sections maintained velocity values along the cross sections.

Spatial interpolation of sample points is a common decision making tool for soil remediation and erosion and deposition studies. Soil properties and contaminant distributions are difficult to model and track even with a large number of sample points in such a heterogeneous system. The spatial interpolation tools in the GIS produce distribution surfaces that can be used for making cost-efficient decisions for remediation strategies, but the results of spatial analysis differ with interpolation techniques.

Spatial interpolation introduces uncertainty to modeling. Attempts to minimize uncertainty included selecting interpolation methods appropriate for the data type. Kriging of contamination sample points attempted to reduce interpolation bias by assigning weights to observational points dependent on distances between the points and estimation locations as well as mutual distances among observational points. Semivariograms helped to assess the spatial dependency of observational data points in which a functional relationship between the spatial pattern of the sampled points and their observed values was defined. Semivariograms for arsenic, cadmium, copper, zinc, and lead concentrations were fit with a spherical model (see Figure 3.3), and parameters from the model were used to interpolate a kriged contamination surface. The error variance for each kriged surface indicates higher variance further from known points. In particular, the error variance was high at the edges of the surface where fewer points were used to interpolate values across the grid. However, most of these areas were beyond the bounding inundation surface and likely had little effect on our results.

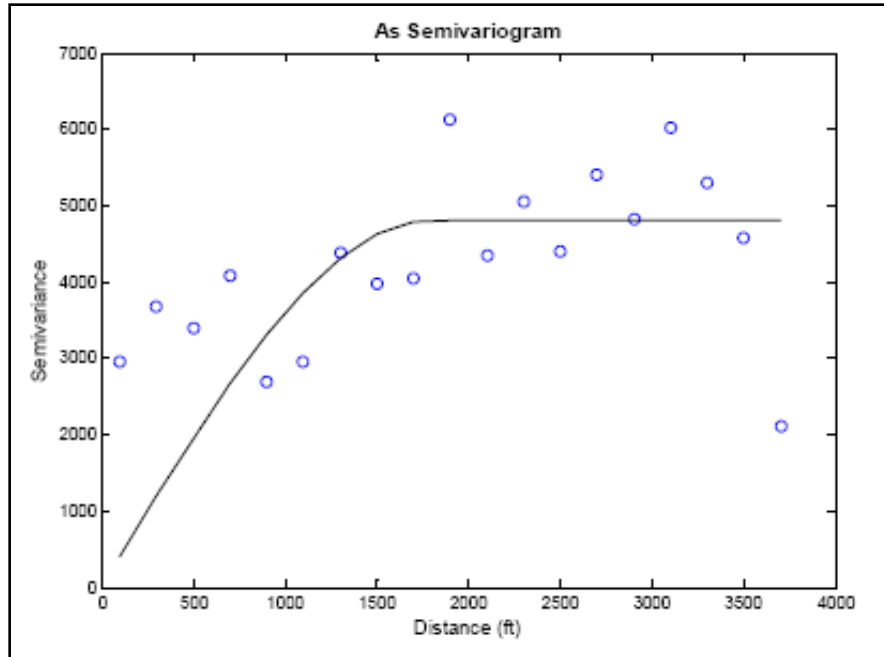


Figure 3.3. The semivariogram for sampled sediment containing arsenic, fit with a spherical model, demonstrates the decreasing similarity of data points (blue dots) with increasing distance from known points.

For the 10, 25, and 100 year flood events, the combination of distribution maps for velocity, critical velocity, sediment size, flood extents, and metal contamination (As, Cu, Cd, Pb, and Zn) help identify areas of potential concern in the wetland. An analysis of the metals of potential concern identified areas where specific metals exceeded preliminary remediation goals for residential screening levels and ecological screening levels. Table 3.5 lists the DEQ and Environmental Protection Agency (EPA) remediation goals for the site.

The velocity surface was compared to the critical velocity surface, and areas where the velocity exceeded the critical velocity were identified. Percentages of velocity exceeding critical velocity were high within the wetland study area and were indicated with a three-dimension elevation map. Spikes in Figure 3.4 indicate areas where velocities exceed critical velocities. Figure 3.4 demonstrates the hazardous areas for the 100 year flood event along with arsenic concentration distributions. For the 10, 25, and 100 year events, estimated velocities exceed critical velocity by 97 percent, 99 percent, and 76 percent, respectively, in the study area (see Table 3.6). Results from the potential hazard analysis indicate increasing hazard regions with larger flood events. Metal concentrations are higher at the entrance of the wetland where tributaries intersect and where the flood wave from the 1975 breach event lost energy and deposited sediment.

Table 3.5. The summary of EPA Region 9 Preliminary Remediation Goals for comparison with soil, mine waste, and tailings sample data assisted with identifying areas where metal concentration levels exceeded screening levels in the upper marsh study area.

a DEQ Action Level for Arsenic in Surface Soil (DEQ Remediation Division, 2005).

b EPA Region 9 Preliminary Remediation Goals (PRGs) for residential soil (October 2004).

c Percentile screening levels for biological effects.

Metal	Aluminum (mg/kg)	Arsenic (mg/kg)	Cadmium (mg/kg)	Copper (mg/kg)	Lead (mg/kg)	Mercury (mg/kg)	Manganese (mg/kg)	Zinc (mg/kg)
Residential PRG	77,000	40 ^a	37 ^b	3,100 ^b	400 ^b	230 ^b	1,800 ^b	23,000 ^b
TEL ^c	--	5.9	0.596	35.7	35	0.174	--	123
PAET ^c	--	19	97.5	340	240	0.16	1,400	500
SEL ^c	--	33	10	110	250	2	1,100	820

Table 3.6. A comparison of the upper marsh area indicates areas where velocities for the 10, 25, and 100 year flood events exceed critical velocities.

Flood Event (year)	Total Area Inundated by 100yr flood in the Upper Marsh	Area Velocity Exceeds Critical Velocity	Percent of Total Marsh Area where $V > V_c$
	(acres)	(acres)	(%)
100	57	43	76
25	38	38	99
10	28	27	98

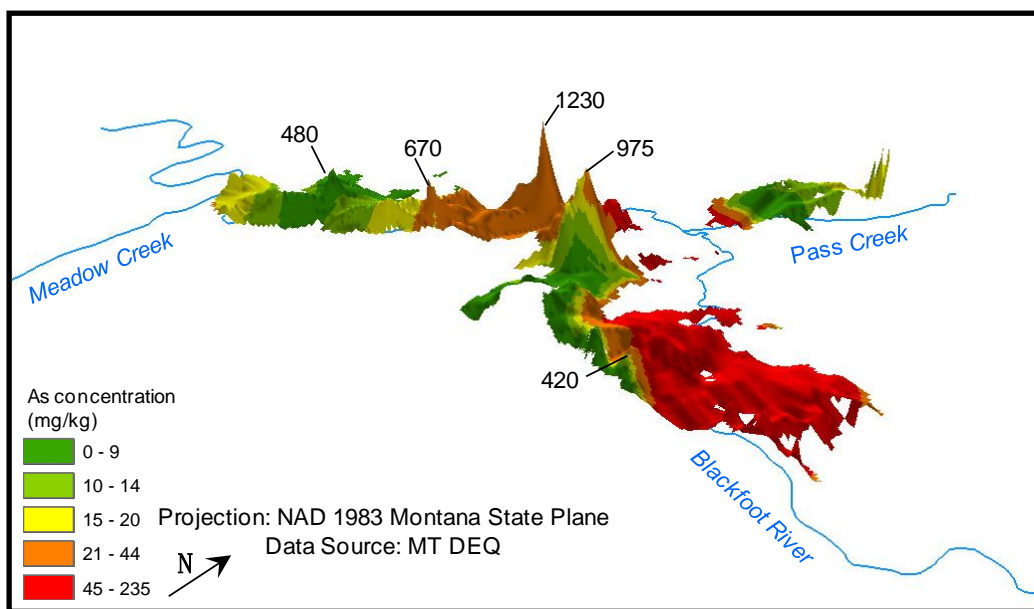


Figure 3.4. For a 100-year flood event, areas of potential concern include those where spikes occur in the surface identifying the magnitude of velocities exceeding critical velocities and those where contaminant sediment levels are significant.

4.0 CONCLUSION

Water resource problems, in particular, flood inundation mapping, rely on robust hydrologic and hydraulic models such as HEC-RAS. Intricate analysis and simulation

capabilities are available with both hydrologic/hydraulic models and GIS, and the integration of the two provides a powerful tool for scientific researchers and policy makers. The widespread availability of spatially distributed data through GIS has made physically based hydrologic models more useable and spurred the development of hydrologic models that take advantage of these new data. This approach for evaluating the potential hazards of metals-trapping wetlands will aid the MT DEQ and the US Forest Service in prioritizing and implementing remediation action items for the UBMC and similar mine reclamation sites. In this study, the coupling of GIS and a hydraulic model through HEC-geoRAS produced an inundation surface only after numerous modeling iterations. The disconnected stream flow results resulted from cell size selection and were influenced by the wide shallow topography of the site. The inundation surface bounded resuspension parameters, critical velocity, sediment size, and metal contamination to model areas of possible resuspension risk. Providing agencies, consultants, and watershed groups with a viable, low cost, computationally efficient method with minimal data requirements for quantifying the risk associated with transport of contaminated sediments out of wetlands will aid these entities in prioritization of restoration efforts and help reduce mining impacts to downstream communities and environments.

Despite the complex nature of the wetland system, the one-dimensional hydraulic model proved to be a sufficient tool to estimate the water surface elevations and flow parameters. Sensitivity analysis showed the one-dimensional hydraulic model to be increasingly sensitive to roughness coefficients at larger discharges. This highlights the need for careful characterization and mapping of roughness values if large flood events are being modeled. Comparison of modeled stream velocity distributions to measured velocity distributions showed deviations from observed data in shallow near-bank and over-bank areas. Further investigation is needed in this area to quantify the effect of these deviations on model output for a variety of discharge events. Thorough investigation of differences between modeled and measured velocity distributions at a range of flows and across several transects at a given site will help practitioners decide whether or not this approach will be useful and may improve confidence in modeled output. We conclude that, if carefully applied, this approach may be a valuable tool for coarse assessments of contaminated sediment mobilization risk in areas where data is limited and/or development of more data/computationally intensive sediment transport, 2D or 3D models is not feasible.

REFERENCES

- Akan, A. O. (2006). *Open Channel Hydraulics*, Elsevier, Burlington, MA.
- Aldridge, B. N., Garrett, J. M., and Highway, D. (1973). *Roughness Coefficients for Stream Channels in Arizona*, US Dept. of the Interior, US Geological Survey.
- Andrews, E. D. (1983). "Entrainment of gravel from naturally sorted riverbed material." *Bulletin of the Geological Society of America*, 94(10), 1225-1231.
- Auble, G. T., Scott, M. L., and Friedman, J. M. (2005). "Use of individualistic streamflow-vegetation relations along the Fremont River, Utah, USA to assess impacts of flow alteration on wetland and riparian areas." *Wetlands*, 25(1), 143-154.
- August, E. E., McKnight, D. M., Hrcir, D. C., and Garhart, K. S. (2002). "Seasonal variability of metals transport through a wetland impacted by mine drainage in the Rocky Mountains." *Environmental Science & Technology*, 36(17), 3779-3786.
- Bendoricchio, G., Luigi Dal Cin, and Jesper Persson. (2000). "Guidelines for free water surface wetland design." *ECOSYSTEMS*, 8, 51-91.
- Benson, M. A., and Dalrymple, T. (1967). "GENERAL FIELD AND OFFICE PROCEDURES FOR INDIRECT DISCHARGE MEASUREMENTS."
- Bergeron, N. E., and Abrahams, A. D. "Estimating shear velocity and roughness length from velocity profiles." *WATER RESOUR RES*, 28(8).
- Brunner, G. W. (2002). "HEC-RAS, River Analysis System Hydraulic Reference Manual, Version 3.1." In: *US Army Corps of Engineers, Hydrologic Engineering Center, CPD-69*, 1-377.
- Chow, V. T. (1959). "Open-channel hydraulics." In: *New York/Tokyo*, McGraw-Hill, 680.
- Cook, S. A. (2007). "Characterization of riparian wetland soils and associated metal concentrations at the headwaters of the Stillwater River, Montana," Montana State University, Bozeman, MT.
- Dollhopf, D. J., Goering, J. D., Rennick, R. B., Morton, R. B., Gauger, W. K., Guckert, J. B., Jones, P. B., Cooksey, K. C., Bucklin, K. E., Weed, R., and Lehman, M. M. (1988). "Hydrochemical, vegetational and microbiological effects of a natural and constructed wetland on the control of acid mine drainage." *RRU 8804*, Montana Abandoned Mine Reclamation Bureau, Helena, MT.
- Fischenich, C., Engineer, R., and Development Center Vicksburg Ms Environmental, L. A. B. (2001). "Stability Thresholds for Stream Restoration Materials." ENGINEER RESEARCH AND DEVELOPMENT CENTER VICKSBURG MS ENVIRONMENTAL LAB.
- Furniss, G., Hinman, N. W., Doyle, G. A., and Runnells, D. D. (1999). "Radiocarbon-dated ferricrete provides a record of natural acid rock drainage and paleoclimatic changes." *Environmental Geology*, 37(1), 102-106.
- Gibbs, R. J. (1973). "Mechanisms of Trace Metal Transport in Rivers." *Science*, 180(4081), 71-73.
- Gurrieri, J. T. (1998). "Distribution of metals in water and sediment and effects on aquatic biota in the upper Stillwater River basin, Montana." *Journal of Geochemical Exploration*, 64(1-3), 83-100.

- Haag, I., Kern, U., and Westrich, B. (2001). "Erosion investigation and sediment quality measurements for a comprehensive risk assessment of contaminated aquatic sediments." *Science of the Total Environment*, 266(1-3), 249-257.
- Hu, J. (Year). "Methods of Generating Surfaces In Environmental GIS Applications." 22-26.11.
- Johnson, G. D., Strickland, M. D., Buyok, J. P., Derby, C. E., and Young, D. P. (1999). "Quantifying impacts to riparian wetlands associated with reduced flows along the Greybull River, Wyoming." *Wetlands*, 19(1), 71-77.
- Julien, P. Y. (1995a). *Erosion and Sedimentation*, Cambridge University Press.
- Julien, P. Y. (1995b). *Erosion and Sedimentation*, Cambridge University Press.
- Kadlec, R. H. (1990). "Overland Flow in Wetlands: Vegetation Resistance." *Journal of Hydraulic Engineering*, 116(5), 691-706.
- Kadlec, R. H., and Knight, R. L. (1996). *Treatment Wetlands*, CRC Press, Boca Raton, Fla.
- Kitanidis, P. K. (1997). *Introduction to Geostatistics: Applications to Hydrogeology*, Cambridge University Press, Cambridge.
- Marcus, W. A., Roberts, K., Harvey, L., and Tackman, G. (1992). "An evaluation of methods for estimating Manning's n in small mountain streams." *Mountain Research and Development*, 12(3), 227-239.
- Marx, D. a. K. T. (1987). *Practical Aspects of Agricultural Kriging*, Arkansas Agricultural Experiment Station, Fayetteville.
- McCoy, J., and Johnston, K. (2001). *Using ArcGIS spatial analyst*, Environmental Systems Research Institute, Redlands.
- Merwade, V., Cook, A., and Coonrod, J. (2008). "GIS techniques for creating river terrain models for hydrodynamic modeling and flood inundation mapping." *Environmental Modelling and Software*, 23(10-11), 1300-1311.
- Moore, J. N. (1992). "Mine effluent effects on non-point source contaminants in the Blackfoot River, Montana." Prepared for Lewis and Clark City-County Health Department. University of Montana, Geology Department, Missoula, MT.
- Ogden, F. L., Garbrecht, J., DeBarry, P. A., and Johnson, L. E. (2001). "GIS and Distributed Watershed Models. II: Modules, Interfaces, and Models." *Journal of Hydrologic Engineering*, 6(6), 515-523.
- Pappenberger, F., Beven, K., Horritt, M., and Blazkova, S. (2005). "Uncertainty in the calibration of effective roughness parameters in HEC-RAS using inundation and downstream level observations." *Journal of Hydrology*, 302(1-4), 46-69.
- Parrett, C., Johnson, D. R. C. A. G. S., United States, and Bureau of Indian Affairs. (2004). *Methods for estimating flood frequency in Montana based on data through water year 1998*, U.S. Dept. of the Interior U.S. Geological Survey ; Denver CO : U.S. Geological Survey Information Services distributor, Reston, Va.
- Schneider, V. R., and Arcement, G. J. (1989). "Guide for Selecting Manning's Roughness Coefficients for Natural Channels and Flood Plains." Available from the US Geological Survey, Books and Open-File Reports Section, Box 25425, Federal Center, Denver, CO 80225-0425. *Water-Supply Paper 2339*, 1989. 38 p, 22 fig, 4 tab, 23 ref.
- Simons, D. B., and Sentürk, F. (1992). *Sediment transport technology: water and sediment dynamics*, Water Resources Publication.
- Spence, L. E. (1975). "Upper Blackfoot River Study, A Preliminary Inventory of Aquatic and Wildlife Resources." Montana Department of Fish and Game, Missoula, Montana.

- Sui, D. Z., and Maggio, R. C. (1999). "Integrating GIS with hydrological modeling: practices, problems, and prospects." *Computers, Environment and Urban Systems*, 23(1), 33-51.
- Tate, E. C., Maidment, D. R., Olivera, F., and Pe, D. J. A. (2002). "Creating a Terrain Model for Floodplain Mapping." *Journal of Hydrologic Engineering*, 7, 100.
- TetraTech. (2007). "Final sampling and analysis plan. 2007 fall sampling event. Remedial investigation. Upper Blackfoot Mining Complex." Montana Department of Environmental Quality, Helena, MT.
- Thompson, J. R., Soerenson, H. R., Gavin, H., and Refsgaard, A. (2004a). "Application of the coupled MIKE SHE/MIKE 11 modelling system to a lowland wet grassland in southeast England." *Journal of Hydrology*, 293(1), 151-179.
- Thompson, J. R., Sørensen, H. R., Gavin, H., and Refsgaard, A. (2004b). "Application of the coupled MIKE SHE/MIKE 11 modelling system to a lowland wet grassland in southeast England." *Journal of Hydrology*, 293(1-4), 151-179.
- Werner, M. G. F. (2001). "Impact of grid size in GIS based flood extent mapping using a 1D flow model." *Physics and Chemistry of the Earth, Part B*, 26(7-8), 517-522.

Evolution of channel morphology and aquatic habitat in the Middle Clark Fork River following removal of Milltown Dam

Basic Information

Title:	Evolution of channel morphology and aquatic habitat in the Middle Clark Fork River following removal of Milltown Dam
Project Number:	2008MT168B
Start Date:	3/1/2008
End Date:	2/28/2010
Funding Source:	104B
Congressional District:	At-Large
Research Category:	Water Quality
Focus Category:	Geomorphological Processes, Sediments, Water Quality
Descriptors:	
Principal Investigators:	Andrew Wilcox, Andrew Wilcox

Publication

1. Wilcox, A. C., D. Brinkerhoff, C. Woelfle-Erskine. 2008. Initial geomorphic responses to removal of Milltown Dam, Clark Fork River, Montana, USA. EOS Trans. AGU. 89(53) Fall Meet. Suppl. Abstract H41I-07.

Montana Water Center / USGS Interim report

Evolution of channel morphology and aquatic habitat in the Middle Clark Fork River following removal of Milltown Dam

Principal Investigator: Andrew Wilcox
Assistant Professor
University of Montana
andrew.wilcox@umontana.edu
406-243-4761

We have been investigating geomorphic processes associated with dam removal in the context of the 2008 removal of Milltown Dam on the Clark Fork River, MT. Funding from the USGS / Montana Water Center seed grant program has provided an opportunity to conduct time-sensitive field data collection and analysis, including geomorphic characterization and geochemical tracer studies, in the months immediately before and after the breach of Milltown Dam. Our Milltown studies have included:

(1) Documentation of the volume, pattern, and timing of reservoir erosion during the 2008 runoff. This effort combined pre- and post-breach topographic data from Milltown reservoir and water surface profile measurements throughout the hydrograph that are being used to reconstruct the spatial and temporal details of sediment evacuation. This effort also entailed comparison of erosion dynamics in an unconfined reservoir reach (the Clark Fork arm of Milltown reservoir) versus a confined reservoir reach (the Blackfoot arm of the reservoir). This analysis documented not only substantial variations in reservoir erosion patterns and mechanisms (vertical incision versus channel widening) as a function of valley confinement, but also large variations in the accuracy of sediment transport modeling predictions in these two reservoir settings.

(2) Collection of bedload transport data during the spring 2008 runoff period, when the initial downstream sediment pulse moved out of Milltown reservoir.

(3) Development of a preliminary sediment budget for Milltown Reservoir following the dam breach, combining reservoir erosion estimates (from (1) above), our bedload data, and USGS suspended flux measurements.

(4) Comparison of measured reservoir erosion and sediment fluxes to predictions based on HEC-6 modeling by project consultants. This analysis indicated that modeling was reasonably accurate in the confined BFR arm of Milltown reservoir but had substantial error in the CFR arm.

(5) Analysis of initial post-removal topographic and textural response upstream and downstream of Milltown Dam. This effort focused on 2 reaches: the lower 4 km of the Blackfoot River (BFR) before its confluence with the CFR, and the CFR within 4 km downstream of Milltown Dam, and entailed pre- and post-breach surveying of 36 cross sections, bed material sampling, and detailed topographic surveys of lateral and mid-channel bars that we hypothesized would be locations of active sediment deposition.

(6) Surveying of longitudinal profiles in the lower BFR and in the CFR from Milltown Dam to 20-km downstream, using a high-resolution, cataraft-based echosounder and GPS system. These data, combined with qualitative observations collected in the course of these boat-

based surveys about locations of sediment deposition and geomorphic change, are being used to identify potential transport versus deposition reaches for the next phase of our study.

(7) Sampling and analysis of the size distribution and metals geochemistry of downstream sediment deposits in order to fingerprint sediment deposits and provide insight into potential ecosystem effects of contaminated sediment deposition. This effort has included sample collection extending over 200 km downstream to Thompson Falls, the next downstream reservoir, at multiple times over the 2008 hydrograph, and measurement of As, Cd, Cu, Zn, Pb, and Hg concentrations.

(8) Collection and initial analysis of imagery. In summer 2008, high-resolution aerial photographs were flown from Milltown reservoir to the CFR's confluence with the Bitterroot River (paid for by Wilcox startup), and airborne-LIDAR was flown in Milltown reservoir by contractors to the State of Montana. The LIDAR data have been used as one component of our analysis of reservoir scour.

(9) Mobilization for data collection, including acquisition of necessary field equipment for boat-based surveying on a river the size of the CFR (PI's startup funds), testing and refining field methods, establishment of field sites, and reconnaissance of additional field sites. Because of this work we are well positioned for the next phase of field data collection.

Our research has already had impacts in terms of outreach, education, and societal importance. Three articles featuring this research appeared in the *Missoulian*. The first of these appeared on the day of the Milltown Dam breach and detailed our efforts to use the dam removal to learn about river processes. The second reported on our findings that erosion and downstream transport of contaminated reservoir sediment had vastly exceeded model predictions and resulted in widespread downstream deposition. These results heightened public understanding of and concern about the *downstream* effects of this dam removal, which had previously received minimal attention as a result of the focus on the remediation and restoration work upstream of the dam, in Milltown reservoir. A third article was written by the PI in an effort to clarify our results. The PI also has spent considerable time discussing our research and results with local environmental groups (e.g., Clark Fork Coalition, Trout Unlimited, American Whitewater), citizens, and other media outlets.

Preliminary science outcomes also include a presentation on this research at the Fall 2008 AGU meeting (Wilcox et al. 2008). Two M.S. theses (James Johnsen, Tim Gilbert) partially supported by the USGS funds will be completed in 2010. The USGS funds have also served as seed money for a full research proposal submitted earlier this year to the National Science Foundation, "Sediment routing in gravel-bed rivers following dam removal," which is pending.

Wilcox, A. C., D. Brinkerhoff, C. Woelfle-Erskine. 2008. "Initial geomorphic responses to removal of Milltown Dam, Clark Fork River, Montana, USA." *EOS Trans. AGU*. 89(53) Fall Meet. Suppl. Abstract H41I-07.

Student Fellowship: How susceptible to chlorine disinfection are detached biofilm particles?

Student Fellowship: How susceptible to chlorine disinfection are detached biofilm particles?

Basic Information

Title:	Student Fellowship: How susceptible to chlorine disinfection are detached biofilm particles?
Project Number:	2008MT172B
Start Date:	3/1/2008
End Date:	12/31/2008
Funding Source:	104B
Congressional District:	At-large
Research Category:	Biological Sciences
Focus Category:	Treatment, Toxic Substances, Water Quality
Descriptors:	
Principal Investigators:	Sabrina Benhke

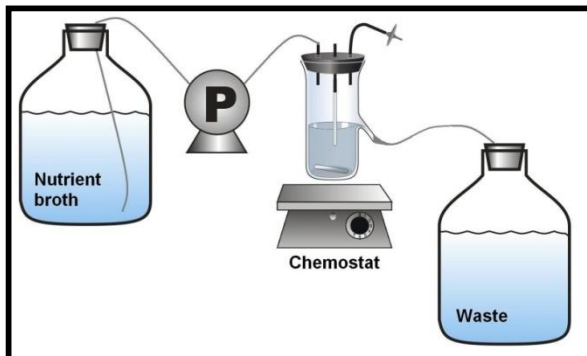
Publication

An update:

How susceptible to chlorine disinfection are detached biofilm particles?

Background:

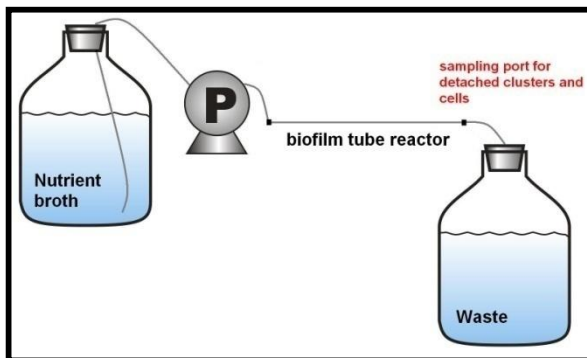
Previously, disinfection experiments have been done with *Salmonella typhimurium* cultures (update May 2008). In June we started performing experiments with *Burkholderia cepacia* under identical conditions.



B. cepacia FS-3 is able to grow in the defined medium consisting of phosphate buffer, 0.1 g/L glucose, 0.018g/L NH_4Cl , and MgSO_4 . Initial experiments have found that the maximum growth rate in this medium is $0.148 \pm 0.024 \text{ h}^{-1}$ which results in a doubling time of about 6 hours.

Samples are taken by removing the lid from the chemostat and using a sterile pipette. The diluted chemostat culture contained single cells as well as clusters up to 100 cells. Clusters

bigger than 100 cells were rare. Most cells are in small clusters of 2 to 5 cells.



B. cepacia FS-3 has been found to establish a biofilm in the silicone tubing of the biofilm tube reactor. The reactor is inoculated with a sterile syringe filled with 10 ml fresh overnight culture followed by a 3 hour attachment period without flow. After this period, the flow is set to 0.9 ml/min resulting in a residence time of about 4 minutes.

Samples of detached cells are removed by collecting effluent in a sterile tube, while samples of biofilm are removed by cutting the

silicone tubing into small (4 cm long) pieces.

Cluster and cells distribution in effluent samples is very similar to what we observed in the chemostat samples. The mechanically detached and homogenized biofilm was also subject to image analysis. Again, a similar pattern to chemostat culture and tube reactor effluent exists.

General Information about experiments:

- 30 min. exposure to Chlorine
- Chlorine added to samples according to a standard curve made with increasing amounts of fresh Chlorine stock in medium without N and C source
- Neutralization of Sodium hypochlorite with Sodium thiosulfate
- Detection limit was 5 CFU/ml or lower for all experiments
- Disaggregation: shear Homogenization at 20,000 rpm for 1 min.

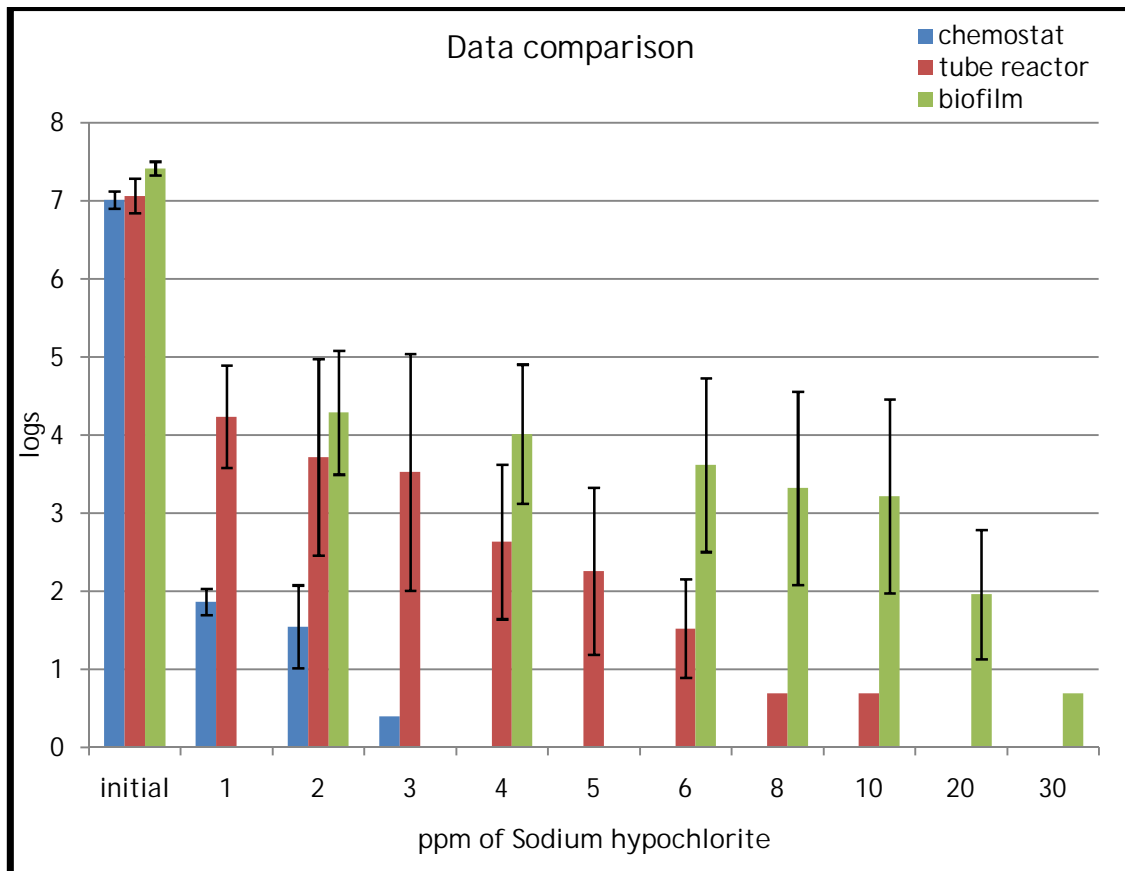
Discussion

Cells and clusters of the chemostat culture are very susceptible to low amounts of Chlorine. In the chemostat, growth is occurring exponentially which is known to make cells more susceptible to disinfection than cells in the stationary phase.

The cluster size distribution of detached biofilm particles and chemostat particles are almost identical and initial cells numbers are very similar. Despite this, detached biofilm clusters are less susceptible to Chlorine. This may be due to an increased amount of extracellular polymeric substances surrounding clusters and cells. This hypothesis is supported by the fact that tube reactor effluent samples consume more free chlorine during the experiment than chemostat samples (for example: 0.86 ppm more Chlorine consumed for tube reactor effluent (on average) upon addition of 2 ppm). This indicates that more (organic) substances in the sample react with the available Chlorine making less of it available for disinfection.

As anticipated, the biofilm is less susceptible to disinfection. The attachment to a surface (silicone tubing) may be protective to the biofilm since Chlorine can attack the biofilm from only one side.

Intuitively, biofilm samples are a more resistant to disinfection than detached biofilm clusters. Initial cell numbers are slightly higher than initial cell numbers for the chemostat culture or the tube reactor effluent.



Student Fellowship: The Consequences of Introgressive Hybridization: Implications for Westslope Cutthroat Trout Conservation

Basic Information

Title:	Student Fellowship: The Consequences of Introgressive Hybridization: Implications for Westslope Cutthroat Trout Conservation
Project Number:	2008MT180B
Start Date:	3/1/2008
End Date:	12/31/2008
Funding Source:	104B
Congressional District:	At-large
Research Category:	Biological Sciences
Focus Category:	Ecology, None, None
Descriptors:	
Principal Investigators:	Matt Corsi

Publication

Montana Water Center/USGS Student Fellowship

**The Consequences of Introgressive Hybridization: Implications for Westslope
Cutthroat Trout Conservation**

by

Matt Corsi
Department of Biological Sciences
University of Montana

Since my last report in June, 2008, I have completed, continued, or begun several projects. Overall, my dissertation project involves examining the distribution of rainbow and cutthroat trout hybrid individuals in the Jocko River basin, examining whether individuals with different hybrid ancestry are different in terms of migration timing, fecundity and growth, as well as developing a population project model to examine the population implications of different management scenarios.

In collaboration with Confederated Salish and Kootenai Tribes, I collected fish returning to spawn and completed collection of fish in tributaries for basin-wide population structure and hybrid assessment. In late summer and early fall, I obtained genotypes for approximately 500 individual trout in the Jocko River System. In addition, I measured fecundity and removed otoliths for age and growth estimates. In the coming spring, I will use these genotypes, along with genotypes collected in previous years, to address migration timing differences between cutthroat trout, rainbow trout, and their hybrids, as well as to test for differences in fecundity among the same groups. Finally these genotypes will allow me to complete a fine-scale basin-wide analysis of the population genetic structure of trout in the Jocko River watershed. Using this population baseline, I hope to be able to determine with reasonable certainty what breeding population was the likely source for migratory fish collected during my study. For those fish that can be reliably assigned to a population, I will examine the relative effects of natal growth environment and individual level of hybridization on growth rates.

I have begun to develop the population projection model that I will use to evaluate alternative management strategies for selective passage of migratory cutthroat trout at an irrigation diversion structure. While this model will eventually include a genetic component to evaluate the hybridization consequences of allowing migratory rainbow-cutthroat trout to pass the diversion structure, I have completed the demographic component of the model. The model suggests, from a purely demographic (not hybridization) standpoint, that passing even a few

migratory individuals above the diversion structure could substantially improve the long-term population viability of populations upstream of the diversion structure. I presented the results of this analysis as part of a poster about management of hybrid populations at the American Fisheries Society 2008 Annual Meeting in Ottawa, Ontario.

The intensive sampling design for fish collection has allowed me to examine both basin-wide and fine scale spatial structure of the cutthroat and rainbow trout population within the Jocko River basin. I am beginning an analysis that will address how various spatial sampling strategies may affect conclusions about hybridization in trout populations. This analysis will allow managers to better design studies to determine if trout populations are hybridized. These initial analyses also have spurred a project addressing how sampling approach for population structure studies have influenced inferences about cutthroat trout life history, genetic migration, and hybridization. Given that these patterns derive from one hybridized population in the Jocko River, MT, I am currently working to pull together other data sets of the spatial pattern of hybridization for westslope cutthroat trout, as well as becoming involved in a project examining the patterns of hybridization in Snake River cutthroat trout in the Gros Ventre River, WY. Initial results from samples that I obtained genotypes for this fall indicate a similar landscape pattern to hybridization as seen in the Jocko River, MT. My project is currently gaining a great deal of momentum, and I will continue to make substantial gains in the coming year. It is also worth noting that I completed my comprehensive exams this fall and passed to candidacy in the doctoral program at the University of Montana.

Student Fellowship: Predictive Modeling of Snowmelt and the Hydrologic Response:

Basic Information

Title:	Student Fellowship: Predictive Modeling of Snowmelt and the Hydrologic Response:
Project Number:	2008MT183B
Start Date:	3/1/2008
End Date:	11/31/2008
Funding Source:	104B
Congressional District:	At-large
Research Category:	Climate and Hydrologic Processes
Focus Category:	Hydrology, Models, Groundwater
Descriptors:	
Principal Investigators:	Tyler Smith

Publication

1. Smith, T. J. and L. A. Marshall (2008). Bayesian methods in hydrologic modeling: A study of recent advancements in Markov chain Monte Carlo techniques, *Water Resources Research*, 44, W00B05, doi:10.1029/2007WR006705.
2. Smith, T. J. 2008. A Conceptual Precipitation-Runoff Modeling Suite: Model Selection, Calibration and Predictive Uncertainty Assessment. M.S. thesis, Montana State Univ., Bozeman, MT.
3. Smith, T, L. Marshall. A Bayesian uncertainty framework for conceptual snowmelt and hydrologic models applied to the Tenderfoot Creek Experimental Forest. *Eos Trans. AGU*, 88(52), Fall Meeting Supplement. American Geophysical Union Fall Meeting. 10-14 December 2007. San Francisco, CA.

Montana Water Center/USGS Student Fellowship Final Report

Predictive Modeling of Snowmelt and the Hydrologic Response

by
Tyler Smith
Department of Civil Engineering
Montana State University

Because of uncertain mathematical descriptions of the physical hydrologic system, hydrologists are faced with uncertainty in the prediction of streamflow from a watershed. This uncertainty is exacerbated in snow-dominated watersheds where the additional complexity of snowpack simulation must be considered. The research performed in accordance with the USGS Fellowship project, *Predictive Modeling of Snowmelt and the Hydrologic Response: Tenderfoot Creek Experimental Forest, MT*, has been successfully completed in order to better understand the trade-off between model structural complexity and predictive performance. In order to quantify this relationship, the project was divided into four primary research objectives. First, a variety of Markov chain Monte Carlo techniques, necessary for model parameter estimation and uncertainty analysis quantification, were explored. Second, a modular modeling framework was established across a range of structural complexity. An integral component to this objective was to synthesize the existing observations from the Stringer Creek watershed, located within Tenderfoot Creek Experimental Forest. Third, the usefulness of alternative data sources for constraining model predictive uncertainty was investigated. Finally, a self-contained graphical user interface was developed to integrate the previous objectives into a freely available modeling software package.

The first objective has successfully resulted in the publication of a paper in a special issue on model uncertainty analysis in *Water Resources Research*¹, where a series of three recently developed Markov chain Monte Carlo algorithms necessary to implement model calibration (parameter estimation) and uncertainty analysis under a Bayesian inferential approach were implemented and compared in their efficiency and effectiveness. This objective builds on findings of past studies², revealing the benefits of newly developed

¹ Smith, T. J., and L. A. Marshall (2008), Bayesian methods in hydrologic modeling: A study of recent advancements in Markov chain Monte Carlo techniques, *Water Resources Research*, 44, W00B05, doi:10.1029/2007WR006705. ² Marshall, L., D. Nott, and A. Sharma (2004), A comparative study of Markov chain Monte Carlo methods for conceptual rainfall-runoff modeling, *Water Resources Research*, 40, W02501, doi:10.1029/2003WR002378.

methods in better characterizing the full distribution of model parameter values (including distribution tails) and in more efficiently searching the parameter space. A predictive modeling framework has been established to analyze the interaction and importance of model structural complexity and model predictive performance. In doing so, thirty unique modular structures, ranging in complexity from very simple to moderately complex, have been developed and included in the modeling suite associated with the modeling framework. The suite of models was constructed in a modular, component-wise fashion to address soil moisture accounting and runoff routing, snowmelt accounting, and semi-distribution of the precipitation inputs to the watershed. This framework then allowed for the comparison of performance by overall structure and based on individual components. Each of the models was assessed based on the criteria of performance, uncertainty, and realism. There was a definite balance between predictive performance and model complexity with similar performance across a range of structural complexities, indicating that process description is important to overall simulation of streamflow in conceptual hydrologic modeling. An alternate data source (snow water equivalents) was used to assess the realism of internal dynamics of each structure. Finally, a self-contained graphical user interface was designed to integrate the multiple layers of predictive hydrologic modeling. The Simulation and Prediction Lab for Analysis of Snowmelt Hydrology (SPLASH) has been successfully programmed to perform model selection, parameter calibration, uncertainty analysis, and model evaluation. This software package simplifies the complexities required to implement a predictive modeling study and shifts the focus toward the modeling problem itself through the application of forward-looking methods in computational hydrology.

Dissemination of Findings

The research supported by this fellowship has resulted in a published paper in the journal *Water Resources Research*, as well as several presentations including the winner of an outstanding student paper award for the Hydrology Section of the 2007 American Geophysical Union Fall Meeting. A complete list of the publications and presentations is listed below.

Smith, T. J. and L. A. Marshall (2008). Bayesian methods in hydrologic modeling: A study of recent advancements in Markov chain Monte Carlo techniques, *Water Resources Research*, 44, W00B05, doi:10.1029/2007WR006705.

Smith, T. J. and L. A. Marshall. 2008. Development and application of a parsimonious snow-hydrologic modeling suite: Investigating the link between model complexity and predictive uncertainty. American Geophysical Union Fall Meeting. 15-19 December 2008. San Francisco, CA.

Marshall, L. A. and T. J. Smith. 2008. A study of recently developed MCMC techniques for efficiently characterizing the uncertainty of hydrologic models. American Geophysical Union Fall Meeting. 15-19 December 2008. San Francisco, CA.

Smith, T. J. and L. A. Marshall. 2008. A flexible modeling framework for rainfall and snowmelt. American Water Resources Association Montana Section 25th Annual Meeting. 2-3 October 2008. Big Sky, MT.

Smith, T. J. and L. A. Marshall. 2008. Advancing Bayesian methods in hydrologic modeling: A study of recently developed Markov chain Monte Carlo techniques. American Statistical Association Montana Chapter Annual Meeting. 16 September 2008. Butte, MT.

Smith, T. J. and L. A. Marshall. 2008. A Bayesian uncertainty framework for conceptual snowmelt and hydrologic models applied to the Tenderfoot Creek Experimental Forest. Montana State University Student Research Celebration. 15 April 2008. Bozeman, MT.

Smith, T. J. and L. A. Marshall. 2007. A Bayesian uncertainty framework for conceptual snowmelt and hydrologic models applied to the Tenderfoot Creek Experimental Forest. American Geophysical Union Fall Meeting. 10-14 December 2007. San Francisco, CA.

Smith, T. J. and L. A. Marshall. 2007. Predictive modeling of snowmelt and the hydrologic response: Tenderfoot Creek Experimental Forest, MT. American Water Resources Association Montana Section 24th Annual Meeting. 11-12 October 2007. Lewistown, MT.

Information Transfer Program Introduction

Information Transfer Program

The Montana Water Center fills the unique role of coordinating Montana University System (MUS) water-related research, and disseminating and applying its findings for the benefit of the people of the state. And, as Montana is a headwaters state to two of the nation's major river drainage basins: the Missouri and the Columbia, how Montana manages its water and aquatic plants and animals can have far ranging impacts downstream. Obviously these are not closed systems. Montana's aquatic resources are also impacted by what comes into the state, be it acid rain, drought, aquatic nuisance species, or wind carried dust and debris that can increase snowpack melt. Of course, climate change is a growing concern and, as research is being done to determine the impact this will have on Montana, the Montana Water Center is part of a multi-disciplinary effort to prepare for what seems to be inevitable change. To prepare people need to be informed, and the Center uses some of its USGS funding to provide forums and outlets for information exchange. During the period March 1, 2008 through February 28, 2009, the Montana Water Center drew on its USGS support to conduct programs listed under the Statewide Education and Outreach project.

Statewide Education and Outreach

Basic Information

Title:	Statewide Education and Outreach
Project Number:	2008MT187B
Start Date:	3/1/2008
End Date:	2/28/2009
Funding Source:	104B
Congressional District:	At-Large
Research Category:	Not Applicable
Focus Category:	Hydrology, Surface Water, Groundwater
Descriptors:	
Principal Investigators:	Steve Guettermann

Publication

1. Whirling Disease Steering Committee of the National Partnership for the Management of Wild and Native Coldwater Fisheries; 2008 Annual Report;
<http://whirlingdisease.montana.edu/pdfs/2008wdi.pdf> (120 pages)
2. Gretchen Rupp, July 2008 Semi-annual report for the Wildfish Habitat Initiative;
http://wildfish.montana.edu/docs/July_2008_semiannual_report.pdf (17 pages)

* Worked closely with faculty researchers to engage students in water-related research, writing papers and professional presentations. In addition, the Water Center encouraged students engaged in water resource studies to present at conferences. The success of these efforts is documented by the fact that student involvement with information transfer through the Montana Water Center rose from approximately two dozen in 2007 to three dozen in 2008.

* Published thirteen Montana Water e-newsletters and distributed them monthly to more than 1,700 professionals, students and decision makers concerned with water resource management; a special edition was published in March that addressed pharmaceuticals in Montana's water, as a response to a national study. Newsletter archives are posted at <http://water.montana.edu/newsletter/archives/default.asp>.

* In the final stages of a Montana Watersheds Coordination Council website redesign at <http://water.montana.edu/mwcc/default.php> - the site is better serving watershed groups throughout the state, which are also becoming more involved with posting watershed information.

* Continued the web information network MONTANA WATER, at <http://water.montana.edu>. Known as Montana's clearinghouse for water information, this website includes an events page, news and announcement updates, an online library, water-resource forums and water source links, a Montana watershed projects database, an expertise directory, water facts and more.

* Completed a project funded by the Montana Department of Environmental Quality to update a statewide watershed projects database. New projects were added from state agency programs, federal programs, watershed groups, and NGOs and is now in the process of being turned over to the Governor's Restoration Initiative program.

* Maintained and circulated a small library of paper documents related to Montana water topics.

* Conducted the state-wide water research meeting on October 2-3, 2008 in Big Sky, Montana. The theme of this 25th annual meeting was Water Sustainability: Challenges for Montana. It was held in conjunction with the Montana Section of the American Water Resources Association. A field trip led by geologist Larry Smith explored the mountainous Big Sky geology and was well attended. The trip also included the Blue Water Task Force which described how development is impacted area streams. The conference attracted nearly 150 Montana researchers and policy makers who took in plenary presentations by Richard Opper, Director of the Montana Department of Environmental Quality, Eloise Kennedy of the Nature Conservancy, Tom Osborne, principal of HydroSolutions, Tom Patton, a hydrogeologist at the Montana Bureau of Mines and Geology and Larry McKay, the GSA Birdsall-Dreiss Distinguished Lecturer for 2008. Over forty researchers presented information on their latest findings along with nearly 30 poster

displays. The web-based archive of this meeting is found at http://awra.org/state/montana/events/conf_archives.htm.

- * Responded to numerous information requests on water topics ranging from invasive aquatic species to water rights to streamside setbacks to contaminants and pollutants in Montana's surface and ground water.

- * Assisted elected and appointed officials, particularly those serving on the Montana Legislative Environmental Quality Council and Water Policy Interim Committee, the Governor's Drought Advisory Committee and the Water Activities Work Group. The Water Policy Interim Committee became a standing committee during Montana's 2009 legislative session and the Water Center expects continued involvement with that group as issues about the state's water and its use and management become more important and the need to use science and collaboration to direct policies becomes more accepted.

- * Sponsored and participated in Montana's 75th Annual Water School September 22-26, 2008 at Montana State University for 300 staff members of water and wastewater utilities. This training covered managing wells and lagoons to process control for water treatment and activated sludge facilities, treatment plant operation, chemical safety, emergency response, quality assurance programs, and more; the Montana Water Center was able to get Dr. Robert D. Morris, acclaimed author of Blue Death, to speak to the public as part of this training.

- * Created and distributed 1500 copies of the black-and-white Montana Water 2009 calendar to elected officials, water resource managers and other partners and supporters; each month features a different Montana water issue and work agencies and NGOs do to mitigate water-related management challenges.

- * Worked with the Bozeman Film Festival to bring a public showing of the award winning film FLOW to a local audience, with subsequent post-viewing discussion about the community's water supply and treatment.

- * Worked with the Montana Department of Environmental Quality and the Montana Department of Transportation to provide professional education to mitigate nonpoint source pollution. The Montana Watercourse provides comparable outreach to watershed groups, teachers, developers, and landowners.

- * Continued to work with the general public answering questions on water quality, water quantity, water rights and sustainability issues.

USGS Summer Intern Program

None.

Student Support					
Category	Section 104 Base Grant	Section 104 NCGP Award	NIWR-USGS Internship	Supplemental Awards	Total
Undergraduate	6	0	0	0	6
Masters	13	0	0	0	13
Ph.D.	3	0	0	0	3
Post-Doc.	0	0	0	0	0
Total	22	0	0	0	22

Notable Awards and Achievements

Other work undertaken by the Montana Water Center includes:

The Whirling Disease Initiative - Research is concentrated on understanding how the disease affects trout populations, and how management actions may intervene in the process. Dissemination of research and testing results to fishery managers is also a focus this year.

The goal of the Whirling Disease Initiative and other research enterprises is to develop a clear understanding of the disease cycle, the predisposing environmental factors, and methods for maintaining fisheries despite its presence. Initiative research has made great strides in the first two areas, and the program is concluding with a focus on assembling, testing and publicizing a toolbox of management methods to support fishery managers as they strive to maintain fisheries in the presence of whirling disease.

Between 1997 and 2006 the Initiative sponsored from six to 20 research projects in each 15-month cycle. A research cycle generally ran from May of one year through December of the following year, allowing for two field seasons. Broad-scale research investigations begun in May 2006 will conclude at the end of June 2009. One hundred and twenty-four research projects have been carried out by university and public-agency scientists, and private firms since 1997. More than \$5.6 million of federal funds and \$4.3 million in matching funds have been expended by these research projects. Typically two to four investigators are involved in each project, and they bring to the project cash or in-kind match of 25 to 150 percent of the amount of the federal grant. Students are involved in most projects, either as technicians or, more often, as graduate research assistants. Summaries of all past and current research projects are available on the Initiative web site at: <http://whirlingdisease.montana.edu/>.

An interactive map of disease incidence is being mounted on the internet, showing up-to-date information for eight states. Research data from projects funded over the entire course of the initiative are being assembled into a database that can be used for synoptic studies. Although not a formal Initiative requirement, publication of research results is strongly encouraged by the Partnership Board and the Steering Committee. To date, at least 70 peer reviewed publications have been produced.

The Small Systems Technical Assistance Center operated by the Water Center is the flagship of a nationwide network that helps small public water utilities provide safe, reliable and affordable drinking water. This year's projects include:

- developing live and electronic training courses on water-system energy efficiency, use of alternative energy sources, water loss testing, and water conservation.
- working with the other TACs to develop a more comprehensive website and research and outreach presence to provide greater nationwide assistance to small public drinking water systems.

The Water Center operates the web site that provides access to the tools developed by all eight technical assistance centers, and co-sponsors the week-long Montana Water School that draws 250 water treatment operators. Its training courses will be presented at a number of national conferences and workshops this year. To date, more than 50,000 water-utility workers have taken the Center's training courses nationwide.

The purpose of the Wild Fish Habitat Initiative is to evaluate the costs and efficacy of measures to bolster wild fish populations, and publicize the findings among fishery and land managers. A report is submitted semi-annually to the U.S. Fish & Wildlife Service. The most recent one can be found at http://wildfish.montana.edu/docs/July_2008_semiannual_report.pdf

This year Initiative investigators continue to:

- evaluate the biology of fluvial Arctic grayling to aid restoration efforts in the Big Hole River - test physical and chemical techniques for eliminating invasive fish species from streams - assess the success of techniques for restoration of cutthroat trout in western watersheds - assemble habitat-restoration case histories to assist land managers and fishery biologists in planning new projects.

The Initiative is a scientific adjunct to the Partners for Fish and Wildlife program operated by the U.S. Fish and Wildlife Service for private landowners, aimed to enhance the effectiveness of that program's habitat restoration projects.

The Montana Watercourse is a statewide program for schools and citizens, providing water information, resources, tools and education. This year's projects include:

- developing and leading water-resource education courses for realtors and teachers - piloting a program of certification for volunteer water quality monitors - updating the Landowner's Guide to Montana Wetlands for both eastern and western Montana - circulating water-resource "teaching trunks" among Montana elementary schools - completed revision of the Guidebook to Montana Ponds, now in its second printing - operating Know-Your-Watershed tours in the Milk and Marias watersheds - organizing the Montana Water Summit for Teachers and Students and received a relatively large grant from Pacific Power & Light in late 2008 for this spring 2009 event.

Antony Berthelote, as a doctoral student at the University of Montana in the Geosciences Department, was awarded a trip to the National AWRA Conference in New Orleans by the Montana Section of the AWRA for his student presentation at the state's water resources conference in Big Sky, Montana, which the Montana Water Center co-sponsors. The title of his presentation was "Field Observations and Groundwater Modeling as Tools to Mitigate Groundwater Supply Impacts During the Removal of Milltown Dam, Western Montana." Much of Tony's work centers on the impact dam removal can have on the adjacent shallow ground water aquifers, which has received little study. Tony combines extensive river monitoring, groundwater monitoring and well inventory data with numerical groundwater modeling techniques to forecast areas that would experience groundwater declines.